Sex-Specific Roles for Melanin-Concentrating Hormone Neurons Linking the Neuroendocrine Reproductive Axis and Sleep

by

Bethany G. Beekly

A dissertation submitted in partial fulfillment
of the requirements for the degree of
Doctor of Philosophy
(Neuroscience)
in the University of Michigan
2023

Doctoral Committee:

Professor Carol F. Elias, Chair
Assistant Professor Christian Burgess
Assistant Professor Ada Eban-Rothschild
Associate Professor David Olson
Assistant Professor Giancarlo Vanini

Bethany G. Beekly

bgbeekly@umich.edu

ORCID iD: 0000-0002-8422-0072

DEDICATION

This dissertation is dedicated to all the talented, powerful women who have inspired and believed in me from my earliest days as a budding scientist. Thank you for building me up every step of the way, ensuring I never doubted for a moment that a scientist could look like me.

I will pay it forward.

Acknowledgements

Thank you to all past and present members of the Elias lab for their profound and ongoing support in all my endeavors, particularly the "wondergrads" I have had the privilege of working with: Natasha and Dania, you both inspire me and are sure to go on to wonderful things. Special thanks are due our fearless leader, my dissertation advisor Dr. Carol Elias. The culture of curiosity, rigor, and respect that makes your lab such a joy to work in trickles down from the top. I couldn't have asked for a better example to aspire to; thank you for setting the bar so high.

To the rest of my dissertation committee – Drs. Christian Burgess, Ada Eban-Rothschild, David Olson, and Giancarlo Vanini – you have consistently made yourselves available despite your extensive research and, in some cases, clinical responsibilities. Your feedback on experimental design, data interpretation, and writing have been invaluable, and your regard has made me feel like a scientist even when I was discouraged. I appreciate you all more than I can express. Special thanks to my close collaborators Giancarlo and Christian, as well as their respective lab members Dr. Viviane Hambrecht-Wiedbusch and doctoral candidate Katherine Furman for the incredible generosity they have shown with their wisdom, time, and resources. We are able to tell a much richer story together!

To our collaborators in the Moenter lab: thank you for your friendship and insights, especially Drs. Laura Burger and Tony DeFazio for their input on experimental design and analysis, and Amanda Gibson for her sage advice both in and out of the lab. Thank you as well to our AMEGOS in the Caswell Diabetes Institute – Drs. Alison Affinati, Martin Myers, Carol

Elias, Paula Goforth, David Olson, and Randy Seeley – and their respective lab members for the camaraderie and productive conversations. Thank you to Drs. Martin Myers and David Olson for the donation of *Tac2*-Cre and eGFP-L10a mice, respectively, and to Alan Rupp, former member of the Myers lab, for graciously donating his time to help with RNAseq data analysis and interpretation.

I owe a massive thank-you to the faculty of the various core facilities I have used during my tenure as a PhD student: Zhe Wu and Nathan Qi (Mouse Metabolic Phenotyping Core); Thom Saunders and Elizabeth Hughes (Transgenic Animal Core); Dana King and Rebecca Tagett (Bioinformatics Core) and Sasha Meshinchi, Eric Rentchler, and Stevel Lentz (Microscopy Core). Your expertise has enabled me to probe questions I could not have otherwise.

To the ULAM staff at the University of Michigan, who work tirelessly to make sure that our experimental animals receive the highest standard of care from birth until the day they exit the study: thank you for your devotion to animal welfare and for making our work possible. Special thanks to Kayla Vore and Aisha Myers, both of whom worked closely with me when I had ongoing experiments that made their jobs more complicated – your efforts did not go unnoticed. We really couldn't do it without you!

Thank you to the Graduate Employee Organization, where I have found countless friends and infinite inspiration. Your commitment to justice can only be described as transcendent, and I am proud to have participated in some small part of the work you have done in my years as a member.

To THE Cohort – your friendship is precious and irreplaceable. I will always be grateful that I got to share this journey with you. Thank you from the bottom of my heart for being you.

Thank you as well to my many dear friends from other NGP cohorts. This program is like family because of you. It is something special to find a place that is as hard to leave as this one.

Last, but most certainly not least, I acknowledge that the work presented in this dissertation was conducted at the University of Michigan, Ann Arbor, located on the ancestral, traditional, and contemporary lands of the Anishinaabeg – The Three Fire Confederacy of the Ojibwe, Odawa, and Potawatomi Nations, as well as the Wyandot Nation. The university resides on land gifted by the three Nations and the Wyandot Nation, along with many other Indigenous Nations, in the 1817 Treaty of Fort Meigs. I acknowledge the language of "gift" in the original treaty entails mutual relationships between treaty parties, respect, and obligation on the part of the settlers. I commit to advocating for Indigenous struggles against ongoing settler-colonization and striving for a decolonized future in all future steps of my career.

TABLE OF CONTENTS

LIST OF TABLES

LIST OF FIGURES

Abstract

My dissertation research has centered around three aspects of reproductive physiology and the role of MCH neurons therein: lactation, the regulation of pubertal timing and fertility, and the effect of gonadal steroids on sleep architecture. Underlying and uniting these distinct elements is a focus on the transcriptional heterogeneity of MCH cells.

Chapter 1 will provide background on MCH and its role in sleep, metabolism, and reproductive physiology. In Chapters 2-5, I focus on the fast neurotransmitter content of MCH cells: most fundamentally, what is the neurochemical identity of different populations of MCH neurons? What are the effects of isolating and disrupting fast neurotransmitter co-release from MCH neurons? Finally, can a consideration of the effects not just of the MCH peptide itself, but co-released neurotransmitters, help to disambiguate some of the seemingly disparate functions of these neurons within the neuroendocrine reproductive axis? In Chapter 6, I consider additional key transcripts beyond the machinery of classical neurotransmission to define subsets of the MCH neuron population and probe their ability to affect the relationship between the sex steroid milieu and sleep. Finally, in Chapter 7, I will integrate the findings of the former chapters and situate them in the broader context of the MCH field, discuss the strengths and weaknesses of my studies, and outline future directions for this work.

Chapter I. Introduction

Project Overview

Defined as "the failure to achieve a successful pregnancy after 12 months or more of appropriate, timed unprotected intercourse or therapeutic donor insemination," infertility is considered a disease by the American Society for Reproductive Medicine and a disability by the US Supreme Court under the Americans with Disabilities Act [1-3]. Each year, hundreds of millions of dollars are poured into assisted reproductive technologies (ARTs), especially *in vitro* fertilization (IVF). It is anticipated that in the next several years, the global IVF market will surpass 40 billion USD, to say nothing of the mental and emotional cost to couples struggling to conceive [4]. Disorders of the reproductive system also have high rates of comorbidity with metabolic dysfunction, certain cancers, and psychiatric illness [5-8].

Reduced and fragmented sleep is associated with infertility in humans. Much of the research on the role of sleep in reproductive function has been in shift workers, who tend to be sleep deprived and/or experience more fragmented sleep. This population also has elevated rates of infertility and poor pregnancy outcomes [9, 10]. Obstructive sleep apnea (OSA) in adults is also correlated with hypogonadism and adverse outcomes of pregnancy. Treatment of OSA not only improves sleep but also ameliorates the associated reproductive issues [11, 12]. These effects are not limited to adults of reproductive age. A striking contrast observed in children with narcolepsy and OSA provides compelling evidence that sleep plays a profound role in the maturation of the reproductive axis. Children with narcolepsy experience precocious puberty at a rate of 17-32% versus the rate of 0.015% reported in the general population, while a diagnosis of OSA predicts significantly delayed pubertal milestones such as breast development in girls [13, 14]. Clearly, there is an urgent need to better understand how the neuroendocrine reproductive axis interacts with sleep.

At the apex of the neuroendocrine reproductive axis, alternately the hypothalamo-pituitary-gonadal (HPG) axis, are gonadotropin-releasing hormone (GnRH) neurons. Episodic release of GnRH drives pulsatile secretion of luteinizing hormone (LH) and follicle-stimulating hormone (FSH) from gonadotropes of the anterior pituitary gland, which in turn act on the gonads to promote maturation of gametes and steroid hormone synthesis. A bout of high-frequency LH pulses is required for both pubertal onset and ovulation. In pubertal development, increased LH secretion is detected before clinical manifestations of puberty. Notably, this rise in LH pulse frequency that precipitates puberty occurs during sleep. Sleep reversal studies in prepubertal boys demonstrated the dependence of increased LH pulse frequency on sleep, not time of day [15]. Since then, several groups have confirmed the association between gonadotropin secretion and sleep during puberty [16-21]. However, in adults, LH pulse frequency is reduced during sleep [22-24]. The neuronal underpinnings of the integration of sleep and gonadotropin secretion are poorly understood.

Neuropeptidergic control of sleep and wakefulness is complex, but melanin-concentrating hormone (MCH) and orexin/hypocretin (ORX/HCRT) are significant contributors. Most brain MCH expression is in neurons of the incertohypothalamic area (IHy, alternatively medial zona incerta, ZIm), the perifornical area (PFx), and the lateral hypothalamic area (LHA), all of which have multiple functions that include sleep/wake regulation [25-27]. Notably, MCH neurons are active during sleep, and optogenetic activation of MCH neurons significantly increases sleep duration [28-33]. MCH neurons also project to areas implicated in reproductive control such as the medial preoptic nucleus (MPO) and the median eminence (ME), which harbor GnRH neuron cell bodies and terminals, respectively [34, 35]. In humans and rodents, MCH terminals are observed in close apposition with GnRH cells, which express MCH receptor 1 (MCHR1) [34-38]. MCH neurons are thus anatomically poised to dually regulate sleep and the reproductive axis. Their functional effect on reproduction is less clear, however, with mixed conclusions about the ability of MCH to stimulate LH secretion. The valence and magnitude of MCH effects on LH appear to depend on both the site of MCH administration and the sex steroid milieu at the time of the experiment [36, 39, 40].

There are many possible explanations for this. Data in rats indicates that MCH neurons migrate from the neural crest in two groups, with an early-arising group that settles in the lateral

hypothalamus and has primarily caudal projection targets including the brainstem; and a late-arising group settling mainly in the medial hypothalamus which mostly targets hypothalamic and cortical neurons [41, 42]. Thus, it stands to reason that subpopulations of MCH neurons may exert different, even opposing effects, on the HPG axis. Sleep architecture also varies with hormonal milieu, suggesting that MCH could coordinate LH secretion with sleep/wake state in a sex-steroid dependent manner [43]. However, the neural underpinnings of biological sex- and gonadal hormone-driven effects on sleep are poorly understood.

Indeed, a major gap in the MCH literature is the lack of basic knowledge of the MCH system in female animals. The MCH system is well-characterized in male mice and rats, but there is little published data in females to describe either the anatomy and colocalized transcripts or the functional effects of MHC neurons. We sought to contribute to the understanding of how MCH neurons interact with the neuroendocrine reproductive axis in both male and female animals with a focus on the MCH system in females. A deeper understanding of the role of sleep in the reproductive axis in both sexes is imperative for the equitable development of effective interventions and treatments for reproductive health across the life span.

Melanin-concentrating hormone

Evolution and anatomy of the MCH system

Melanin-concentrating hormone (MCH) is a cyclic 19-amino acid (aa) neuropeptide derived from a propeptide called pre-pro-melanin-concentrating hormone (ppMCH) encoded by the *Pmch* gene [44, 45]. In mammals, MCH is expressed primarily in the brain but may exhibit low levels of expression in peripheral tissues including lung, thyroid, and the gastrointestinal tract [46]. Most MCH expression is in neurons of the incertohypothalamic area (IHy, alternatively medial zona incerta, ZIm), the perifornical area (PFx), and the lateral hypothalamic area (LHA) [25-27], all of which are involved in essential functions like energy balance, reproduction, and the stress response [47-51]. The MCH peptide is most often thought of as a major homeostatic integrator with roles in a wide range of neuroendocrine processes.

The precise origin of the *Pmch* gene in vertebrates remains an open question in the field, though distantly MCH-related genes have been suggested in *Aplysia californica* (California sea hare),

Ciona intestinalis, (vase tunicate), *Branchiostoma floridae* (Florida lancelet), and *Caenorhabditis elegans* (roundworm) [44]. The earliest-diverging organisms in which neuronal MCH expression is reported are the lampreys (order Petromyzontiformes) [52-54]. However, MCH was first described in chum salmon in the 1980s, where it is expressed in the hypothalamus and subsequently enters the blood stream via the neurohypophysis [55]. The primary function of MCH in salmonids, which gave the peptide its name, is to facilitate adaptive color change: it aggregates melanin to cause a paling of the scales, opposing the action of α-melanocyte-stimulating hormone (αMSH), which disperses pigment granules within melanophores to make the scales appear darker [55].

As it happens, these seemingly unrelated functions are actually the result of a gene duplication that occurred after the teleost divergence, resulting in two MCH-coding genes in this clade with distinctive sequences, distribution, and functions, referred to as "*Pmcha*," analogous to the ubiquitous vertebrate *Pmch* gene, and "*Pmchb*," specific to teleost fishes [56]. The peptide originated by *Pmcha* in the teleost fishes is nearly identical to mammalian *Pmch,* with three conservative substitutions in the ring structure: Ile^{2} replaces Phe^{2}, Val^{9} replaces Leu^{9}, and Ala^{19} replaces Val^{19}. There may be additional, likely conservative, substitutions that are species-specific; for instance, *Cyprinus carpio* (the common carp) may have an additional substitution, Ile^{4} replacing Met^{4} [56]. The *Pmchb* gene differs markedly from mammalian *Pmch* and from *Pmcha*. It is intronless and encodes a 17-aa cyclic peptide with two substitutions on the N-terminus preceding the ring structure—Thr^{2} replaces Met^{4} and Met^{3} replaces Leu^{5}—and one non-conservative substitution in the C-terminal sequence outside the ring—Glu^{16} replaces Gln^{18}—in addition to the same substitutions inside the ring described above [56]. As *Pmchb* is not present in mammals, and mammalian reproduction is the focus of this work, all further mention of the *Pmch* gene and its peptide product in teleost fishes will refer to *Pmcha*.

In addition to MCH, there are at least two other peptide products of the mammalian *Pmch* gene, the 13-aa neuropeptide glutamic acid-isoleucine (NEI)[1] and the 19-aa neuropeptide glycine-glutamic acid (NGE)[2], which originate from ppMCH, as well as both coding and noncoding non-

[1] In salmonids, due to an amino acid substitution, there exists an analogous transcript that is referred to as neuropeptide glutamic acid-valine (NEV) [57].
[2] In salmonids, due to an amino acid substitution, there exists an analogous transcript which is referred to as neuropeptide proline-glutamic acid (NPE) [57].

canonical transcripts including the alternative-splicing gene product MCH-gene-overprinted-polypeptide (MGOP) and the antisense-RNA-overlapping-MCH (AROM) [44, 58-60] (For review, see [61, 62]). In the hominid lineage, two chimeric genes called *PMCH-Linked* 1 and 2 with transcriptional regulatory function have also been reported and are understood to have arisen through a complex process of exon shuffling, retrotransposition of antisense *Pmch* mRNA, *de nov*o creation of novel splice sites, and spontaneous chromosomal duplication events [63].

In rodents and primates, most MCH neurons also contain NEI and NGE [34, 44, 64, 65]. In addition to NEI and NGE, some MCH neurons produce the neuropeptide cocaine- and amphetamine-regulated transcript (CART) and express the gene for secretogranin II (*ScgII*) which is cleaved into two secreted peptides, secretoneurin and EM66 [66]. (For review, see [67-70]). Finally, MCH neurons express numerous genes involved in the synthesis, packaging, and release of the classical neurotransmitters GABA and glutamate, which are the central nervous system's predominant inhibitory and excitatory neurotransmitters, respectively [66, 71-74]. The question of whether functional glutamatergic or GABAergic signaling actually occurs in MCH neurons is a contentious one; the topic of classical neurotransmission in MCH neurons will be covered more extensively in chapters 4 and 5.

MCH neuron morphology varies somewhat between clades; the focus of this morphological discussion will be the mammalian MCH system [75]. The majority of mammalian MCH-expressing cells are large, multipolar neurons of irregular or rounded shape with between 2 and 5 primary dendrites, many secondary dendritic branches, and occasional tertiary branches [76]. The second most numerous MCH neuronal subtype are fusiform cells, which are more elongated, almost always have two primary dendrites, and exhibit significantly less secondary and tertiary branching than multipolar cells [76]. These are primarily located in the ZIm (*unpublished observations*). Finally, a small percentage of MCH neurons are the crescent type; these cells are located very close to blood vessels and as such their sickle shape is most likely due to displacement by the blood vessel; it seems likely that they constitute a portion of the population of fusiform cells, as they too usually have two primary dendrites and very little secondary or tertiary branching [76]. Regardless of cell morphology, the MCH peptide's subcellular localization is primarily in the soma and around the nucleus, differentiating it from NEI, which, while colocalized nearly 100% with MCH, primarily occupies proximal dendrites and axonal

projections [76]. High-magnification images of MCH immunoreactivity illustrate that, while MCH expression in the soma is dense, it is concentrated into discrete puncta, suggesting that most MCH is contained within vesicles [76].

Localization of MCH neurons in the brain is variable across families of organisms and even between closely related species (i.e., mice and rats). Painting in broad strokes, this population has evolved from a relatively small ependymal/subependymal population in the dorsomedial hypothalamus that is closely associated with the third ventricle to a large, dispersed population of neurons primarily located in the lateral hypothalamus [56]. In the lampreys and early jawed vertebrates, MCH cells border the third ventricle and constitute part of the paraventricular organ (PVO), a highly-vascularized brain region not found in mammals which is situated outside the blood-brain barrier and as such releases many hypothalamic hormones into circulation [53, 54, 77-79]. MCH projections are observed primarily in olfactory regions, the habenular nucleus (a regulator of monoaminergic neurons which contributes, among other things, to the modulation of sleep-wake cycles), and the spinal cord [54, 80]. Beginning with ray-finned fishes (Actinopterygians), these periventricular neurons become two distinct populations, dorsal and ventral, and the innervation of the neurohypophysis as well as the adenohypophysis becomes more apparent. The earliest precursors to a true lateral hypothalamic locus of MCH expression are observed in Actinopterygii with the emergence of a population in the lateral tuberal nucleus (NLT) of *Lepisosteus osseus* (longnose gar), though they retain the dorsomedial ventricular population as well.

The teleost fishes comprise an infraclass of the ray-finned fishes [52]. At the point that they diverge from other Actinopterygii, around 320 MYA, MCH expression patterns begin to more closely resemble that which is observed in mammals, with the bulk of MCH expression being localized in the NLT [81]. On the other hand, in Sarcopterygii (the lobe-finned fishes), which originate the tetrapod lineage and diverged from Actinopterygii about 425 MYA, the primarily dorsomedial ventricular localization of the MCH cells is retained, and a smaller group of MCH cells appears in the peripheral layers of the ventral hypothalamus, extremely close to the base of the brain [56, 82]. MCH projection targets are similar in teleost and lobe-finned fishes, with fibers observed in the neurohypophysis, thalamic nuclei, the pretectal region, the preoptic area of the hypothalamus, and throughout the telencephalon [81, 83-86].

The lateralization of MCH neurons in the tetrapod lineage did not come about until the Sauropsid/Synapsid divergence, which gives rise to modern birds and reptiles (Sauropsida) and mammals (Synapsida). The Sauropsids express significant MCH populations in the dorsomedial periventricular nucleus and the LHA, with projections to olfactory regions, septal nuclei including the MS/NDB, hippocampus, preoptic area and other hypothalamic nuclei, pretectal area, optic lobes, and numerous sites in the brainstem and spinal cord [87]. MCH fiber density in hippocampus, thalamus, and olfactory regions is higher in the non-Avian Sauropsids and brainstem/spinal cord projections, being more concentrated to specific nuclei in Aves compared to the diffuse, abundant projections observed in non-Avian Sauropsids [87].

Synapsida experiences the most pronounced lateralization of the MCH population, with virtually complete loss of the dorsomedial periventricular population in favor of large populations in the LHA and ZIm/IHy. It is important to reinforce at this point that the lateralization of the MCH system has thus occurred multiple times throughout the course of evolutionary history. This instance of convergent evolution gives us a clue as to the evolution of the peptide's function: as the MCH populations migrate laterally, they gain access to large fiber tracts—the infundibulum in those fishes which exhibit this lateral migration, and the medial forebrain bundle (mfb) in organisms of the tetrapod lineage. In so doing, MCH neurons are able to engage with an exponentially greater number of both inputs and outputs, greatly expanding their capacity as major integrators of homeostatic information and modulators of a diverse array of systems.

The mammalian MCH system is best described in common model organisms such as *Mus musculus* (laboratory mice) and *Rattus norvegicus* (laboratory rats), and as such, these will be the representatives of family Muridae for this discussion. In the male rat, *Pmch* mRNA is found in the ZIm/IHy, LHA (anterior, tuberal, and posterior subdivisions), anterior periventricular nucleus (PeA), the caudal part of the anterior hypothalamic nucleus (ANH), olfactory tubercle (within the islands of Calleja), pontine sites within the paramedian reticular formation, and the internuclear region, a band of cells situated in between the dorsomedial and ventromedial hypothalamic nuclei (DMH; VMH), though peptide expression is only clearly visible in ZIm/IHy, PFx and LHA [25, 62, 88]. Female rats possess these same populations and additionally exhibit *Pmch* mRNA in the caudal laterodorsal tegmental nucleus (LDTc) [89]. Furthermore, in lactating dams, transient *Pmch* mRNA expression is observed in the preoptic area (POA), periventricular

preoptic nucleus (PVpo), and the paraventricular nucleus of the hypothalamus (PVH) in the final week of lactation before weaning [90, 91]. In mice, *Pmch* mRNA is largely restricted to the LHA, PFx, and IHy, with some expression in the dorsomedial nucleus of the hypothalamus (DMH) [92, 93]. While sexual dimorphisms have not been investigated in the sexually naïve mouse, our group has demonstrated transient expression in lactating female mice around lactation day 19 in the POA and PVH as well as the anterodorsal thalamic nucleus and lateral septum [94]. Extensive comparison of these and other less commonly-used muroid species can be found in [76].

The distribution of MCH varies significantly between mammalian clades. Sheep (*Ovis aries*), for instance, appear to lack MCH neurons in the ZIm/IHy, and this population is also smaller and more caudolateral in the tufted capuchin monkey (*Cebus apella*[3]); in the domestic cat (*Felis catus*) the entire localization of the MCH population is shifted significantly dorsally as compared to other mammals discussed here [56, 64, 95-97]. In humans, MCH mRNA and peptide are detected in the LHA, ZIm, DMH, and the dorsal hypothalamic area (DHA) which is located dorsal to the DMH [27, 98-100]. Of note, in both *Homo sapiens* and *Mus musculus,* a ring-shaped structure of MCH neurons has been reported, in the DHA in humans and LHA in mice, and it has been suggested that this may constitute a sub-structure/neurochemical division within the LHA referred to as the "LHA shell" [27, 56, 76]. Evaluating the collective significance of these variations is challenging given the small number of mammalian species in which MCH mRNA and/or peptide expression has been systematically characterized. They may suggest subtly different functional priorities resulting from access to different neurochemical subpopulations within the hypothalamus and to particular aspects of the mfb, which houses many topographically distinct compartments [101].

From their earliest Petromyzontidae origins, the MCH neurons have exhibited a distinctive pattern of projections illustrative of two unique modes of signaling. Some of their axons project locally within the hypothalamus, as well as more extensively throughout the brain in more recently-diverged fishes, reptiles, and tetrapods, in a manner suggestive of typical

[3] In the original description of MCH in a new world monkey, the species was identified as *Cebus apella* (Bittencourt et al., 1998). The taxonomic identification of the monkeys used in these early experiments has since been revised. Those animals are now more closely identified with members of genus *Sapajus*, though controversy remains on this topic (see also Battagello et al., 2017; Diniz et al., "A Tale of Two Peptides")

neurotransmission; others project directly to the ventricles, particularly the third ventricle (3V), indicative of a capacity to signal by "volume transmission," that is, by depositing the contents of their synaptic vesicles directly in to the cerebrospinal fluid (CSF) to be distributed throughout the brain [53-55, 102, 103].

Of those axons which project in a more typical fashion to various sites throughout the brain, data in the mouse and rat has illustrated that there are two developmentally, neurochemically, and hodologically distinct groups [41, 42, 104]. During embryonic development, MCH-destined neurons are generated roughly between E10 and E16 in mice and rats, and they settle in the mantle layer in a lateral-to-medial gradient. Thus, the group which settles first, around E11, is situated more laterally, forming clusters of cell bodies located dorsolateral to the fornix. Around E13 the second group of MCH neurons begin to settle; some will end up in the more lateral regions of the hypothalamus, but most will pass the earlier-arising population to settle in the rostromedial zona incerta and perifornical area [42].

The transcriptional profiles of the two populations also diverge early as a result of a Sonic hedgehog-controlled genetic cascade. The earlier-arising, caudolateral population is defined by the expression of *Scg2* and *Nrxn3*, while the later-arising, rostromedial projection is defined by the expression of *Nptx1*, *Lypd1*, *Parm1*, *Amigo2*, *Cartpt*, and *Tacr3* [41]. The caudolateral population has mostly descending projections, while the rostromedial population has primarily local and ascending projections, though both groups have projection targets in the cortex, pons, brainstem, spinal cord, and hypothalamus [41, 42, 104].

The MCH receptor

In humans, two receptors for MCH have been identified, MCHR1 and MCHR2, but MCHR2 has been less thoroughly characterized because functional MCHR2 is absent in rodents [105-109]. MCHR1 is a 353-aa rhodopsin-family GPCR previously known as the orphan receptor SLC-1 or GPR24 which shares about 40% homology with human somatostatin receptors, but it is highly specific to MCH [110-119]. The sequence of MCHR1 is largely conserved, with a high degree of homology between primate, rodent, fish, and amphibian cDNA sequences in those representatives of each that have been studied [110-118]. MCHR1 mRNA can be observed in the majority of olfactory and limbic structures, notably taenia tecta, olfactory tubercle, piriform cortex, and nucleus accumbens (shell); hippocampus, and to a lesser extent in the neocortex;

hypothalamus, some intralaminar thalamic nuclei, brainstem, reticular formation, and spinal cord [113]. It is also found at lower levels in some peripheral tissues such as brown adipose cells, pancreas, and pituitary gland [103, 120].

MCHR1 is capable of dual and somewhat contradictory actions [121, 122]. It inhibits adenylyl cyclase and subsequently suppress cAMP accumulation [115]. It can also mobilize intracellular Ca^{2+} ions, presumably through the phospholipase C pathway, and primarily in the context of very high concentrations of MCH [111, 115]. This would seem to suggest that MCHR1 may couple to either $G\alpha_{i/o}$ and $G\alpha_q$, though it has been demonstrated to show a higher affinity for $G\alpha_i$ proteins [113, 115, 121, 123] (reviewed in [124]). An alternate explanation to $G\alpha_q$ coupling which has been proposed is that intracellular Ca^{2+} ions are mobilized through the activation of phospholipase Cβ (PLCβ) mediated by release of βγ subunits from heterotrimeric $G\alpha_{i/o}$ ($G\alpha_{i3}$) proteins [113, 116]. In either case, it seems that the valence of MCH action may vary between target regions depending on the availability of different G protein subunits. Additional review of the electrophysiological effects of MCH on various populations of hypothalamic neurons can be found in [125].

Regulation of MCH and MCH receptor expression

A number of factors can affect the activity of MCHR1. Periplakin, a component of the desmosome, the neurite-outgrowth factor neurochondrin, and RSG8, one of the GTPase-activating proteins for G_α protein subunits, can all reduce MCH-binding-induced calcium mobilization by interacting with the receptor's C-terminus tail [126, 127]. The significance of many specific residues in MCHR1 to its structure, cell surface expression, and ligand binding have been reviewed in [122]; mutations to any of these residues can impair normal MCH signaling. Melanocortin receptor accessory protein 2 (MRAP2), a transmembrane protein known to regulate the cell surface expression of several GPCRs and found abundantly in the hypothalamus, regulates the availability of the receptor for ligand binding by controlling whether it is expressed on the cell surface. The binding of MCH itself, in the manner of many GPCRs, also induces the internalization of the receptor, meaning that the regulation of MCH and MCHR1 expression are often linked and inversely related. [128-133].

MCH neurons receive afferents from many neuronal populations. Many of these neuropeptidergic inputs may also affect *Pmch* expression levels. For instance, the melanocortin 4

receptor (MC-4R) is present on MCH-expressing neurons, and administration of MC-4R antagonists upregulates MCH expression [134]. MCH neurons also receive inputs from neuropeptide Y (NPY), agouti-related peptide (AgRP), and pro-opiomelanocortin (POMC) neurons, and thus the MCH system is potentially regulated by these peptides as well, though the details and mechanisms behind this theory are not well-studied.

Gonadal hormones regulate MCH neurotransmission, though the mechanism depends on which hormone is being considered. Administration of the androgenic hormones dehydroepiandrosterone (DHEA) and dihydrotestosterone (DHT) to ovariectomized female mice upregulates *Pmch* mRNA expression in the hypothalamus [135]. On the other hand, MCH and MCHR1 protein are decreased by acute high-dosage estradiol treatment in ovariectomized female rats, and in intact rats, MCH and MCHR1 protein are reduced in the periovulatory phase when estrogen is at its highest relative to other cycle stages [136, 137]. Progesterone alone does not affect MCH expression in ovariectomized or estradiol-primed female rats, and in fact may attenuate the reduction in MCH-ir cells observed in the IHy with estradiol injection alone [137, 138]. Progesterone receptor blockade, however, also increases the number of MCH-ir neurons in the IHy as well as serum levels of MCH [137]. [136]. Relatedly, MCH expression has been reported to fluctuate with the reproductive cycle in the common carp. Elevated MCH expression can be observed during the preparatory phase of the carp's reproductive cycle, as well as during the post-spawning/post-spermiation and pre-spawning/pre-spermiation phases, while expression is at its zenith during the spawning/spermiation phase [139]. MCH levels also fluctuate with age and developmental stage [140, 141]. As gonadal steroids are often associated with transcriptional regulation, it is surprising that these changes so far appear limited to protein levels. At the level of gene expression, assessed using real-time quantitative PCR, no changes have been documented to either *Pmch* or *Mchr1* expression in association with gonadal steroid hormone manipulations

Environmental neuroendocrine disruptors can modulate *Pmch* expression. For instance, diethylhexyl phthalate (DEHP), a widely utilized phthalate plasticizer, results in significantly elevated *Pmch* levels [142]. In this way, environmental contaminants may be linked directly to the etiology of neuropsychiatric disorders, as correlations have been shown between baseline levels of MCH and anxious/depressive behaviors. Rats selectively bred for low

locomotion/exploration in a novel environment are used as a rodent model for depressive/anxious behavior. In these "bred low responder" (BLR) mice, *Pmch* mRNA is increased by 44% in the hypothalamus and hippocampal CA1 MCHR1 is reduced by 14% as compared to "bred high responders" (BHR), which are naturally resilient to anxiety and depression like behaviors [143]. Relatedly, acupuncture has been shown to upregulate *Pmch* expression [144]. It has been suggested that regulation of *Pmch* expression mediates the positive response of patients with dyskinesias to acupuncture therapy [144]. Although the precise mechanisms that underlie this response are unclear, one possibility that unites these data with the association between elevated MCH and higher risk of neuropsychiatric disorder is that inflammation and the neuroimmune response contribute to the effect of environmental contaminants, stressors, and acupuncture therapy on *Pmch* gene expression levels, though the valence of the eventual outcome is context-dependent.

Unsurprisingly, given MCH's potent sleep-promoting capabilities and well-established role in metabolism, *Pmch* and *Mchr1* expression levels can be modulated by energy status, circadian rhythms, and sleep pressure. Broadly, MCH is understood to be an orexigenic peptide that is downregulated by satiety signals. In leptin-deficient (ob/ob) mice, *Pmch* expression levels are elevated, an effect which can be attenuated by the administration of exogenous leptin [145, 146]. In broiler hens, it has been shown that *Pmch* levels are highest in fasted hens, followed by hens which have been fasted and subsequently refed for two hours before sacrifice, with the lowest *Pmch* expression levels associated with normal fed conditions [140]. *Pmch* mRNA is also regulated by energy state in the common carp, though not in quite the same manner as that observed in birds and mammals: after normal feeding, *Pmch* is at its highest; it is *reduced* by fasting, and increased relative to fasting with refeeding [139].

Mchr1 mRNA is higher in the frontal cortex and hippocampus of rats during the light phase (when rats are predominantly sleeping) [147]. This can be reduced by selectively REM-sleep depriving the rats [147]. REM sleep deprivation and subsequent REM rebound, as well as chronic sleep restriction (not REM-specific), elevate MCH levels in the CSF, indicating that MCH expression levels, release, or both are upregulated by sleep pressure [147]. Furthermore, sleep disruptions result in circadian fluctuations in MCH CSF levels and *Pmch* gene expression that are not observed in control conditions, such as the fact that under selective REM sleep

deprivation and subsequent rebound REM sleep, *Pmch* gene expression, like the receptor gene expression, is significantly higher in light phase than in the dark phase, which was not the case with general sleep restriction, or in control animals—in these groups, a significant difference was observed only in the receptor levels [147].

Functions of MCH

Mammalian MCH is associated with a wide variety of processes. It has some autonomic functions including central regulation of the cardiovascular system and regulation of respiration via multisynaptic connections with motor neurons of the diaphragm, most specifically the central hypercapnic chemoreflex [148-151]. The MCH system also has a role in olfactory integration, which may at least partly explain the effects it has on parental care, aggression, and even food seeking [152-154]. Transient MCH expression is observed in the rostral hypothalamus in late lactation, which could be related to olfaction but seems to be more likely associated with suckling-induced oxytocin secretion [155]. MCH can also affect other facets of reproductive physiology by modulating gonadotropin secretion from the pituitary gland, though again, the contexts in which it exerts stimulatory vs. inhibitory action are not fully understood [36, 39].

MCH has been implicated in psychiatric disease, though the nature of its effects is not always clear. Intracerebroventricular injection of MCH in male rats has been shown to increase exploration of novel environments and time spent in the open arms of an elevated plus maze, all of which are considered reductions in anxiety-like behavior, but MCH receptor antagonists have also been observed to have anxiolytic and antidepressant effects in diet-induced obese male rats [156, 157]. The MCH system is also a substrate for drug addiction, with MCH receptor antagonism resulting in suppression of both cocaine- and alcohol-seeking behavior in male rats [158, 159]. Finally, the MCH system is implicated in learning and memory, seemingly by increasing hippocampal synaptic transmission [160, 161].

However, the most established roles for MCH are in the central regulation of metabolism and the control of vigilance states, especially rapid eye movement (REM) sleep. These functions are also the most directly relevant to my thesis work and will be discussed in greater detail in the sections to follow.

MCH and Central Regulation of Metabolism

Central control of metabolism and appetite is comprised of neural and neuroendocrine components [162, 163]. Hypothalamic neuroendocrine cells may be associated with the posterior pituitary and secrete end hormones directly into the main circulation, or they may be associated with the anterior pituitary and secrete releasing/inhibiting hormones into the hypophyseal portal system [162, 164]. End hormones induce direct effects on their target organs, while releasing hormones stimulate second-order neuroendocrine cells in the anterior pituitary, which in turn release stimulating hormones to elicit effects on target tissues [162, 164]. Inhibiting hormones have a more nuanced, modulatory action that works to suppress the release of the specific pituitary hormone in question [164].

Some populations of neuroendocrine cells also have non-neuroendocrine aspects. Pituitary-projecting cells may have additional projection targets within the brain where they release either neuropeptides or amino acid neurotransmitters such as glutamate, or there may be separate populations of cells which utilize releasing hormones as neurotransmitters rather than endocrine factors [162]. Corticotropin-releasing hormone (CRH) neurons, for example, comprise a neuroendocrine population in the paraventricular hypothalamic nucleus (PVH) which releases CRH to the anterior pituitary but also participates in canonical glutamatergic neurotransmission, as well as an extrahypothalamic population which modulates food intake through entirely non-endocrine mechanisms [162, 165].

There are also many hypothalamic neuropeptides associated with the regulation of energy balance that do not have direct neuroendocrine functions such as endocannabinoids, pro-opiomelanocortin (POMC), neuropeptide Y (NPY), agouti-related peptide (AgRP), neurotensin (Nts), cocaine- and amphetamine-regulated transcript (CART), orexin/hypocretin (OC/HCRT), and MCH. Other primarily-peripheral signaling molecules glucagon-like peptide 1 (GLP-1), cholecystokinin (CCK), leptin, and ghrelin can also act as neurotransmitters in the brain, thereby contributing to the central control of metabolism and appetite [166].

There exists a large body of evidence in support of MCH as an orexigenic peptide. Transgenic models of overexpression of the *Pmch* gene exhibit increased feeding and body weight [167]. *Pmch* expression is upregulated in conditions of negative energy balance or the absence of satiety signals like leptin, and its central administration can promote an acute increase in food

intake [145, 146, 168, 169]. Chronic intracerebroventricular administration of MCH to male mice on high-fat diet results in elevated food intake, weight gain, adiposity, hyperinsulinemia and hyperleptinemia [170, 171]. Chronic administration of an MCHR1 agonist also increases food intake, body weight, and adiposity in male rats, while MCHR1 antagonists significantly reduce food intake and reverse diet-induced obesity-related hyperinsulinemia, hyperleptinemia, hypercholesterolemia, and hyperinsulinemia [172, 173]. As a result, the MCH system has been a promising and attractive target for novel anti-obesity therapies in recent years.

MCH and the Neurobiology of Sleep

Sleep is a critical survival function that is largely conserved across taxa, though variation in sleep architecture is observed in invertebrates, non-avian reptiles, and amphibians (for review see [174]). Henceforth, sleep in mammals will be discussed, as it has undergone the most thorough characterization.

Behaviorally, sleep is a rapidly reversible state that can be distinguished from wakefulness by the closing of the eyes, adoption of species-specific stereotyped postures, and an increased arousal threshold [175]. Using electroencephalography (EEG), mammalian and avian sleep can be broken down into distinct phases, leading us to classify vigilance into three basic states using: (1) wakefulness (W), for which the EEG is characterized by low amplitude, high frequency waveforms; (2) non-rapid eye movement (NREM) sleep, also known as slow-wave sleep (SWS), for which the EEG is characterized by higher amplitude, slower waveforms reflecting synchronous oscillations of neuronal activity, with the highest power typically observed in the delta frequency; and (3) rapid eye movement (REM) sleep, also known as paradoxical sleep (PS) for its resemblance to waking EEG signatures, though it may be distinguished from wake by the more organized, “sawtooth”-like theta-frequency waveforms [176-178]. The normal cycle of state transitions observed in drug-free animals is W-NREM-REM-W, with at least a brief wake event separating each bout of sleep, sometimes referred to as a “microarousal.”

Neural control of sleep and wakefulness is complex and remains incompletely understood, despite a wealth of research on the topic. Early research on the induction of sleep proposed the existence of an “ascending reticular activating system” (ARAS) in which a neuronal network in the brainstem activates forebrain, thalamic, and cortical nuclei to modulate vigilance state [179]. Over time, conceptualization of the ARAS has changed, but the notion of a network of nuclei

working in tandem using assorted neurotransmitters to promote arousal has largely stood the test of time. Sleep-wake regulatory circuitry is governed by mutually inhibitory circuits involving both classical neurotransmission (i.e., GABA and glutamate) and additional neuropeptides. In general terms, glutamate, being the brain's primary excitatory neurotransmitter, is associated with arousal while GABA, the brain's primary inhibitory transmitter, is considered sleep-promoting. The reality, however, is less clear-cut: GABAergic signaling can lead to disinhibition of arousal circuitry, which can in turn promote wakefulness, while glutamatergic excitation of inhibitory interneurons can be sleep-promoting [180] (for review, see [181]).

Many other neurotransmitter systems are involved in modulation of sleep-wake state including REM- and wake-promoting acetylcholine neurons of the pedunculopontine and laterodorsal tegmental nuclei and the basal forebrain; norepinephrine neurons in the locus coeruleus; arousal-promoting monoaminergic neurons in the dorsal raphe nuclei, nucleus accumbens, and prefrontal cortex; arousal-promoting histaminergic neurons of the tuberomammillary nucleus; and sleep-promoting adenosine neurons in the basal forebrain [181-187]. Furthermore, early electrophysiological studies found the lateral hypothalamus to be an important hypothalamic site of sleep-wake control [188, 189]. Indeed, numerous neuropeptidergic neurons situated largely in the hypothalamus have been shown to modulate vigilance state, including, but not limited to, those expressing galanin, melatonin, oxytocin, neuropeptide Y, somatostatin, ghrelin, substance P, orexin/hypocretin, and melanin-concentrating hormone [28, 181, 190-198].

MCH neurons are another critical component of the neuropeptidergic regulation of vigilance state. They are particularly active during and important for the induction of REM sleep. When mice are REM-sleep deprived for 72 hours prior to sacrifice, cFos expression (a correlate of neuronal activation) is significantly decreased in MCH neurons as compared with control mice that are allowed to recover for three hours following the 72 hours of REM sleep deprivation [199]. Electrophysiological recordings combined with juxtacellular labeling of neurons in adult male Long-Evans rats subsequently found MCH neurons to be selectively active during sleep, particularly during REM sleep [28]. Optogenetically stimulating MCH neurons for 24 hours (1 minute on, 4 minutes off, at 10 or 30 Hz) significantly increases the total time spent in both NREM and REM sleep and reduces the latency to sleep onset during the dark phase [31]. Optogenetically stimulating MCH neurons at the onset of a REM sleep episode, as determined

by cortical EEG, significantly lengthens the REM sleep epoch, and stimulation during NREM reduces the latency to a REM transition, but optogenetically silencing them reduces both the frequency and amplitude of hippocampal theta rhythms without significantly altering the duration of the bout of REM sleep [30, 32]. More recently, though MCH neurons were previously believed to be largely silent during wake, it has been shown that a subset of MCH neurons are active during novel object exploration [33].

Taken together, these data seem to indicate that MCH neurons play a more unique role in the induction rather than the maintenance of REM sleep, but they are also sufficient, though not necessary, for the maintenance of a REM epoch, suggesting some functional redundancy in the neural circuitry which maintains theta rhythms following the transition to REM. Their relationship to REM sleep seems tightly linked to their ability to modulate theta rhythms, a conclusion which is further supported by the recent evidence that MCH neuron activation can be observed during wakefulness during specific contexts, that is, during tasks which elicit strong theta rhythm activity. Whether their role in REM and theta rhythms is in any way modulated by sex is unknown.

Sex variables do have documented effects on both subjective and objective measures of sleep [200-202]. Women have longer REM sleep duration than age-matched men, but shorter phase 1 and non-REM sleep durations [203]. The amplitudes of core body temperature (CBT) and melatonin rhythms differ as well, with men exhibiting higher CBT amplitudes on average while women have higher melatonin amplitudes [204]. Diurnal rhythms of core body temperature (CBT) are advanced about an hour on average in women compared to men; some studies report a corresponding advancement of the diurnal melatonin rhythm, though this is more controversial [203-207]. Interestingly, women are twice as likely to report disordered sleep as men, but there is little to no data to directly support this: for all the differences in sleep and related parameters that have been observed, none would indicate a deficit in sleep quality. The difference may be a matter of circadian rhythm (women tend to sleep earlier and wake earlier if allowed to follow their preferred sleep schedule, a fact which is supported by the advanced melatonin rhythms) and thus a state of desynchrony between circadian rhythm and actual sleep behavior caused by work, family obligations, and other lifestyle factors could contribute to feelings of tiredness.

Furthermore, the female reproductive cycle appears to impose an additional layer of sleep regulation, with increased NREM sleep duration but decreased REM sleep duration and amplitude of CBT diurnal rhythms observed during the luteal as compared to the follicular phase of the menstrual cycle in adult women [208, 209]. In particular, women frequently report insomnia during the luteal phase of the menstrual cycle. Yet once again, these reports cannot be fully explained by existing data: total sleep time, latency to sleep onset, number of awakenings, duration of awakenings, and morning vigilance are all found to be unaffected by the menstrual cycle, at least by existing measures. These findings would suggest that the levels of circulating estradiol and/or progesterone impact certain features of sleep and circadian rhythms, but also may independently alter perception of sleep quality via affective or other pathways. For instance, the anxiety and depressive symptoms associated with the pre-menstrual period could distort the perceived difficulty of falling asleep and feeling of being rested.

It is also the case that the way sleep develops and fluctuates across the lifespan is different between the sexes. Sleep depth and structure and circadian rhythms undergo many changes across the lifespan that are sexually dimorphic (see Chapter 6; [210, 211]). It is likely that a combination of organization and activational effects culminate in the biological sex differences which result in disparities in sleep health. Poor sleep should be of great concern as it is associated with numerous comorbidities such as obesity, depression, and infertility [9, 10, 212-220]. Ultimately, since women and girls are much more likely to present with these concerns, healthcare equity requires that we understand what factors predispose women and girls to insomnia and other sleep disruptions.

To achieve this, it will be important to understand mechanisms by which the neural circuits controlling vigilance stages interact with the HPG axis. MCH neurons have been associated with the HPG axis, specifically with LH release. GnRH neurons express the receptor for MCH and, if primed with estradiol, in cultured hypothalamic explants they will release GnRH following MCH application [36, 37, 138]. Furthermore, MCH injection into the female rat brain affects LH release in a manner which seems to depend on both site of injection and the ovarian hormone milieu, though the precise relationship between these variables is not well understood [36, 221, 222].

Hypothesis: Because of their established relationship to sleep and the fact that they have a demonstrated ability to affect pituitary LH secretion in a manner dependent on gonadal hormones, we hypothesized that MCH neurons are involved in the temporal integration of sleep patterns and LH secretion, and that this action is modulated by sex steroids.

Objectives:

The overarching objective of our studies was to better understand how *Pmch* neurons engage with gonadal hormones and the neuroendocrine reproductive axis in male and female animals in order to identify a mechanism by which they could coordinate the temporal relationship between sleep and LH secretion. We approached this objective with two distinct but related sub-aims: to characterize the transcriptional and hodological profiles of subpopulations of MCH neurons; and to parse the respective reproductive and metabolic contributions of MCH and glutamatergic neurotransmission in MCH neurons.

In Chapter 2, we assess the validity of our animal model in both males and females and in diverse physiological states. We demonstrate that in commercially available *Pmch*-Cre mice, there is a dissociation between *Pmch* mRNA and Cre-induced reporter gene expression in late lactation and concluded that we required a new mouse model for our purposes (Beekly at al., *Frontiers in Neuroanatomy*, 2020).

In Chapter 3, we describe the generation of a new *Pmch*-iCre knockin mouse using CRISPR/Cas9 technology. Our new animal resolves the issues of dissociated *Pmch* and Cre expression described in Chapter 2 and expresses iCre-induced GFP expression in the preoptic area during lactation. This chapter will be combined with Chapter 5 in preparation for submission to *Journal of Neuroscience* for publication.

Chapter 4 is a comprehensive review of the literature on classical neurotransmission from MCH neurons which includes our own analysis of several existing RNA-seq datasets. The purpose of this review was to gain a better understanding of the factors which might affect neurochemical identity and whether classical neurotransmitter content of MCH neurons could be context-specific. We conclude that most MCH neurons in adult mice are primarily glutamatergic, but there may be contexts in which MCH neurons release GABA. (Beekly at al., *Frontiers in Neuroendocrinology*, resubmitted with revisions).

In Chapter 5, based on our conclusions in Chapter 4, we investigate the metabolic and reproductive effects of deleting VGLUT2 from MCH neurons in male and female mice. We generated *Pmch*$^{\Delta VGLUT2}$ mice and evaluated numerous metabolic and reproductive variables. We report sex-dependent effects of VGLUT2 deletion in MCH neurons on spontaneous motor activity, glucose handling, pubertal timing, and reproductive efficiency. The finding that males and females exhibited different phenotypes when VGLUT2 was deleted from MCH neurons supported our theory that MCH neurons may be modulated by gonadal steroids.

Thus, in Chapter 6 we seek out other key transcripts in MCH neurons which could explain how MCH neurons respond to gonadal hormones. We determined that a subset of MCH neurons in the PFx expresses the neurokinin-B receptor (NKB; NK3R), and furthermore that estrogen-sensitive kisspeptin-neurokinin B-dynorphin (KNDy) neurons of the arcuate project to regions where MCH neurons are located. We proposed that ARH NKB inputs to PFx MCH/NK3R neurons modulate sleep in a sex-steroid dependent manner. To test this hypothesis, we expressed channelrhodopsin in KNDy neurons, optogenetically stimulated KNDy neuron terminals in the PFx, and observed changes to the EEG as well as spontaneous activity and food and water intake. While male mice and female mice under low estradiol conditions were largely unresponsive, females supplemented with exogenous estradiol exhibited reduced REM and NREM sleep time and increased wake time during the dark phase. Our findings reveal a novel potential estradiol-dependent role for the KNDy-MCH neuron circuit in the integration of gonadal steroids and sleep in female mice.

Finally, Chapter 7 will comprise the integration of the findings of the preceding chapters and a discussion of the strengths and weaknesses of our studies. It will situate what we have learned about the MCH system in the broader context of the MCH field and outline questions and future experiments for the continuation of this work.

References

1. Medicine, P.C.o.t.A.S.f.R., *Definitions of infertility and recurrent pregnancy loss: a committee opinion.* Fertility and Sterility, 2012. **99**(1): p. 63.
2. *Bragdon vs. Abbott*, in *U.S. Case Law*. 1998, Supreme Court of the United States.
3. Silveira, M.A., et al., *GnRH Neuron Activity and Pituitary Response in Estradiol-Induced vs Proestrous Luteinizing Hormone Surges in Female Mice.* Endocrinology, 2017. **158**(2): p. 356-366.

4. Research, G.V., *In-Vitro Fertilization (IVF) Market Size, Share & Trends Analysis Report By Type, By Instrument (Disposable Devices, Culture Media, Capital Equipment), By End Use, By Region, And Segment Forecasts, 2019 - 2026*. 2019.
5. Pories, W.J., et al., *Who would have thought it? An operation proves to be the most effective therapy for adult-onset diabetes mellitus.* Ann Surg, 1995. **222**(3): p. 339-50; discussion 350-2.
6. Escobar-Morreale, H.c.F., et al., *The Polycystic Ovary Syndrome Associated with Morbid Obesity May Resolve after Weight Loss Induced by Bariatric Surgery.* The Journal of Clinical Endocrinology & Metabolism, 2005. **90**(12): p. 6364-6369.
7. Tarín, J.J., et al., *Infertility etiologies are genetically and clinically linked with other diseases in single meta-diseases.* Reproductive Biology and Endocrinology, 2015. **13**(1): p. 31.
8. Berg, B.J. and J.F. Wilson, *Psychiatric morbidity in the infertile population: a reconceptualization.* Fertil Steril, 1990. **53**(4): p. 654-61.
9. Mahoney, M.M., *Shift work, jet lag, and female reproduction.* Int J Endocrinol, 2010. **2010**: p. 813764.
10. Stocker, L.J., et al., *Influence of shift work on early reproductive outcomes: a systematic review and meta-analysis.* Obstet Gynecol, 2014. **124**(1): p. 99-110.
11. Mosko, S.S., E. Lewis, and J.F. Sassin, *Impaired sexual maturation associated with sleep apnea syndrome during puberty: a case study.* Sleep, 1980. **3**(1): p. 13-22.
12. Chen, Y.H., et al., *Obstructive sleep apnea and the risk of adverse pregnancy outcomes.* Am J Obstet Gynecol, 2012. **206**(2): p. 136.e1-5.
13. Poli, F., et al., *High prevalence of precocious puberty and obesity in childhood narcolepsy with cataplexy.* Sleep, 2013. **36**(2): p. 175-81.
14. Shaw, N.D., et al., *Obstructive sleep apnea (OSA) in preadolescent girls is associated with delayed breast development compared to girls without OSA.* J Clin Sleep Med, 2013. **9**(8): p. 813-8.
15. Kapen, S., et al., *Effect of Sleep-Wake Cycle Reversal on Luteinizing Hormone Secretory Pattern in Puberty.* 1974. **39**: p. 293-9.
16. Apter, D., et al., *Gonadotropin-releasing hormone pulse generator activity during pubertal transition in girls : pulsatile and diurnal patterns of circulating gonadotropins.* Journal of Clinical Endocrinology and Metabolism, 1993 **76**(4): p. 940-949.
17. Dunkel, L., et al., *Developmental changes in 24-hour profiles of luteinizing hormone and follicle-stimulating hormone from prepuberty to midstages of puberty in boys.* 1992. **74**: p. 890-7.
18. Landy, H., et al., *Sleep Modulation of Neuroendocrine Function: Developmental Changes in Gonadotropin-Releasing Hormone Secretion during Sexual Maturation.* 1990. **28**: p. 213-7.
19. Mitamura, R., et al., *Diurnal Rhythms of Luteinizing Hormone, Follicle-Stimulating Hormone, and Testosterone Secretion before the Onset of Male Puberty 1.* 1999. **84**: p. 29-37.
20. E. Oerter, et al., *Gonadotropin Secretory Dynamics During Puberty in Normal Girls and Boys.* 1990. **71**: p. 1251-8.
21. Penny, R., N. O. Olambiwonnu, and S. D. Frasier, *Episodic fluctuations of serum gonadotropins in pre and post-pubertal girls and boys.* 1977. **45**: p. 307-11.

22. Boyar, R., et al., *Synchronization of Augmented Luteinizing Hormone Secretion with Sleep during Puberty.* 1972. **287**: p. 582-6.
23. R. McCartney, C., *Maturation of Sleep–Wake Gonadotrophin-Releasing Hormone Secretion Across Puberty in Girls: Potential Mechanisms and Relevance to the Pathogenesis of Polycystic Ovary Syndrome.* 2010. **22**: p. 701-9.
24. Shaw, N., et al., *Insights into Puberty: The Relationship between Sleep Stages and Pulsatile LH Secretion.* 2012. **97**.
25. Bittencourt, J., et al., *The melanin-concentrating hormone system of the rat brain: an immuno-and hybridization histochemical characterization.* Journal of Comparative Neurology, 1992. **319**(2): p. 218-245.
26. Sita, L., C. Elias, and J. Bittencourt, *Connectivity pattern suggests that incerto-hypothalamic area belongs to the medial hypothalamic system.* 2007. **148**: p. 949-69.
27. Elias, C.F., et al., *Chemically defined projections linking the mediobasal hypothalamus and the lateral hypothalamic area.* J Comp Neurol, 1998. **402**(4): p. 442-59.
28. Hassani, O., M. Gee Lee, and B. Jones, *Melanin-concentrating hormone neurons discharge in a reciprocal manner to orexin neurons across the sleep-wake cycle.* 2009. **106**: p. 2418-2422.
29. Verret, L., et al., *A role of melanin-concentrating hormone producing neurons in the central regulation of paradoxical sleep.* 2003. **4**: p. 19.
30. Jego, S., et al., *Optogenetic identification of a rapid eye movement sleep modulatory circuit in the hypothalamus.* 2013. **16**.
31. Konadhode, R., et al., *Optogenetic Stimulation of MCH Neurons Increases Sleep.* 2013. **33**: p. 10257-63.
32. Tsunematsu, T., et al., *Optogenetic Manipulation of Activity and Temporally Controlled Cell-Specific Ablation Reveal a Role for MCH Neurons in Sleep/Wake Regulation.* 2014. **34**: p. 6896-909.
33. Blanco-Centurion, C., et al., *Dynamic Network Activation of Hypothalamic MCH Neurons in REM Sleep and Exploratory Behavior.* The Journal of Neuroscience, 2019: p. 0305-19.
34. Attademo, A.M., et al., *Neuropeptide Glutamic Acid-Isoleucine May Induce Luteinizing Hormone Secretion via Multiple Pathways.* Neuroendocrinology, 2006. **83**(5-6): p. 313-24.
35. G.P. Gallardo, M., S. R. Chiocchio, and J. H. Tramezzani, *Changes of melanin-concentrating hormone related to LHRH release in the median eminence of rats.* 2005. **1030**: p. 152-8.
36. Murray, J., et al., *Evidence for a Stimulatory Action of Melanin-Concentrating Hormone on Luteinising Hormone Release Involving MCH1 and Melanocortin-5 Receptors.* 2006. **18**: p. 157-67.
37. S Williamson-Hughes, P., K. Grove, and M.S. Smith, *Melanin concentrating hormone (MCH): A novel neural pathway for regulation of GnRH neurons.* 2005. **1041**: p. 117-24.
38. Skrapits, K., et al., *Lateral hypothalamic orexin and melanin-concentrating hormone neurons provide direct input to gonadotropin-releasing hormone neurons in the human.* 2015. **9**: p. 348.
39. Gonzalez, M., B. Baker, and C. Wilson, *Stimulatory effect of melanin-concentrating hormone on luteinising hormone release.* Neuroendocrinology, 1997. **66**: p. 254-262.

40. MacKenzie, F., M. James, and C. Wilson, *Changes in dopamine activity in the zona incerta (ZI) over the rat oestrous cycle and the effect of lesions of the ZI on cyclicity: further evidence that the incerto-hypothalamic tract has a stimulatory role in the control of LH release.* Brain Research, 1988. **444**: p. 75-78.
41. Croizier, S., et al., *Development of posterior hypothalamic neurons enlightens a switch in the prosencephalic basic plan.* PLoS One, 2011. **6**(12): p. e28574.
42. Cvetkovic, V., et al., *Characterization of subpopulations of neurons producing melanin-concentrating hormone in the rat ventral diencephalon.* J Neurochem, 2004. **91**(4): p. 911-9.
43. Koehl, M., S.E. Battle, and F.W. Turek, *Sleep in female mice: a strain comparison across the estrous cycle.* Sleep, 2003. **26**(3): p. 267-72.
44. Nahon, J.L., et al., *The rat melanin-concentrating hormone messenger ribonucleic acid encodes multiple putative neuropeptides coexpressed in the dorsolateral hypothalamus.* Endocrinology, 1989. **125**(4): p. 2056-65.
45. Vitale, R.M., et al., *Conformational features of human melanin-concentrating hormone: an NMR and computational analysis.* Chembiochem, 2003. **4**(1): p. 73-81.
46. Breton, C., et al., *Structure and regulation of the mouse melanin-concentrating hormone mRNA and gene.* Mol Cell Neurosci, 1993. **4**(3): p. 271-84.
47. Arrigoni, E., M.J.S. Chee, and P.M. Fuller, *To eat or to sleep: That is a lateral hypothalamic question.* Neuropharmacology, 2019. **154**: p. 34-49.
48. Joseph, D.N. and S. Whirledge, *Stress and the HPA Axis: Balancing Homeostasis and Fertility.* Int J Mol Sci, 2017. **18**(10).
49. Oyola, M.G. and R.J. Handa, *Hypothalamic-pituitary-adrenal and hypothalamic-pituitary-gonadal axes: sex differences in regulation of stress responsivity.* Stress, 2017. **20**(5): p. 476-494.
50. Kaprara, A. and I.T. Huhtaniemi, *The hypothalamus-pituitary-gonad axis: Tales of mice and men.* Metabolism, 2018. **86**: p. 3-17.
51. Yamashita, T. and A. Yamanaka, *Lateral hypothalamic circuits for sleep-wake control.* Curr Opin Neurobiol, 2017. **44**: p. 94-100.
52. Kumar, S. and S.B. Hedges, *A molecular timescale for vertebrate evolution.* Nature, 1998. **392**(6679): p. 917-20.
53. al-Yousuf, S. and N. Mizuno, *Electron microscopic identification of axons containing melanin-concentrating hormone in the lamprey, Lampetra fluviatilis L.* Neurosci Lett, 1991. **128**(2): p. 249-52.
54. Bird, D.J., et al., *The distribution of melanin-concentrating hormone in the lamprey brain.* Gen Comp Endocrinol, 2001. **121**(3): p. 232-41.
55. Kawauchi, H., et al., *Characterization of melanin-concentrating hormone in chum salmon pituitaries.* Nature, 1983(305): p. 321–323.
56. Diniz, G.B. and J.C. Bittencourt, *The Melanin-Concentrating Hormone (MCH) System: A Tale of Two Peptides.* Front Neurosci, 2019. **13**: p. 1280.
57. Nahon, J.-L., *The melanin-concentrating hormone: from the peptide to the gene.* Critical reviews in neurobiology, 1994. **8**(4): p. 221-262.
58. Toumaniantz, G., J.C. Bittencourt, and J.L. Nahon, *The rat melanin-concentrating hormone gene encodes an additional putative protein in a different reading frame.* Endocrinology, 1996. **137**(10): p. 4518-21.

59. Borsu, L., F. Presse, and J.L. Nahon, *The AROM gene, spliced mRNAs encoding new DNA/RNA-binding proteins are transcribed from the opposite strand of the melanin-concentrating hormone gene in mammals.* J Biol Chem, 2000. **275**(51): p. 40576-87.
60. Moldovan, G.L., et al., *Inhibition of homologous recombination by the PCNA-interacting protein PARI.* Mol Cell, 2012. **45**(1): p. 75-86.
61. Bittencourt, J. and M.E. Celis, *Anatomy, function and regulation of neuropeptide EI (NEI).* Peptides, 2008. **29**(8): p. 1441-50.
62. Bittencourt, J.C., *Anatomical organization of the melanin-concentrating hormone peptide family in the mammalian brain.* Gen Comp Endocrinol, 2011. **172**(2): p. 185-97.
63. Courseaux, A. and J.L. Nahon, *Birth of two chimeric genes in the Hominidae lineage.* Science, 2001. **291**(5507): p. 1293-7.
64. Bittencourt, J.C., et al., *The distribution of melanin-concentrating hormone in the monkey brain (Cebus apella).* Brain Res, 1998. **804**(1): p. 140-3.
65. Bittencourt, J.C. and C.F. Elias, *Melanin-concentrating hormone and neuropeptide EI projections from the lateral hypothalamic area and zona incerta to the medial septal nucleus and spinal cord: a study using multiple neuronal tracers.* Brain Res, 1998. **805**(1-2): p. 1-19.
66. Mickelsen, L.E., et al., *Single-cell transcriptomic analysis of the lateral hypothalamic area reveals molecularly distinct populations of inhibitory and excitatory neurons.* Nat Neurosci, 2019. **22**(4): p. 642-656.
67. Zhao, E., H. Hu, and V.L. Trudeau, *Secretoneurin as a hormone regulator in the pituitary.* Regul Pept, 2010. **165**(1): p. 117-22.
68. Troger, J., et al., *Granin-derived peptides.* Prog Neurobiol, 2017. **154**: p. 37-61.
69. Trudeau, V.L., *Neuroendocrine Control of Reproduction in Teleost Fish: Concepts and Controversies.* Annu Rev Anim Biosci, 2022. **10**: p. 107-130.
70. Ahmadian-Moghadam, H., M.S. Sadat-Shirazi, and M.R. Zarrindast, *Cocaine- and amphetamine-regulated transcript (CART): A multifaceted neuropeptide.* Peptides, 2018. **110**: p. 56-77.
71. Mickelsen, L.E., et al., *Neurochemical Heterogeneity Among Lateral Hypothalamic Hypocretin/Orexin and Melanin-Concentrating Hormone Neurons Identified Through Single-Cell Gene Expression Analysis.* eNeuro, 2017. **4**(5).
72. Nectow, A.R., et al., *Rapid Molecular Profiling of Defined Cell Types Using Viral TRAP.* Cell Rep, 2017. **19**(3): p. 655-667.
73. Rose, C.R., et al., *Molecular and cellular physiology of sodium-dependent glutamate transporters.* Brain Res Bull, 2018. **136**: p. 3-16.
74. Blanco-Centurion, C., et al., *VGAT and VGLUT2 expression in MCH and orexin neurons in double transgenic reporter mice.* IBRO Rep, 2018. **4**: p. 44-49.
75. Baker, B.I., *Melanin-concentrating hormone: a general vertebrate neuropeptide.* Int Rev Cytol, 1991. **126**: p. 1-47.
76. Diniz, G., et al., *Melanin-concentrating hormone peptidergic system: Comparative morphology between muroid species.* The Journal of Comparative Neurology, 2019. **527**(18): p. 2973-3001.
77. Nozaki, M., T. Tsukahara, and H. Kobayashi, *An immunocytochemical study on the distribution of neuropeptides in the brain of certain species of fish.* BIOMEDICAL RESEARCH-TOKYO, 1983. **4**: p. 135-143.

78. Röhlich, P. and B. Vigh, *Electron microscopy of the paraventricular organ in the sparrow (Passer domesticus).* Zeitschrift für Zellforschung und Mikroskopische Anatomie, 1967. **80**(2): p. 229-245.
79. Meurling, P. and E.M. Rodríguez, *The paraventricular and posterior recess organs of elasmobranchs: a system of cerebrospinal fluid-contacting neurons containing immunoreactive serotonin and somatostatin.* Cell and tissue research, 1990. **259**: p. 463-473.
80. Stephenson-Jones, M., et al., *Evolutionary conservation of the habenular nuclei and their circuitry controlling the dopamine and 5-hydroxytryptophan (5-HT) systems.* Proc Natl Acad Sci U S A, 2012. **109**(3): p. E164-73.
81. Baker, B.I. and D.J. Bird, *Neuronal organization of the melanin-concentrating hormone system in primitive actinopterygians: evolutionary changes leading to teleosts.* J Comp Neurol, 2002. **442**(2): p. 99-114.
82. Croizier, S., et al., *The vertebrate diencephalic MCH system: a versatile neuronal population in an evolving brain.* Front Neuroendocrinol, 2013. **34**(2): p. 65-87.
83. Naito, N., et al., *Immunocytochemical identification of melanin-concentrating hormone in the brain and pituitary gland of the teleost fishes Oncorhynchus keta and Salmo gairdneri.* Cell and tissue research, 1985. **242**: p. 41-48.
84. Baker, B., et al., *Cloning and expression of melanin-concentrating hormone genes in the rainbow trout brain.* Neuroendocrinology, 1995. **61**(1): p. 67-76.
85. Suzuki, M., et al., *Influence of environmental colour and diurnal phase on MCH gene expression in the trout.* Journal of neuroendocrinology, 1995. **7**(4): p. 319-328.
86. Vallarino, M., et al., *Melanin-concentrating hormone system in the brain of the lungfish Protopterus annectens.* J Comp Neurol, 1998. **390**(1): p. 41-51.
87. Cardot, J., D. Fellmann, and C. Bugnon, *Melanin-concentrating hormone-producing neurons in reptiles.* Gen Comp Endocrinol, 1994. **94**(1): p. 23-32.
88. Swanson, L.W., *The hypothalamus*, in *The Handbook of Chemical Neuroanatomy: Integrated systems of the CNS*, A. Bjorklund, T. Hokfelt, and L.W. Swanson, Editors. 1987, Elsevier: Amsterdam. p. 1-124.
89. Rondini, T.A., et al., *Melanin-concentrating hormone is expressed in the laterodorsal tegmental nucleus only in female rats.* Brain Res Bull, 2007. **74**(1-3): p. 21-8.
90. Rondini, T.A., et al., *Chemical identity and connections of medial preoptic area neurons expressing melanin-concentrating hormone during lactation.* J Chem Neuroanat, 2010. **39**(1): p. 51-62.
91. Knollema, S., et al., *Novel hypothalamic and preoptic sites of prepro-melanin-concentrating hormone messenger ribonucleic Acid and Peptide expression in lactating rats.* J Neuroendocrinol, 1992. **4**(6): p. 709-17.
92. Elias, C.F., et al., *Characterization of CART neurons in the rat and human hypothalamus.* J Comp Neurol, 2001. **432**(1): p. 1-19.
93. Broberger, C., *Hypothalamic cocaine-and amphetamine-regulated transcript (CART) neurons: histochemical relationship to thyrotropin-releasing hormone, melanin-concentrating hormone, orexin/hypocretin and neuropeptide Y.* Brain research, 1999. **848**(1-2): p. 101-113.
94. Beekly, B.G., et al., *Dissociated Pmch and Cre Expression in Lactating Pmch-Cre BAC Transgenic Mice.* Frontiers in Neuroanatomy, 2020. **14**(60).

95. Tillet, Y., M. Batailler, and D. Fellmann, *Distribution of melanin-concentrating hormone (MCH)-like immunoreactivity in neurons of the diencephalon of sheep.* J Chem Neuroanat, 1996. **12**(2): p. 135-45.
96. Chaillou, E., et al., *Sensitivity of Galanin-and Melanin-Concentrating Hormone-Containing Neurones to Nutritional Status: An Immunohistochemical Study in the Ovariectomized Ewe.* Journal of neuroendocrinology, 2003. **15**(5): p. 459-467.
97. Chometton, S., et al., *Different distributions of preproMCH and hypocretin/orexin in the forebrain of the pig (Sus scrofa domesticus).* Journal of Chemical Neuroanatomy, 2014. **61**: p. 72-82.
98. Thannickal, T.C., Y.-Y. Lai, and J.M. Siegel, *Hypocretin (orexin) cell loss in Parkinson's disease.* Brain, 2007. **130**(6): p. 1586-1595.
99. Aziz, A., et al., *Hypocretin and melanin-concentrating hormone in patients with Huntington disease.* Brain pathology, 2008. **18**(4): p. 474-483.
100. Krolewski, D.M., et al., *Expression patterns of corticotropin-releasing factor, arginine vasopressin, histidine decarboxylase, melanin-concentrating hormone, and orexin genes in the human hypothalamus.* Journal of Comparative Neurology, 2010. **518**(22): p. 4591-4611.
101. Nieuwenhuys, R., L.M. Geeraedts, and J.G. Veening, *The medial forebrain bundle of the rat. I. General introduction.* J Comp Neurol, 1982. **206**(1): p. 49-81.
102. Lord, M.N., et al., *Melanin-concentrating hormone and food intake control: Sites of action, peptide interactions, and appetition.* Peptides, 2021. **137**: p. 170476.
103. Presse, F., et al., *The melanin-concentrating hormone receptors: neuronal and non-neuronal functions.* Int J Obes Suppl, 2014. **4**(Suppl 1): p. S31-6.
104. Brischoux, F., et al., *Time of genesis determines projection and neurokinin-3 expression patterns of diencephalic neurons containing melanin-concentrating hormone.* Eur J Neurosci, 2002. **16**(9): p. 1672-80.
105. Hill, J., et al., *Molecular cloning and functional characterization of MCH2, a novel human MCH receptor.* J Biol Chem, 2001. **276**(23): p. 20125-9.
106. Sailer, A.W., et al., *Identification and characterization of a second melanin-concentrating hormone receptor, MCH-2R.* Proc Natl Acad Sci U S A, 2001. **98**(13): p. 7564-9.
107. Wang, S., et al., *Identification and pharmacological characterization of a novel human melanin-concentrating hormone receptor, mch-r2.* J Biol Chem, 2001. **276**(37): p. 34664-70.
108. Tan, C.P., et al., *Melanin-concentrating hormone receptor subtypes 1 and 2: species-specific gene expression.* Genomics, 2002. **79**(6): p. 785-92.
109. Logan, D.W., et al., *The structure and evolution of the melanocortin and MCH receptors in fish and mammals.* Genomics, 2003. **81**(2): p. 184-91.
110. An, S., et al., *Identification and characterization of a melanin-concentrating hormone receptor.* Proc Natl Acad Sci U S A, 2001. **98**(13): p. 7576-81.
111. Bächner, D., et al., *Identification of melanin concentrating hormone (MCH) as the natural ligand for the orphan somatostatin-like receptor 1 (SLC-1).* FEBS Lett, 1999. **457**(3): p. 522-4.
112. Chambers, J., et al., *Melanin-concentrating hormone is the cognate ligand for the orphan G-protein-coupled receptor SLC-1.* Nature, 1999. **400**(6741): p. 261-5.

113. Lembo, P.M., et al., *The receptor for the orexigenic peptide melanin-concentrating hormone is a G-protein-coupled receptor.* Nat Cell Biol, 1999. **1**(5): p. 267-71.
114. Saito, Y., *[Searching for neurotransmitters as cognate ligands of orphan G protein-coupled receptor: finding receptor for melanin-concentrating hormone].* Nihon Shinkei Seishin Yakurigaku Zasshi, 2001. **21**(3): p. 77-82.
115. Saito, Y., et al., *Molecular characterization of the melanin-concentrating-hormone receptor.* Nature, 1999. **400**(6741): p. 265-9.
116. Shimomura, Y., et al., *Isolation and identification of melanin-concentrating hormone as the endogenous ligand of the SLC-1 receptor.* Biochem Biophys Res Commun, 1999. **261**(3): p. 622-6.
117. Kolakowski, L.F., et al., *Characterization of a human gene related to genes encoding somatostatin receptors.* FEBS Lett, 1996. **398**(2-3): p. 253-8.
118. Lakaye, B., et al., *Cloning of the rat brain cDNA encoding for the SLC-1 G protein-coupled receptor reveals the presence of an intron in the gene.* Biochim Biophys Acta, 1998. **1401**(2): p. 216-20.
119. Aizaki, Y., et al., *Distinct roles of the DRY motif in rat melanin-concentrating hormone receptor 1 in signaling control.* Peptides, 2009. **30**(5): p. 974-981.
120. Balber, T., et al., *Radiopharmaceutical Evidence for MCHR1 Binding Sites in Murine Brown Adipocytes.* Front Endocrinol (Lausanne), 2019. **10**: p. 324.
121. Hawes, B.E., et al., *The melanin-concentrating hormone receptor couples to multiple G proteins to activate diverse intracellular signaling pathways.* Endocrinology, 2000. **141**(12): p. 4524-32.
122. Chung, S., Y. Saito, and O. Civelli, *MCH receptors/gene structure-in vivo expression.* Peptides, 2009. **30**(11): p. 1985-1989.
123. Eberle, A.N., et al., *Expression and characterization of melanin-concentrating hormone receptors on mammalian cell lines.* Peptides, 2004. **25**(10): p. 1585-95.
124. Sarret, P. and A. Beaudet, *Neurotensin receptors in the central nervous system. Handbook of chemical neuroanatomy. Vol. 20. Peptide receptors, Part II*. 2002, Amsterdam: Elsevier. p.
125. Gao, X.B., *Electrophysiological effects of MCH on neurons in the hypothalamus.* Peptides, 2009. **30**(11): p. 2025-30.
126. Murdoch, H., et al., *Periplakin interferes with G protein activation by the melanin-concentrating hormone receptor-1 by binding to the proximal segment of the receptor C-terminal tail.* J Biol Chem, 2005. **280**(9): p. 8208-20.
127. Francke, F., et al., *Interaction of neurochondrin with the melanin-concentrating hormone receptor 1 interferes with G protein-coupled signal transduction but not agonist-mediated internalization.* J Biol Chem, 2006. **281**(43): p. 32496-507.
128. Chan, L.F., et al., *MRAP and MRAP2 are bidirectional regulators of the melanocortin receptor family.* Proc Natl Acad Sci U S A, 2009. **106**(15): p. 6146-51.
129. Chaly, A.L., et al., *The Melanocortin Receptor Accessory Protein 2 promotes food intake through inhibition of the Prokineticin Receptor-1.* Elife, 2016. **5**.
130. Rouault, A.A.J., A.A. Lee, and J.A. Sebag, *Regions of MRAP2 required for the inhibition of orexin and prokineticin receptor signaling.* Biochim Biophys Acta Mol Cell Res, 2017. **1864**(12): p. 2322-2329.
131. Srisai, D., et al., *MRAP2 regulates ghrelin receptor signaling and hunger sensing.* Nat Commun, 2017. **8**(1): p. 713.

132. Asai, M., et al., *Loss of function of the melanocortin 2 receptor accessory protein 2 is associated with mammalian obesity.* Science, 2013. **341**(6143): p. 275-8.
133. Wang, M., et al., *Determination of the Interaction and Pharmacological Modulation of MCHR1 Signaling by the C-Terminus of MRAP2 Protein.* Front Endocrinol (Lausanne), 2022. **13**: p. 848728.
134. Hanada, R., et al., *Differential regulation of melanin-concentrating hormone and orexin genes in the agouti-related protein/melanocortin-4 receptor system.* Biochem Biophys Res Commun, 2000. **268**(1): p. 88-91.
135. Mo, Q., et al., *Genome-wide analysis of DHEA- and DHT-induced gene expression in mouse hypothalamus and hippocampus.* J Steroid Biochem Mol Biol, 2009. **114**(3-5): p. 135-43.
136. Santollo, J. and L.A. Eckel, *Oestradiol decreases melanin-concentrating hormone (MCH) and MCH receptor expression in the hypothalamus of female rats.* J Neuroendocrinol, 2013. **25**(6): p. 570-9.
137. Duarte, J.C.G., J.G.P. Ferreira, and J.C. Bittencourt, *Melanin-concentrating hormone regulation by estradiol and progesterone in the incerto-hypothalamic area.* Peptides, 2023. **163**: p. 170975.
138. Murray, J.F., et al., *The influence of gonadal steroids on pre-pro melanin-concentrating hormone mRNA in female rats.* J Neuroendocrinol, 2000. **12**(1): p. 53-9.
139. Xu, J., et al., *Characterization and expression of melanin-concentrating hormone (MCH) in common carp (Cyprinus carpio) during fasting and reproductive cycle.* Fish Physiol Biochem, 2019. **45**(2): p. 805-817.
140. Simon, Á., et al., *Feeding state and age dependent changes in melanin-concentrating hormone expression in the hypothalamus of broiler chickens.* Acta Biochim Pol, 2018. **65**(2): p. 251-258.
141. Piórkowska, K., et al., *Transcriptomic Changes in Broiler Chicken Hypothalamus during Growth and Development.* Int J Genomics, 2018. **2018**: p. 6049469.
142. Lin, H., et al., *In Utero Exposure to Diethylhexyl Phthalate Affects Rat Brain Development: A Behavioral and Genomic Approach.* Int J Environ Res Public Health, 2015. **12**(11): p. 13696-710.
143. García-Fuster, M.J., et al., *The melanin-concentrating hormone (MCH) system in an animal model of depression-like behavior.* Eur Neuropsychopharmacol, 2012. **22**(8): p. 607-13.
144. Kim, Y.K., et al., *Acupuncture Alleviates Levodopa-Induced Dyskinesia via Melanin-Concentrating Hormone in Pitx3-Deficient aphakia and 6-Hydroxydopamine-Lesioned Mice.* Mol Neurobiol, 2019. **56**(4): p. 2408-2423.
145. Qu, D., et al., *A role for melanin-concentrating hormone in the central regulation of feeding behaviour.* Nature, 1996. **380**(6571): p. 243-7.
146. Mondal, M.S., M. Nakazato, and S. Matsukura, *Characterization of orexins (hypocretins) and melanin-concentrating hormone in genetically obese mice.* Regul Pept, 2002. **104**(1-3): p. 21-5.
147. Dias Abdo Agamme, A.L., et al., *MCH levels in the CSF, brain preproMCH and MCHR1 gene expression during paradoxical sleep deprivation, sleep rebound and chronic sleep restriction.* Peptides, 2015. **74**: p. 9-15.

148. Li, N., E. Nattie, and A. Li, *The role of melanin concentrating hormone (MCH) in the central chemoreflex: a knockdown study by siRNA in the lateral hypothalamus in rats.* PLoS One, 2014. **9**(8): p. e103585.
149. Takakura, A.C., *A new neuromodulatory mechanism in the lateral hypothalamus regulating the hypercapnic ventilatory response in conscious rats.* Exp Physiol, 2022. **107**(11): p. 1212-1213.
150. Badami, V.M., et al., *Distribution of hypothalamic neurons with orexin (hypocretin) or melanin concentrating hormone (MCH) immunoreactivity and multisynaptic connections with diaphragm motoneurons.* Brain Res, 2010. **1323**: p. 119-26.
151. Benarroch, E.E., *Control of the cardiovascular and respiratory systems during sleep.* Auton Neurosci, 2019. **218**: p. 54-63.
152. Adams, A.C., et al., *Ablation of the hypothalamic neuropeptide melanin concentrating hormone is associated with behavioral abnormalities that reflect impaired olfactory integration.* Behav Brain Res, 2011. **224**(1): p. 195-200.
153. Alachkar, A., et al., *Inactivation of the melanin concentrating hormone system impairs maternal behavior.* Eur Neuropsychopharmacol, 2016. **26**(11): p. 1826-1835.
154. Orikasa, C., *Neural Contributions of the Hypothalamus to Parental Behaviour.* Int J Mol Sci, 2021. **22**(13).
155. Alvisi, R.D., et al., *Suckling-induced Fos activation and melanin-concentrating hormone immunoreactivity during late lactation.* Life Sci, 2016. **148**: p. 241-6.
156. Monzón, M.E. and S.R. De Barioglio, *Response to novelty after i.c.v. injection of melanin-concentrating hormone (MCH) in rats.* Physiol Behav, 1999. **67**(5): p. 813-7.
157. Borowsky, B., et al., *Antidepressant, anxiolytic and anorectic effects of a melanin-concentrating hormone-1 receptor antagonist.* Nat Med, 2002. **8**(8): p. 825-30.
158. Chung, S., et al., *The melanin-concentrating hormone system modulates cocaine reward.* Proc Natl Acad Sci U S A, 2009. **106**(16): p. 6772-7.
159. Cippitelli, A., et al., *Suppression of alcohol self-administration and reinstatement of alcohol seeking by melanin-concentrating hormone receptor 1 (MCH1-R) antagonism in Wistar rats.* Psychopharmacology (Berl), 2010. **211**(4): p. 367-75.
160. Adamantidis, A. and L. de Lecea, *A role for Melanin-Concentrating Hormone in learning and memory.* Peptides, 2009. **30**(11): p. 2066-70.
161. Varas, M., et al., *Melanin concentrating hormone increase hippocampal synaptic transmission in the rat.* Peptides, 2002. **23**(1): p. 151-5.
162. Yoo, E.S., J. Yu, and J.W. Sohn, *Neuroendocrine control of appetite and metabolism.* Exp Mol Med, 2021. **53**(4): p. 505-516.
163. Valassi, E., M. Scacchi, and F. Cavagnini, *Neuroendocrine control of food intake.* Nutr Metab Cardiovasc Dis, 2008. **18**(2): p. 158-68.
164. Hiller-Sturmhöfel, S. and A. Bartke, *The endocrine system: an overview.* Alcohol Health Res World, 1998. **22**(3): p. 153-64.
165. Nieuwenhuizen, A.G. and F. Rutters, *The hypothalamic-pituitary-adrenal-axis in the regulation of energy balance.* Physiol Behav, 2008. **94**(2): p. 169-77.
166. Diéguez, C., et al., *Hypothalamic control of lipid metabolism: focus on leptin, ghrelin and melanocortins.* Neuroendocrinology, 2011. **94**(1): p. 1-11.
167. Ludwig, D.S., et al., *Melanin-concentrating hormone overexpression in transgenic mice leads to obesity and insulin resistance.* J Clin Invest, 2001. **107**(3): p. 379-86.

168. Presse, F., et al., *Melanin-concentrating hormone is a potent anorectic peptide regulated by food-deprivation and glucopenia in the rat.* Neuroscience, 1996. **71**(3): p. 735-45.
169. Rossi, M., et al., *Melanin-concentrating hormone acutely stimulates feeding, but chronic administration has no effect on body weight.* Endocrinology, 1997. **138**(1): p. 351-5.
170. Ito, M., et al., *Characterization of MCH-mediated obesity in mice.* Am J Physiol Endocrinol Metab, 2003. **284**(5): p. E940-5.
171. Gomori, A., et al., *Chronic intracerebroventricular infusion of MCH causes obesity in mice. Melanin-concentrating hormone.* Am J Physiol Endocrinol Metab, 2003. **284**(3): p. E583-8.
172. Mashiko, S., et al., *Antiobesity effect of a melanin-concentrating hormone 1 receptor antagonist in diet-induced obese mice.* Endocrinology, 2005. **146**(7): p. 3080-6.
173. Shearman, L.P., et al., *Chronic MCH-1 receptor modulation alters appetite, body weight and adiposity in rats.* Eur J Pharmacol, 2003. **475**(1-3): p. 37-47.
174. Rattenborg, N.C. and G. Ungurean, *The evolution and diversification of sleep.* Trends Ecol Evol, 2023. **38**(2): p. 156-170.
175. Joiner, W.J., *Unraveling the Evolutionary Determinants of Sleep.* Curr Biol, 2016. **26**(20): p. R1073-R1087.
176. Saper, C.B., et al., *Sleep state switching.* Neuron, 2010. **68**(6): p. 1023-42.
177. Steriade, M., D.A. McCormick, and T.J. Sejnowski, *Thalamocortical oscillations in the sleeping and aroused brain.* Science, 1993. **262**(5134): p. 679-85.
178. Saper, C.B. and P.M. Fuller, *Wake-sleep circuitry: an overview.* Curr Opin Neurobiol, 2017. **44**: p. 186-192.
179. Moruzzi, G. and H.W. Magoun, *Brain stem reticular formation and activation of the EEG. 1949.* J Neuropsychiatry Clin Neurosci, 1995. **7**(2): p. 251-67.
180. Mondino, A., et al., *Glutamatergic Neurons in the Preoptic Hypothalamus Promote Wakefulness, Destabilize NREM Sleep, Suppress REM Sleep, and Regulate Cortical Dynamics.* J Neurosci, 2021. **41**(15): p. 3462-3478.
181. Holst, S.C. and H.P. Landolt, *Sleep-Wake Neurochemistry.* Sleep Med Clin, 2022. **17**(2): p. 151-160.
182. Alam, M.N., et al., *Adenosinergic modulation of rat basal forebrain neurons during sleep and waking: neuronal recording with microdialysis.* J Physiol, 1999. **521 Pt 3**: p. 679-90.
183. Lee, M.G., et al., *Cholinergic basal forebrain neurons burst with theta during waking and paradoxical sleep.* J Neurosci, 2005. **25**(17): p. 4365-9.
184. Takahashi, K., J.S. Lin, and K. Sakai, *Neuronal activity of histaminergic tuberomammillary neurons during wake-sleep states in the mouse.* J Neurosci, 2006. **26**(40): p. 10292-8.
185. Takahashi, K., et al., *Locus coeruleus neuronal activity during the sleep-waking cycle in mice.* Neuroscience, 2010. **169**(3): p. 1115-26.
186. Jacobs, B.L. and C.A. Fornal, *Activity of serotonergic neurons in behaving animals.* Neuropsychopharmacology, 1999. **21**(2 Suppl): p. 9S-15S.
187. Popa, D., et al., *Contribution of 5-HT2 receptor subtypes to sleep-wakefulness and respiratory control, and functional adaptations in knock-out mice lacking 5-HT2A receptors.* J Neurosci, 2005. **25**(49): p. 11231-8.
188. Steininger, T.L., et al., *Sleep-waking discharge of neurons in the posterior lateral hypothalamus of the albino rat.* Brain Res, 1999. **840**(1-2): p. 138-47.

189. Alam, M.N., et al., *Sleep-waking discharge patterns of neurons recorded in the rat perifornical lateral hypothalamic area.* J Physiol, 2002. **538**(Pt 2): p. 619-31.
190. Colwell, C.S., *Linking neural activity and molecular oscillations in the SCN.* Nat Rev Neurosci, 2011. **12**(10): p. 553-69.
191. Berson, D.M., F.A. Dunn, and M. Takao, *Phototransduction by retinal ganglion cells that set the circadian clock.* Science, 2002. **295**(5557): p. 1070-3.
192. Shen, Y.C., et al., *Roles of Neuropeptides in Sleep-Wake Regulation.* Int J Mol Sci, 2022. **23**(9).
193. Konadhode, R.R., D. Pelluru, and P.J. Shiromani, *Neurons containing orexin or melanin concentrating hormone reciprocally regulate wake and sleep.* Front Syst Neurosci, 2014. **8**: p. 244.
194. Murck, H., et al., *Galanin has REM-sleep deprivation-like effects on the sleep EEG in healthy young men.* J Psychiatr Res, 1999. **33**(3): p. 225-32.
195. Beranek, L., et al., *Central administration of the somatostatin analog octreotide induces captopril-insensitive sleep responses.* Am J Physiol, 1999. **277**(5): p. R1297-304.
196. Weikel, J.C., et al., *Ghrelin promotes slow-wave sleep in humans.* Am J Physiol Endocrinol Metab, 2003. **284**(2): p. E407-15.
197. Antonijevic, I.A., et al., *Neuropeptide Y promotes sleep and inhibits ACTH and cortisol release in young men.* Neuropharmacology, 2000. **39**(8): p. 1474-81.
198. Raymond, J.S., et al., *The influence of oxytocin-based interventions on sleep-wake and sleep-related behaviour and neurobiology: A systematic review of preclinical and clinical studies.* Neurosci Biobehav Rev, 2021. **131**: p. 1005-1026.
199. Verret, L., et al., *A role of melanin-concentrating hormone producing neurons in the central regulation of paradoxical sleep.* BMC Neurosci, 2003. **4**: p. 19.
200. Baker, F.C. and H.S. Driver, *Self-reported sleep across the menstrual cycle in young, healthy women.* J Psychosom Res, 2004. **56**(2): p. 239-43.
201. Baker, F.C. and H.S. Driver, *Circadian rhythms, sleep, and the menstrual cycle.* Sleep Med, 2007. **8**(6): p. 613-22.
202. Hrozanova, M., et al., *Sex differences in sleep and influence of the menstrual cycle on women's sleep in junior endurance athletes.* PLoS One, 2021. **16**(6): p. e0253376.
203. Boivin, D.B., et al., *Diurnal and circadian variation of sleep and alertness in men vs. naturally cycling women.* Proc Natl Acad Sci U S A, 2016. **113**(39): p. 10980-5.
204. Cain, S.W., et al., *Sex differences in phase angle of entrainment and melatonin amplitude in humans.* J Biol Rhythms, 2010. **25**(4): p. 288-96.
205. Lazar, A.S., et al., *Circadian period and the timing of melatonin onset in men and women: predictors of sleep during the weekend and in the laboratory.* J Sleep Res, 2013. **22**(2): p. 155-9.
206. Van Reen, E., et al., *Sex of college students moderates associations among bedtime, time in bed, and circadian phase angle.* J Biol Rhythms, 2013. **28**(6): p. 425-31.
207. Burgess, H.J. and C.I. Eastman, *The dim light melatonin onset following fixed and free sleep schedules.* J Sleep Res, 2005. **14**(3): p. 229-37.
208. Shechter, A., F. Varin, and D.B. Boivin, *Circadian variation of sleep during the follicular and luteal phases of the menstrual cycle.* Sleep, 2010. **33**(5): p. 647-56.
209. Shechter, A., et al., *Nocturnal polysomnographic sleep across the menstrual cycle in premenstrual dysphoric disorder.* Sleep Med, 2012. **13**(8): p. 1071-8.

210. Mong, J.A., et al., *Sleep, rhythms, and the endocrine brain: influence of sex and gonadal hormones.* J Neurosci, 2011. **31**(45): p. 16107-16.
211. Franco, P., et al., *Sleep during development: Sex and gender differences.* Sleep Med Rev, 2020. **51**: p. 101276.
212. Chaput, J.P., et al., *The role of insufficient sleep and circadian misalignment in obesity.* Nat Rev Endocrinol, 2023. **19**(2): p. 82-97.
213. Palagini, L., et al., *Sleep, insomnia and mental health.* J Sleep Res, 2022. **31**(4): p. e13628.
214. Sciarra, F., et al., *Disruption of Circadian Rhythms: A Crucial Factor in the Etiology of Infertility.* Int J Mol Sci, 2020. **21**(11).
215. Beroukhim, G., E. Esencan, and D.B. Seifer, *Impact of sleep patterns upon female neuroendocrinology and reproductive outcomes: a comprehensive review.* Reprod Biol Endocrinol, 2022. **20**(1): p. 16.
216. Sen, A. and H.M. Hoffmann, *Role of core circadian clock genes in hormone release and target tissue sensitivity in the reproductive axis.* Mol Cell Endocrinol, 2020. **501**: p. 110655.
217. Parsons, M.J., et al., *Social jetlag, obesity and metabolic disorder: investigation in a cohort study.* Int J Obes (Lond), 2015. **39**(5): p. 842-8.
218. Wang, Y.Q., et al., *The Neurobiological Mechanisms and Treatments of REM Sleep Disturbances in Depression.* Curr Neuropharmacol, 2015. **13**(4): p. 543-53.
219. Miljevic, A., et al., *Alterations in EEG functional connectivity in individuals with depression: A systematic review.* J Affect Disord, 2023.
220. Helm, K., et al., *Neuronal connectivity in major depressive disorder: a systematic review.* Neuropsychiatr Dis Treat, 2018. **14**: p. 2715-2737.
221. Wu, M., et al., *Gonadotropin inhibitory hormone inhibits basal forebrain vGluT2-gonadotropin-releasing hormone neurons via a direct postsynaptic mechanism.* J Physiol, 2009. **587**(Pt 7): p. 1401-11.
222. Tsukamura, H., et al., *Intracerebroventricular administration of melanin-concentrating hormone suppresses pulsatile luteinizing hormone release in the female rat.* J Neuroendocrinol, 2000. **12**(6): p. 529-34.

Chapter II. Transient MCH Expression in Late Lactation: Dissociated *Pmch* and Cre Expression in Lactating *Pmch*-Cre BAC Transgenic Mice

Abstract

The melanin-concentrating hormone (MCH) system plays a role in many physiological processes including reproduction and lactation. However, research regarding the function of MCH on different aspects of the reproductive function lags, due in part to a lack of validated genetic models with which to interrogate the system. This is particularly true in the case of female reproduction, as the anatomy and function of the MCH system is not well-characterized in the female mouse. We set out to determine whether the commercially available *Pmch*-Cre transgenic mouse line is a viable model to study the role of MCH neurons in distinct female reproductive states. We found that *Pmch* is transiently expressed in several nuclei of the rostral forebrain at the end of lactation. This includes the medial subdivision of the medial preoptic nucleus, the paraventricular nucleus of the hypothalamus, the ventral subdivision of the lateral septum, the anterodorsal preoptic nucleus and the anterodorsal nucleus of the thalamus. The *Pmch* expression in these sites, however, does not reliably induce Cre expression in the *Pmch*-Cre (BAC) transgenic mouse, making this line an inadequate model with which to study the role of MCH in behavioral and/or neuroendocrine adaptations of lactation. We also contribute to the general knowledge of the anatomy of the murine MCH system by showing that lactation-induced *Pmch* expression in the rostral forebrain is mostly observed in GABAergic (VGAT) neurons, in contrast to the typical MCH neurons of the tuberal and posterior hypothalamus which are glutamatergic (VGLUT2).

Background

The melanin-concentrating hormone (MCH) system has been implicated in a diverse array of fundamental physiological processes such as metabolic regulation, stress response, and sleep [1-4]. Several studies have provided compelling evidence that MCH neurons also regulate aspects of reproductive function such as the release of luteinizing hormone (LH) and lactation [5, 6].

While MCH neurons have widespread projections throughout the brain, they originate from a discrete region of the hypothalamus [7-12]. In rats, MCH expression is almost exclusively restricted to cell bodies in the incertohypothalamic area (IHy, aka rostromedial zona incerta or ZIm), the lateral hypothalamic area (LHA), and the perifornical area (PFx). The distribution of MCH neurons in mice and rats—and, indeed, in all rodents in which the system has been studied—follows a similar basic plan. However, close study of the mouse and rat reveals some key differences, including a population of periventricular MCH neurons seen in rats but not in mice, and the absence of more posterior groups in the mouse [7, 13]. Interestingly, MCH is transiently observed in the medial preoptic area (MPO), the periventricular preoptic nucleus, and the most rostral parts of the paraventricular nucleus of the hypothalamus (PVH) of female rats during lactation [5, 14] and, to a lesser extent, in the MPO of the mouse [5, 13, 14]. The role of MPO MCH expression in the lactating rodents is unclear, potentially due to a lack of validated models with which to study this phenomenon. Indeed, functional studies in mice lag behind the anatomy of the MCH system, as the majority of the experiments referenced up to this point which involve reproductive function were performed in rats.

In the present study, we sought to determine whether the commercially available Tg(*Pmch*-cre)1Lowl/J ("*Pmch*-Cre") transgenic mouse line [15] is a viable model to interrogate the role of the MCH system in female physiology. The *Pmch*-Cre mouse was developed using a bacterial artificial chromosome (BAC) containing the coding region for Cre recombinase flanked by upstream and downstream regulatory elements of the *Pmch* gene [15]. This technique is moderately efficient and used to be a common method of introducing DNA sequences in the genome of a model organism. However, the loci of insertion for the BAC is random: it is incorporated into a genomic site with a unique set of regulatory elements, potentially imposing additional layers of regulation on Cre expression. It may also fail to recapitulate epigenetic regulation that occurs at the native gene locus and relies on enhancers that may be located

hundreds of thousands of bases up- or downstream [16, 17]. The unpredictable nature of this method necessitates thorough validation, which has not been performed in female mice, particularly in lactating dams.

In addition to defining the locations of MCH expression during lactation, we sought to determine whether these MCH neurons potentially release γ-aminobutyric acid (GABA), glutamate, both, or neither of the classical fast neurotransmitters. We used brain tissue from Cre-driven reporter lines expressing GFP in neurons expressing the vesicular glutamate transporter (VGLUT2) or the vesicular GABA transporter (VGAT) to verify the fast neurotransmitter phenotype of MCH neurons in different brain regions.

Methods

Mice

Animal Care

Mice were housed in a vivarium at the University of Michigan with a 12/12 light/dark cycle and *ad libitum* access to food and water. The mice received phytoestrogen-reduced Envigo diet 2016 (16% protein/4% fat), except during breeding when mice were fed phytoestrogen-reduced Envigo diet 2019 (19% protein/8% fat). Phytoestrogen-reduced diet is routinely used in our laboratory to avoid the effects of exogenous estrogens on mouse physiology. All procedures and experiments were carried out in accordance with the guidelines established by the National Institutes of Health Guide for the Care and Use of Laboratory Animals and approved by the University of Michigan Committee on Use and Care of Animals (Animal Protocol #8712).

Pmch-Cre;eGFP mice

Commercially available *Pmch*-Cre (Tg(*Pmch*-Cre)1Lowl/J, JAX®; stock # 014099) mice were used. This mouse model was developed using a BAC containing a Cre coding sequence downstream of the mouse pro-melanin concentrating hormone (*Pmch*) promoter [15].

The *Pmch*-Cre mice were crossed with two different mouse lines carrying Cre-inducible reporter genes. First, *Pmch*-Cre mice were crossed with the B6;129-*Gt(ROSA)26Sor*^{tm2Sho}/J line (JAX®; stock # 004077, "R26-eGFP"). This mouse carries a targeted mutation of the *R26* locus with a loxP-flanked transcriptional blocking cassette preventing the expression of CAG promoter-driven enhanced green fluorescent protein (eGFP) reporter [20]. Cre-mediated excision of the

blocking cassette in *Pmch*-Cre;R26-eGFP mice results in expression of GFP in cells expressing Cre.

Pmch-Cre mice were also crossed with the B6;129S4-*Gt(ROSA)26Sor*$^{tm9(EGFP/Rpl10a)Amc}$/J line (JAX®; stock # 024750, "eGFP-L10a"), kindly donated by Dr. David Olson (University of Michigan), to generate *Pmch*-Cre;eGFP-L10a reporter mice. The eGFP-L10a mice express a chimeric L10a ribosomal subunit fused to enhanced green fluorescent protein. Successful Cre-mediated excision results in expression of the eGFP::L10A fusion protein in Cre-expressing tissues [21]. Due to the ribosomal eGFP fusion, this mouse model enables a strong fluorescent signal to accumulate in cell bodies.

Vgat-Cre;eGFP and Vglut2-Cre;eGFP mice

Vgat-IRES-Cre:*Slc32a1*$^{tm2(cre)Lowl/J}$ (JAX® mice, Stock # 016962) and Vglut2-IRES-Cre: S*lc17a6*$^{tm2(cre)Lowl/}$J (JAX® mice, Stock # 016963) mice were crossed with eGFP-L10a reporter to generate mice which express GFP in VGAT- or VGLUT2-expressing cells, respectively (Vgat-Cre;eGFP-L10a and Vglut2-Cre;eGFP-L10a mice) [22].

Genotyping

All mice were genotyped before experiments by extracting DNA from tail tip biopsies using the REDExtract-N-Amp™ Tissue PCR Kit, catalog no. XNAT (Sigma-Aldrich®). PCR was performed with a Bio-Rad C1000™ Thermal Cycler and included positive (DNA from the original JAX mice) and negative (sterile water) controls. Primer sequences can be found in Table 2-1.

Experimental Groups

Sexually naïve adult male *Pmch*-Cre;eGFP mice (8-12 weeks of age) were used. Adult female mice were divided into sexually naïve (8-10 weeks of age) and lactating groups (16-18 weeks of age) for a total of 3 experimental groups (n=4 per group). An additional group of females (n=4) was evaluated 5 days after weaning as control for the lactation group. Experimental groups were evaluated in both reporter lines: *Pmch*-Cre;R26-eGFP and *Pmch*-Cre;eGFP-L10a.

Additionally, Vgat-Cre;eGFP-L10a and Vglut2-Cre;eGFP-L10a dams were bred with Vglut2-Cre and Vgat-Cre males to generate two more lactation groups in which to assess the fast neurotransmitter phenotype of MCH neurons (n=3 per group).

Perfusion and Histology

Tissue collection

Adult male *Pmch*-Cre;eGFP mice were euthanized and brains harvested between 8-12 weeks of age. Sexually naïve females, 8-10 weeks of age, were ascertained to be in diestrus before tissue was harvested. Brains were collected from lactating females on day 19 of lactation (16-18 weeks of age).

All mice were anesthetized with isoflurane and transcardially perfused with saline prepared with diethyl pyrocarbonate (DEPC)-treated water followed by 10% neutral buffered formalin for 10 min. Following perfusion, brains were dissected and postfixed in 20% sucrose/10% buffered formalin overnight at 4°C, then cryoprotected in 20% sucrose in DEPC-treated 1× phosphate buffered saline (PBS) overnight at 4°C. Brains were sectioned with a freezing Leica SM2010 R microtome (4 series, 30-µm thickness, in the frontal plane). Sections were stored at -20°C in RNAse-free cryoprotectant (20% glycerol, 30% ethylene glycol in DEPC-PBS).

Radioactive in situ *hybridization*

Single-label radioactive *in situ* hybridization (ISH) was performed on one series of brain sections from each animal. Sections were mounted onto RNAse-free SuperFrost Plus slides (Fisher Scientific). Mounted tissue was fixed in 4% paraformaldehyde in DEPC-treated 1×PBS for 20 min, dehydrated in increasing concentrations of ethanol, cleared of lipids using xylenes, and subsequently rehydrated in decreasing concentrations of ethanol. The slides were pretreated by microwaving in sodium citrate buffer (pH 6.0), then dehydrated again in increasing concentrations of ethanol, air-dried, and stored at -20˚C [23-25].

The *Pmch* cDNA (template) was produced from mouse hypothalamic RNA and used to amplify a 478 bp sequence in the coding region of the *Pmch* gene (IDT, Inc). Primer sequences are delineated in Table 2-1. The *Pmch* riboprobe was generated by *in vitro* transcription using ^{35}S-UTP as the radioisotope. ^{35}S -labeled *Pmch* probe was diluted in hybridization solution (50 % formamide, 10 mM Tris-HCl pH 8.0, 0.01% of yeast tRNA, 0.05% of total yeast RNA, 10 mM dithiothreitol/DTT, 10% dextran sulfate, 0.3 M NaCl, 1 mM EDTA, and 1× Denhardt's solution) and applied to slides, which were allowed to hybridize overnight at 55°C, as routinely done by our group [24]. Following post-hybridization treatment with RNAse, stringency washes with saline sodium citrate (SSC) buffer and dehydration in increasing concentrations of ethanol,

sections were dried at room temperature and slides were placed in X-ray film cassettes with BMR-2 film (Kodak, Rochester, NY, USA) for 1 day (tuberal and posterior levels of the hypothalamus) or 4 days (rostral forebrain). Slides were then dipped in NTB autoradiographic emulsion (Kodak), dried for 3 hours and stored in light-protected slide boxes at 4˚C for 6 days (tuberal and posterior levels of the hypothalamus) or 14 days (rostral forebrain). Slides were developed with Dektel developer (Kodak, VWR, Radnor, PA, USA), dehydrated in increasing concentrations of ethanol, cleared in xylenes and coverslipped with DPX mounting medium (Electron Microscopy Sciences).

Dual-label Immunohistochemistry

Dual-label immunohistochemistry (IHC) for MCH or NEI and GFP was performed in one series of brain sections from each animal. Sections were blocked for 30 min in 3% normal donkey serum (NDS) and incubated overnight in chicken anti-GFP (1:10,000, Aves Labs, AB_2307317) and either rabbit anti-MCH (1:5,000, Phoenix Pharmaceuticals, AB_2722682) or rabbit anti-NEI (1:15,000, kindly provided by Dr. Paul Sawchenko, Salk Institute for Biological Studies, La Jolla, CA) followed by secondary antisera (goat anti-chicken conjugated to Alexa Fluor™ 488 AB_2534096, and donkey anti-rabbit conjugated to Alexa Fluor™ 594 AB_141637) for 1 h (1:500, Thermo Fisher Scientific). Sections were mounted onto gelatin-coated slides, air-dried, and coverslipped with Fluoromount G mounting medium (Electron Microscopy Sciences).

In one series of brain sections from lactating dams (n=3), a tyramide signal amplification (TSA) procedure was used. Briefly, sections were incubated for 10 mins in 10% H_2O_2 to block endogenous peroxidase activity, followed by a 1 h blocking step in 3% NDS. They were incubated overnight in rabbit anti-MCH (1:30,000). The next day, sections were incubated for 1 h in donkey anti-rabbit biotinylated secondary antibody (1:500, Jackson ImmunoResearch Laboratories AB_2340593) followed by 1 h in avidin-biotin complex (ABC) solution (1:500, Vector Laboratories). Finally, they were incubated in tyramide reagent (1:250, Perkin Elmer) + 0.003% H_2O_2 followed by 30 min in AlexaFluor™ 594-conjugated streptavidin (1:1000, Thermo Fisher Scientific) before mounting and coverslipping with FluoroMount G mounting medium.

Dual label in situ hybridization (ISH) and immunohistochemistry (IHC)

Dual-label ISH and IHC were performed to determine the colocalization of Pmch mRNA and Vgat-Cre or Vglut2-Cre GFP-ir [26]. Briefly, free-floating sections from lactating females

(n=3/genotype) were treated with 0.1% sodium borohydride for 15 min and 10 min with 0.25 % acetic anhydride in DEPC-treated 0.1 M triethanolamine (TEA, pH 8.0). Sections were incubated overnight at 50°C in the hybridization solution containing the ^{35}S-*Pmch* riboprobe. Subsequently, sections were treated with RNase A for 30 min and submitted to stringency washes in SSC (sodium chloride-sodium citrate buffer). Sections were blocked (3% BSA in PBS-Triton) then incubated with anti-GFP antibody (1:5,000) overnight at 4 °C. Sections were incubated for 1.5 h in a goat anti-chicken AlexaFluor 488 antibody and mounted onto SuperFrost plus slides. After overnight air drying, slides were dehydrated in increasing concentrations of ethanol and dipped in NTB-2 autoradiographic emulsion (Kodak), dried and stored in light-protected boxes at 4 °C for 3 weeks. Finally, slides were developed with D-19 developer (Kodak), dehydrated in graded ethanol, cleared in xylenes, and coverslipped with DPX mounting medium.

Fluorescent in situ hybridization

Fluorescent *in situ* hybridization for *Pmch* and *Slc32a1* was performed using the RNAscope® fluorescent multiplex detection Kit (Advanced Cell Diagnostics, cat. no. 320850) as previously described [27]. Briefly, mice were deeply anesthetized with isoflurane and decapitated. Brains were collected and immediately frozen on dry ice, then cut into 6 series of 16-µm sections on a cryostat at -20°C and mounted onto Superfrost Plus slides. Slides were heated at 60°C, then immersed in 10% buffered formalin for 2 h at 4°C. They were dehydrated in increasing concentrations of ethanol, cleared in xylenes, and rehydrated in decreasing concentrations of ethanol. Next, slides were boiled for 10 min in sodium citrate buffer and incubated for 10 min in 0.03% sodium dodecyl sulfate. Slides were subsequently dried at room temperature and a hydrophobic barrier was drawn around the sections. From this point forward, steps were carried out in humidity control trays to prevent sections from drying. Endogenous peroxidase activity was blocked with a 10-min incubation with H_2O_2 followed by rinsing with nuclease-free water. RNAscope protease III was then applied and slides were heated for 30 min at 40°C before once again rinsing with nuclease-free water. Hybridization was performed by applying pre-warmed target positive and negative control probes to sections and heating for 2 h at 40°C. Then, the amplification of each probe (AMP 1-2) was performed sequentially, incubating for 30 minutes at 40°C then rinsing in wash buffer after each Multiplex FL v2 Amp solution. The slides were developed using two RNAscope Multiplex FL v2 HRP-C*n* solutions where *n*=1-2 (one probe per channel). For each channel, this was performed by incubating in RNAscope Multiplex FL v2

HRP-C*n* for 15 min at 40°C, rinsing with wash buffer, incubating for 30 min at 40°C with TSA+ Fluorescein (Akoya Biosciences, cat. no. SKU NEL741001KT), incubating in RNAscope Multiplex FL v2 HRP blocker for 15 minutes at 40°C, and rinsing once more with wash buffer. Finally, slides were counterstained with DAPI and coverslipped with ProLong Gold antifade mounting medium (ThermoFisher Scientific).

Analysis methods and generation of photomicrographs

Slides from each cohort of *Pmch*-Cre/GFP mice were examined under an Axio Imager M2 Microscope or a SteREO DiscoveryV8 (Zeiss). The digital Allen Brain Atlas was used as a reference to determine relative location within the hypothalamus and identify the primary sites containing MCH-immunoreactivity, GFP-immunoreactivity, and *Pmch* mRNA expression. Images were acquired with a digital camera (Axiocam, Zeiss) using Zen software. All sections were examined, and single- and dual-labeled cells were quantified in 20× magnification using ImageJ with the Cell Counter plugin in one representative section of each area of interest (i.e., IHy, PFx, LHA). For data illustration, only sharpness, contrast, and brightness were adjusted.

Results

Pmch expression and MCH immunoreactivity in tuberal and posterior hypothalamus are similar in naïve male, female, and lactating mice.

In situ hybridization for *Pmch* was performed in brain sections from sexually naïve males and females in diestrus to visualize the distribution of *Pmch* mRNA and assess whether it is sexually dimorphic and/or distinct in lactating females. Intense hybridization signal was observed in males in cells of the IHy, LHA, and PFx with virtually no signal elsewhere in the brain. Populations of MCH cells were identified in the IHy as characterized by their relatively dorsal location within the hypothalamus, just below the thalamus. Populations of MCH cells were defined in the LHA and PFx using other nearby structures including the fornix, optic tract, and internal capsule. There was no difference in the distribution pattern of *Pmch* mRNA between the two groups that could be visually ascertained (Figure 2-1A-B, D-E). Furthermore, the distribution of *Pmch* mRNA in IHy, LHA and PFx of the lactating dams was also similar to that of the sexually naïve male and female mouse (Figure 2-1C, F).

To assess if the distribution of the MCH peptide is similar in all three groups, MCH-immunoreactivity (MCH-ir) was examined and compared in sexually naïve male and female as

well as lactating female mouse brains. Abundant MCH-ir was observed in perikarya and fibers in the IHy, LHA, and PFx, in all groups in accordance with the mRNA pattern and previous studies [7, 13]. No clear difference in the distribution pattern of MCH-ir was observed between groups (Figure 2-1G-L)

A subset of GFP+ neurons in the perifornical area (PFx) does not express MCH-ir

MCH- and Cre-induced GFP-ir were compared in sexually naïve male and female as well as lactating *Pmch*-Cre;R26-eGFP mouse brains. Virtually all GFP+ neurons expressed MCH-ir in the IHy and LHA (Figure 2-2A-F). However, a population of GFP+ neurons that do not express MCH-ir was consistently observed in the PFx of all groups of mice. To assess whether this was an artifact of our reporter gene, we repeated this experiment with a different reporter line. In *Pmch*-Cre;eGFP-L10a mice, the same population of GFP+/MCH- cells was observed in all three groups (Figure 2-2G-I). These neurons are primarily found lateral to the fornix at the level of the tuberal division of the LHA. The GFP+/MCH- cells have a distinctive small, circular morphology and cluster together near the fornix. A few such neurons were occasionally observed in other regions of the hypothalamus, primarily in the dorsal IHy, but without a consistent distribution pattern among mice from the same group.

Since MCH is just one of several peptide products of the *Pmch* transcript, the other major one being NEI, we evaluated NEI- and GFP-ir to determine whether the PFx GFP+/MCH- neuronal population expresses NEI. Abundant NEI-ir was observed in virtually all GFP-ir perikarya and fibers in the IHy, and LHA of all three groups, showing that, as reported in rats [7], virtually all hypothalamic MCH neurons also contain NEI. However, a population of small GFP immunoreactive neurons in the PFx was also negative for NEI-ir. This GFP+/NEI- subset of neurons presumably overlaps with the population of GFP+/MCH- neurons previously described (Fig 2-2G-H).

***Pmch* is expressed in several nuclei of the rostral forebrain in lactating mouse**

To further map Cre-induced GFP distribution, we initially performed a comprehensive analysis of *Pmch* expression in the rostral forebrain of lactating (day 19) mice. As previously described in lactating rats, we observe *Pmch* expression in the MPO and PVH of lactating mice. However, the pattern of mRNA distribution was distinct comparing both murine species. At the level of the anterior commissure, *Pmch* expression in the MPO is restricted to the periventricular nucleus and

medial subdivision of medial preoptic nucleus (MPNm) with some lateral spreading below and above to include the anterodorsal preoptic nucleus (ADP) and the principal subdivision of the bed nucleus of the stria terminalis (BSTpr) (Figure 2-3A-C). *Pmch* mRNA was also observed in the rostral PVH (Figure 2-3D) and forebrain regions where it has not been reported in the rat. We found a moderate to dense population of *Pmch* cells in the lateral septum (LS,) and the anterodorsal nucleus of the thalamus (AD) just lateral to the stria medullaris (Figure 2-3E-F).

Expression of *Pmch* and Cre-induced GFP-ir are dissociated in lactating *Pmch*-Cre mice

GFP-ir was examined in rostral forebrain of lactating *Pmch*-Cre;R26-eGFP and *Pmch*-Cre;eGFP-L10a dams. The latter reporter strain was preferred because the GFP fluorescence was more intense. Despite this more intense signal, little to no GFP-ir was observed in the MPO and inconsistent GFP-ir was observed in the PVH (Figure 2-4A-C). This contrasts with the gene expression data, which shows high *Pmch* mRNA expression in these regions. Sparse GFP-ir cells were detected in the BSTpr and LS (Figure 2-4C-D). Furthermore, a group of GFP-ir cells was consistently observed in the dorsal aspect of the medial septum (MS), where no *Pmch* mRNA was observed (Figure 2-4E). Finally, GFP-ir was also seen in the AD (Figure 2-4F). To assess if a delay in Cre and GFP expression was the cause of this inconsistency, a group of females was perfused 5 days after weaning (or 7 days post lactation day 19). No differences in eGFP-ir was observed compared to females perfused at lactation day 19. Collectively, our findings indicate that *Pmch* and Cre expression are incongruent: a large number of *Pmch* neurons do not express GFP-ir and a group of GFP+ neurons in the dorsal MS does not express *Pmch*.

Expression of vGluT2 and vGAT differs in subsets of *Pmch* neurons

To gain insights into the fast neurotransmitter phenotype of MCH neurons we used Vgat- and Vglut2-Cre;eGFP-L10a reporter mice, dual label ISH and immunohistochemistry and dual label ISH.

Dual immunofluorescence was performed in brains from Vgat- and Vglut2-Cre;eGFP-L10a reporter mice to assess the colocalization of MCH-ir and GFP-ir in sexually naïve males and females in diestrus, and in nursing dams on day 19 of lactation. In the LHA, IHy, and PFx, as previously suggested by single-cell RNA sequencing data [18], MCH-ir in all groups colocalized with Vglut2-Cre;eGFP (Figure 2-5A-C). Sporadic MCH immunoreactive cells colocalized with Vgat-Cre;eGFP (Figure 2-5D-F).

In the rostral forebrain of lactating dams, MCH-ir and NEI-ir were very low and inconsistent, and *Pmch*-Cre induced GFP-ir did not label MCH neurons. To evaluate coexpression with the transcript, we used brain sections of the Vgat- and Vglut2-Cre;eGFP reporter mice. *In situ* hybridization for *Pmch* in combination with immunohistochemical amplification of GFP fluorescent signal was performed in all three mouse groups. In the LHA, IHy, and PFx, *Pmch* mRNA in all groups of mice colocalized with Vglut2-Cre;eGFP primarily, and sporadically with Vgat-Cre;eGFP, consistent with our immunohistochemical data. In the lactating dams, colocalization was less clear. *Pmch* mRNA in the MPO, PVH, LS, and AD colocalized primarily with Vgat-Cre;eGFP and not Vglut2-eGFP (Figure 2-6A-C). Because this result contradicts recent studies [19], we performed fluorescent ISH using RNAscope to further examine colocalization of *Pmch* with *Slc32a1* (VGAT). The findings were unambiguous and demonstrated that virtually all *Pmch* expressing neurons coexpress *Slc32a1* (Figure 2-6D-F).

In summary, our findings indicate that MCH neurons in the LHA, PFx, and IHy are overwhelmingly glutamatergic, and those in the rostral forebrain induced during lactation are mostly GABAergic.

Discussion

In this study, we assessed if the commercially available Tg(*Pmch*-cre)1Lowl/J transgenic mouse line [15] is a viable model to interrogate the role of the MCH system in the female reproductive function. We found that in male and female (diestrous and lactating) mice, a group of Cre-induced GFP-expressing cells that do not express MCH- or NEI-ir is consistently observed in the PFx. In lactating dams, *Pmch* expression is observed in the MPO and anterior PVH, and in previously unreported forebrain nuclei, i.e., LS and AD. However, most of these sites do not show Cre-induced GFP-ir in the Tg(*Pmch*-cre)1Lowl/J transgenic mouse line. We also found that typical MCH neurons in the tuberal and posterior hypothalamus coexpress VGLUT2 (*Slc17a6*) whereas lactation-induced *Pmch* expression in rostral forebrain is mostly observed in VGAT (*Slc32a1*) neurons.

This Tg(*Pmch*-cre)1Lowl/J mouse model shares many similarities with the C57BL/6-Tg(*Pmch*-cre)1Rck/J line. Both lines utilize a BAC transgene. The promoter for the C57BL/6-Tg(*Pmch*-cre)1Rck/J line is somewhat larger, including 108 kb upstream of the MCH gene in the BAC regulatory element as opposed to the 64 kb in the Tg(*Pmch*-cre)1Lowl/J. The strains also have

nearly identical penetrance and specificity. [15, 28] Ultimately, we chose to focus on the Tg(*Pmch*-cre)1Lowl/J line because it is used and cited more frequently, making our findings applicable to more researchers in the field [15, 29, 30].

Whereas most previous studies have been focused on peptide distribution, here we gave special attention to the distribution and expression of the *Pmch* gene. As previously described for MCH-ir, *Pmch* expression is very similar in naïve male and female mice with clear anterior and posterior patterns of distribution [13]. The anterior pattern of mRNA expression is characterized by distinct populations of neurons in the IHy, PFx, and a few neurons in the LHA (anterior division), while the posterior pattern primarily consists of dense expression in the LHA (tuberal division) and PFx. We have further shown that virtually all MCH-ir cells express GFP (and thus Cre recombinase) in the *Pmch*-Cre reporter mouse, indicating that Cre expression in the Tg(*Pmch*-Cre)1Lowl/J BAC transgenic mouse line is highly penetrant. It is worth mentioning that we observe higher penetrance than what was demonstrated in the originating publication [15]. This is likely due to the use of a ribosomal protein-associated reporter line, which is more concentrated in the soma, whereas the original publication validated the model used a TdTomato reporter, which is expressed in fibers and thus yields a more diluted signal [21, 31].

However, we observe some GFP-ir cells which do not express MCH located in the PFx. The cause for this discrepancy is not evident, but an artifact (ectopic expression) of the BAC transgene is a reasonable explanation, calling into question the specificity of Cre expression. Alternatively, MCH could play a developmental role in these cells. If its production is turned off by adulthood, MCH-ir and *Pmch* would not be detected by our assays, yet GFP signal would still be visible as it is driven by a ubiquitous promoter. Future work will be necessary to address this question by characterizing hypothalamic *Pmch* mRNA and MCH peptide expression at various timepoints in the developing mouse brain.

In lactating mice, *Pmch* expression is clearly different from rats [5]. While in rats, *Pmch* expression is triggered at mid-lactation and becomes dense in the MPN and PVH, in mice, *Pmch* is observed only at the end of lactation (day 19) at low to moderate levels specifically in the MPNm [19] and anterior PVH. Notably, the mice also show lactation-induced *Pmch* in previously unreported brain sites, including the LS, the ADP, the ventral BSTpr and the anterior AD. The role of MCH system in these sites is not known. Furthermore, the inconsistency of Cre-

mediated GFP expression indicate that the *Pmch*-Cre BAC transgenic mouse model is not useful for investigating transient MCH expression in lactating dams. Sacrificing lactating dams 5 days after weaning the offspring to allow more time for Cre-mediated recombination and GFP expression did not change the low to nonexistent levels of GFP-ir in the MPNm of the lactating dam.

Turning on MCH production for just several days at the end of lactation suggests that its role is highly specific and time sensitive. If this is the case, it may indicate that MCH in these neurons is subjected to unique epigenetic regulation what may not be reproduced in the BAC sequence. Moreover, differences at the level of transcription, such as the use of enhancers, that inform MCH production and processing could interfere with Cre expression in these cells if the enhancers are not located within the BAC transgene. A BAC genomic clone containing 64 kb upstream and 34 kb downstream of *Pmch* gene was used to generate the original MCH-Cre mice with the goal of capturing most of the gene's regulatory elements [15]. However, mammalian enhancers can be located as far as one million base pairs from the transcriptional start site of the gene in question [16, 17, 32]. Thus, it is possible that important enhancer activity has been excluded from the BAC regulatory element.

It has been suggested that prolactin-induced phosphorylation of STAT5 (pSTAT5) has a role in the lactation-induced MCH-ir in the MPO. STAT5 is a known activator protein for hundreds of enhancers, particularly those implicated in pregnancy- and lactation-associated genes [19, 33]. The seven STAT family proteins are all believed to target the same palindromic core motif, TTCN_{2-4}GAA. STAT5A and B in particular have a strong preference for palindromic core motifs of N_3 [34]. A brief search using DNASTAR Lasergene software shows that approximately 50 sites per 100 kb contain sequence TTCN_3GAA, yielding close to 500 potential pSTAT5 binding sites upstream of the *Pmch* gene regulatory element that are potentially missing from the BAC regulatory elements. Whereas these are clearly speculations, it is possible that regulatory sequences essential for *Pmch* expression during lactation are not included in the BAC used in this mouse model.

For the purposes of anatomical and specific functional studies, i.e. viral injections, tract tracing or colocalization with other transcripts and peptides, this may be an acceptable model because

nearly all of the Cre-expressing cells are indeed MCH-positive neurons with the exception of the small, highly localized population of PFx neurons that are easy to identify.

It has long been debated whether MCH neurons release GABA, glutamate, both, or neither of the classical fast neurotransmitters. In rats, it has been documented that MCH neurons of the tuberal hypothalamus express *Gad1* (glutamic acid decarboxylase or GAD67), the enzyme that catalyzes the decarboxylation of glutamate to GABA, and the vesicular GABA transporter (VGAT) can be found in MCH terminals [35, 36]. However, glutamate has been observed in MCH cells and demonstrated to be released from MCH terminals [37, 38]. Using a different reporter system, however, others claim that these neurons are neither GABAergic nor glutamatergic [39]. The glutamatergic-leaning transcriptional profile of hypothalamic MCH neurons has largely been reinforced with the availability of advanced genomic techniques, i.e. single-cell RNA sequencing [18]. Our data using distinct methodologies is in agreement with the latter and demonstrates that the typical MCH neurons in the tuberal hypothalamus are essentially glutamatergic. It is also worth mentioning that our findings are not contradictory to previous studies in rats showing that MCH neurons coexpress GAD67. Species differences should not be ignored as the colocalization of MCH and GAD67 or lack thereof in mice has not been shown. The presence of GAD67 indicates that the cell has the necessary machinery to synthetize GABA from glutamate [40, 41]. Whether this process is observed in specific physiological state(s) in MCH neurons of the mouse hypothalamus needs further investigation.

Transient MCH expression in the rat MPO, on the other hand, has been shown to occur in GAD67 expressing neurons [14]. Using immunohistochemistry and radioactive ISH we show that transient lactation-induced MCH expression is largely restricted to VGAT+ neurons, though in the MPO sporadic *Pmch* mRNA can apparently be also found in VGLUT2+ neurons. RNAscope confirms that most of lactation-induced *Pmch* neurons coexpress *Slc32a1* (VGAT). This contrast in fast neurotransmitter phenotype could underlie fundamental differences in the function and properties of these transient MCH neurons as compared with their counterparts elsewhere in the hypothalamus. However, it also contradicts the recent finding that MCH neurons in the LHA, PFx, and IHy express neither Vglut2, Vglut3, nor Vgat [19]. As aforementioned, this difference may arise from our use of an eGFP-L10a reporter strain rather than a TdTomato reporter. Because L10 is a ribosomal protein, it concentrates in the cytoplasm for ease of visualization whereas TdTomato also labels terminals, diluting the signal [21, 31].

We conclude that the *Pmch*-Cre mouse model is unsuitable for studying the role of MCH during lactation. Any Cre-dependent manipulations will not target the neurons which transiently express MCH during lactation, especially in the MPNm, PVH and LS, where the mRNA/GFP-ir discrepancy is most pronounced. This presents a need to develop other methods for investigating these neurons, which could involve the development of another transgenic mouse line. It would be particularly beneficial to use a knock-in strategy to increase specificity and congruence of Cre and *Pmch* expression in both sexes and all physiological states.

Table 2-1. Primer sequences used for genotyping mice and performing radioactive *in situ* hybridization.

Primer	**Purpose**	**Sequence**
Common Forward	*Pmch*-iCre Genotyping	GAA AAG ATA AGG CCT TCA AGT GCT
Internal + Control Reverse	*Pmch*-iCre Genotyping	GAT CTT TCT GCA GTA TCT TCC TTC
Transgene Reverse	*Pmch*-iCre Genotyping	ATC GAC CGG TAA TGC AGG CAA
Forward	R26-eGFP Genotyping	AAG TTC ATC TGC ACC ACC G
Reverse	R26-eGFP Genotyping	TCC TTG AAG AAG ATG GTG CG
Forward 1	L10-eGFP Genotyping	GAG GGG AGT GTT GCA ATA ACC
Forward 2	L10-eGFP Genotyping	TCT ACA AAT GTG GTA GAT CCA GGC
Reverse	L10-eGFP Genotyping	CAG ATG ACT ACC TAT CCT CCC
Forward	*Pmch* cDNA Template for ISH	(CAG AGA TGC AAT TAA CCC TCA CTA AAG GGA GA) AGC ATC AAA CTA AGG ATG GCA
Reverse	*Pmch* cDNA Template for ISH	(CCA AGC CCT CTA ATA CGA CTC ACT ATA GGG AGA) GCA TAC ACC TGA GCA TGT CAA AA

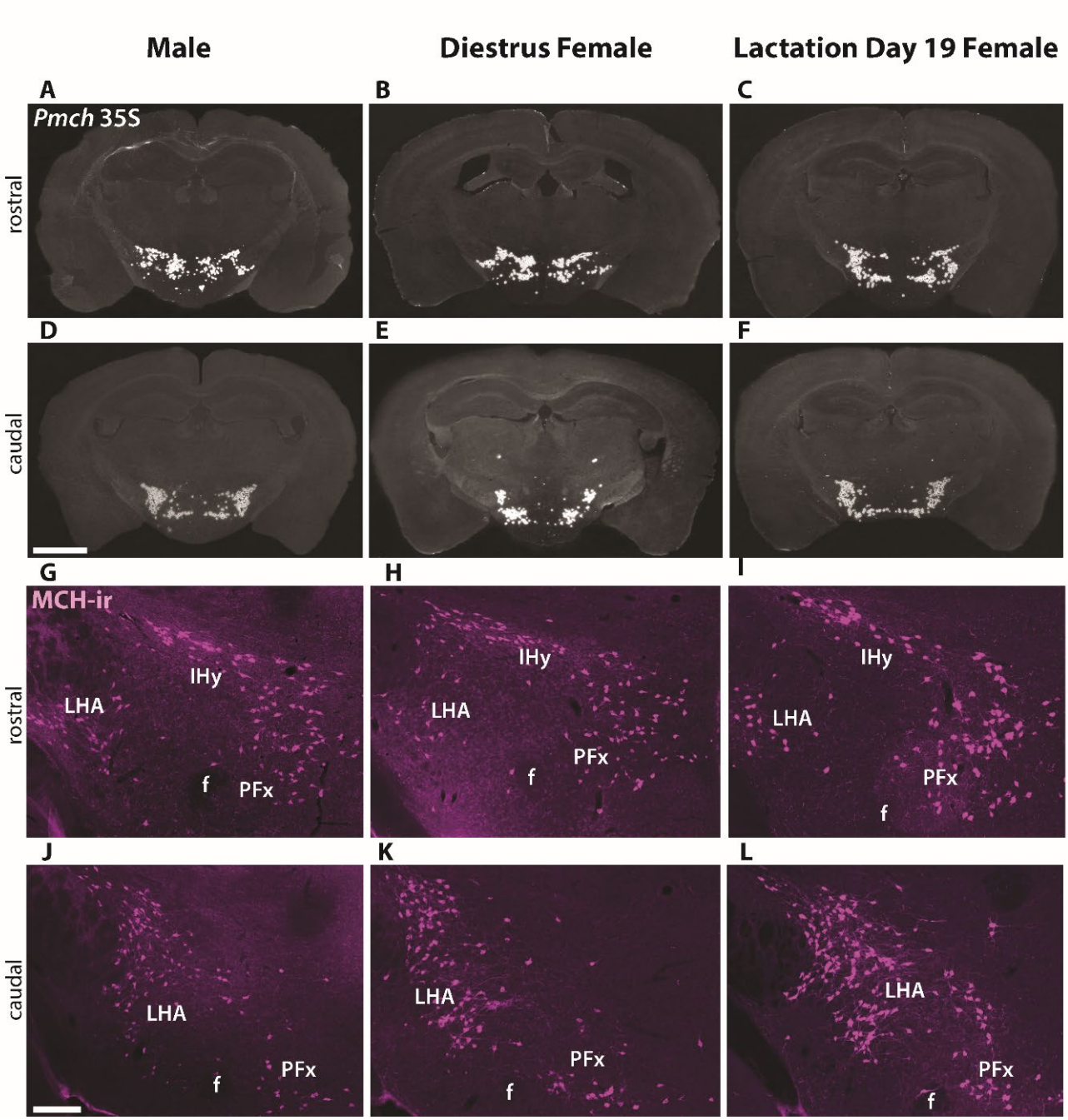

Figure 2-1. *Pmch* expression and MCH-immunoreactivity in the tuberal hypothalamus are similar in naïve male, sexually naïve diestrous female, and lactating mice. *A-F* Dark field micrographs showing the distribution of *Pmch* mRNA (silver grains) in rostral *(A-C)* and caudal *(D-F)* aspects of the tuberal hypothalamus in all three groups of mice: sexually naïve male *(A, D)*, diestrous female *(B, E)* and lactating *(C, F)* mice. *G-L* Fluorescent micrographs showing the distribution of MCH-ir in cells of the rostral *(G-I)* and caudal *(J-L)* aspects of the tuberal hypothalamus in sexually naïve male *(G, J)*, diestrous female *(H, K)* and lactating *(I, L)* mice.
Scale bar: (A-F) 1000µm, (G-L) 200µm.
Abbreviations: f, fornix; IHy, incertohypothalamic area; LHA, lateral hypothalamic area; PFx, perifornical area.

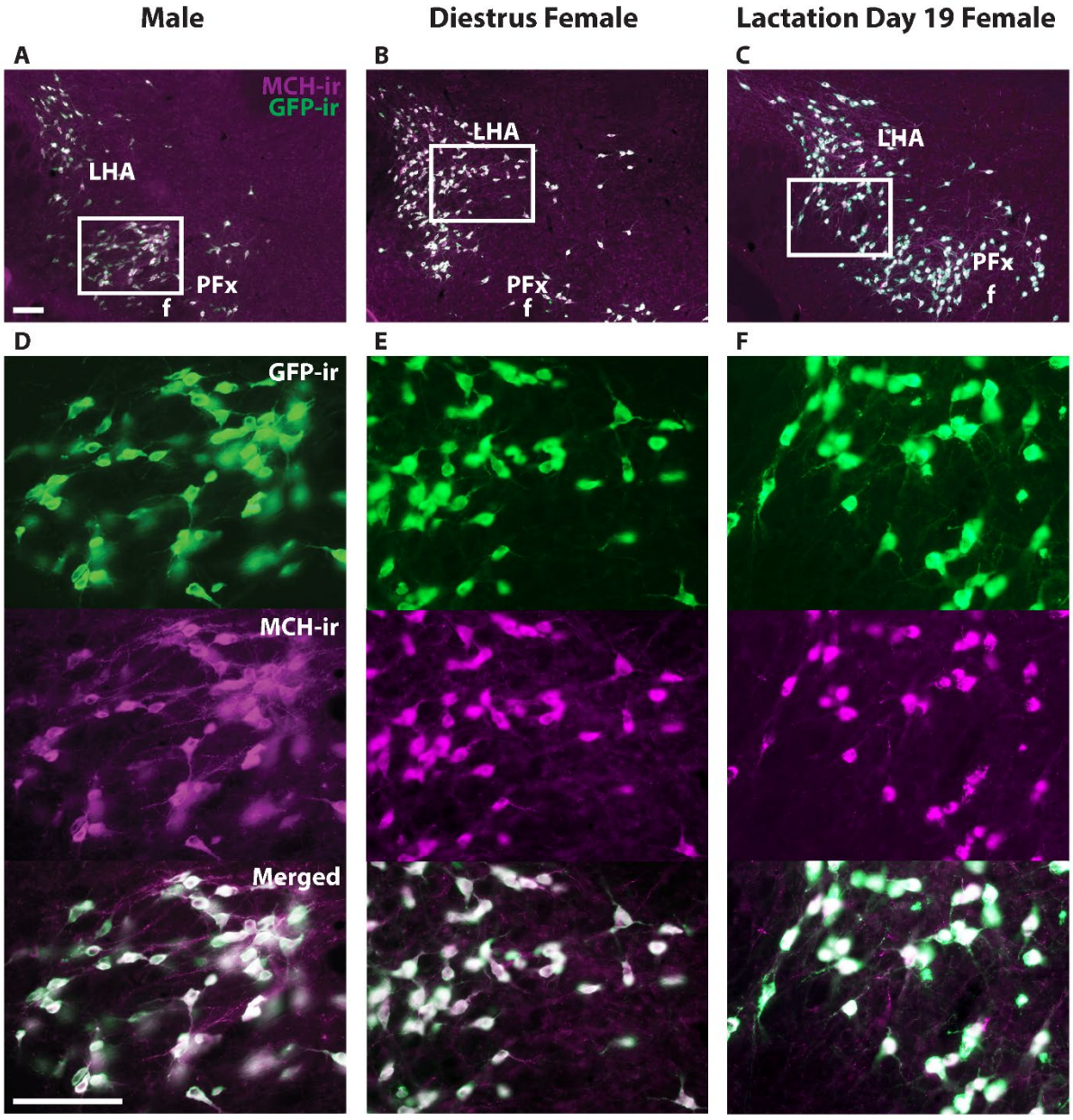

Figure 2-2. The majority of GFP+ neurons in the hypothalamus of *Pmch*-Cre;eGFP mice express MCH-immunoreactivity (-ir). Fluorescent micrographs showing the colocalization of GFP-ir and MCH-ir in the lateral hypothalamus of *Pmch*-Cre;eGFP-L10a male (*A*), sexually naïve diestrus (*B*) and lactating (day 19) mice (*C*). Scale bars: 100 μm.

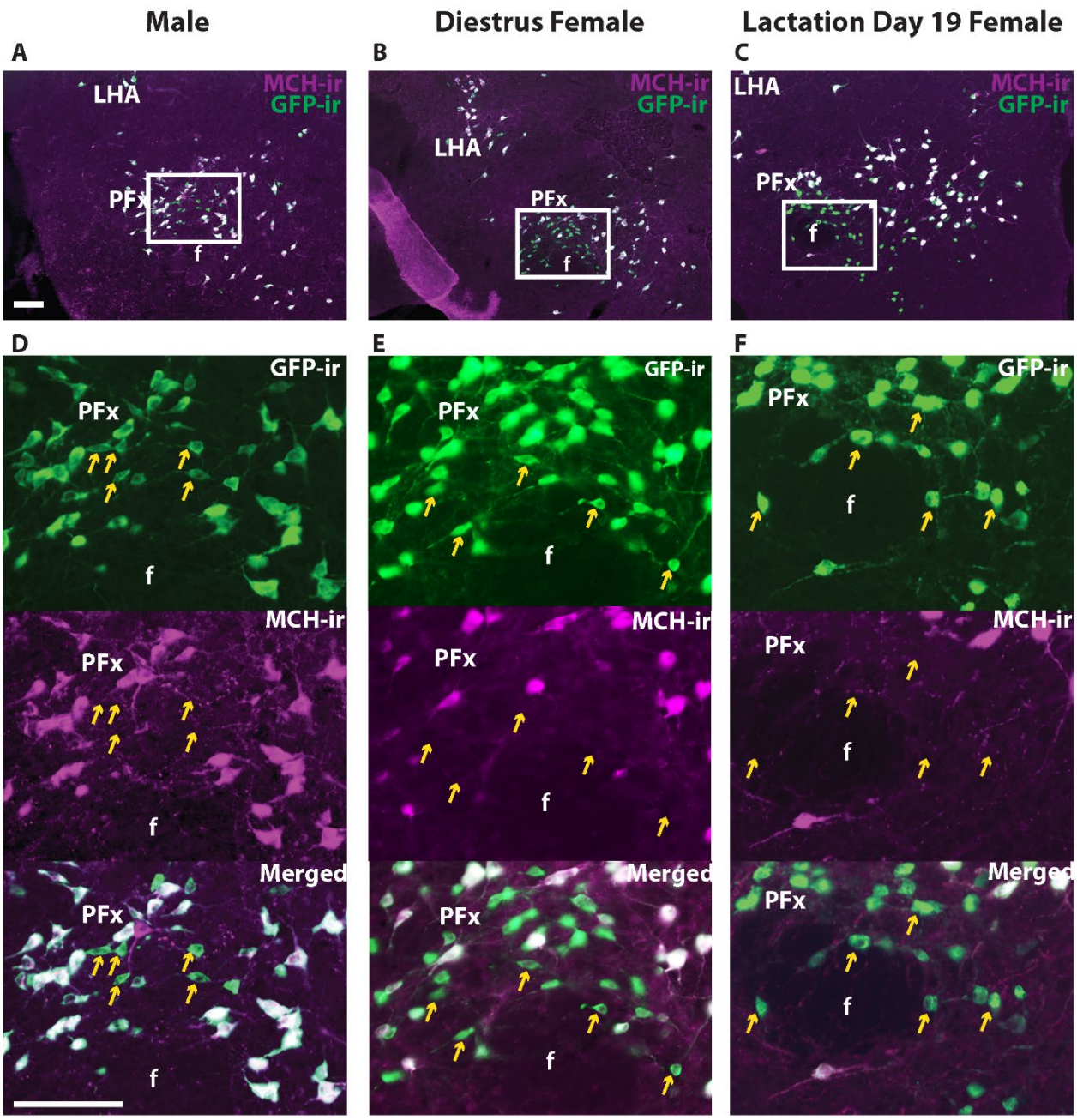

Figure 2-3. A subset of GFP+ neurons in the perifornical area does not express MCH-ir. Fluorescent micrographs showing GFP-ir and MCH-ir in the perifornical area (PFx) of a Pmch-Cre;eGFP male (*A*), diestrus female (*B*), and lactating dam (*C*). Note the presence of a subset of GFP-ir neurons in all groups that do not express MCH-ir (arrows). Sections are between 74 and 77 of 132 (Allen Mouse Brain Atlas, 2004).
Scale bars: 100 µm.
Abbreviations: f, fornix LHA, lateral hypothalamic area; PFx, perifornical area.

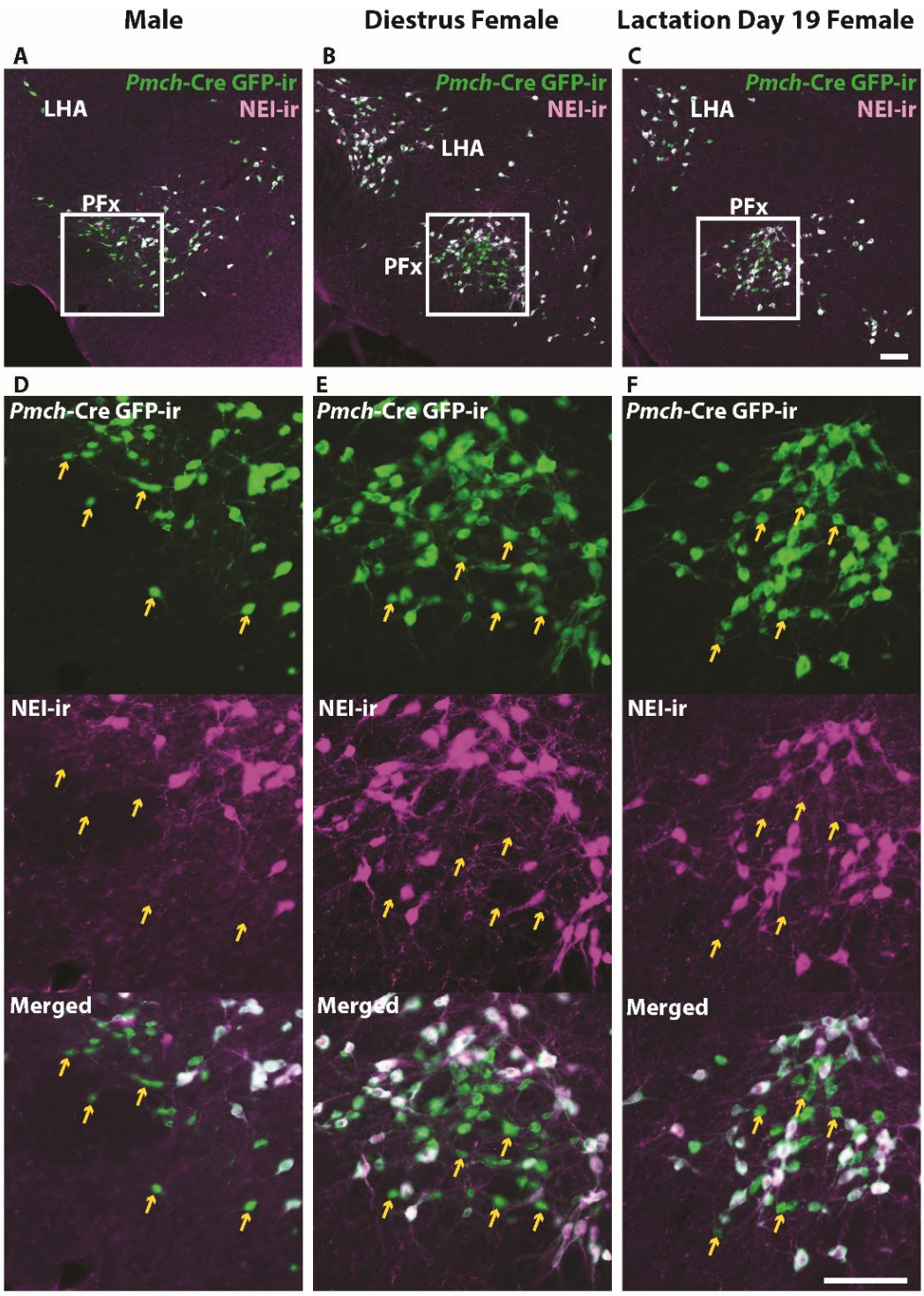

Figure 2-4. GFP+ /MCH- neurons in the perifornical area do not express NEI-ir. Fluorescent micrographs showing GFP-ir and NEI-ir in the perifornical area (PFx) of a *Pmch*-Cre;eGFP male (*A*), diestrus female (*B*), and lactating dam (*C*). Note the presence of a subset of GFP-ir neurons in all groups that do not express NEI-ir (arrows) which appears to correspond to the similar group of neurons observed that express GFP-ir but not MCH-ir. Sections are between 74 and 77 of 132 (Allen Mouse Brain Atlas, 2004).
Scale bars (A–D) and (E–F): 100 μm.
Abbreviations: f, fornix LHA, lateral hypothalamic area; PFx, perifornical area.

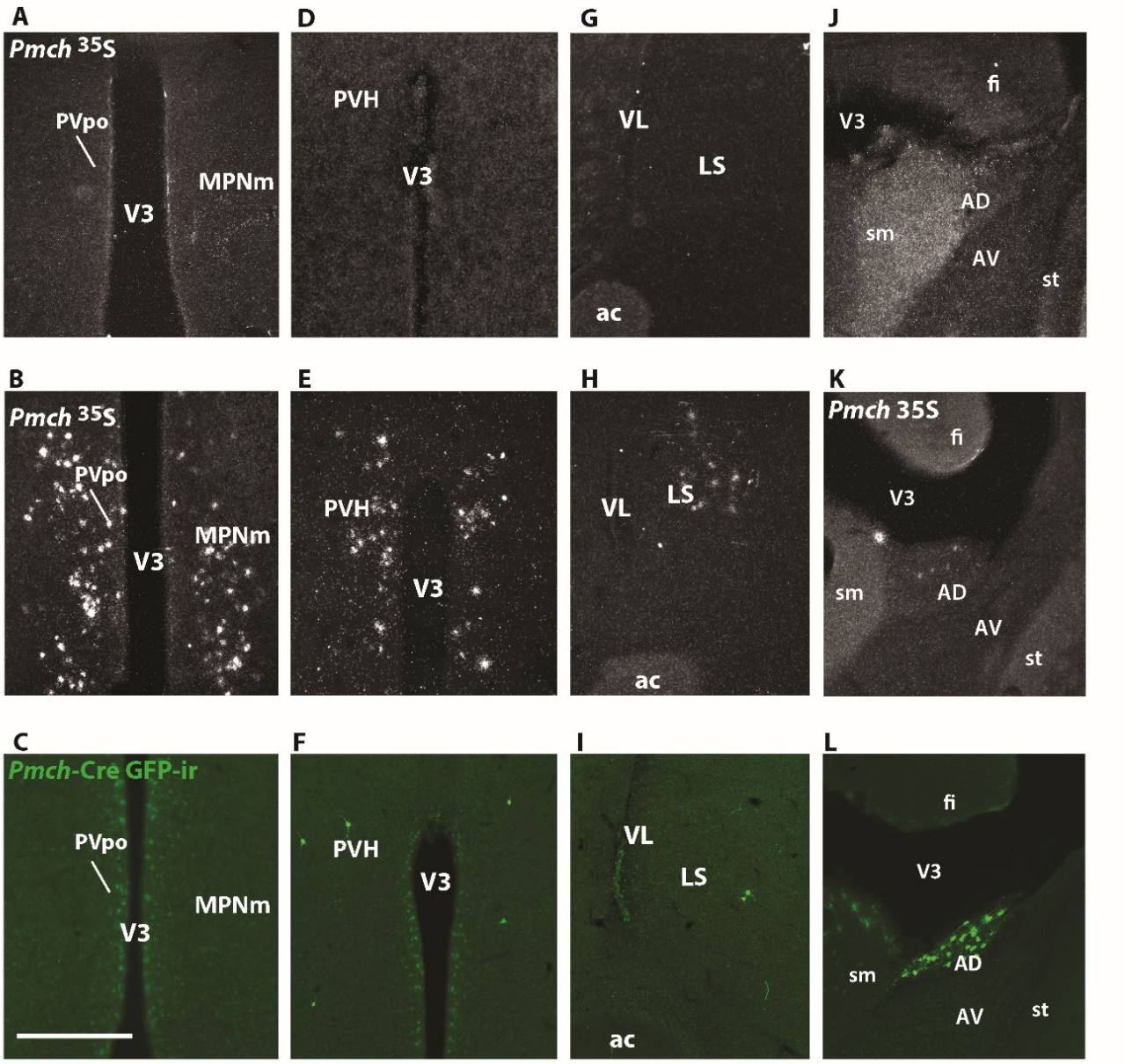

Figure 2-5. Expression of *Pmch* and Cre-induced GFP-ir are dissociated in several nuclei of the rostral forebrain in lactating dams. *A* Dark field photomicrograph of the medial preoptic nucleus (MPN) of a sexually naïve female in diestrus. *B* Dark field photomicrograph of the MPN of a lactation day 19 female. *C* Fluorescent photomicrograph of the MPN of a lactation day 19 female. *D* Dark field photomicrograph of the paraventricular nucleus (PVH) of a sexually naïve female in diestrus. *E* Dark field photomicrograph of the PVH of a lactation day 19 female. *F* Fluorescent photomicrograph of the PVH of a lactation day 19 female. *G* Dark field photomicrograph of the lateral septum (LS) of a sexually naïve female in diestrus. *H* Dark field photomicrograph of the LS of a lactation day 19 female. *I* Fluorescent photomicrograph of the LS of a lactation day 19 female. *J* Dark field photomicrograph of the anterodorsal thalamic nucleus (AD) of a sexually naïve female in diestrus. *K* Dark field photomicrograph of the AD of a lactation day 19 female. (L) Fluorescent photomicrograph of the AD of a lactation day 19 female. Images are taken from levels 54/132 (MPNm), 58/132 (PVH), 50/132 (LS), and 58/132 (AD) (Allen Mouse Brain Atlas, 2004). Scale bar (A–L): 200 µm.
Abbreviations: ac, anterior commissure; AV, anteroventral nucleus of the thalamus; fi, fimbria; sm, stria medullaris; st, stria terminalis; V3, third ventricle; VL, lateral ventricle.

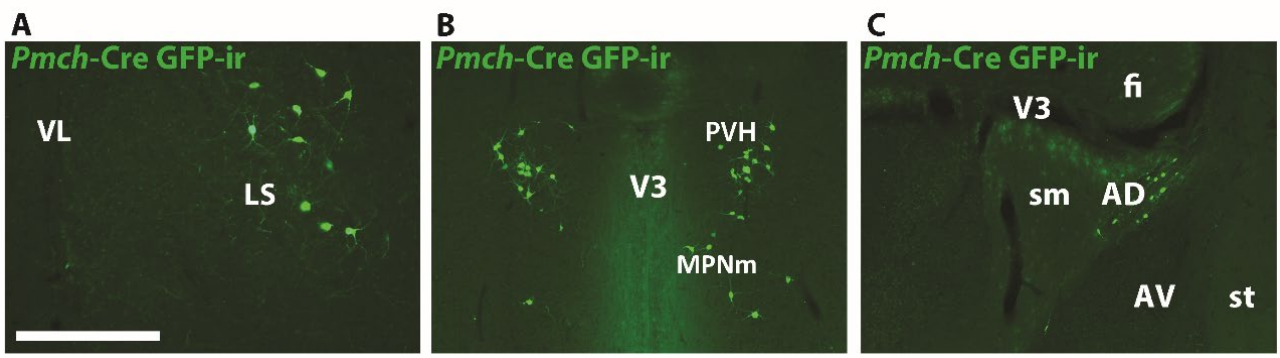

Figure 2-6. Cre-induced GFP expression in lactation-specific regions of the rostral forebrain is unchanged post-lactation.
Fluorescent micrographs showing GFP-ir in the LS *(A)*, PVH *(B)*, MPNm *(C)*, and AD *(D)* of female mice five days post-weaning. Images are taken from levels 54/132 (MPNm), 50/132 (LS), and 58/132 (PVH/AD) (Allen Mouse Brain Atlas).
Scale bar (A–D): 200 µm.
Abbreviations: AD, anterodorsal nucleus of the thalamus; AV, anteroventral nucleus of the thalamus; fi, fimbria; LS, lateral septum; MPNm, medial preoptic nucleus, medial part; sm, stria medullaris; st, stria terminalis; V3, third ventricle; VL, lateral ventricle.

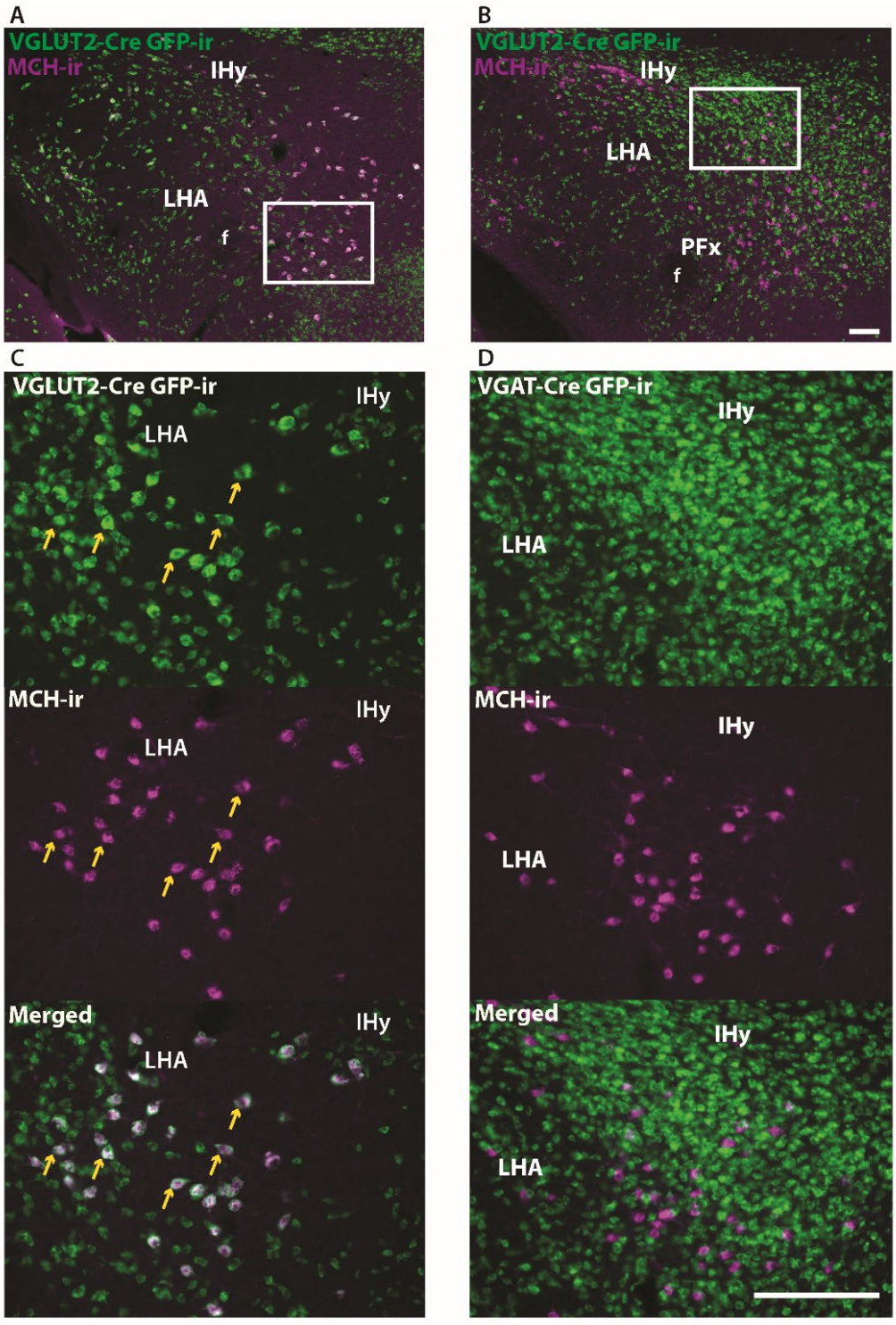

Figure 2-7. MCH- and Vglut2-Cre GFP-immunoreactivity are coexpressed in neurons of the tuberal and posterior hypothalamus. *A-C* Immunohistochemistry for MCH and GFP in the lateral hypothalamus of Vglut2-Cre;eGFP mice shows that MCH-ir neurons predominantly colocalize with VGLUT2 (arrows). *D-F* Immunohistochemistry for MCH and GFP in the lateral hypothalamus of Vgat-Cre;eGFP mice shows that MCH-ir neurons do not colocalize with VGAT. Images depict tissue from postpartum females on lactation day 19, but the same result was observed in sexually naïve males and females.
Scale bar: 200µm.
Abbreviations: IHy, incertohypothalamic area; LHA, lateral hypothalamic area.

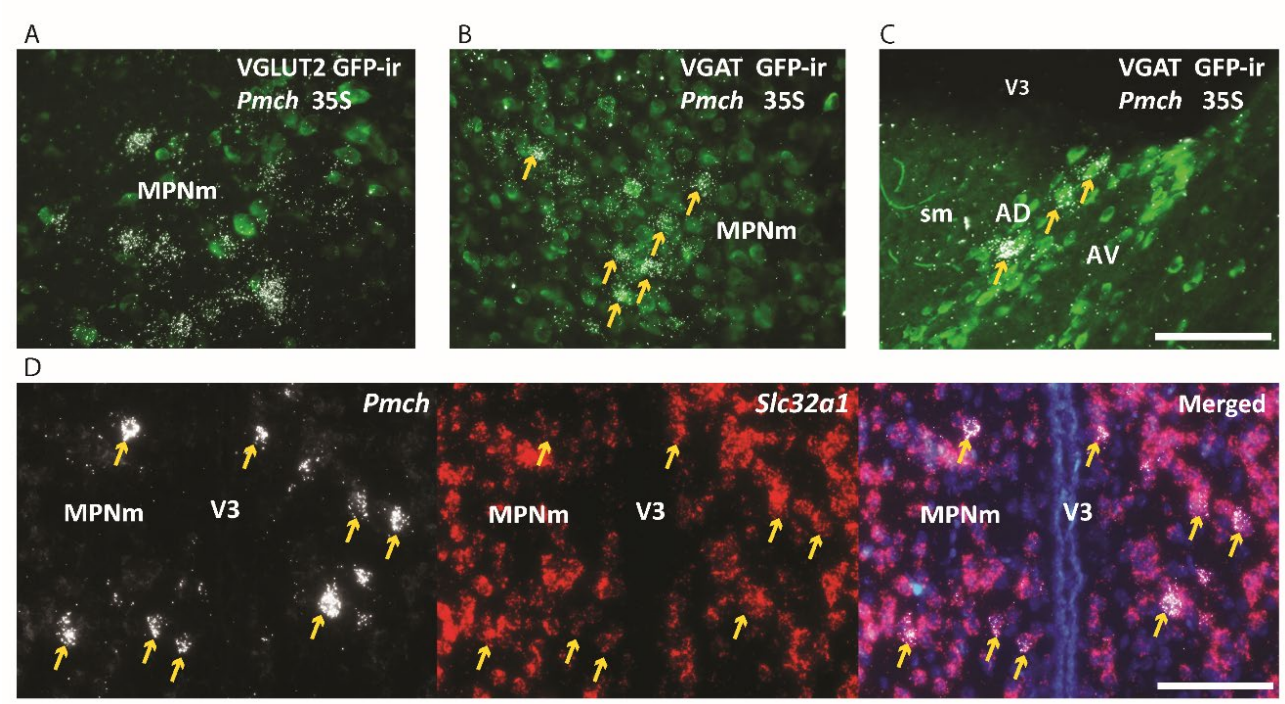

Figure 2-8. *Pmch* is expressed in rostral forebrain neurons that coexpress *Slc32a1* (VGAT). *A-B* Fluorescent and dark field micrographs showing the majority of *Pmch* in the MPN do not colocalize with VGLUT2 *(A)* but do colocalize with VGAT *(B)*. *(C)* Fluorescent and dark field micrograph showing the majority of *Pmch* in the AD also colocalizes with VGAT. *D-F* Fluorescent micrographs showing coexpression (arrows) of *Pmch* (white) and *Slc32a1* (red) in medial aspect of the medial preoptic nucleus (MPNm) using RNAscope® technology. DAPI counterstain in blue.
Scale bar: 100µm.
Abbreviations: AD, anterodorsal nucleus of the thalamus; AV, anteroventral nucleus of the thalamus; MPNm, medial preoptic nucleus, medial part; sm, stria medullaris; VL, lateral ventricle; V3, third ventricle.

References

1. Bahjaoui-Bouhaddi, M., et al., *Insulin treatment stimulates the rat melanin-concentrating hormone-producing neurons.* Neuropeptides, 1994. **27**(4): p. 251-8.
2. Qu, D., et al., *A role for melanin-concentrating hormone in the central regulation of feeding behaviour.* Nature, 1996. **380**(6571): p. 243-7.
3. Baker, B.I., D.J. Bird, and J.C. Buckingham, *Salmonid melanin-concentrating hormone inhibits corticotrophin release.* J Endocrinol, 1985. **106**(2): p. R5-8.
4. Verret, L., et al., *A role of melanin-concentrating hormone producing neurons in the central regulation of paradoxical sleep.* BMC Neurosci, 2003. **4**: p. 19.
5. Knollema, S., et al., *Novel hypothalamic and preoptic sites of prepro-melanin-concentrating hormone messenger ribonucleic Acid and Peptide expression in lactating rats.* J Neuroendocrinol, 1992. **4**(6): p. 709-17.
6. Attademo, A.M., et al., *Neuropeptide Glutamic Acid-Isoleucine May Induce Luteinizing Hormone Secretion via Multiple Pathways.* Neuroendocrinology, 2006. **83**(5-6): p. 313-24.
7. Bittencourt, J., et al., *The melanin-concentrating hormone system of the rat brain: an immuno-and hybridization histochemical characterization.* Journal of Comparative Neurology, 1992. **319**(2): p. 218-245.
8. Sita, L., C. Elias, and J. Bittencourt, *Connectivity pattern suggests that incerto-hypothalamic area belongs to the medial hypothalamic system.* 2007. **148**: p. 949-69.
9. Elias, C.F., et al., *Chemically defined projections linking the mediobasal hypothalamus and the lateral hypothalamic area.* J Comp Neurol, 1998. **402**(4): p. 442-59.
10. Bittencourt, J.C. and C.F. Elias, *Melanin-concentrating hormone and neuropeptide EI projections from the lateral hypothalamic area and zona incerta to the medial septal nucleus and spinal cord: a study using multiple neuronal tracers.* Brain Res, 1998. **805**(1-2): p. 1-19.
11. Elias, C.F. and J.C. Bittencourt, *Study of the origins of melanin-concentrating hormone and neuropeptide EI immunoreactive projections to the periaqueductal gray matter.* Brain Res, 1997. **755**(2): p. 255-71.
12. Casatti, C.A., et al., *Distribution of melanin-concentrating hormone neurons projecting to the medial mammillary nucleus.* Neuroscience, 2002. **115**(3): p. 899-915.
13. Diniz, G., et al., *Melanin-concentrating hormone peptidergic system: Comparative morphology between muroid species.* The Journal of Comparative Neurology, 2019.
14. Rondini, T.A., et al., *Chemical identity and connections of medial preoptic area neurons expressing melanin-concentrating hormone during lactation.* J Chem Neuroanat, 2010. **39**(1): p. 51-62.
15. Kong, D., et al., *Glucose stimulation of hypothalamic MCH neurons involves K(ATP) channels, is modulated by UCP2, and regulates peripheral glucose homeostasis.* Cell Metab, 2010. **12**(5): p. 545-52.
16. Krivega, I. and A. Dean, *Enhancer and promoter interactions-long distance calls.* Curr Opin Genet Dev, 2012. **22**(2): p. 79-85.
17. Dean, A., *On a chromosome far, far away: LCRs and gene expression.* Trends Genet, 2006. **22**(1): p. 38-45.
18. Mickelsen, L.E., et al., *Single-cell transcriptomic analysis of the lateral hypothalamic area reveals molecularly distinct populations of inhibitory and excitatory neurons.* Nat Neurosci, 2019. **22**(4): p. 642-656.

19. Teixeira, P.D.S., et al., *Regulation and neurochemical identity of melanin-concentrating hormone neurons in the preoptic area of lactating mice.* J Neuroendocrinol, 2019: p. e12818.
20. Mao, X., et al., *Activation of EGFP expression by Cre-mediated excision in a new ROSA26 reporter mouse strain.* Blood, 2001. **97**(1): p. 324-6.
21. Liu, J., et al., *Cell-specific translational profiling in acute kidney injury.* J Clin Invest, 2014. **124**(3): p. 1242-54.
22. Vong, L., et al., *Leptin action on GABAergic neurons prevents obesity and reduces inhibitory tone to POMC neurons.* Neuron, 2011. **71**(1): p. 142-54.
23. Sibony, M., et al., *Enhancement of mRNA in situ hybridization signal by microwave heating.* Laboratory Investigation, 1995. **73**(4): p. 586-91.
24. Frazão, R., et al., *Shift in Kiss1 cell activity requires estrogen receptor α.* J Neurosci, 2013. **33**(7): p. 2807-20.
25. Mohsen, Z., et al., *Sexually dimorphic distribution of Prokr2 neurons revealed by the Prokr2-Cre mouse model.* Brain Struct Funct, 2017. **222**(9): p. 4111-4129.
26. Garcia-Galiano, D., et al., *PI3Kα inactivation in leptin receptor cells increases leptin sensitivity but disrupts growth and reproduction.* JCI Insight, 2017. **2**(23).
27. Wang, F., et al., *RNAscope: a novel in situ RNA analysis platform for formalin-fixed, paraffin-embedded tissues.* J Mol Diagn, 2012. **14**(1): p. 22-9.
28. Jego, S., et al., *Optogenetic identification of a rapid eye movement sleep modulatory circuit in the hypothalamus.* 2013. **16**.
29. Varin, C., P.H. Luppi, and P. Fort, *Melanin-concentrating hormone-expressing neurons adjust slow-wave sleep dynamics to catalyze paradoxical (REM) sleep.* Sleep, 2018. **41**(6).
30. Dilsiz, P., et al., *MCH Neuron Activity Is Sufficient for Reward and Reinforces Feeding.* Neuroendocrinology, 2020. **110**(3-4): p. 258-270.
31. Madisen, L., et al., *A robust and high-throughput Cre reporting and characterization system for the whole mouse brain.* Nat Neurosci, 2010. **13**(1): p. 133-40.
32. Maston, G.A., S.K. Evans, and M.R. Green, *Transcriptional regulatory elements in the human genome.* Annu Rev Genomics Hum Genet, 2006. **7**: p. 29-59.
33. Yamaji, D., et al., *Sequential activation of genetic programs in mouse mammary epithelium during pregnancy depends on STAT5A/B concentration.* Nucleic Acids Res, 2013. **41**(3): p. 1622-36.
34. Ehret, G.B., et al., *DNA binding specificity of different STAT proteins. Comparison of in vitro specificity with natural target sites.* J Biol Chem, 2001. **276**(9): p. 6675-88.
35. Sapin, E., et al., *A very large number of GABAergic neurons are activated in the tuberal hypothalamus during paradoxical (REM) sleep hypersomnia.* PLoS One, 2010. **5**(7): p. e11766.
36. del Cid-Pellitero, E. and B.E. Jones, *Immunohistochemical evidence for synaptic release of GABA from melanin-concentrating hormone containing varicosities in the locus coeruleus.* Neuroscience, 2012. **223**: p. 269-276.
37. Chee, M.J., E. Arrigoni, and E. Maratos-Flier, *Melanin-concentrating hormone neurons release glutamate for feedforward inhibition of the lateral septum.* J Neurosci, 2015. **35**(8): p. 3644-51.
38. Schneeberger, M., et al., *Functional analysis reveals differential effects of glutamate and MCH neuropeptide in MCH neurons.* Mol Metab, 2018. **13**: p. 83-89.

39. Blanco-Centurion, C., et al., *Dynamic Network Activation of Hypothalamic MCH Neurons in REM Sleep and Exploratory Behavior.* The Journal of Neuroscience, 2019: p. 0305-19.
40. ROBERTS, E. and S. FRANKEL, *gamma-Aminobutyric acid in brain: its formation from glutamic acid.* J Biol Chem, 1950. **187**(1): p. 55-63.
41. Martin, D.L., *Regulatory properties of brain glutamate decarboxylase.* Cell Mol Neurobiol, 1987. **7**(3): p. 237-53.

Chapter III. Generation of *Pmch*-iCre Mice Using CRISPR/Cas9 Technology

Abstract

The use of bacterial artificial chromosomes (BACs) was once an extremely common method of genome engineering, and many transgenic animals created using this technology are still in wide use today. However, BAC transgenes are typically 80-200 kb in size and thus may be incapable of fully capturing the regulatory landscape of a gene, which may have promoter elements or enhancer regions located hundreds of thousands of bases away from the gene locus itself. This means that BAC transgene expression may not always reliably reflect expression patterns of the gene of interest, particularly in unique physiological circumstances such as lactation.

Previously, our group documented a dissociation between *Pmch* mRNA expression and Cre-induced reporter gene expression in commercially available BAC transgenic *Pmch*-Cre mice in lactating dams. As described in Chapter 2, *Pmch* mRNA, but not reporter gene, can be observed in the preoptic area and paraventricular nucleus of the hypothalamus in late lactation. We believed this could be due to a distant promoter region implicated in lactation-specific activation of *Pmch* gene expression which was not captured in the BAC transgene. To facilitate further investigation of the role of *Pmch* expression in the rostral hypothalamus during lactation, including the epigenetic regulation required for its activation, we used CRISPR/Cas9 technology to generate a novel *Pmch*-iCre knockin mouse line. The new transgenic mouse exhibits reporter gene expression in the POA and PVH of lactating dams which is in line with mRNA levels determined through *in situ* hybridization. It also exhibits GFP expression in additional sites, some of which have not been previously associated with the *Pmch* gene in mice, and some of which have not been reported at all; we believe these to be putative sites of developmental *Pmch* expression. If this is the case, this mouse line will facilitate the study of the *Pmch* system and its epigenetic regulation in diverse physiological states and enable the systematic characterization of the developmental role of the *Pmch* system.

Background

The generation of transgenic animals as scientific tools took off in the latter half of the 20th century when biologists began injecting exogenous genetic material into fertilized eggs [1, 2]. Early constructs for transgenesis largely consisted of short promoter transgenes such as those utilizing the pCAGs and ROSA26 promoters as well as the lentiviral *Ubc* and adenovirus EIIa promoters, as well as promoters from defined cell/tissue types like fat or neural cell promoters in order to drive tissue-specific transgene expression [3-12]. However, it quickly became clear that the regulatory elements for the genes being targeted were spread over a far larger area than could be captured in these 1-3 kb constructs. Subsequently, many early transgenic mice were generated by introducing a much larger (~200 kb) bacterial artificial chromosome (BAC) transgene into mouse embryos by pronuclear injection and implanting the modified embryos into pseudopregnant dams. A BAC transgene is created via the incorporation of a DNA construct containing the desired DNA fragment (i.e., reporter gene, modification cassette, etc.) flanked by homologous sequences from the BAC genomic DNA to facilitate integration of the fragment via homologous recombination in competent *E. coli* [13]. The BACs carrying the desired sequence can then be purified from cells by negative selection. Yeast and phage chromosomes have also been used to this end (YACs and PACs, respectively), but BACs have predominated as they have the advantages of greater stability and resistance to position effects than their yeast and phage counterparts, the ability to carry up to several hundred kilobases of DNA, and the ease of using bacteria for introduction of exogenous DNA and DNA purification [14, 15].

BAC transgenic animals have proven a powerful mechanism for studying developmental biology, gene expression and regulation, protein function, neural circuits, and potential gene therapy models. Mice generated by this method continue to be widely used across many disciplines of biology. However, there are several important considerations that accompany their use. There can be variation in transgene copy number, which may affect expression and integrity of the transgene (although the size of the BAC often limits the number of copies that are integrated to one) [16]. Furthermore, as discussed in Chapter 2, once a BAC transgene is injected into a fertilized embryo, the locus of insertion for the BAC is essentially random, which introduces the possibility that promoters and enhancers around the insertion site may impose additional layers of regulation on the expression of the transgene that are unrelated to the target gene [17, 18]. It also means the BAC may fail to recapitulate the entire regulatory landscape that

occurs at the native gene locus of the target gene, as enhancer regions for a given gene may be located many hundreds of kilobases up- or downstream, making them impossible to capture even in an extremely large BAC construct [19].

To avoid such "position effects" and the loss of control sequences that regulate transgene expression, gene targeting—the introduction of exogenous genomic DNA into a mammalian cell—can be performed directly in mouse embryonic stem (ES) cells in essentially the same way as it is in BACs. The desired sequence is flanked with arms of homology to encourage site-specific homologous recombination, although pronuclear injection of DNA constructs alone into mouse ES cells is inefficient [20-24]. The process is greatly enhanced by the addition of an engineered nuclease to induce a double-stranded break (DSB) at a target sequence, which can subsequently be repaired by one of two cellular processes: error-prone non-homologous end joining (NHEJ), in which DSBs are simply re-ligated with a high chance of creating insertion/deletion mutations (indels); or high-fidelity homology-directed repair (HDR), which utilizes a DNA template to repair the break by homologous recombination [25]. Zinc-finger endonucleases (ZFNs) and transcription activator-like effector nucleases (TALENs) are two commonly used technologies which employ the strategy of tethering a site-specific DNA binding protein to an endonuclease catalytic domain. ZFNs are fusions of the nuclease domain of a bacterial restriction enzyme, most often *Fok1*, and a DNA-binding zinc finger protein targeted to a specific nucleotide sequence, while TALENs are derived from transcription activator-like effectors from the genus of plant pathogens *Xanthomas* [26, 27].

More recently, the clustered regularly interspaced short palindromic repeats/CRISPR associated (CRISPR/Cas) system has gained traction as the most efficient, flexible, and specific method to date of introducing genetic mutations. CRISPR is a component of many prokaryotic adaptive immune systems which uses nucleases guided by specific RNA sequences to cleave foreign DNA [28-34]. CRISPR RNA (crRNA) recognizes and facilitates the destruction of foreign DNA sequences by forming a complex with a nuclease known as a CRISPR-associated (Cas9) protein. Each system is composed of Cas genes, noncoding RNAs, and a unique array of repetitive elements ("direct repeats") interleaved with *protospacers*—short, variable DNA sequences which are derived from exogenous (i.e., pathogenic) DNA [28, 35-37]. Collectively, the direct repeats and protospacers make up the crRNA array [35]. A given crRNA array, together with a

trans-activating crRNA (tracrRNA), comprise a crRNA unit containing a 20 bp guide sequence and a partial direct repeat. To make things even more efficient, in the lab, the crRNA and tracrRNA can be fused together into what is known as a "single guide RNA" (sgRNA).

The sgRNA is injected into ES cells along with the Cas protein to induce a DSB at a sequence determined by the guide RNA sequence. The guide sequence directs the Cas protein to the specific DNA target to be cleaved according to standard base pairing rules, but a short (2-6 bp) *protospacer-adjacent motif* (PAM) sequence must also flank the target sequence in order for the Cas protein to recognize the site and induce a DSB. In bacteria, the PAM sequence is recognized by Cas1 and Cas2, which are responsible for excising small DNA fragments from invading pathogens such as bacteriophages and integrating these into the crRNA array. The PAM sequence is never found in the direct repeats of the crRNA array, thus preventing the cell's Cas9 from destroying its own crRNA array. In the context of genetic engineering, this means that when designing CRISPR reagents, one must first identify locations of PAM sequences in the approximate location of the gene of interest and select potential guide sequences adjacent to PAM sequences.

In the study of reproductive neuroendocrinology, it is extremely important that any genetic modifications targeted to expression of a particular gene reflect that gene's expression across the lifespan and in diverse physiological contexts. Sexual differentiation, pubertal development, conspecific interactions including sexual interactions, pregnancy, lactation, and reproductive senescence are associated with epigenetic changes that may rely on enhancer regions far outside the limits of even the largest BAC transgenes [38-47]. The work covered in Chapter 2 describes the study of *Pmch*-driven expression of Cre recombinase using a BAC transgenic mouse model in lactating female mice and demonstrates that the existing commercially available *Pmch*-Cre mice may not be suitable for studying MCH in all physiological states, particularly lactation, because *Pmch* mRNA and Cre-induced reporter gene expression are found to be dissociated in the rostral hypothalamus during late lactation in the female mouse [18].

For this reason, we generated a new *Pmch*-Cre knockin mouse in collaboration with the University of Michigan's Transgenic Animal Model Core, ensuring that Cre recombinase expression would be subjected to the control of *all* regulatory elements present at the native *Pmch* gene locus. Given the already diverse and rapidly growing arsenal of tools and technology

available for CRISPR/*Cas* mediated genome editing, CRISPR/Cas9 technology was used to insert the sequence for codon-improved Cre recombinase ("iCre") between the final protein-coding codon and the termination codon of the *Pmch* gene, located on chromosome 10 in mouse (chromosome 12 in human, chromosome 7 in rat). The iCre sequence applies mammalian codon usage to the prokaryotic Cre sequence and thus contains numerous base substitutions which do not alter the peptide sequence but do improve Cre expression and reduce the chances of epigenetic silencing in mammals [48]. Our new animal model resolved the immediate issue of dissociated Cre and *Pmch* expression in the forebrain and rostral hypothalamus of lactating dams: *Pmch*-iCre;eGFP-L10a reporter mice show GFP expression in the expected cells of the POA, PVH, and forebrain nuclei of lactating dams where *Pmch* mRNA has been described in our lab [18]. Furthermore, these reporter mice have revealed the presence of GFP (a marker of Cre recombinase activity and a surrogate for *Pmch* expression), likely indicative of developmental MCH expression, in additional regions throughout the brain where MCH has not been previously reported.

Our findings open up major new avenues for research into epigenetic regulation of *Pmch* gene expression and the developmental role of MCH in the central nervous system. They also necessitate the careful consideration of each experiment's needs from its model organism. Future studies of the MCH system must consider whether it is more constructive to restrict Cre expression to those neurons which express MCH in adulthood, at the expense of potentially missing some conditional and/or transient expression; or to fully recapitulate the entire regulatory landscape of the *Pmch* gene in regulation of reporter genes and other modification cassettes, knowing that a significant number of neurons may be altered that are not actively expressing the MCH peptide.

Methods

Mice

Animal Care

Mice were housed in a vivarium at the University of Michigan with a 12/12 light/dark cycle and ad libitum access to food and water. While in the UM Transgenic Animal Core vivarium, animals received LabDiet 5008 (26% protein/16% fat). While in our lab's vivarium, the mice received phytoestrogen-reduced Envigo diet 2016 (16% protein/4% fat), except during breeding

when mice were fed phytoestrogen-reduced Envigo diet 2019 (19% protein/8% fat) to accommodate additional nutritional needs of pregnant and nursing dams. Phytoestrogen-reduced diet is routinely used in our laboratory to avoid the effects of exogenous estrogens on mouse physiology. All procedures and experiments were carried out in accordance with the guidelines established by the National Institutes of Health Guide for the Care and Use of Laboratory Animals and approved by the University of Michigan Committee on Use and Care of Animals (Animal Protocol # PRO00009706 [UM Transgenic Animal Core] and PRO00010420 [Elias Lab]).

Generation of transgenic Pmch-*iCre mice using CRISPR/Cas9 technology*

Clustered Regularly Interspaced Short Palindromic Repeats (CRISPR) and the CRISPR-associated protein Cas9 (CRISPR/Cas9) technology was used to insert codon improved Cre recombinase ("iCre") into the *Pmch* gene between the final protein-coding codon and the termination codon of the mouse *Pmch* (Ensembl gene ENSMUSG00000035383) in the same reading frame, as previously described [49, 50]. The endogenous *Pmch* polyadenylation signal in the 3' UTR is intact.

Design and validation of CRISPR reagents

The CRISPOR algorithm was used to identify specific single guide RNA targets (sgRNA) predicted to cut the chromosome near codon 165 [51]. sgRNA C258G1 (Table 3-1) with a high cutting frequency determination (CFD) specificity score of 88 [52] was obtained in the form of chemically modified synthetic sgRNA from MilliporeSigma [53]. Recombinant *Streptomyces pyogenes* Cas9 endonuclease was obtained from MilliporeSigma (CAS9PROT). C258G1 was assembled into sgRNA/Cas9 ribonucleoprotein (RNP) complexes (30 ng/ul sgRNA + 50 ng/ul Cas9) and tested by mouse zygote microinjection to determine if it induced chromosome breaks, as previously described [54]. Briefly, after RNP microinjection, zygotes were cultured *in vitro* to the blastocyst stage (about 64 cells per blastocyst). Subsequently, DNA was extracted from individual blastocysts and subjected to PCR and amplicon DNA sequencing to identify small insertions/deletions (indels) at the Cas9/sgRNA cut sites, indicative of NHEJ repair of DSBs induced by sgRNA/Cas9 complexes (Figure 3-1B,C). The amplicon size was 519 bp. Primer sequences used for PCR amplification and Sanger sequencing can be found in Table 3-1.

After the demonstration of effective Cas9 cleavage of the target, a Megamer® single-stranded DNA donor (Integrated DNA Technologies) was synthesized to serve as a template for high-fidelity HDR which included a P2A self-cleaving peptide sequence with a Gly-Ser-Gly linker between the last Pmch codon and the start of the iCre sequence and arms of homology (5' end: 100 bp; 3' end: 101 bp of genomic sequence) flanking the sgRNA target [55]. Numerous silent base substitutions were made in these homologous arms to discourage repeated recognition and cleavage at the target site as is routinely done by the UM Transgenic Animal Core [56].

Generation of transgenic founders

To generate mice carrying the *Pmch* iCre knockin, zygotes were obtained from the mating of B6SJLF1 (Jackson Laboratory stock no. 100012) female and male mice. Pronuclear microinjections were performed as previously described [57]. The microinjection mixture contained sgRNA C258G1 (30ng/ul) complexed with WTCAS9 protein (50ng/ul) and 10ng/ul of ssDNA. Surviving zygotes were transferred to pseudopregnant females. 106 potentially gene edited generation zero (G0) founder pups were screened for the iCre knockin by PCR amplicon sequencing. Those positive for iCre were subsequently sequenced at the 5' and 3' junctions to verify correct orientation of the donor fragment. Primers used for genotyping can be found in Table 3-1. G0 founder animals carrying the mutation were mated to wild type mice for germline transmission to G1 pups. Germline transmission was confirmed by genotyping the G1 animals for iCre as described above.

Validation of the Pmch-iCre mouse model

Single- and dual-label immunohistochemistry

Presence of functional iCre recombinase was confirmed by mating iCre positive G1 pups to B6;129S4-*Gt(ROSA)26Sor*$^{tm9(EGFP/Rpl10a)Amc}$/J mice kindly provided by Dr. David Olson, University of Michigan, and commercially available at JAX® (stock #024750, "eGFP-L10a") and checking the brains of the resulting adult male and female G2 offspring for GFP expression.

Cre-induced GFP expression was systematically mapped after four generations of backcrossing to wild-type mice (G4 mice). Adult sexually naïve male and female *Pmch*-iCre;eGFP-L10a mice as well as postpartum female *Pmch*-iCre;eGFP-L10a mice on day 19 of lactation (n=3 each) were deeply anesthetized with isoflurane and perfused with 10% formalin. Brains were dissected, postfixed for 2 hours in 10% formalin, and cryoprotected overnight using a solution of 20%

sucrose in PBS. Coronal sections (30 μm thickness, 4 series) were collected with a freezing microtome and stored in a cryoprotectant solution (20% glycerol/30% ethylene glycol in DEPC-treated PBS) at −20°C.

Dual-label immunohistochemistry (IHC) for MCH and GFP was performed in one series of brain sections from each animal. Antigen unmasking was performed as follows: free-floating sections were incubated in 1% NaOH and 1% H_2O_2 in dH_20 for 10 mins, then in 0.3% glycine in PBS for 10 mins, then in 0.03% sodium dodecyl sulfate (SDS) in PBS, with 3 washes in fresh PBS between each step. Sections were next blocked for 30 min in PBS-T with 3% normal donkey serum (NDS) and subsequently incubated overnight in blocking solution with chicken anti-GFP (1:10,000, Aves Labs, AB_2307317) and rabbit anti-MCH (1:5,000, Phoenix Pharmaceuticals, AB_2722682). Sections were rinsed three times in fresh PBS and incubated in PBS with secondary antisera (1:500 goat anti-chicken conjugated to Alexa FluorTM 488, AB_2534096, and 1:500 donkey anti-rabbit conjugated to Alexa FluorTM 594, AB_141637) for 1 h (Thermo Fisher Scientific). Sections were mounted onto gelatin-coated slides, air-dried, and coverslipped with Fluoromount G mounting medium (Electron Microscopy Sciences).

Analysis methods and generation of photomicrographs

Slides were examined under an Axio Imager M2 Microscope or a SteREO DiscoveryV8 (Zeiss). The digital Allen Mouse Brain Atlas was used as a reference to determine relative location within the hypothalamus and identify the primary sites containing MCH and GFP immunoreactivity. Images were acquired with a digital camera (Axiocam, Zeiss) using Zen software. Single- and dual-labeled cells were quantified in 20× magnification using ImageJ with the Cell Counter plugin in one representative section of each area of interest (i.e., IHy, PFx, LHA). For data illustration, only sharpness, contrast, and brightness were adjusted.

Results

A specific and active sgRNA was designed which cleaves the mouse *Pmch* gene 7 bp from its termination codon.

The CRISPOR algorithm was used to identify specific single guide RNA targets (sgRNA) predicted to cut the chromosome near codon 165 in exon 3 of the mouse *Pmch* gene (Figure 3-1A) [51]. This algorithm uses a constantly-updated database of the success of various guide sequences in different species and assigns sgRNAs a cutting frequency determination (CFD)

specificity score which predicts the activity and specificity of a given guide sequence to assign it a single numeral score that enables the quick comparison of potential guides [52]. sgRNA C258G1 (Table 3-1) was found to have a high CFD specificity score of 88 and deemed the most promising candidate. C258G1 was assembled into sgRNA/Cas9 ribonucleoprotein (RNP) complexes (30 ng/ul sgRNA + 50 ng/ul Cas9) and tested by mouse zygote microinjection to determine if it induced chromosome breaks, as previously described [54]. DNA was extracted from blastocysts and subjected to PCR to amplify a 519 bp fragment of the *Pmch* gene surrounding the putative cut site (Table 3-1). Amplicons were submitted to Eurofins Genomics for standard Sanger sequencing to determine if the sgRNA induced chromosome breaks as shown by "peaks-on-peaks" patterns in Sanger chromatograms that indicate the presence of multiple PCR templates that are present as a result of NHEJ repair of DSBs [58]. C258G1 induced chromosome breaks 7 bp from the termination codon (Figure 3-1B-C).

Five transgenic founders were generated which correctly integrated iCre into *Pmch,* exhibited normal fertility, and achieved germline transmission of the iCre knockin
Following demonstration of sgRNA activity, a single-stranded oligonucleotide DNA donor (ssODN) was designed and synthesized to serve as a template for high-fidelity HDR. The ssODN included a P2A self-cleaving peptide sequence with a Gly-Ser-Gly linker between the last Pmch codon and the start of the iCre sequence and arms of homology approximately 100 bp in length flanking the sgRNA target to facilitate homologous recombination (Figure 3-1D) [55]. To generate mice carrying the *Pmch* iCre knockin, zygotes were obtained from the mating of wild-type mice. Subsequently, a mixture of sgRNA C258G1 complexed with WTCAS9 protein and the ssODN were microinjected into the zygotes. Surviving zygotes were transferred to pseudopregnant females.

106 potentially gene edited generation zero (G0) chimeric founder pups were screened for the iCre knockin by PCR. Of these, 19 were determined to be iCre positive (Figure 3-1D). A fragment at both the 3' and 5' ends of the ssODN, spanning the junction between the ssODN and the endogenous genome, was used to screen those 19 G0 mice for correct integration of the iCre sequence. 18 mice were positive for the 3' junction fragment and of those, 5 mice were positive for both the 3' and 5' junction bands (Figure 3-1E,F). Those 5 mice were presumed to contain the iCre sequence incorporated into the genome in the correct orientation.

G0 founder animals carrying the mutation were mated to wild type mice to determine germline transmission to G1 pups. Germline transmission was confirmed by genotyping for iCre in G1 pups as above. The mice are observed to be of normal fertility and body weight.

Primer sequences used to genotype for iCre and to amplify the 5' and 3' junction fragments can be found in Table 3-1.

Presence of functional iCre recombinase was confirmed by breeding *Pmch*-iCre mice to a reporter line.

The functionality of the iCre recombinase was confirmed by mating G1 *Pmch*-iCre mice to a Cre-inducible reporter line ("eGFP-L10a") and checking the brains of resulting adult male and female G2 offspring for appropriate GFP expression using immunohistochemistry for MCH and GFP. All MCH-immunoreactive cells were found to express GFP (Figure 3-2). Furthermore, GFP expression was observed in the POA and PVH of dams on lactation day 19 in accordance with previously documented *Pmch* mRNA expression in late lactation ([18, 59-62], Chapter 2) (Figure 3-3A, B). Interestingly, we also observe sparse GFP labeling in the PVH of both virgin male and female mice, though it appears to be reduced in the male, and in the POA of virgin females, but not males (Figure 3-3C-F).

The dense cluster of very small, round GFP+/MCH- cells surrounding the fornix, particularly at the level of the tuberal LHA, that we reported in the BAC transgenic line ([18, 59-62], Chapter 2) is also present in our new *Pmch*-iCre knock-in. (Figure 3-4A). There are also GFP+/MCH- cells of similar morphology in the dorsal aspect of the ZIm as well, expanding into the external medullary lamina of the thalamus (Figure 3-4B). In addition, we observe GFP+/MCH- cells in a number of sites throughout the brain where *Pmch* mRNA has not been previously reported in the mouse, though some have been documented in the rat brain. GFP+/MCH- cells are observed in the olfactory tubercle, concentrated in the islands of Calleja, and in the pontine reticular formation, as has been reported [63] (Figure 3-5A-C). Novel sites of dense GFP expression include the taenia tecta, primarily the ventral part (TTv); the piriform cortex, layer 1 (PIR1); the medial septum/diagonal band (MS/NDB), the ventral part of the lateral septum (LSv), the arcuate nucleus; the lateral geniculate nucleus, especially the ventral part (LGv)[1]; the external cuneate

[1] Expression in the LGv appears to be sexually dimorphic, with GFP visible at more levels of the nucleus in females than in males. Specifically, in females, GFP can be seen in the most rostral aspect of the LGv, when the LGv is

nucleus (ECU); principal sensory nucleus of the trigeminal nerve (PSV); the spinal nucleus of the hypoglossal nerve (XII); and (Figure 3-5C-O).

Discussion

In the present study, we describe the generation and characterization of a transgenic knockin model for the study of the MCH system. The *Pmch*-iCre mice express iCre recombinase driven by the *Pmch* promoter, visualized by crossing to eGFP-L10a reporter mice. The pattern of iCre-induced GFP expression was assessed in mice heterozyogus for the mutation and compared with previous published data as well as our group's analysis of MCH peptide and *Pmch* mRNA distribution [18, 64]. Further validation of the mouse model was performed using dual label immunohistochemistry. Expression of iCre-induced GFP and MCH immunoreactivity were largely congruent. In late lactation dams, iCre-induced GFP expression aligns with lactation-induced *Pmch* mRNA expression in the POA and PVH ([18], Chapter 2). All MCH+ cells expressed GFP. GFP+/MCH- cells were also observed in several additional sites, which may be regions of developmental *Pmch* expression. The heterozygous animals are fertile and have no obvious abnormal metabolic phenotype.

Interestingly, GFP is also observed in the POA and PVH of sexually naïve females and, to a lesser extent, males, though expression is not as high as it is during late lactation in either group. While transient expression of *Pmch* has been documented in this region in lactating dams, it has never been reported previously in sexually naïve male or female animals ([18, 59-62]; Chapter 2). Indeed, we observe a clear gradient of expression, with the lowest levels found in sexually naïve male mice, moderate expression in sexually naïve female mice, and, as discussed previously, the highest levels seen in sexually experienced females on lactation day 19. We report a similar "gradient" of GFP expression in the paraventricular hypothalamic nucleus, another region previously only believed to express *Pmch* in late-lactation dams; beyond its putative role in lactation and parental care, this region is a hub for neuroendocrine and autonomic control, associated with many systems including, but not limited to, reproduction, stress, and metabolism [65]. Thus, expression here could be related to the organization of numerous

situated more dorsally, very close to the fourth ventricle. In males, it does not appear until the middle part of the LGv.

neuroendocrine circuits and processes, though the differences in expression levels seem to indicate some connection to both lactation and to biological sex.

It is plausible that low levels of *Pmch* expression in these areas during early development help establish the circuitry which is later re-activated during lactation, though this does not explain the presence of sparse GFP labeling in this region in the sexually naïve male. Future studies should investigate whether GFP levels in the male can be modulated by exposure to pups and, given the clear significance of the *Pmch* gene to the olfactory system, perhaps other pheromonal and/or reproduction-oriented stimuli such as a sexually receptive female. GFP is also observed in both sexes in the lateral septum, ventral part (LSv), where changes in prolactin receptor expression have also been documented in the LSv during lactation in rats [66].

Finally, GFP is observed in the arcuate nucleus of the hypothalamus (ARH). It has been suggested based on immunohistochemical competition experiments that cross-reactivity with epitopes on MCH, NEI, or NGE could account for a-MSH described in the dorsolateral hypothalamus, in addition to several other peptides [63]. In particular, α-MSH has a C-terminal amide motif in common with NEI, and faint labeling of cells in the ARH which are believed to be α-MSH+, but not NEI+, has been reported with the use of anti-NEI antibodies [63]. This faint labeling is reported only with the use of colchicine pretreatment, suggesting that a high concentration of α-MSH in the cell is required—but an alternate explanation could be that these neurons express NEI in development, but expression levels are too low, at least in adulthood, to detect without some means of concentrating the peptide in the perikarya. Or, perhaps the faint labeling is truly due to cross-reactivity of the NEI antibody with epitopes on α-MSH, but developmental expression of one or more products of the *Pmch* gene is required for the organization of circuits involving α-MSH neurons of the ARH. Given the strong relationship between α-MSH and MCH, this seems particularly plausible.

The complexity of the MCH system cannot be overstated. It is always important to consider these additional peptide products of the *Pmch* gene, as well as both coding and noncoding non-canonical transcripts including the alternative-splicing gene product MCH-gene-overprinted-polypeptide (MGOP) and the antisense-RNA-overlapping-MCH (AROM) [67-70] (For additional review, see [71, 72]). Every site of GFP expression documented here, not just the ARH, might be expressing or NEI, NGE, or some non-canonical transcript with an as-of-yet

undefined regulatory role within the cell. It may utilize more than one of these peptides, either concurrently, or at different points throughout development. Extensive characterization of the sites of GFP reported here at different prenatal timepoints will be required to understand the scope of developmental *Pmch* expression and function.

In future experiments utilizing Cre driver lines to probe the *Pmch* system, it must be carefully considered whether the BAC transgenic *Pmch*-Cre mouse model or this novel *Pmch*-iCre knock-in will best serve the experimenter's purposes. *Pmch* expression during early postnatal development, i.e., the first two months of life, has been shown to be important for normal energy homeostasis [73]. However, the contributions of co-expressed neurotransmitters in MCH neurons to energy homeostasis during this time period has not been thoroughly investigated, nor has the role of *Pmch* expression during prenatal development on metabolism or other functions. This new transgenic mouse line has revealed previously unreported brain regions to be putative developmental sites of *Pmch* expression. Future experiments should be dedicated to the systematic characterization of *Pmch* mRNA expression in the developing brain to confirm that developmental *Pmch* expression can explain the sites of GFP+/MCH- cells and, if so, to map expression in specific areas to given developmental time points in an effort to begin to understand its neurodevelopmental function.

Given that other products of the *Pmch* gene besides the MCH peptide itself likely are differentially regulated, the new *Pmch* knockin may also be beneficial, as the use of a knock-in at the endogenous gene locus rather than a randomly incorporated BAC transgene ensures that the regulation of not just MCH but also NEI, NGE, and other gene products of the *Pmch* gene, are fully recapitulated with the expression of iCre recombinase. Finally, in situations where it is important that iCre recombinase expression reflects *Pmch* gene expression in diverse physiological states, such as lactation, the new mouse model described here will likely do so more reliably, as its situation at the endogenous *Pmch* gene locus means its regulation more completely recapitulates that of the *Pmch* gene itself.

In the case of conditional knockins/knockouts or functional manipulations like chemo- or optogenetics, particularly if MCH neurons of the ZIm and tuberal hypothalamus are the focus, using the original BAC transgenic mouse may prove more practical. The BAC transgenic *Pmch*-Cre mouse reliably expresses Cre recombinase in ZIm, PFx, and LHA MCH+ neurons in adult

mice without the extensive confounds and caveats that come with developmentally-driven Cre recombinase expression in regions outside the area of interest.

Acknowledgements

We acknowledge Thomas L. Saunders, Elizabeth Hughes, Wanda Filipiak, and Galina Gavrilina and the Transgenic Animal Model Core of the University of Michigan's Biomedical Research Core Facilities for design and production of the Pmch iCre transgenic mice. Research reported in this publication was supported by the National Cancer Institute of the National Institutes of Health under award number P30CA046592.

Table 3-1. Primer sequences used in the generation of a new *Pmch*-iCre mouse.

Name	**Sequence**	**Purpose**
sgRNA C258G1	TTGGCAAGTCTGATACCTGC (TGG)	Single-guide RNA for generation of Pmch-iCre mice
Blastocyst DNA—Forward	CCATAGGAAGGAGAGATTTTGACAGTGAG	Amplify blastocyst DNA around cut site for sequencing
Blastocyst DNA—Reverse	GCAGAATTATGCAGAACTTTTGTGAGGTT	Amplify blastocyst DNA around cut site for sequencing
iCre FWD Primer	GACAGGCAGGCCTTCTCTGAA	Check for presence of iCre recombinase sequence
iCre REV Primer	CTTCTCCACACCAGCTGTGGA	Check for presence of iCre recombinase sequence
5' Junction Site—Forward	GAGATTTTGACATGCTCAGGTGT	Verify donor construct integration in correct orientation
5' Junction Site—Reverse	CAGGTGCTGTTGGATGGTCT	Verify donor construct integration in correct orientation
3' Junction Site—Forward	GCCCTTCTGACTCCAATGCT	Verify donor construct integration in correct orientation
3' Junction Site—Reverse	TGTGAGGTTTAATGCACACGTC	Verify donor construct integration in correct orientation

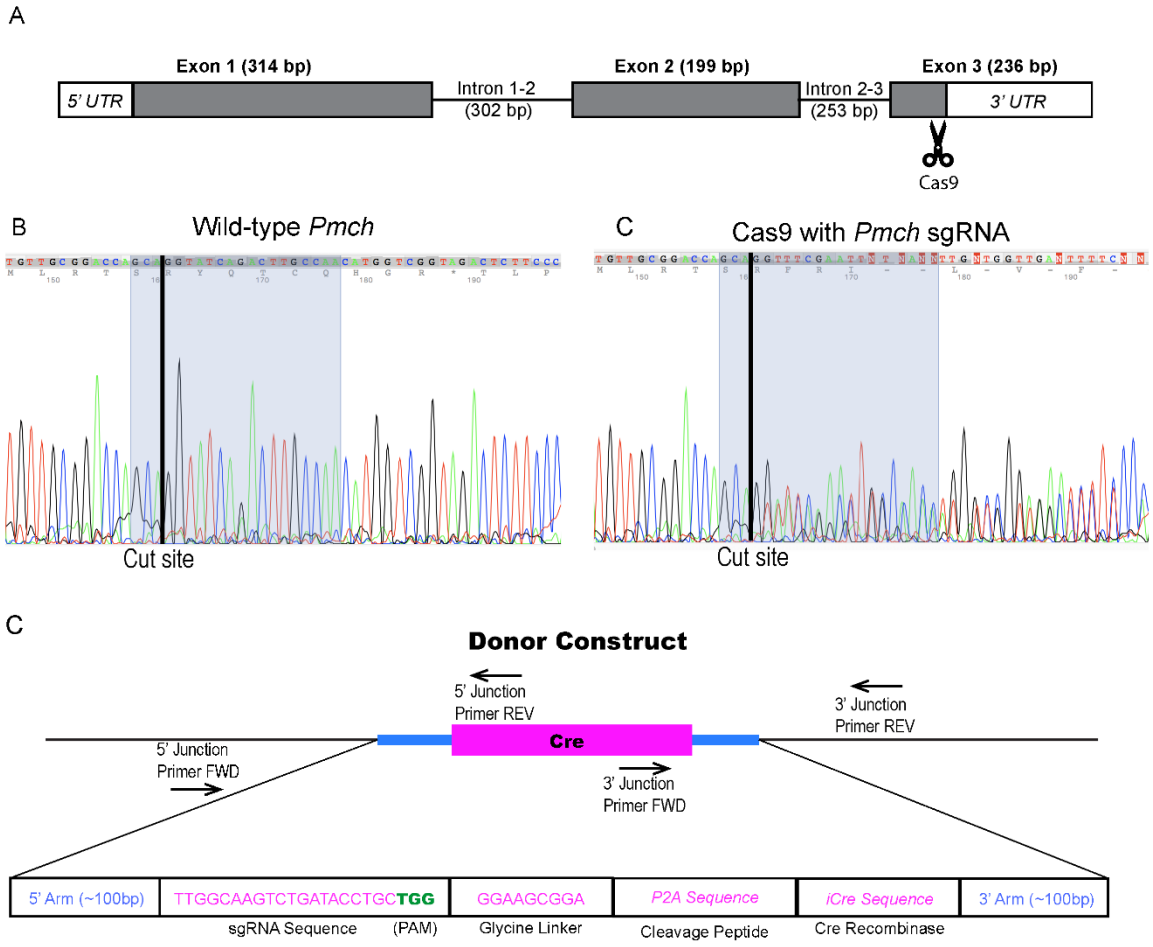

Figure 3-1: Overview of generation of a novel *Pmch*-iCre knockin mouse model using CRISPR/Cas9 technology. (A) Schematic showing site in Exon 3 of the murine *Pmch* gene where the construct containing the iCre sequence is to be inserted. (B, C) Sanger sequencing chromatogram of WT (B) and sample (C) blastocysts. Note that the WT blastocyst shows single resolved peaks while sample blastocyst DNA exhibits "peaks on peaks" indicative of non-homologous end joining and subsequent insertion/deletion mutations. (D) Schematic diagram of the donor construct used to generate *Pmch*-iCre mice showing the position of 5' and 3' junction site primers used to confirm integration of the donor construct in the correct orientation.

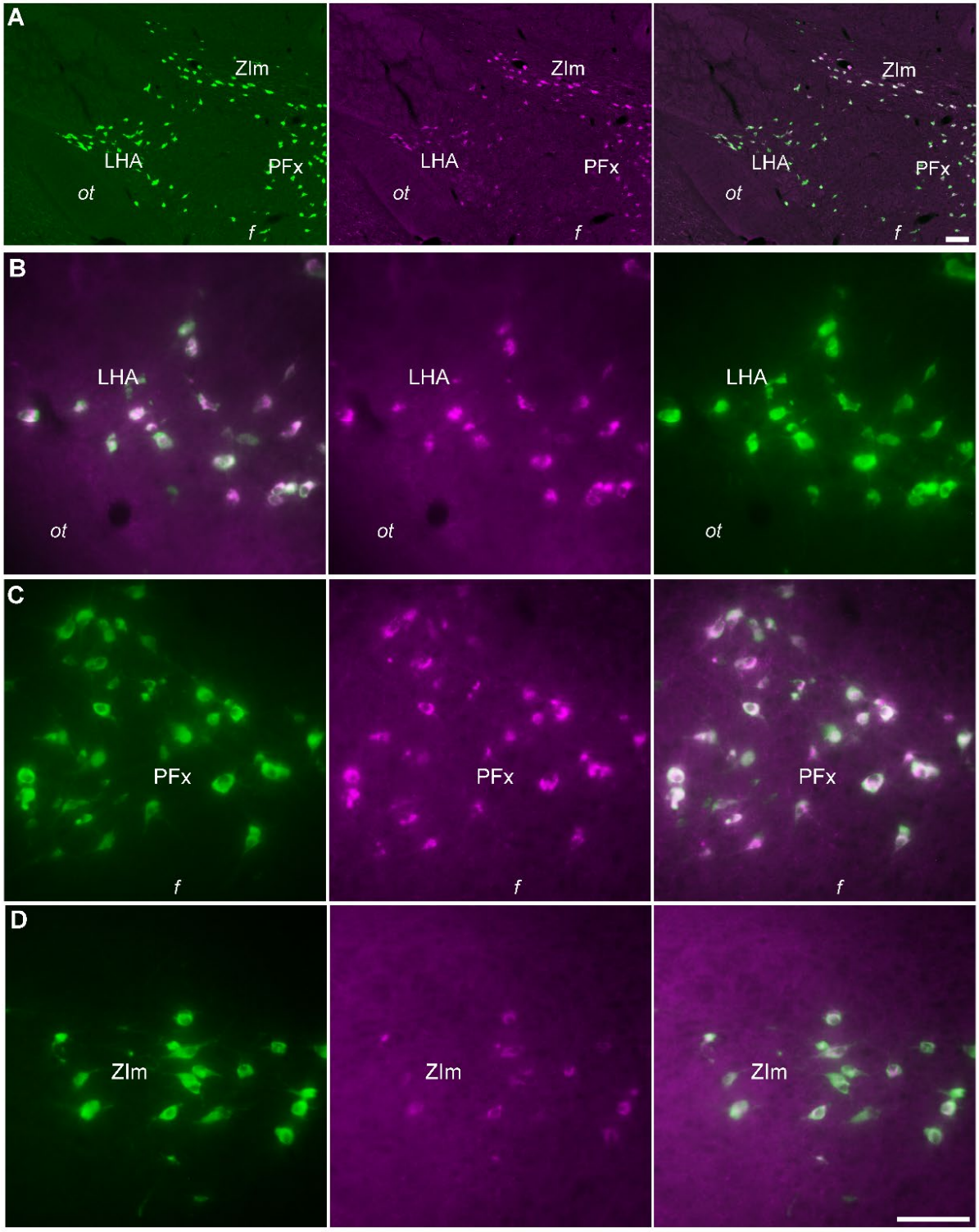

Figure 3-2. Virtually 100% of MCH+ neurons colocalize GFP when *Pmch*-iCre mice are bred to eGFP-L10a reporter line. (A) Distribution of Cre-induced GFP expression (*left*), MCH-immunoreactive cells (*center*) and merged images showing virtually 100% colocalization of GFP and MCH immunoreactivity (*right*). (B) High-magnification image of the LHA showing colocalization (*right*) of GFP (*left*) and MCH immunoreactive cells (*center*). (C) High-magnification image of the PFx showing colocalization (*right*) of GFP (*left*) and MCH immunoreactive cells (*center*). (D) High-magnification image of the ZIm showing colocalization (*right*) of GFP (*left*) and MCH immunoreactive cells (*center*). Scale bars=100µm. *Abbreviations:* f=fornix, LHA=lateral hypothalamic area, PFx=perifornical area, ZIm=zona incerta, medial part.

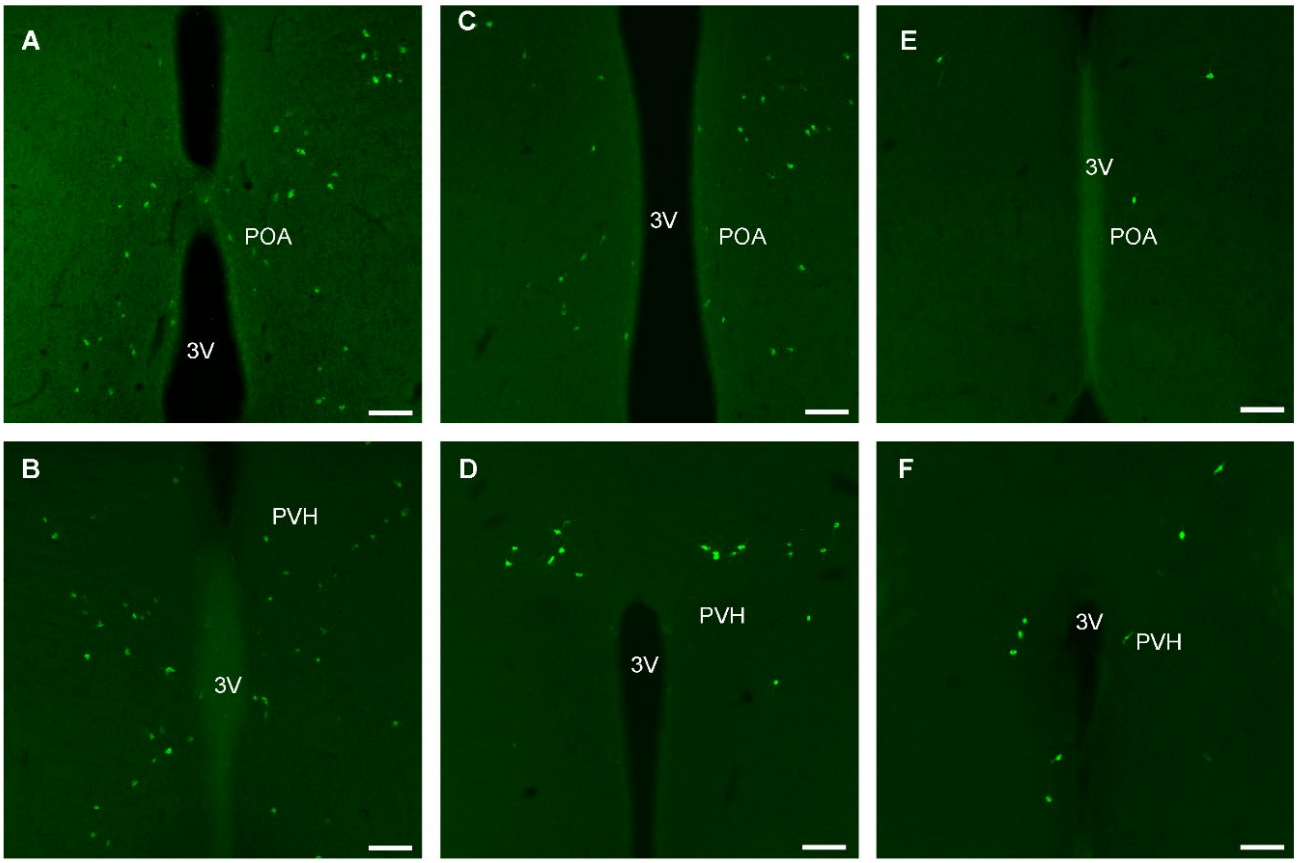

Figure 3-3. Cre-induced GFP expression in the POA and PVH of lactating *Pmch*-iCre dams recapitulates previously observed *Pmch* mRNA expression levels, but also sparsely labels cells in the POA and PVH of sexually naïve male and female mice. (A) POA of lactating female. (B) PVH of lactating female. (C) POA of sexually naïve female. (D) PVH of sexually naïve female. (E) POA of sexually naïve male. (F) PVH of sexually naïve male. Scale bars=100µm. *Abbreviations: POA=preoptic area, PVH=paraventricular hypothalamic nucleus, 3V=third ventricle*.

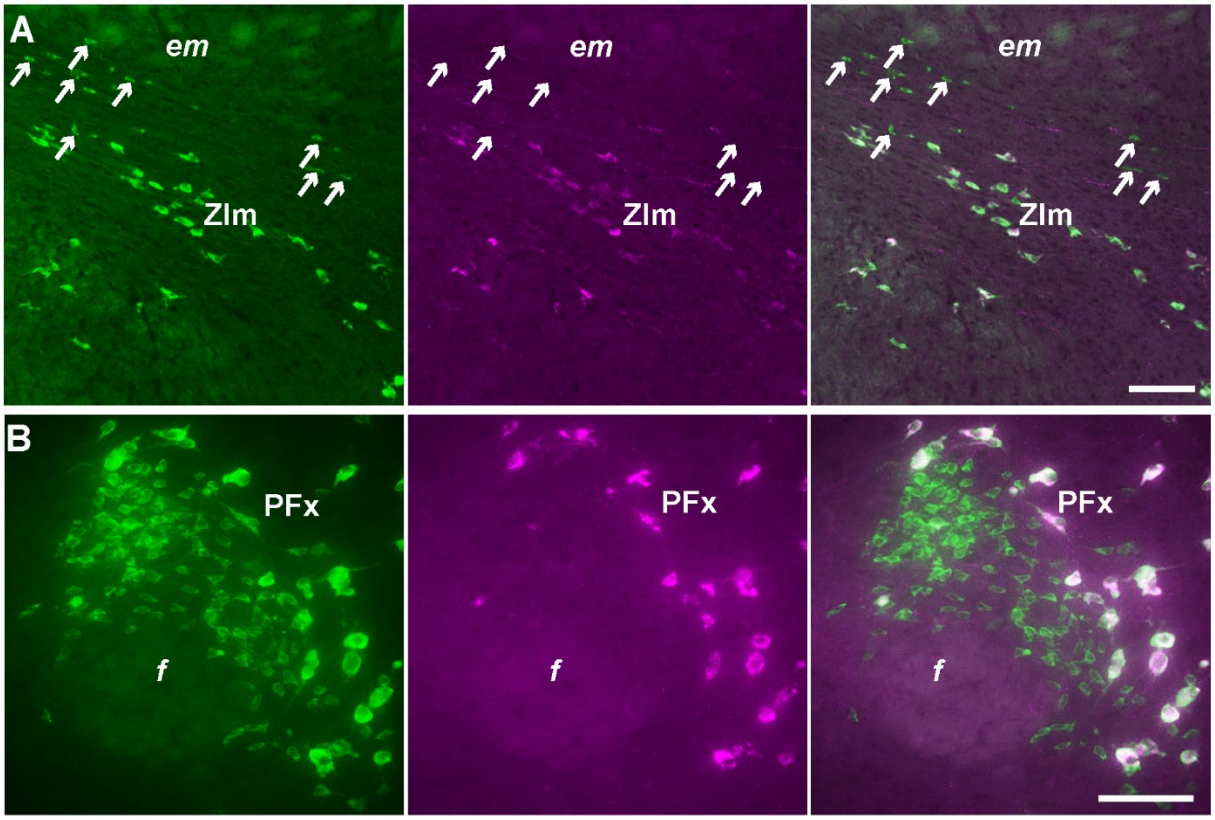

Figure 3-4. GFP+/MCH- cells are observed in the PFx and dorsal aspect of ZIm in *Pmch*-iCre male and female mice. (A) Distribution of Cre-induced GFP expression (*left*), MCH-immunoreactive cells (*center*) and merged images showing the presence of numerous GFP+/MCH- cells in the dorsal aspect of the ZIm. (A) Distribution of Cre-induced GFP expression (*left*), MCH-immunoreactive cells (*center*) and merged images showing the presence of numerous GFP+/MCH- cells in the dorsolateral aspect of the PFx. Scale bars=100µm. *Abbreviations: em=external medullary lamina of the thalamus, f=fornix, PFx=perifornical area, ZIm=zona incerta, medial part.*

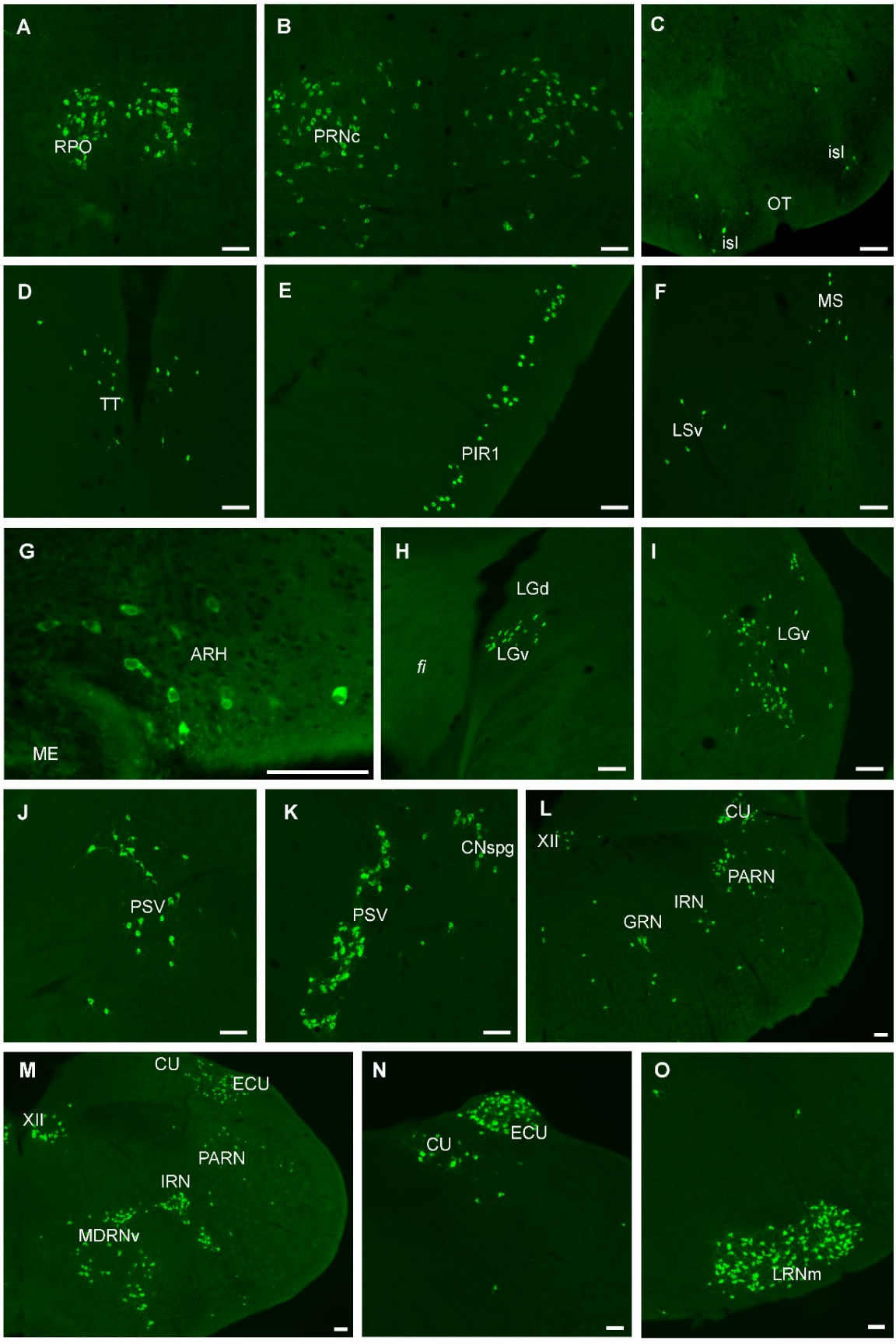
A
RPO
B
PRNc
C
isl
OT
isl
D
TT
E
PIR1
F
MS
LSv
G
ARH
ME
H
LGd
LGv
fi
I
LGv
J
PSV
K
CNspg
PSV
L
CU
XII
PARN
IRN
GRN
M
CU
ECU
XII
PARN
IRN
MDRNv
N
ECU
CU
O
LRNm

Figure 3-5. Several regions in the forebrain and brainstem express GFP but not MCH in the adult mouse when *Pmch*-iCre mice are bred to eGFP-L10a reporter line. *A* Moderate to dense GFP labeling is observed in the RPO. *B* Moderate GFP labeling is observed in the PRNc. *C* Moderate GFP labeling is observed in the OT, particularly in the islets of Calleja. *D* Moderate labeling is observed in the TT, primarily the ventral part. *E* Moderate to dense GFP labeling is observed in PIR1. *F* Sparse to moderate labeling is observed in the LSv and MS. *G* Sparse to moderate labeling is observed in the ARH. *H, I* Moderate to dense labeling is observed in the LG. *J,K* Moderate to dense labeling is observed in CNspg and PSV. *L-O* Moderate labeling is observed in CU, ECU, GRN, IRN, LRNm, mDRNv, PARN, and XII. Note that the density of labeling varies at different levels of the reticular nuclei and the ECU.
Scale bars=100μm.
Abbreviations: ARH=arcuate nucleus of the hypothalamus; CN=cochlear nucleus; CU=cuneate nucleus; ECU=external cuneate nucleus; GRN=gigantocellular reticular nucleus; IRN=intermediate reticular nucleus; isl=islands of Calleja; LGd=lateral geniculate body, dorsal part; LGv=lateral geniculate body, ventral part; LRNm=lateral reticular nucleus, magnocellular part; LSv=lateral septum, ventral part; ME=median eminence; MS=medial septum; MDRNv=medullary reticular nucleus, ventral part; OT=olfactory tubercle; PIR1=piriform cortex, layer 1; PARN=parvicellular reticular nucleus; PRNc=pontine reticular nucleus, caudal part; PSV=principal sensory nucleus of the trigeminal nerve; RPO=nucleus raphe pontis; TT=taenia tecta; XII=hypoglossal nucleus.

References

1. Saunders, T.L., *The History of Transgenesis.* Methods Mol Biol, 2020. **2066**: p. 1-26.
2. Jackson, D.A., R.H. Symons, and P. Berg, *Biochemical method for inserting new genetic information into DNA of Simian Virus 40: circular SV40 DNA molecules containing lambda phage genes and the galactose operon of Escherichia coli.* Proc Natl Acad Sci U S A, 1972. **69**(10): p. 2904-9.
3. Saunders, T., *New Transgenic Technologies*, in *Movement Disorders: Genetics and Models*, M.S. LeDoux, Editor. 2015.
4. Hayashi, S. and A.P. McMahon, *Efficient recombination in diverse tissues by a tamoxifen-inducible form of Cre: a tool for temporally regulated gene activation/inactivation in the mouse.* Developmental biology, 2002. **244**(2): p. 305-318.
5. Lee, Y.-j., et al., *Elevated global SUMOylation in Ubc9 transgenic mice protects their brains against focal cerebral ischemic damage.* PloS one, 2011. **6**(10): p. e25852.
6. Miyazaki, J., *Efficient selection for high-expression transfectants with a novel eukaryotic vector.* Gene, 1989. **79**: p. 269-277.
7. Lois, C., et al., *Germline transmission and tissue-specific expression of transgenes delivered by lentiviral vectors.* science, 2002. **295**(5556): p. 868-872.
8. Kisseberth, W.C., et al., *Ubiquitous expression of marker transgenes in mice and rats.* Developmental biology, 1999. **214**(1): p. 128-138.
9. Kato, T., et al., *Phenotypic characterization of transgenic mice overexpressing neuregulin-1.* PloS one, 2010. **5**(12): p. e14185.
10. Madisen, L., et al., *A robust and high-throughput Cre reporting and characterization system for the whole mouse brain.* Nat Neurosci, 2010. **13**(1): p. 133-40.
11. Valet, P., et al., *Understanding adipose tissue development from transgenic animal models.* J Lipid Res, 2002. **43**(6): p. 835-60.
12. van de Sluis, B. and J.W. Voncken, *Transgene design.* Methods Mol Biol, 2011. **693**: p. 89-101.
13. Yang, X.W., P. Model, and N. Heintz, *Homologous recombination based modification in Escherichia coli and germline transmission in transgenic mice of a bacterial artificial chromosome.* Nat Biotechnol, 1997. **15**(9): p. 859-65.
14. Heintz, N., *BAC to the future: the use of bac transgenic mice for neuroscience research.* Nat Rev Neurosci, 2001. **2**(12): p. 861-70.
15. Giraldo, P. and L. Montoliu, *Size matters: use of YACs, BACs and PACs in transgenic animals.* Transgenic Res, 2001. **10**(2): p. 83-103.
16. Chandler, K.J., et al., *Relevance of BAC transgene copy number in mice: transgene copy number variation across multiple transgenic lines and correlations with transgene integrity and expression.* Mamm Genome, 2007. **18**(10): p. 693-708.
17. Dean, A., *On a chromosome far, far away: LCRs and gene expression.* Trends Genet, 2006. **22**(1): p. 38-45.
18. Beekly, B.G., et al., *Dissociated Pmch and Cre Expression in Lactating Pmch-Cre BAC Transgenic Mice.* Frontiers in Neuroanatomy, 2020. **14**(60).
19. Krivega, I. and A. Dean, *Enhancer and promoter interactions-long distance calls.* Curr Opin Genet Dev, 2012. **22**(2): p. 79-85.
20. Thomas, K.R. and M.R. Capecchi, *Site-directed mutagenesis by gene targeting in mouse embryo-derived stem cells.* Cell, 1987. **51**(3): p. 503-12.

21. Smithies, O., et al., *Insertion of DNA sequences into the human chromosomal beta-globin locus by homologous recombination.* Nature, 1985. **317**(6034): p. 230-4.
22. Thomas, K.R. and M.R. Capecchi, *Introduction of homologous DNA sequences into mammalian cells induces mutations in the cognate gene.* Nature, 1986. **324**(6092): p. 34-8.
23. Hasty, P. and A. Bradley, *Gene targeting vectors for mammalian cells*, in *Gene Targeting: A Practical Approach*, A. Joyner, Editor. 1993, Oxford University Press: Oxford, UK.
24. Lin, F.L., K. Sperle, and N. Sternberg, *Recombination in mouse L cells between DNA introduced into cells and homologous chromosomal sequences.* Proc Natl Acad Sci U S A, 1985. **82**(5): p. 1391-5.
25. Jasin, M. and R. Rothstein, *Repair of strand breaks by homologous recombination.* Cold Spring Harb Perspect Biol, 2013. **5**(11): p. a012740.
26. Carbery, I.D., et al., *Targeted genome modification in mice using zinc-finger nucleases.* Genetics, 2010. **186**(2): p. 451-9.
27. Urnov, F.D., et al., *Genome editing with engineered zinc finger nucleases.* Nat Rev Genet, 2010. **11**(9): p. 636-46.
28. Barrangou, R., et al., *CRISPR provides acquired resistance against viruses in prokaryotes.* Science, 2007. **315**(5819): p. 1709-12.
29. Horvath, P. and R. Barrangou, *CRISPR/Cas, the immune system of bacteria and archaea.* Science, 2010. **327**(5962): p. 167-70.
30. Wiedenheft, B., S.H. Sternberg, and J.A. Doudna, *RNA-guided genetic silencing systems in bacteria and archaea.* Nature, 2012. **482**(7385): p. 331-8.
31. Deveau, H., J.E. Garneau, and S. Moineau, *CRISPR/Cas system and its role in phage-bacteria interactions.* Annu Rev Microbiol, 2010. **64**: p. 475-93.
32. Makarova, K.S., et al., *Evolution and classification of the CRISPR-Cas systems.* Nat Rev Microbiol, 2011. **9**(6): p. 467-77.
33. Bhaya, D., M. Davison, and R. Barrangou, *CRISPR-Cas systems in bacteria and archaea: versatile small RNAs for adaptive defense and regulation.* Annu Rev Genet, 2011. **45**: p. 273-97.
34. Garneau, J.E., et al., *The CRISPR/Cas bacterial immune system cleaves bacteriophage and plasmid DNA.* Nature, 2010. **468**(7320): p. 67-71.
35. Ran, F.A., et al., *Genome engineering using the CRISPR-Cas9 system.* Nat Protoc, 2013. **8**(11): p. 2281-2308.
36. Marraffini, L.A. and E.J. Sontheimer, *CRISPR interference limits horizontal gene transfer in staphylococci by targeting DNA.* Science, 2008. **322**(5909): p. 1843-5.
37. Brouns, S.J., et al., *Small CRISPR RNAs guide antiviral defense in prokaryotes.* Science, 2008. **321**(5891): p. 960-4.
38. Gegenhuber, B. and J. Tollkuhn, *Epigenetic Mechanisms of Brain Sexual Differentiation.* Cold Spring Harb Perspect Biol, 2022. **14**(11).
39. Manotas, M.C., et al., *Genetic and Epigenetic Control of Puberty.* Sex Dev, 2022. **16**(1): p. 1-10.
40. Fang, Q., et al., *Individuality and Transgenerational Inheritance of Social Dominance and Sex Pheromones in Isogenic Male Mice.* J Exp Zool B Mol Dev Evol, 2016. **326**(4): p. 225-36.

41. Stolzenberg, D.S. and H.S. Mayer, *Experience-dependent mechanisms in the regulation of parental care.* Front Neuroendocrinol, 2019. **54**: p. 100745.
42. Andrawus, M., L. Sharvit, and G. Atzmon, *Epigenetics and Pregnancy: Conditional Snapshot or Rolling Event.* Int J Mol Sci, 2022. **23**(20).
43. Sjoeholm, A., et al., *Region-, neuron-, and signaling pathway-specific increases in prolactin responsiveness in reproductively experienced female rats.* Endocrinology, 2011. **152**(5): p. 1979-88.
44. Sapsford, T.J., et al., *Differential sensitivity of specific neuronal populations of the rat hypothalamus to prolactin action.* J Comp Neurol, 2012. **520**(5): p. 1062-77.
45. Wang, S., et al., *Identification and functional analysis of m 6 A in the mammary gland tissues of dairy goats at the early and peak lactation stages.* Front Cell Dev Biol, 2022. **10**: p. 945202.
46. Bilmez, Y., G. Talibova, and S. Ozturk, *Dynamic changes of histone methylation in mammalian oocytes and early embryos.* Histochem Cell Biol, 2022. **157**(1): p. 7-25.
47. Bilmez, Y., G. Talibova, and S. Ozturk, *Expression of the histone lysine methyltransferases SETD1B, SETDB1, SETD2, and CFP1 exhibits significant changes in the oocytes and granulosa cells of aged mouse ovaries.* Histochem Cell Biol, 2022. **158**(1): p. 79-95.
48. Shimshek, D.R., et al., *Codon-improved Cre recombinase (iCre) expression in the mouse.* Genesis, 2002. **32**(1): p. 19-26.
49. Cong, L., et al., *Multiplex genome engineering using CRISPR/Cas systems.* Science, 2013. **339**(6121): p. 819-23.
50. Quadros, R.M., et al., *Easi-CRISPR: a robust method for one-step generation of mice carrying conditional and insertion alleles using long ssDNA donors and CRISPR ribonucleoproteins.* Genome Biol, 2017. **18**(1): p. 92.
51. Haeussler, M., et al., *Evaluation of off-target and on-target scoring algorithms and integration into the guide RNA selection tool CRISPOR.* Genome Biol, 2016. **17**(1): p. 148.
52. Cram, D., et al., *WheatCRISPR: a web-based guide RNA design tool for CRISPR/Cas9-mediated genome editing in wheat.* BMC Plant Biol, 2019. **19**(1): p. 474.
53. Hendel, A., et al., *Chemically modified guide RNAs enhance CRISPR-Cas genome editing in human primary cells.* Nat Biotechnol, 2015. **33**(9): p. 985-989.
54. Sakurai, T., et al., *A single blastocyst assay optimized for detecting CRISPR/Cas9 system-induced indel mutations in mice.* BMC Biotechnol, 2014. **14**: p. 69.
55. Jasin, M. and J.E. Haber, *The democratization of gene editing: Insights from site-specific cleavage and double-strand break repair.* DNA Repair (Amst), 2016. **44**: p. 6-16.
56. Kim, J.H., et al., *High cleavage efficiency of a 2A peptide derived from porcine teschovirus-1 in human cell lines, zebrafish and mice.* PLoS One, 2011. **6**(4): p. e18556.
57. Van Keuren, M.L., et al., *Generating transgenic mice from bacterial artificial chromosomes: transgenesis efficiency, integration and expression outcomes.* Transgenic Res, 2009. **18**(5): p. 769-85.
58. Etard, C., et al., *Tracking of Indels by DEcomposition is a Simple and Effective Method to Assess Efficiency of Guide RNAs in Zebrafish.* Zebrafish, 2017. **14**(6): p. 586-588.
59. Rondini, T.A., et al., *Chemical identity and connections of medial preoptic area neurons expressing melanin-concentrating hormone during lactation.* J Chem Neuroanat, 2010. **39**(1): p. 51-62.

60. Alvisi, R.D., et al., *Suckling-induced Fos activation and melanin-concentrating hormone immunoreactivity during late lactation.* Life Sci, 2016. **148**: p. 241-6.
61. Teixeira, P.D.S., et al., *Regulation and neurochemical identity of melanin-concentrating hormone neurons in the preoptic area of lactating mice.* J Neuroendocrinol, 2019: p. e12818.
62. Knollema, S., et al., *Novel hypothalamic and preoptic sites of prepro-melanin-concentrating hormone messenger ribonucleic Acid and Peptide expression in lactating rats.* J Neuroendocrinol, 1992. **4**(6): p. 709-17.
63. Bittencourt, J., et al., *The melanin-concentrating hormone system of the rat brain: an immuno-and hybridization histochemical characterization.* Journal of Comparative Neurology, 1992. **319**(2): p. 218-245.
64. Diniz, G., et al., *Melanin-concentrating hormone peptidergic system: Comparative morphology between muroid species.* The Journal of Comparative Neurology, 2019. **527**(18): p. 2973-3001.
65. Qin, C., J. Li, and K. Tang, *The Paraventricular Nucleus of the Hypothalamus: Development, Function, and Human Diseases.* Endocrinology, 2018. **159**(9): p. 3458-3472.
66. Mann, P.E. and R.S. Bridges, *Prolactin receptor gene expression in the forebrain of pregnant and lactating rats.* Brain Res Mol Brain Res, 2002. **105**(1-2): p. 136-45.
67. Nahon, J.L., et al., *The rat melanin-concentrating hormone messenger ribonucleic acid encodes multiple putative neuropeptides coexpressed in the dorsolateral hypothalamus.* Endocrinology, 1989. **125**(4): p. 2056-65.
68. Toumaniantz, G., J.C. Bittencourt, and J.L. Nahon, *The rat melanin-concentrating hormone gene encodes an additional putative protein in a different reading frame.* Endocrinology, 1996. **137**(10): p. 4518-21.
69. Borsu, L., F. Presse, and J.L. Nahon, *The AROM gene, spliced mRNAs encoding new DNA/RNA-binding proteins are transcribed from the opposite strand of the melanin-concentrating hormone gene in mammals.* J Biol Chem, 2000. **275**(51): p. 40576-87.
70. Moldovan, G.L., et al., *Inhibition of homologous recombination by the PCNA-interacting protein PARI.* Mol Cell, 2012. **45**(1): p. 75-86.
71. Bittencourt, J. and M.E. Celis, *Anatomy, function and regulation of neuropeptide EI (NEI).* Peptides, 2008. **29**(8): p. 1441-50.
72. Bittencourt, J.C., *Anatomical organization of the melanin-concentrating hormone peptide family in the mammalian brain.* Gen Comp Endocrinol, 2011. **172**(2): p. 185-97.
73. Mul, J.D., et al., *Pmch expression during early development is critical for normal energy homeostasis.* Am J Physiol Endocrinol Metab, 2010. **298**(3): p. E477-88.

Chapter IV. Fast neurotransmitter identity of MCH neurons: do contents depend on context?

Abstract

Hypothalamic melanin-concentrating hormone (MCH) neurons participate in many fundamental neuroendocrine processes. While some of their effects can be attributed to MCH itself, others appear to depend on co-released neurotransmitters. Historically, the subject of fast neurotransmitter co-release from MCH neurons has been contentious, with data to support MCH neurons releasing GABA, glutamate, both, and neither. Rather than assuming a position in that debate, this review considers the evidence for all sides and presents an alternative explanation: neurochemical identity, including classical neurotransmitter content, is subject to change. With an emphasis on the variability of experimental details, we posit that MCH neurons may release GABA and/or glutamate at different points according to environmental and contextual factors. Through the lens of the MCH system, we offer evidence that the field of neuroendocrinology would benefit from a more nuanced and dynamic interpretation of neurotransmitter identity.

Introduction

Melanin-concentrating hormone (MCH) is a cyclic 19-amino acid (aa) neuropeptide encoded by the *Pmch* gene which was first described in teleost fishes, where it aggregates melanin in the scales to facilitate adaptive color change [1]. In mammals, MCH neurons serve as major homeostatic integrators with roles in a wide range of neuroendocrine processes. Most MCH expression in the brain is in neurons of the incertohypothalamic area (IHy, alternatively medial zona incerta, ZIm), the perifornical area (PFx), and the lateral hypothalamic area (LHA) [2-4], all of which are involved in essential functions like energy balance, reproduction, and the stress response [5-9]. MCH neurons are perhaps best known for their role in sleep regulation. They are active during sleep, and optogenetic stimulation of MCH neurons significantly increases sleep duration, particularly that of REM sleep [10-16]. Additionally, MCH neurons have a well-documented role in feeding, body weight regulation, and glucose sensing [17-19]. They are

putative regulators of reproductive physiology, projecting to areas such as the medial preoptic nucleus (MPO) and the median eminence (ME), which harbor gonadotropin-releasing hormone (GnRH) cell bodies and terminals, respectively [20, 21]. The MCH peptide has also been implicated in immune function [22]; psychiatric disorders including drug addiction [23]; depression and anxiety [24]; learning and memory [25]; and olfaction, aggression, and parental behavior [26, 27]. With such a diverse array of neuroendocrine functions, many of which pertain to existing nation- and worldwide health crises such as obesity, infertility, mental health, and substance use disorders, there is an urgent need to more completely understand how these neurons operate in a variety of physiological and environmental contexts.

In addition to MCH, there are at least two other peptide products of the mammalian *Pmch* gene, the 13-aa neuropeptide glutamic acid-isoleucine (NEI) and the 19-aa neuropeptide glycine-glutamic acid (NGE), as well as both coding and noncoding non-canonical transcripts [28-32] (For review, see [33, 34]). In rodents and primates, most MCH neurons also contain NEI and NGE [28, 35-37]. In addition to NEI and NGE, some MCH neurons produce the neuropeptide cocaine- and amphetamine-regulated transcript (CART) and express the gene for secretogranin II (*ScgII*) which is cleaved into two secreted peptides, secretoneurin and EM66 [38]. (For review, see [39-42]). Finally, MCH neurons express numerous genes involved in the synthesis, packaging, and release of the classical neurotransmitters GABA and glutamate, which are the central nervous system's predominant inhibitory and excitatory neurotransmitters, respectively [38, 43-46].

Both GABA and glutamate are found extensively throughout the hypothalamus, and their co-release with other hypothalamic neuropeptides is well-documented [38, 47-51]. However, the question of whether MCH neurons co-release GABA, glutamate, both, or neither has been a surprisingly contentious one for decades. Rather than offering clarity, technical improvements in histological and molecular methods like *in situ* hybridization and single-cell RNA sequencing have only muddied the waters further by increasing the pool of data supporting each claim. Getting to the bottom of this conundrum is of critical importance, as consideration of co-released neurotransmitters and peptides should be incorporated into every aspect of MCH research. Particularly where its implications for sleep, metabolism, and psychiatric disease are concerned, there is potential for the development of therapeutics targeting the MCH system; parsing MCH

effects *vs* effects of other co-released peptides and neurotransmitters in MCH neurons may inform the design of future clinical studies.

In this review, we discuss the histological, physiological, and molecular evidence for GABA and glutamate release from MCH neurons. Rather than attempt to "resolve" the question of co-transmission in MCH neurons, we emphasize the wide variety of experimental methods and conditions used in published studies and present an alternative interpretation: neurochemical identity, including classical neurotransmitter content, is not a static property. We are often too quick to dismiss a result that does not agree with accepted findings. However, if technical errors can be, within reason, ruled out as the sole cause of the variation, we may benefit from slowing down and getting curious about these inconsistencies. MCH neurons may preferentially use GABA or glutamate at different points across the lifespan of an organism according to developmental stage, life history events, sex, estrous cycle stage, and/or environmental and other contextual factors. Defining these nuances will require great attention to scientific methods and experimental designs.

Histology

Markers of canonical fast neurotransmission

Perhaps the simplest way to frame the question of classical neurotransmitter co-release is to ask whether GABA and/or glutamate colocalize with MCH. Methods to directly label GABA and glutamate are limited in mice, although antibodies with reactivity in rats do exist. Colocalization of MCH- and glutamate-immunoreactivity has been reported in the rat LHA [52]. More commonly, histological studies target other components of the cellular machinery associated with GABAergic and glutamatergic neurotransmission. However, the many components of GABA and glutamate synthesis, packaging, and release are imperfect indicators, with some providing a more reliable proxy for actual GABAergic or glutamatergic transmission than others (Table 4-1).

One common marker used to identify GABAergic cells is glutamic acid decarboxylase-67 (*Gad1*/GAD67), one of two enzymes responsible for the conversion of glutamate to GABA. An early study using radioactive *in situ* hybridization in brain sections from adult male rats to characterize neurons expressing CART in the LHA found that 75% of neurons containing CART mRNA (*Cartpt*) also contained *Pmch*, while 53% of *Cartpt* cells contained *Gad1* [53]. While not

the focus of the study, this finding does imply that a subset of *Pmch*+ neurons must also be *Gad1*+. Subsequent studies sought to further characterize this *Pmch+/Gad1+* population, showing that the majority—85-87%—of *Pmch*+ neurons in the LHA co-expressed *Gad1* in adult male mice and rats [12, 54, 55].

More recently, it was reported that a significant percentage but nevertheless a minority of MCH neurons expressed GAD67 immunoreactivity. In this study, the retrograde tracer Fluorogold (FG) was injected into the cerebrospinal fluid (CSF) of adult male rats to identify MCH neurons that have access to the cerebral ventricles. Of the approximately 1/3 of MCH neurons contacting the ventricles ("MCH+/FG+ neurons"), 45% were immunoreactive to GAD67, while 23.5% of those that did not contact the ventricles ("MCH+/FG- neurons") were immunoreactive to GAD67 [56]. This works out to just over 30% of the entire population of MCH neurons expressing GAD67, with clear differences in incidence observed between hodologically distinct populations. As mentioned in the Introduction, MCH expression is not limited to the LHA *per se*, extending into the neighboring IHy and PFx. The incongruity of these data may therefore reflect the presence of differing transcriptional profiles between subpopulations as defined by the locations of the perikarya as well as the dendrites. It is also possible that *Gad1* mRNA is transcribed in many more MCH cells than effectively translated into protein, leaving it in reserve to be quickly translated if the need arises. In this case, *in situ* hybridization would detect a greater percentage of dual-labeled cells than immunohistochemistry.

An additional enzyme capable of converting glutamate to GABA is glutamic acid decarboxylase-65 (*Gad2*/GAD65). While the two GAD enzymes are very similar in structure, kinetics, and function, they serve distinct roles within the cell. GAD67 primarily synthesizes GABA that is used for extra-synaptic and metabolic purposes, while GAD65 regulates the vesicular pool of GABA for release [57]. This makes *Gad2*/GAD65 expression potentially more relevant to the question of co-released neurotransmitters than *Gad1*/GAD67. Unfortunately, very few studies have examined the expression of *Gad2*/GAD65 in MCH neurons. Using mice expressing channelrhodopsin-eYFP in MCH neurons (*Pmch*-Cre;ChR2-eYFP mice) and antibodies against GAD65, a study showed GAD65 puncta in YFP+ fibers contacting paraventricular oxytocin neurons of lactating female mice as well as adult male mice that had been exposed to pups [58]. To our knowledge, this study constitutes the only published data regarding the presence of GAD65 immunoreactivity in lateral hypothalamic MCH cells. It is worth highlighting the

physiological state of the mice used; the possibility that GAD65 expression in MCH cells is specific to a certain reproductive state such as pregnancy, lactation, or parental care cannot be ruled out. Further immunohistochemical and sequencing experiments should be performed to resolve this ambiguity.

There is precedent for suspecting lactation-specific alterations to the MCH system: a population of neurons in the medial preoptic area (MPO) transiently express MCH in lactating mice and rats [59, 60]. Those MCH neurons have been shown using radioisotope-labeled riboprobes to co-express *Gad1* in the rat [61]. Our lab has strengthened this claim by using RNAscope to show that MPO *Pmch*+ neurons also express the gene for vesicular GABA transporter (VGAT/*Slc32a1*) in the mouse [62]. However, we and others have used both RNAscope and VGAT/VGLUT2-GFP reporter lines to show that in mice, *Pmch/Slc32a1* and MCH/VGAT colocalization is restricted to the MPO of lactating dams, while 97-100% of constitutively-MCH+ neurons express VGLUT2/*Slc17a6* and not VGAT/*Slc32a1* in virgin males, virgin females, and lactating females [62, 63].

As the process of packaging neurotransmitter into vesicles is directly related to the release of neurotransmitter into the synaptic cleft, the presence of transporter-associated genes may be considered a more reliable marker for cells which participate in canonical GABA and/or glutamate release than synthesis-associated genes. Thus, we find the presence of VGLUT2 and the absence of VGAT to be compelling evidence that MCH neurons in the LHA, IHy, and ZIm release glutamate transported by VGLUT2, while the presence of VGAT and absence of VGLUT2 supports the model of GABA transported by VGAT in transitory MPO MCH neurons. Yet these results are contradicted by other studies which showed virtually no colocalization of MCH immunoreactivity with VGAT-GFP/VGAT-EYFP, VGLUT2-GFP/VGLUT2-EYFP, or VGLUT3 immunoreactivity in the MPO of lactating mice, and no or only a very small amount of colocalization between VGLUT2-GFP and MCH immunoreactivity in the LHA of male, female, and lactating mice [46, 60].

Expression of glutamatergic transmission markers was also investigated in ventricle projecting MCH neurons of male rats. No *Slc17a6* (VGLUT2), *Slc17a7* (VGLUT1), or *Slc17a8* (VGLUT3) mRNA was observed in MCH+/FG+ cells [56]. We cannot speculate as to the presence of vesicular glutamate transporters in the other ~66% of MCH neurons that do not contact the CSF based on this study, as MCH+/FG- neurons were not assessed in this instance. However,

elsewhere, high levels of *Slc17a6* in the IHy and scattered expression of *Slc17a8* throughout the LHA were reported in rats, but despite MCH neurons being abundant in both of these hypothalamic sites, no colocalization of MCH with either vesicular glutamate transporter was observed [64].

The failure to detect one or more of these markers could always be an artifact of the probes, transgenic mice, and/or antibodies being used—for instance, the VGLUT3 antibody commonly used in mice labels cell bodies in the hypothalamus poorly, preferentially labeling dendrites instead [60]. The procedures involved in generating histological data can introduce a high degree of variability: subtle differences in tissue fixation and preparation, temperature, and pH are just a few factors which may result in an antibody performing well in one experiment and poorly in another. Some reporters also label perikarya less effectively (e.g., TdTomato and ChR2-eYFP); when the labeling of cell bodies is important, a reporter suited to that purpose such as L10eGPF may be more reliable (Figure 4-1A, B). Furthermore, the number of alleles with the transgene is often not declared when using Cre lines in combination with Cre-driven reporters, but there are instances where this has been shown to make a difference in reporter gene expression. For example, our group has noted that mice hemizygous for LepR-Cre have fewer reporter-labeled cells in the arcuate nucleus than mice homozygous for LepR-Cre. We also note that reporter expression in LepR-Cre;TdTomato mice homozygous for LepR-Cre appears more similar to leptin-induced PSTAT3 immunoreactivity in the arcuate nucleus, reinforcing that mice homozygous for LepR-Cre exhibit reporter expression that is more true to actual LepR expression levels (Figure 4-1C-E).

Without diverse techniques to corroborate a finding and a granular degree of experimental detail, any given study is challenging to evaluate on its own. This is particularly relevant for females as physiologic conditions such as pregnancy/parturition and lactation have the potential to transiently alter the MCH system. Such alterations might feasibly include neurotransmitter co-release. Such physiological changes and contexts may result in similar alterations to other neuronal populations that are yet undocumented. Some combinatorial effect of the specific subpopulation of neurons, physiological state, sex, and/or the sexual experience of the animal (i.e., naïve or of proven fertility) may ultimately determine neurotransmitter identity.

The puzzle is complicated further by the fact that it is not common practice in all fields of neuroscience to report whether animals used for histology were single *vs* group housed, had ever

been used for breeding, were cycling regularly or were in a particular estrous cycle phase, etc. Indeed, these are often considered more relevant to physiology or behavioral experiments and are usually afterthoughts for histology. Yet it is well-established that such variables can alter gene expression. VGAT and VGLUT expression is incredibly dynamic throughout early development [65]. Even in adulthood, expression levels of VGAT, GAD67, VGLUT2, and VGLUT3 can be modulated by numerous factors including physical lesions to the brain, alterations to the serotonin system, and dopaminergic inputs [66-68]. Furthermore, "dual-phenotype" neurons have been identified in the preoptic area of female rats, and their ratios of VGAT- and VGLUT2-positive vesicles fluctuate with estradiol levels [69].

Markers of non-canonical fast neurotransmission

While VGAT and VGLUTs are indicators of a cell's ability to canonically release GABA and glutamate, respectively, it's important to note they do not necessarily predict whether a cell *does* release GABA or glutamate under given physiological conditions. Conversely, it has also been shown that neither VGAT nor GAD enzymes are strictly required for GABAergic neurotransmission. Non-canonical methods of GABA release which utilize vesicular monoamine transporter 2 (VMAT2/*Slc18a2*) instead of VGAT have been documented [70]. Furthermore, midbrain dopamine neurons lack GAD67, GAD65, and VGAT and cannot participate in *de novo* GABA synthesis. Instead, they seem to recycle GABA for co-release using two membrane GABA transporters, GAT1 (*Slc6a1*) and GAT3 (*Slc6a11*) to reuptake GABA and subsequently release it in a VMAT2-dependent manner [71, 72]. Mice lacking GAT1 in dopamine neurons ($Dat^{\text{IRES-Cre/+}}$;$Gat1^{\text{fl/fl}}$) and controls ($Dat^{\text{IRES-Cre/+}}$;$Gat1^{+/+}$) were subjected to optogenetic stimulation in the substantia nigra, which in wild-type mice will elicit GABA-dependent iPSCs. The iPSCs were abolished in the $Dat^{\text{IRES-Cre/+}}$;$Gat1^{\text{fl/fl}}$ mice, demonstrating that GAT1 is required for these neurons to release GABA and thus revealing a novel mechanism for non-canonical GABAergic neurotransmission [72].

Some have chosen to bypass the machinery of synthesis and release entirely, focusing instead on other components of the pre- and postsynaptic membrane. As these are fairly plastic, they may provide a more accurate snapshot of signaling activity that is actually occurring at a given time. In adult male mice, rats, and rabbits, *Slc1a1* (excitatory amino acid transporter 3 [EAAT3], a sodium-dependent transporter found on the presynaptic membrane that is responsible for

glutamate reuptake from the synaptic cleft) is observed in LHA MCH cells [64]. This would reinforce that MCH neurons likely also *release* glutamate. By contrast, MCH+ terminals in rats can be observed in close apposition with gephyrin-positive neurons in the locus coeruleus [66]. Since gephyrin is a marker of GABAergic synapses, this was taken as evidence that MCH neurons release GABA. These data do not necessarily contradict one another: that MCH neurons projecting to the locus coeruleus are GABAergic does not preclude other MCH neurons from being glutamatergic. A summary of these histological data can be found in Table 4-2.

As there are numerous markers of canonical GABA- and glutamatergic cells and circuits and even more associated with noncanonical methods of neurotransmitter release, it is clear that there are limits to the utility of histology alone to address our question. Although developments like the Brainbow toolbox and spatially resolved transcriptomic data (MERFISH, spatial transcriptomics, Slide-seq, etc.) are beginning to make this limitation obsolete, historically we have been restricted to *in situ* visualization of just a few genes or proteins at a time. Thus, an alternative approach is to use quantitative molecular techniques to look for enrichment of GABA- and glutamatergic markers and see how that data fits into the full transcriptomic landscape. These techniques have the added advantage of being relatively unconstrained by *a priori* hypotheses.

Molecular Biology

An early "semi-qualitative" RT-qPCR study of hand-picked MCH cells from brain sections of male rats showed slight enrichment of *Slc17a7*, *Gad1*, and *Gad2* [73]. More than a decade later, viral translating ribosome affinity purification (vTRAP) and RNA sequencing were used to isolate and profile MCH neurons on a larger scale. In this approach, Cre-dependent adeno-associated viral (AAV) vectors engineered to express eGFP-L10a are injected into the brains of Cre-driver mice including *Pmch-Cre* BAC transgenic mice. Cells can then be dissociated and fluorescently labeled cells immunoprecipitated for sequencing, thus enabling the sequencing of specific cell populations [44, 74, 75]. Using this technique, similar enrichment of both *Gad1* and *Gad2* has been observed (1.8- and 1.6-fold, respectively), as well as *Slc17a6* (2.1-fold) and *Slc17a8* (2.88-fold) in mice 3-4 months of age (sex not reported) [63]. Importantly, *Slc32a1* was not enriched, which would indicate that MCH cells are unlikely to participate in canonical GABA release. Slight enrichment of *Gad2* has only been reported in one other study which

utilized fluorescence activated cell sorting (FACS)-assisted single-cell qPCR [43]. The presence of *Slc17a6* and *Gad1* and the absence of *Slc32a1* in virtually all MCH neurons have since been corroborated with drop-seq performed on hypothalamus of wild type juvenile male and female mice [38, 76], FACS-assisted single-cell qPCR performed on lateral hypothalamus from Pmch-Cre;eYFP juvenile male and female mice [43], and single-nucleus sequencing from ZsGreen^{MCH} adult male mice [77]. A summary of these data can be found in Table 4-2.

With this type of data, strain differences in Cre driver lines and fluorescent reporter lines as well as potential artifacts of FACS must be acknowledged, but in this instance, congruence is observed between multiple sequencing data sets utilizing a variety of methods and transgenic mice. This might lead us to dismiss the seemingly atypical finding of high *Gad2* enrichment in MCH cells using hand-picked and vTRAP-isolated cells. However, we once again encourage an alternate interpretation: does species (rat vs. mouse) have an effect? Is there something unique about the experimental conditions that led to the observation of *Gad2* enrichment in MCH cells isolated by vTRAP? These mice were the only ones which required a stereotaxic injection into the LHA to induce the fluorescence in MCH neurons used for cell sorting. Could the upregulation of GABAergic signaling genes in MCH neurons be related to a mild inflammatory response induced by the viral injection? Further speculation would be possible if more details were given about the experimental animals used in these experiments such as sex, the time of day when tissue was collected, vivarium and other housing conditions, etc.

Analysis of existing datasets

Given these considerations, we were curious whether pooling sequencing data from multiple studies could offer any clues to interpretation. Could re-clustering *only* MCH neurons from whole-hypothalamus sequencing experiments reveal additional insights? Might there be any relevant clusters that appear in just one experiment? We thus analyzed data from three published datasets: Mickelsen et al. 2019 [38]; Rossi et al. 2019 [76]; and Jiang et al. 2020 [77]—henceforth referred to as A, B, and C, respectively (Figure 4-2). The three data sets are difficult to integrate due to variations in experimental design and different numbers of MCH cells. Despite this, we were able to generate a harmonized dataset using the Seurat CCA approach. We then clustered this harmonized dataset into 6 populations using graph-based clustering (Figure 4-2A-D). All details and scripts can be found at http://github.com/alanrupp/beekly-mch-2022.

Of the 6 clusters, 3 are likely artifacts. Cluster 1 is enriched for oligodendrocyte marker genes and likely represents MCH/oligodendrocyte doublets. Cluster 5 had few exclusive marker genes, was poorly integrated across datasets, and had low *Pmch* expression, suggesting it is an amalgamation of various neurons and not a bona fide population. Cluster 6 had few enriched markers and poor gene detection, suggesting it represents low read-depth cells (Figure 4-2C).

Clusters 3 and 4 appear to comprise conventional MCH neurons. They have the highest *Pmch* expression and robust transcriptomes with unique genes. They have the highest *Pmch* expression and robust transcriptomes with unique genes. Notably, cluster 4 is a well-described subpopulation of rostromedial MCH neurons which express the neurokinin-B receptor *Tac3r* and *Cartpt* [78-81]. Further analysis revealed no major differences between clusters 3 and 4 in fast neurotransmitter identity genes. This suggests that neurotransmitter use is not dependent on transcriptional subpopulation identity and is instead likely context-dependent or stochastic (Figure 4-2C). As each study reported individually, our conclusion based on the pooled data is that the majority of MCH neurons express *Gad1* but not *Gad2* or *Slc32a1*, and a significant percentage of MCH neurons express Slc17a6. This would indicate that MCH neurons do not engage in canonical GABAergic signaling but likely use GABA for other (i.e., metabolic) purposes, and that many MCH neurons are glutamatergic (Figure 4-2F-K). Additionally, *Slc1a1*, the gene which codes for EAAT3, was expressed in a significant percentage of MCH neurons. This is yet another likely indicator that MCH neurons participate in glutamatergic signaling (Figure 4-2N).

Cluster 2 was only observed in dataset C and has comparatively low *Pmch* expression. As this dataset was the only one to use FACS, it could be argued that this subpopulation of neurons is a result of technical artifact, particularly because it bears some resemblance to Cluster 5 (non bona fide MCH neurons). However, it may be distinct enough to warrant its own cluster. Dataset C was also the largest dataset, with 1266 cells *vs* 150 and 61 cells in data sets A and B, respectively. It is possible that cluster 2 constitutes a small subpopulation of MCH neurons which was not captured by the other two studies. Notably, Cluster 2 is unique in that it shows enrichment of *Gad2* (Figure 4-2K). We suspect that this could represent a genuine MCH population and that its small size might explain why only select few studies report *Gad2* enrichment in MCH cells. Even beyond the presence of *Gad2* enrichment, these cells exhibit a

very different transcriptional profile from both Cluster 3 and Cluster 4. That observation further invites the question of whether this population, if indeed a genuine MCH neuron population, responds to a very specific stimulus, be it internal or external, and therefore whether it can be observed in all physiologic states, exert unique effects, etc. If it is an authentic MCH neuron population, it is certainly worthy of further exploration. Rigorous control of sex, age, physiological conditions, and experimental procedures in future single-cell sequencing studies as well as the ability to sequence a high percentage of the total MCH neurons will be necessary to clarify the significance of these observations.

In section 2, we described some non-canonical methods of GABAergic signaling that have been observed in neurons outside the MCH system. In addition to *de novo* synthesis, GABA may be taken up and recycled from the synapse via GAT1 (*Slc6a1)* and GAT3 (*Slc6a11)* [72]. *Slc6a1* and *Slc6a11* are both found in MCH neurons, with *Slc6a11* expressed in a higher number of cells (Figure 4-2L-M) [38]. It is therefore possible that MCH neurons could release GABA that is derived from synaptic reuptake even where *Gad2* is lacking. The question of vesicular release, however, remains, since MCH neurons lack *Slc32a1.* In the absence of VGAT, VMAT2 may be used for synaptic GABA release [70]. However, the currently available data indicates that MCH neurons in 21-day-old mice lack VMAT2. Whether MCH neurons of adult male and female mice (or rats) express VMAT2 is unknown [43].

While at least some MCH neurons may have the means to synthesize GABA *de novo* and/or to recycle GABA from the synapse, their ability to release it, lacking both VGAT and VMAT2, remains to be explained. The presence of alternative transporters that could facilitate non-canonical GABA release like VMAT1 (*Slc18a1*) and vesicular polyamine transporter (VPAT, *Slc18b1*) should be explored in MCH neurons. Should another likely candidate be identified, the study of non-canonical GABAergic co-transmission in midbrain dopamine neurons may serve as a roadmap for further research on the potential of MCH neurons to exhibit a similar synaptic strategy.

Physiology and Behavior

Thus far, we have considered the debate over MCH-GABA/glutamate co-release as a question of "what's there?" Based on the expression of numerous genes and peptides, we attempt to extrapolate the answer to the arguably more pertinent question of "what happens?" Circuit- and

systems-level experiments have sought to provide more direct insight into this question by investigating the downstream effects of MCH neuron activation.

Slice Electrophysiology

A study using Cre-dependent ChR2-eYFP viral vectors in adult male and female Pmch-Cre mice showed that by holding MCH neurons at a voltage of -60 mV and optogenetically stimulating MCH terminals adjacent to wake-promoting histaminergic (HA) neurons in the tuberomammillary nucleus (TMN), bicuculline-sensitive (i.e., GABA-dependent) IPSCs are evoked in postsynaptic neurons. They categorized their observed latency of 5.36 ± 2.9 ms as consistent with a monosynaptic connection, and concluded that MCH neurons suppress wake via release of GABA onto HA neurons [12]. The high standard error of the latency, however, permits an alternate interpretation: both poly- and monosynaptic connections may have been activated by their paradigm, in which case the reported latency would correspond to an average of the latencies associated with each effect.

A similar voltage-clamp experiment in male and female mice probed the role of MCH projections to the lateral septum (LS). Depending on the voltage with which MCH neurons were held, both IPSCs and EPSCs could be elicited in postsynaptic LS neurons. When holding MCH neurons at -60 mV (as in the previous study), optogenetic stimulation of MCH terminals in the LS evoked kynurenic acid-sensitive (i.e., glutamate-dependent) *EPSCs* while at -5 mV stimulation of MCH terminals resulted in bicuculline-sensitive IPSCs in the postsynaptic cell. The latency to EPSC was 3.5 ± 0.3 ms, which they state is consistent with a monosynaptic connection; while the latency to IPSC was 6.3 ± 0.3 ms, which they state is more consistent with a polysynaptic connection. The authors suggest a mechanism involving polysynaptic GABA PSCs in the LS driven by monosynaptic glutamate PSCs. This interpretation is supported by the use of TTX to prevent polysynaptic events; in this control, IPSCs, but not EPSCs, were abolished [82].

Again, it should be emphasized that these data aren't mutually exclusive. An MCH neuron might release either GABA or glutamate depending on the identity of its downstream target cell. For instance, an MCH neuron projecting to the LS may release glutamate while one projecting to the TMN releases GABA. Because of this, it is challenging to capture a complete picture of neurotransmitter corelease from MCH neurons using *in vitro* electrophysiology when only one

target population is measured. Furthermore, the particulars of the stimulation and recording parameters can influence the results. These two studies used slightly different photostimulation paradigms and came to opposite conclusions, which could suggest that an MCH neuron's "decision" to release GABA or glutamate depends on factors like frequency of stimulation and the integration of multiple synaptic inputs.

In vivo data

Metabolism

MCH neurons have a well-established role in metabolism and energy balance. Much of this data has been in regards to the MCH peptide itself since it was first demonstrated that MCH-knockout ("MCH-KO") mice are hyperactive, hypophagic, and lean more than two decades ago [83]. Since then, we have learned that MCH-KO mice are protected from high fat diet-induced obesity and development of insulin resistance; that *over*expressing MCH causes obesity as well as insulin resistance; and that MCH peptide can regulate pancreatic islet cells and induce insulin release [84-88].

To eliminate the interference of compensatory developmental effects that may occur in genetic knockout or overexpression models, it has also been shown that chemogenetic manipulation of MCH neurons induces comparable changes in feeding. Adult male rats stereotaxically injected with an adeno-associated virus containing an excitatory designer receptor exclusively activated by designer drugs (DREADDs, hM3Dq) driven by a *Pmch*-specific promoter showed an acute increase in food intake following injection of clozapine-*N*-oxide (CNO). This effect is completely abolished by treatment with the MCH receptor-1 antagonist H6408 [56], suggesting that MCH neurotransmission via its receptor is necessary for this effect.

Considering all of these data, one might conclude that the metabolic effects of MCH neurons are dependent solely on MCH peptide itself. However, when the metabolic phenotypes of male MCH neuronal ablation (diphtheria toxin), MCH-KO, and transgenic *Pmch*-Cre;*Slc17a6*$^{fl/fl}$ mice (which lack VGLUT2 in MCH neurons) are compared, a unique effect of glutamatergic transmission in MCH neurons begins to emerge. All three experimental groups exhibit decreased body weight and adiposity, increased locomotor activity, late-onset hypophagia, attenuated weight gain on high-fat diet, and reductions in circulating leptin [63, 89]. These data point to some functional redundancy between MCH and glutamate release from MCH neurons in the context of energy balance.

By contrast, specific indicators of glucose sensing and handling differed between groups. MCH neuronal ablation and conditional VGLUT2 deletion in MCH neurons, but not global MCH-KO, result in reduced sucrose preference and improved glucose tolerance [63]. These data suggest a role for MCH peptide in body weight regulation, but also a glutamate-dependent mechanism by which MCH neurons contribute to glucose homeostasis. Given the findings related to MCH peptide action on pancreatic islet cells and its effects on insulin resistance, it appears that MCH and glutamatergic signaling from MCH neurons must work synergistically for optimal regulation of energy balance.

These results are reminiscent of data reported regarding agouti-related peptide (AgRP) neurons, another hypothalamic population of critical importance to energy homeostasis. AgRP neurons in adult male mice were shown to release GABA and neuropeptide Y to induce rapid, transient changes in feeding behavior, while the release of AgRP itself led to delayed and prolonged alterations in feeding [90]. Whether MCH and glutamatergic neurotransmission have a similar relationship is unknown. Importantly, whether females in distinct physiological states (cycling, pregnant, lactating) show similar responses has also not been investigated.

Collectively, these data demonstrate one thing clearly: understanding of complex behavior requires meticulous experimental design to parse the acute *vs* the chronic and the constitutive *vs* the inducible effects, to say nothing of the localized *vs* the global, or the potential effects of internal and external environment. In all likelihood, the metabolic effects of MCH, GABA, and/or glutamate release from MCH neurons are nuanced and context dependent.

It will also be essential that both sexes be represented in future studies. The effects of biological sex and steroid hormones on metabolism are inarguable, yet females are severely underrepresented in the experiments described. Chemogenetic stimulation of MCH neurons in particular has documented sex-dependent effects on feeding behavior: MCH action at its receptor in the nucleus accumbens shell (ACBsh), whether by chemogenetic stimulation of MCH neurons or direct injection of MCH peptide in the ACBsh, increases chow and sucrose consumption in male but not female rats. This effect seems to be estradiol-mediated, as ovariectomized rats exhibit an orexigenic effect of MCH in the ACBsh more similar to male rats, and this phenotype is attenuated when the ovariectomized rats are given estradiol replacement [91]. For additional review of sex differences in metabolism, see [92].

Strain differences must also be accounted for, particularly when transgenic mice are used. While not specifically documented where glutamatergic signaling in MCH neurons is concerned, there are many demonstrated instances of background strain effects on the role of MCH in metabolism and glucose handling. Overexpression of MCH results in increased body weight on a C57BL/6 background, but not on an FVB background, although this was assessed only in males [84]. On a C57BL/6 background, a proportionally greater reduction in body weight is observed, but a greater increase in heat production and locomotor activity is seen in the 129 strain. MCH-KO mice also eat more chow on 129 compared to C57BL/6 background, and high fat diet elevates insulin in C57BL/6 but not in 129 mice, which likely explains the apparent discrepancy between body weight and energy expenditure. These differences have been shown in both males and females [85].

Given the functional redundancy of MCH and glutamate neurotransmission from MCH cells in the regulation of energy balance, it may be supposed that the observed metabolic effects of disrupting glutamate release from MCH cells could depend in part upon the background strain of the mice used in a similar manner. While studies using both sexes have come to the same conclusions regarding strain differences in males and females, it will be important to continue to ensure that any effects of background strain on fast neurotransmission in MCH neurons considers both sexes.

Sleep

As alluded to in the Introduction, MCH neurons also serve a wide range of functions beyond metabolism, particularly sleep—and their effects may be just as nuanced in the context of these other functions as in that of metabolism. Indeed, some of the most compelling evidence in support of physiologically relevant glutamate co-release comes from sleep experiments. *Pmch*-Cre;*Slc17a6*$^{fl/fl}$ adult male mice exhibit reduced REM sleep during the dark phase, suggesting that glutamatergic signaling in MCH neurons is required for normal diurnal variations of REM sleep [93]. These data are similarly indicative of some functional redundancy between MCH and glutamate release from MCH neurons, because optogenetic stimulation of MCH neurons in *Pmch*-Cre;*Slc17a6*$^{fl/fl}$ mice still promotes REM sleep. As previously mentioned, background strain effects have been documented for the role of MCH neurons in metabolism, so it is worth investigating whether these results can be reproduced on different background strains.

Importantly, to our knowledge none of these data include females, despite the fact that sex variables have well established effects on sleep. For example, adult women have shorter phase 1 sleep and non-REM sleep duration, but longer REM sleep duration, compared to age-matched men [94]. Diurnal rhythms of core body temperature (CBT) are advanced about an hour on average in women compared to men; some studies report a corresponding advancement of the diurnal melatonin rhythm, though this is more controversial [94-98]. The amplitude of CBT and melatonin rhythm differ as well, with men exhibiting higher CBT amplitudes on average while women have higher melatonin amplitudes [98]. Furthermore, the female reproductive cycle appears to impose an additional layer of sleep regulation, with decreased REM sleep duration and amplitude of CBT diurnal rhythms observed during the luteal as compared to the follicular phase of the menstrual cycle in adult women [99]. This would suggest that the levels of circulating estradiol and/or progesterone may impact sleep architecture. For additional review of sex differences in sleep, see [100].

Reproductive physiology

In addition to impacting sleep architecture, ovarian hormones modulate the effect that MCH neurons can exert on reproductive function. We believe it is worth highlighting some of these data, as they constitute further evidence that MCH neuron activity is highly context-dependent—a fact which does not necessarily apply to the MCH peptide alone.

At the apex of the neuroendocrine reproductive axis, gonadotropin-releasing hormone (GnRH) neurons release GnRH, which enters the pituitary portal blood system to stimulate secretion of luteinizing hormone (LH) and follicle-stimulating hormone (FSH) from the anterior pituitary gland. LH and FSH act on the gonads to induce synthesis and secretion of sex steroid hormones as well as maturation of gametes. Of particular note is a brief period of greatly upregulated GnRH neuron firing and subsequent LH release, known as the "LH surge," which is required for ovulation to occur in females.

GnRH neurons express the MCH receptor MCHR1, a G_i-coupled GPCR [101-103]. MCH-immunoreactive fibers also closely appose GnRH neurons [103, 104]. Although anatomically poised to excite GnRH neurons, the actual ability of MCH neurons to affect pituitary hormone release, as well as the valence of that effect, appears to be gated by estradiol and progesterone levels. In cultured hypothalamic explants, incubation with MCH induces GnRH neurons to release GnRH only if the cultures are first primed with estradiol [105]. Injecting MCH into the

preoptic area, where GnRH neurons are located, as well as the median eminence, where GnRH neuron projections are found, stimulates LH release in ovariectomized rats with estradiol replacement, but not without estradiol [106]. Conversely, in "surge model" rats, which receive a curated schedule of estradiol and progesterone doses following ovariectomy to generate a predictably-timed LH surge, the intracerebroventricular (ICV) injection of MCH attenuates this LH surge [107].

This could indicate that the relative levels of ovarian hormones mediate the effect of MCH on pituitary hormone secretion. It may also suggest that there are different, even opposing, effects of MCH in specific target regions. The activation of other cell populations when MCH is injected ICV could be responsible for the inhibition of LH in the second study. The argument for different effects of MCH in different target cells is supported by the finding that MCH can *suppress* the induction of GnRH by kisspeptin, another hypothalamic neuropeptide which is a potent activator of GnRH neurons, but only in a subpopulation of GnRH neurons [101]. The possibility that circulating gonadal hormones and/or specific neuronal projection targets mediate fast neurotransmitter release from MCH neurons cannot be ruled out and ought to be explored. Documenting sex differences and potential different effects of MCH and neurotransmitter co-release obtained in specific physiological states is, again, fundamental to advance the field.

Discussion

Collectively, it is our opinion that the data published to date offers clearer, more substantial support for glutamate co-release from MCH neurons. Studies demonstrating the presence of VGLUT2, needed for packaging and release of glutamate, combined with the absence of GAD65 and VGAT, needed for canonical release of GABA, greatly outnumber those suggesting either the absence of VGLUT2 or the presence of GAD65 and/or VGAT. Furthermore, *in vitro* and *in vivo* studies point to a functional role for glutamate release in MCH cells by showing significant effects of the loss of glutamate signaling machinery from MCH neurons. However, these data are biased in favor of glutamate co-release; to date, no studies have been performed using MCH-specific knockouts of any component of GABAergic signaling. Whether mice lacking *Gad1* and/or *Gad2* in MCH neurons (or, indeed, any of the components of non-canonical GABAergic transmission mentioned in Sections 2 and 3) exhibit sleep, metabolic, olfactory, reproductive, or other abnormalities is of great interest and should be pursued in future studies. Beyond this, there

are numerous gaps in the existing evidence which must be addressed to reach a compelling conclusion.

Given the heterogeneity of MCH neurons and their targets, future studies should attempt to address specific subsets of MCH neurons rather than treating the population as a monolith. Images showing the sites of viral vectors injections, optic fiber placement, neuronal harvesting, etc. should be provided when studying such a large and heterogeneous population. We now have the projection-specific and intersectional tools needed to map and manipulate highly specific circuits in the brain. Their use in our understanding of the MCH system is warranted.

More consistent representation of both sexes should also be prioritized, and with this, studies in females should monitor the estrous cycle and avoid pooling data from females across estrous cycle stages until no estrous cycle effect is demonstrated. Realistically, knowing that it is not always feasible to include this many conditions in one study, investigators should endeavor to report as much detail as possible about their experimental animals and design to foster consistency across multiple studies and research groups and facilitate the interpretation of published data. Body weights, physiological states (e.g., cycling, lactating), housing conditions, and ages of animals are relevant variables. In all of this, the possibility that something as fundamental as neurochemical identity may be flexible should be considered, and seemingly discrepant results approached with curiosity rather than frustration. There is much to learn from context-dependent modulation of excitatory and inhibitory tone from MCH neurons—and many other systems.

Balancing excitation and inhibition ("E/I balance") at the single-neuron and circuit levels is important developmentally and for the stability of mature circuits [108, 109]. Failure to maintain the appropriate E/I balance is associated with numerous neurological disorders as epilepsy, autism-spectrum disorders, dementia, and psychiatric illness [109-111]. Subtle alterations in levels of input activity are constantly being corrected for by neurons and circuits in otherwise healthy brains to preserve E/I balance, though very little is understood about this process [108]. We do know that neurons can change their neurotransmitter identity in response to exercise, injury, and photoperiod-induced stress [112-114].

E/I balance is typically attributed to neuronal excitability and/or structural alterations at the synapse, particularly in relation to GABAergic interneurons [109]. To our knowledge, the notion

that E/I imbalance depends on transcriptional regulation of GABA and glutamate signaling machinery of projection neurons has not been directly investigated. Yet other neuropeptides can be upregulated and downregulated according to age, environmental conditions, and physiological states [115-118]. It is therefore plausible that such a mechanism could influence the production of the classical neurotransmitters as well.

We argue that the neuroendocrinology field would benefit from a more nuanced interpretation of neurochemical identity that allows for change on a relatively short timescale with development, aging, environmental conditions, and physiological states as part of a coordinated response to E/I balance changes. Neuronal identities are not static, even—or perhaps especially—when the neurons in questions perform fundamental functions of survival like energy homeostasis and reproduction. Given the contention surrounding the field of MCH neuron co-transmission and the inconsistency of findings, it is our expectation that employing a more dynamic evaluation of fast neurotransmitter identity in distinct physiological conditions will orient the field to the missing pieces of the puzzle the MCH system has become in neuroendocrine regulation.

Acknowledgments

This study was supported by funding from National Institute of Health (grant numbers R01HD069702, R01HD096324 [CFE]; T32HD079342, F31HD102160 [BGB]; and 1R01DK129366-01 [CRB]), the Michigan Diabetes Research Center Pilot and Feasibility Award, and the Whitehall Foundation New Investigator Grant (#2018-08-50 [CRB]).

Table 4-1: Components of GABA and glutamate synthesis, packaging, and release. Glutamate-associated genes highlighted in gray.

Gene name	Protein abbreviation	Protein name	Function
Gad1	GAD67	Glutamic acid decarboxylase-67	Catalyzes synthesis of cytoplasmic GABA from glutamate for extrasynaptic and metabolic uses.
Gad2	GAD65	Glutamic acid decarboxylase-65	Catalyzes synthesis of GABA from glutamate; regulates the vesicular pool of GABA available for synaptic release.
Slc32a1	Vgat	Vesicular GABA transporter	Responsible for vesicular storage and subsequent exocytosis of GABA.
Abat	GABA-T	4-aminobutyrate aminotransferase	Breaks GABA down into succinic semialdehyde + glutamate.
Slc18a1	VMAT1	Vesicular monoamine transporter 1	Facilitates non-canonical GABA release into the synapse. Less common in the brain than VMAT2.
Slc18a2	VMAT2	Vesicular monoamine transporter 2	Facilitates non-canonical GABA release into synapses.
Slc6a1	GAT1	Solute carrier family 6 member 1	Sodium-dependent membrane GABA transporter. Tranports GABA from the synaptic cleft into presynaptic terminals. Expressed in both neurons and non-neuronal cell types.
Slc6a11	GAT3	Solute carrier family 6 member 11	Sodium-dependent membrane GABA transporter. Tranports GABA from the synaptic cleft into presynaptic terminals. Predominantly in glial cells.
Slc17a7	VGluT1	Vesicular glutamate transporter 1	Loads glutamate into synaptic vesicles. Considered a marker of canonical glutamate neurons. Mainly in cerebral cortex, hippocampus and cerebellum.
Slc17a6	VGluT2	Vesicular glutamate transporter 2	Loads glutamate into synaptic vesicles. Considered a marker of canonical glutamate neurons. Mainly in thalamus, hypothalamus, and brainstem.
Slc17a8	VGluT3	Vesicular glutamate transporter 3	Loads glutamate into synaptic vesicles. Found in neurons that use other neurotransmitters besides glutamate. Low in cerebral cortex, hippocampus, striatum and raphe nuclei.
Slc1a1	EAAT3	Excitatory amino acid transporter 3	Sodium-dependent transporter found on presynaptic membranes. Reuptakes glutamate from the synaptic cleft.
Gphn	Geph	Gephyrin	Postsynaptic density protein. Facilitates anchoring of GABA receptors in postsynaptic membranes.
Slc18b1	VPAT	Vesicular polyamine transporter	Transports monoamines and polyamines using an electrochemical gradient of H^+.

Table 4-2. Highlights from published data describing the presence or absence of GABA and glutamate associated proteins and/or genes in MCH neurons. Abbreviations: CSF, cerebral spinal fluid; IHy, incertohypothalamic area; LC, locus coeruleus; LHA, lateral hypothalamic area; POA, preoptic area; ZIm, medial zona incerta.

Amino Acids & Proteins	Immunohistochemistry	Notes	References
VGluT1	0% of CSF-projecting	Adult male Sprague-Dawley rats	Noble et al., *Cell Metab* 2018
VGluT2	0% of CSF-projecting	Adult male Sprague-Dawley rats	Noble et al., *Cell Metab* 2018
	LHA: 0%	Adult male Sprague-Dawley rats	Collin et al., *Eur J Neurosci* 2003
	LHA: 0%	Adult male and female mice	Blanco-Centurion et al., *IBRO Rep* 2018
	POA: 0%	Adult female mice, multiple strains, late lactation	Teixeira et al., *J Neuroendocrinol* 2019
VGluT3	0% of CSF-projecting	Adult male Sprague-Dawley rats	Noble et al., *Cell Metab* 2018
	LHA: 0%	Adult male Sprague-Dawley rats	Collin et al., *Eur J Neurosci* 2003
	POA: 4.5%	Adult female mice, multiple strains, late lactation	Teixeira et al., *J Neuroendocrinol* 2019
VGaT	LHA: 0%	Adult male Sprague-Dawley rats	Collin et al., *Eur J Neurosci* 2003
	LHA: 0%	Adult male and female mice	Blanco-Centurion et al., *IBRO Rep* 2018
	POA: 2.7%	Adult female mice, multiple strains, late lactation	Teixeira et al., *J Neuroendocrinol* 2019
EAAT3	LHA: Present	Adult male Sprague-Dawley rats	Collin et al., *Eur J Neurosci* 2003
Glutamate	LHA: Present	Adult male and female Sprague-Dawley rats; humans (age and sex unspecified)	Abrahamson et al., *Neuroreport* 2001
GAD67	45% CSF projecting 23% non-CSF projecting	Adult male Sprague-Dawley rats	Noble et al., *Cell Metab* 2018
GAD65	LHA: Present	Adult male and female sexually experienced mice	Kato et al., *Sci Rep* 2021
GABA	LHA: Present	Adult male and female sexually experienced mice	Kato et al., *Sci Rep* 2021
Gephyrin	Fibers in apposition to Geph+ neurons (LC)	Adult male Sprague-Dawley rats	Del Cid-Pellitero et al., *Neurosci* 2012
Genes	*In situ* hybridization	Notes	References
Slc17a7	LHA: 0%	Adult male Sprague-Dawley rats	Noble et al., *Cell Metab* 2018
Slc17a6	LHA: 0%	Adult male Sprague-Dawley rats	Noble et al., *Cell Metab* 2018
	LHA: 100% POA: 0%	Adult male, adult virgin female, and late-lactation mice	Beekly et al., *Front Neuroanat* 2020

Slc17a6	LHA/PFx/ZIm: 98%	Adult mice, unspecified sex	Schneeberger et al., *Mol Metab* 2018
Slc17a8	LHA: 0%	Adult male Sprague-Dawley rats	Noble et al., *Cell Metab* 2018
Slc32a1	LHA: 0% POA: 100%	Adult male, adult virgin female, and late-lactation mice	Beekly et al., *Front Neuroanat* 2020
Gad1	IHy/ LHA: 85%	Adult male Sprague-Dawley rats	Elias et al., *J Chem Neuroanat* 2008
	ZIm/LHA: 85%	Adult male Sprague-Dawley rats	Sapin et al., *PLoS One* 2010
	LHA: 85 %	Adult male *Pmch*-Cre mice	Jego et al., *Nat Neurosci* 2013
	POA: 95%	Adult female Sprague-Dawley rats in late lactation	Rondini et al., *J Chem Neuroanat* 2010

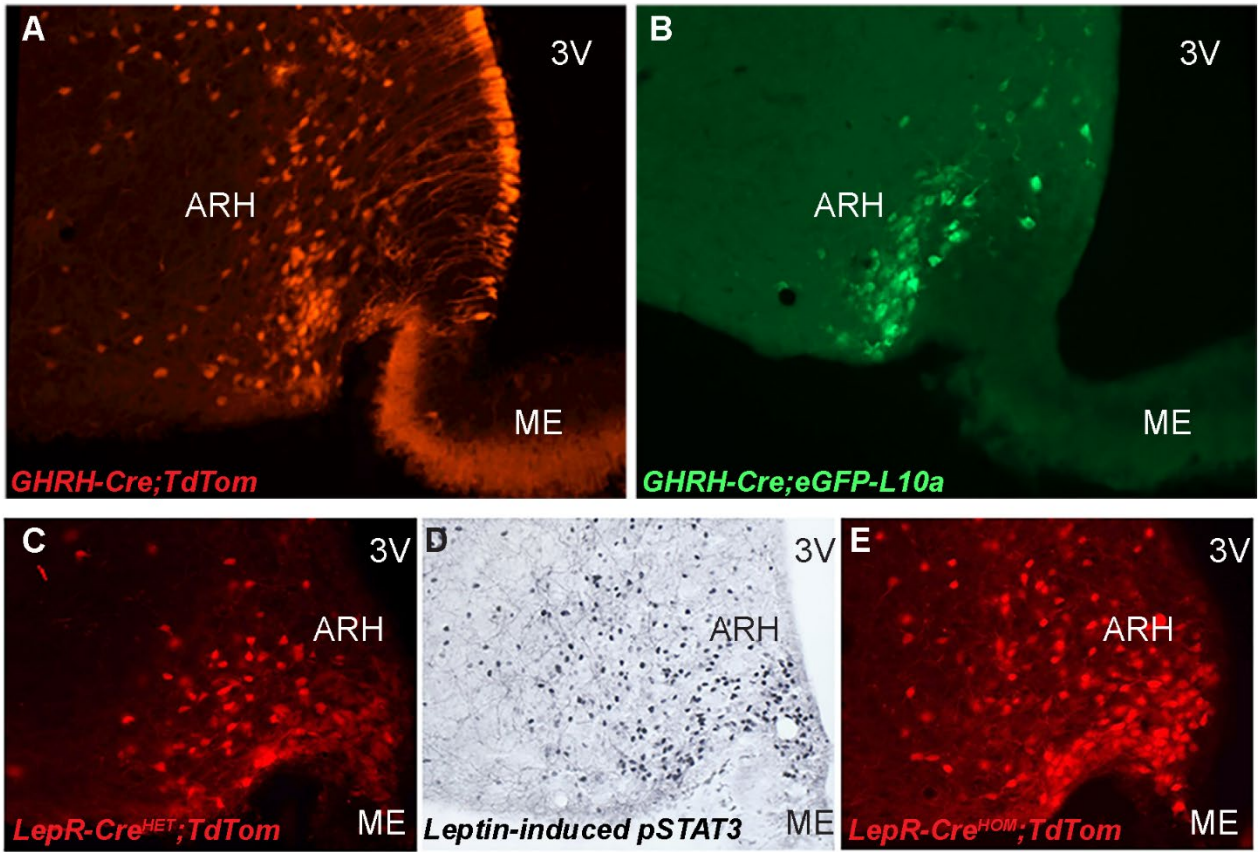

Figure 4-1. Different reporter genes and number of alleles with the transgene can affect results. (A) Fluorescent micrographs showing TdTomato expression in GHRH-Cre;TdTomato mouse. Note strong labeling of arcuate nucleus (ARH) neurons, tanycytes, and fibers projecting to the median eminence (ME). (B) Fluorescent micrographs showing eGFP-L10a expression in GHRH-Cre;eGFP-L10a mouse. Note only labeling of arcuate nucleus neurons. (C) Fluorescent micrographs showing TdTomato expression in a LepRb-Cre;TdTomato mouse hemizygous for Cre. (D) Bright field micrographs showing leptin induced PSTAT3 expression. (E) Fluorescent micrographs showing TdTomato expression in LepRb-Cre;TdTomato mouse homozygous for Cre. *Abbreviations*: 3V, third ventricle.

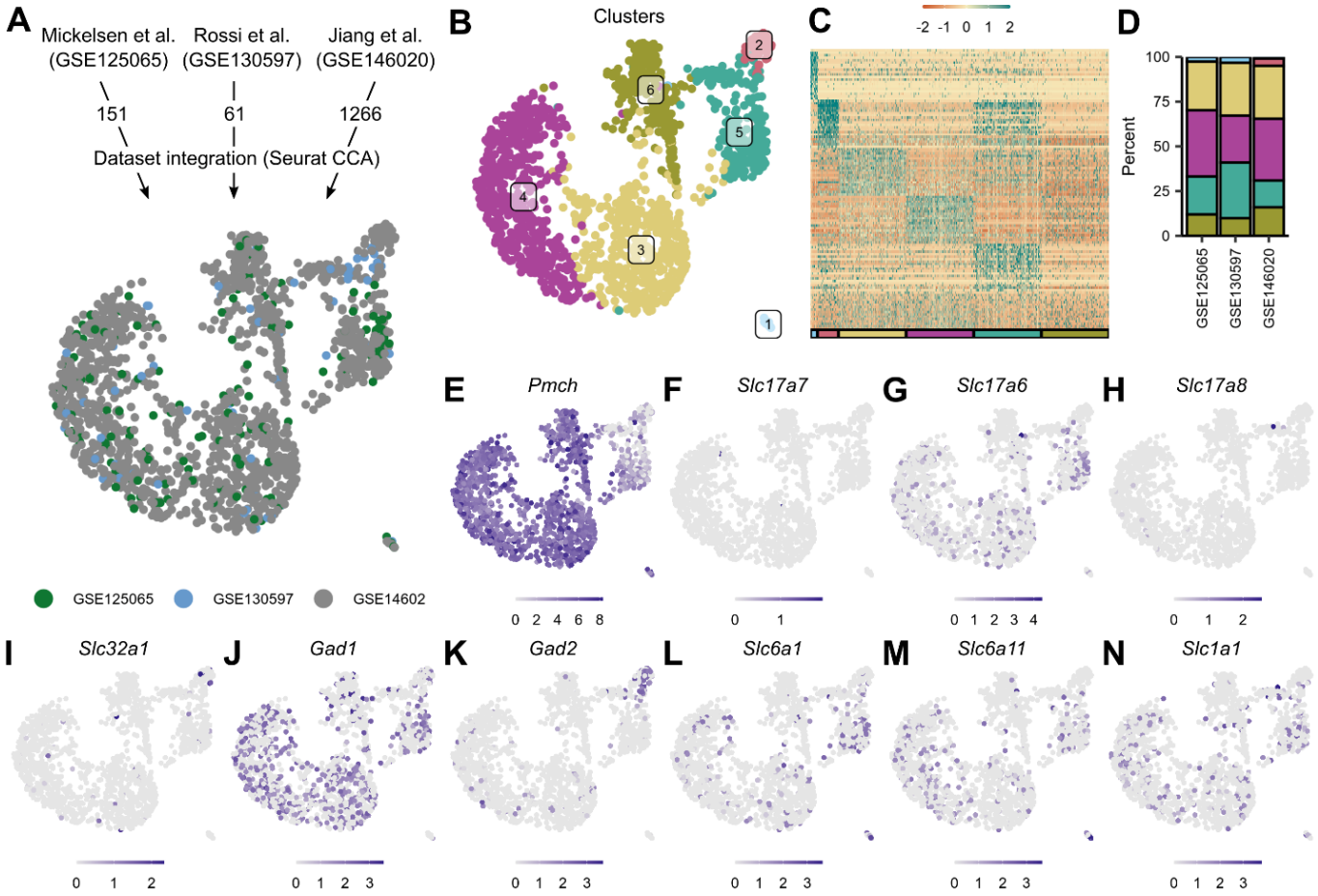

Figure 4-2. MCH neuron transcriptome data from three published single-cell sequencing studies was further analyzed for genes associated with fast neurotransmission. (A) Visualization of dataset integration using the Seurat CCA approach. (B) Summary of major MCH neuron clusters. (C) Heat map of gene expression for the six clusters. Note that Cluster 1 is enriched for oligodendrocyte marker genes and is presumed to comprise MCH/oligodendrocyte doublets; Cluster 5 had few exclusive marker genes, poor integration, and low *Pmch* expression, and is thus presumed not to be a bona fide MCH neuron population; and Cluster 6 has few enriched markers and is presumed to comprise low read depth cells. (D) Bar graph displaying the breakdown of the percentage of MCH neurons in each cluster derived from each of the three analyzed datasets. (E) *Pmch* gene expression in each of the six clusters. Darker colors correspond to greater enrichment. (F-N) Expression of various fast neurotransmitter signaling machinery genes in each cluster. Darker colors correspond to greater enrichment.

References

1. Kawauchi, H., et al., *Characterization of melanin-concentrating hormone in chum salmon pituitaries.* Nature, 1983(305): p. 321–323.
2. Bittencourt, J., et al., *The melanin-concentrating hormone system of the rat brain: an immuno-and hybridization histochemical characterization.* Journal of Comparative Neurology, 1992. **319**(2): p. 218-245.
3. Sita, L., C. Elias, and J. Bittencourt, *Connectivity pattern suggests that incerto-hypothalamic area belongs to the medial hypothalamic system.* 2007. **148**: p. 949-69.
4. Elias, C.F., et al., *Chemically defined projections linking the mediobasal hypothalamus and the lateral hypothalamic area.* J Comp Neurol, 1998. **402**(4): p. 442-59.
5. Arrigoni, E., M.J.S. Chee, and P.M. Fuller, *To eat or to sleep: That is a lateral hypothalamic question.* Neuropharmacology, 2019. **154**: p. 34-49.
6. Joseph, D.N. and S. Whirledge, *Stress and the HPA Axis: Balancing Homeostasis and Fertility.* Int J Mol Sci, 2017. **18**(10).
7. Oyola, M.G. and R.J. Handa, *Hypothalamic-pituitary-adrenal and hypothalamic-pituitary-gonadal axes: sex differences in regulation of stress responsivity.* Stress, 2017. **20**(5): p. 476-494.
8. Kaprara, A. and I.T. Huhtaniemi, *The hypothalamus-pituitary-gonad axis: Tales of mice and men.* Metabolism, 2018. **86**: p. 3-17.
9. Yamashita, T. and A. Yamanaka, *Lateral hypothalamic circuits for sleep-wake control.* Curr Opin Neurobiol, 2017. **44**: p. 94-100.
10. Hassani, O., M. Gee Lee, and B. Jones, *Melanin-concentrating hormone neurons discharge in a reciprocal manner to orexin neurons across the sleep-wake cycle.* 2009. **106**: p. 2418-2422.
11. Verret, L., et al., *A role of melanin-concentrating hormone producing neurons in the central regulation of paradoxical sleep.* 2003. **4**: p. 19.
12. Jego, S., et al., *Optogenetic identification of a rapid eye movement sleep modulatory circuit in the hypothalamus.* 2013. **16**.
13. Konadhode, R., et al., *Optogenetic Stimulation of MCH Neurons Increases Sleep.* 2013. **33**: p. 10257-63.
14. Tsunematsu, T., et al., *Optogenetic Manipulation of Activity and Temporally Controlled Cell-Specific Ablation Reveal a Role for MCH Neurons in Sleep/Wake Regulation.* 2014. **34**: p. 6896-909.
15. Blanco-Centurion, C., et al., *Dynamic Network Activation of Hypothalamic MCH Neurons in REM Sleep and Exploratory Behavior.* The Journal of Neuroscience, 2019: p. 0305-19.
16. Potter, L.E. and C.R. Burgess, *The melanin-concentrating hormone system as a target for the treatment of sleep disorders.* Frontiers in Neuroscience, 2022.
17. Al-Massadi, O., et al., *Multifaceted actions of melanin-concentrating hormone on mammalian energy homeostasis.* Nat Rev Endocrinol, 2021. **17**(12): p. 745-755.
18. Lord, M.N., et al., *Melanin-concentrating hormone and food intake control: Sites of action, peptide interactions, and appetition.* Peptides, 2021. **137**: p. 170476.
19. Qu, D., et al., *A role for melanin-concentrating hormone in the central regulation of feeding behaviour.* Nature, 1996. **380**(6571): p. 243-7.

20. Costa, H.C., et al., *Characterisation and origins of melanin-concentrating hormone immunoreactive fibres of the posterior lobe of the pituitary and median eminence during lactation in the Long-Evans rat.* J Neuroendocrinol, 2019. **31**(9): p. e12723.
21. Arroyo, A., et al., *Expression of kv4.3 voltage-gated potassium channels in rat gonadotrophin-releasing hormone (GnRH) neurons during the estrous cycle.* Reprod Sci, 2011. **18**(2): p. 136-44.
22. Lakaye, B., et al., *Melanin-concentrating hormone and immune function.* Peptides, 2009. **30**(11): p. 2076-80.
23. Morganstern, I., G. Gulati, and S.F. Leibowitz, *Role of melanin-concentrating hormone in drug use disorders.* Brain Res, 2020. **1741**: p. 146872.
24. Rana, T., et al., *Exploring the role of neuropeptides in depression and anxiety.* Prog Neuropsychopharmacol Biol Psychiatry, 2022. **114**: p. 110478.
25. Adamantidis, A. and L. de Lecea, *A role for Melanin-Concentrating Hormone in learning and memory.* Peptides, 2009. **30**(11): p. 2066-70.
26. Adams, A.C., et al., *Ablation of the hypothalamic neuropeptide melanin concentrating hormone is associated with behavioral abnormalities that reflect impaired olfactory integration.* Behav Brain Res, 2011. **224**(1): p. 195-200.
27. Orikasa, C., *Neural Contributions of the Hypothalamus to Parental Behaviour.* Int J Mol Sci, 2021. **22**(13).
28. Nahon, J.L., et al., *The rat melanin-concentrating hormone messenger ribonucleic acid encodes multiple putative neuropeptides coexpressed in the dorsolateral hypothalamus.* Endocrinology, 1989. **125**(4): p. 2056-65.
29. Toumaniantz, G., J.C. Bittencourt, and J.L. Nahon, *The rat melanin-concentrating hormone gene encodes an additional putative protein in a different reading frame.* Endocrinology, 1996. **137**(10): p. 4518-21.
30. Borsu, L., F. Presse, and J.L. Nahon, *The AROM gene, spliced mRNAs encoding new DNA/RNA-binding proteins are transcribed from the opposite strand of the melanin-concentrating hormone gene in mammals.* J Biol Chem, 2000. **275**(51): p. 40576-87.
31. Moldovan, G.L., et al., *Inhibition of homologous recombination by the PCNA-interacting protein PARI.* Mol Cell, 2012. **45**(1): p. 75-86.
32. Courseaux, A. and J.L. Nahon, *Birth of two chimeric genes in the Hominidae lineage.* Science, 2001. **291**(5507): p. 1293-7.
33. Bittencourt, J. and M.E. Celis, *Anatomy, function and regulation of neuropeptide EI (NEI).* Peptides, 2008. **29**(8): p. 1441-50.
34. Bittencourt, J.C., *Anatomical organization of the melanin-concentrating hormone peptide family in the mammalian brain.* Gen Comp Endocrinol, 2011. **172**(2): p. 185-97.
35. Bittencourt, J.C., et al., *The distribution of melanin-concentrating hormone in the monkey brain (Cebus apella).* Brain Res, 1998. **804**(1): p. 140-3.
36. Attademo, A.M., et al., *Neuropeptide Glutamic Acid-Isoleucine May Induce Luteinizing Hormone Secretion via Multiple Pathways.* Neuroendocrinology, 2006. **83**(5-6): p. 313-24.
37. Bittencourt, J.C. and C.F. Elias, *Melanin-concentrating hormone and neuropeptide EI projections from the lateral hypothalamic area and zona incerta to the medial septal nucleus and spinal cord: a study using multiple neuronal tracers.* Brain Res, 1998. **805**(1-2): p. 1-19.

38. Mickelsen, L.E., et al., *Single-cell transcriptomic analysis of the lateral hypothalamic area reveals molecularly distinct populations of inhibitory and excitatory neurons.* Nat Neurosci, 2019. **22**(4): p. 642-656.
39. Zhao, E., H. Hu, and V.L. Trudeau, *Secretoneurin as a hormone regulator in the pituitary.* Regul Pept, 2010. **165**(1): p. 117-22.
40. Troger, J., et al., *Granin-derived peptides.* Prog Neurobiol, 2017. **154**: p. 37-61.
41. Trudeau, V.L., *Neuroendocrine Control of Reproduction in Teleost Fish: Concepts and Controversies.* Annu Rev Anim Biosci, 2022. **10**: p. 107-130.
42. Ahmadian-Moghadam, H., M.S. Sadat-Shirazi, and M.R. Zarrindast, *Cocaine- and amphetamine-regulated transcript (CART): A multifaceted neuropeptide.* Peptides, 2018. **110**: p. 56-77.
43. Mickelsen, L.E., et al., *Neurochemical Heterogeneity Among Lateral Hypothalamic Hypocretin/Orexin and Melanin-Concentrating Hormone Neurons Identified Through Single-Cell Gene Expression Analysis.* eNeuro, 2017. **4**(5).
44. Nectow, A.R., et al., *Rapid Molecular Profiling of Defined Cell Types Using Viral TRAP.* Cell Rep, 2017. **19**(3): p. 655-667.
45. Rose, C.R., et al., *Molecular and cellular physiology of sodium-dependent glutamate transporters.* Brain Res Bull, 2018. **136**: p. 3-16.
46. Blanco-Centurion, C., et al., *VGAT and VGLUT2 expression in MCH and orexin neurons in double transgenic reporter mice.* IBRO Rep, 2018. **4**: p. 44-49.
47. Dicken, M.S., R.E. Tooker, and S.T. Hentges, *Regulation of GABA and glutamate release from proopiomelanocortin neuron terminals in intact hypothalamic networks.* J Neurosci, 2012. **32**(12): p. 4042-8.
48. Venner, A., et al., *Reassessing the Role of Histaminergic Tuberomammillary Neurons in Arousal Control.* J Neurosci, 2019. **39**(45): p. 8929-8939.
49. Horvath, T.L., et al., *A GABA-neuropeptide Y (NPY) interplay in LH release.* Peptides, 2001. **22**(3): p. 473-81.
50. Dicken, M.S., A.R. Hughes, and S.T. Hentges, *Gad1 mRNA as a reliable indicator of altered GABA release from orexigenic neurons in the hypothalamus.* Eur J Neurosci, 2015. **42**(9): p. 2644-53.
51. Romanov, R.A., et al., *Molecular interrogation of hypothalamic organization reveals distinct dopamine neuronal subtypes.* Nat Neurosci, 2017. **20**(2): p. 176-188.
52. Abrahamson, E.E., R.K. Leak, and R.Y. Moore, *The suprachiasmatic nucleus projects to posterior hypothalamic arousal systems.* Neuroreport, 2001. **12**(2): p. 435-40.
53. Elias, C.F., et al., *Characterization of CART neurons in the rat and human hypothalamus.* J Comp Neurol, 2001. **432**(1): p. 1-19.
54. Elias, C.F., et al., *Melanin-concentrating hormone projections to areas involved in somatomotor responses.* J Chem Neuroanat, 2008. **35**(2): p. 188-201.
55. Sapin, E., et al., *A very large number of GABAergic neurons are activated in the tuberal hypothalamus during paradoxical (REM) sleep hypersomnia.* PLoS One, 2010. **5**(7): p. e11766.
56. Noble, E.E., et al., *Control of Feeding Behavior by Cerebral Ventricular Volume Transmission of Melanin-Concentrating Hormone.* Cell Metab, 2018. **28**(1): p. 55-68.e7.
57. Grone, B.P. and K.P. Maruska, *Three Distinct Glutamate Decarboxylase Genes in Vertebrates.* Sci Rep, 2016. **6**: p. 30507.

58. Kato, Y., et al., *Involvement of MCH-oxytocin neural relay within the hypothalamus in murine nursing behavior.* Sci Rep, 2021. **11**(1): p. 3348.
59. Knollema, S., et al., *Novel hypothalamic and preoptic sites of prepro-melanin-concentrating hormone messenger ribonucleic Acid and Peptide expression in lactating rats.* J Neuroendocrinol, 1992. **4**(6): p. 709-17.
60. Teixeira, P.D.S., et al., *Regulation and neurochemical identity of melanin-concentrating hormone neurons in the preoptic area of lactating mice.* J Neuroendocrinol, 2019: p. e12818.
61. Rondini, T.A., et al., *Chemical identity and connections of medial preoptic area neurons expressing melanin-concentrating hormone during lactation.* J Chem Neuroanat, 2010. **39**(1): p. 51-62.
62. Beekly, B.G., et al., *Dissociated Pmch and Cre Expression in Lactating Pmch-Cre BAC Transgenic Mice.* Frontiers in Neuroanatomy, 2020. **14**(60).
63. Schneeberger, M., et al., *Functional analysis reveals differential effects of glutamate and MCH neuropeptide in MCH neurons.* Mol Metab, 2018. **13**: p. 83-89.
64. Collin, M., et al., *Plasma membrane and vesicular glutamate transporter mRNAs/proteins in hypothalamic neurons that regulate body weight.* Eur J Neurosci, 2003. **18**(5): p. 1265-78.
65. Boulland, J.L., et al., *Expression of the vesicular glutamate transporters during development indicates the widespread corelease of multiple neurotransmitters.* J Comp Neurol, 2004. **480**(3): p. 264-80.
66. Del Cid-Pellitero, E. and B.E. Jones, *Immunohistochemical evidence for synaptic release of GABA from melanin-concentrating hormone containing varicosities in the locus coeruleus.* Neuroscience, 2012. **223**: p. 269-76.
67. Mendez, J.A., et al., *Developmental and target-dependent regulation of vesicular glutamate transporter expression by dopamine neurons.* J Neurosci, 2008. **28**(25): p. 6309-18.
68. Chung, E.K., et al., *Up-regulation in expression of vesicular glutamate transporter 3 in substantia nigra but not in striatum of 6-hydroxydopamine-lesioned rats.* Neurosignals, 2006. **15**(5): p. 238-48.
69. Ottem, E.N., et al., *Dual-phenotype GABA/glutamate neurons in adult preoptic area: sexual dimorphism and function.* J Neurosci, 2004. **24**(37): p. 8097-105.
70. Tritsch, N.X., J.B. Ding, and B.L. Sabatini, *Dopaminergic neurons inhibit striatal output through non-canonical release of GABA.* Nature, 2012. **490**(7419): p. 262-6.
71. Tritsch, N.X., et al., *Midbrain dopamine neurons sustain inhibitory transmission using plasma membrane uptake of GABA, not synthesis.* Elife, 2014. **3**: p. e01936.
72. Melani, R. and N.X. Tritsch, *Inhibitory co-transmission from midbrain dopamine neurons relies on presynaptic GABA uptake.* Cell Rep, 2022. **39**(3): p. 110716.
73. Harthoorn, L.F., et al., *Multi-transcriptional profiling of melanin-concentrating hormone and orexin-containing neurons.* Cell Mol Neurobiol, 2005. **25**(8): p. 1209-23.
74. Kong, D., et al., *Glucose stimulation of hypothalamic MCH neurons involves K(ATP) channels, is modulated by UCP2, and regulates peripheral glucose homeostasis.* Cell Metab, 2010. **12**(5): p. 545-52.
75. Zanetti, M.E., et al., *Immunopurification of polyribosomal complexes of Arabidopsis for global analysis of gene expression.* Plant Physiol, 2005. **138**(2): p. 624-35.

76. Rossi, M.A., et al., *Obesity remodels activity and transcriptional state of a lateral hypothalamic brake on feeding.* Science, 2019. **364**(6447): p. 1271-1274.
77. Jiang, H., et al., *MCH Neurons Regulate Permeability of the Median Eminence Barrier.* Neuron, 2020. **107**(2): p. 306-319.e9.
78. Croizier, S., et al., *A comparative analysis shows morphofunctional differences between the rat and mouse melanin-concentrating hormone systems.* PLoS One, 2010. **5**(11): p. e15471.
79. Croizier, S., et al., *Development of posterior hypothalamic neurons enlightens a switch in the prosencephalic basic plan.* PLoS One, 2011. **6**(12): p. e28574.
80. Cvetkovic, V., et al., *Characterization of subpopulations of neurons producing melanin-concentrating hormone in the rat ventral diencephalon.* J Neurochem, 2004. **91**(4): p. 911-9.
81. Brischoux, F., et al., *Time of genesis determines projection and neurokinin-3 expression patterns of diencephalic neurons containing melanin-concentrating hormone.* Eur J Neurosci, 2002. **16**(9): p. 1672-80.
82. Chee, M.J., E. Arrigoni, and E. Maratos-Flier, *Melanin-concentrating hormone neurons release glutamate for feedforward inhibition of the lateral septum.* J Neurosci, 2015. **35**(8): p. 3644-51.
83. Shimada, M., et al., *Mice lacking melanin-concentrating hormone are hypophagic and lean.* Nature, 1998. **396**(6712): p. 670-4.
84. Ludwig, D.S., et al., *Melanin-concentrating hormone overexpression in transgenic mice leads to obesity and insulin resistance.* J Clin Invest, 2001. **107**(3): p. 379-86.
85. Kokkotou, E., et al., *Mice with MCH ablation resist diet-induced obesity through strain-specific mechanisms.* Am J Physiol Regul Integr Comp Physiol, 2005. **289**(1): p. R117-24.
86. Jeon, J.Y., et al., *MCH-/- mice are resistant to aging-associated increases in body weight and insulin resistance.* Diabetes, 2006. **55**(2): p. 428-34.
87. Tadayyon, M., et al., *Expression of melanin-concentrating hormone receptors in insulin-producing cells: MCH stimulates insulin release in RINm5F and CRI-G1 cell-lines.* Biochem Biophys Res Commun, 2000. **275**(2): p. 709-12.
88. Pissios, P., et al., *Melanin concentrating hormone is a novel regulator of islet function and growth.* Diabetes, 2007. **56**(2): p. 311-9.
89. Whiddon, B.B. and R.D. Palmiter, *Ablation of neurons expressing melanin-concentrating hormone (MCH) in adult mice improves glucose tolerance independent of MCH signaling.* J Neurosci, 2013. **33**(5): p. 2009-16.
90. Krashes, M.J., et al., *Rapid versus delayed stimulation of feeding by the endogenously released AgRP neuron mediators GABA, NPY, and AgRP.* Cell Metab, 2013. **18**(4): p. 588-95.
91. Terrill, S.J., et al., *Nucleus accumbens melanin-concentrating hormone signaling promotes feeding in a sex-specific manner.* Neuropharmacology, 2020. **178**: p. 108270.
92. Anversa, R.G., et al., *A review of sex differences in the mechanisms and drivers of overeating.* Front Neuroendocrinol, 2021. **63**: p. 100941.
93. Naganuma, F., et al., *Melanin-concentrating hormone neurons promote rapid eye movement sleep independent of glutamate release.* Brain Struct Funct, 2019. **224**(1): p. 99-110.

94. Boivin, D.B., et al., *Diurnal and circadian variation of sleep and alertness in men vs. naturally cycling women.* Proc Natl Acad Sci U S A, 2016. **113**(39): p. 10980-5.
95. Lazar, A.S., et al., *Circadian period and the timing of melatonin onset in men and women: predictors of sleep during the weekend and in the laboratory.* J Sleep Res, 2013. **22**(2): p. 155-9.
96. Van Reen, E., et al., *Sex of college students moderates associations among bedtime, time in bed, and circadian phase angle.* J Biol Rhythms, 2013. **28**(6): p. 425-31.
97. Burgess, H.J. and C.I. Eastman, *The dim light melatonin onset following fixed and free sleep schedules.* J Sleep Res, 2005. **14**(3): p. 229-37.
98. Cain, S.W., et al., *Sex differences in phase angle of entrainment and melatonin amplitude in humans.* J Biol Rhythms, 2010. **25**(4): p. 288-96.
99. Shechter, A., F. Varin, and D.B. Boivin, *Circadian variation of sleep during the follicular and luteal phases of the menstrual cycle.* Sleep, 2010. **33**(5): p. 647-56.
100. Spitschan, M., et al., *Sex differences and sex bias in human circadian and sleep physiology research.* Elife, 2022. **11**.
101. Wu, M., et al., *Melanin-concentrating hormone directly inhibits GnRH neurons and blocks kisspeptin activation, linking energy balance to reproduction.* Proc Natl Acad Sci U S A, 2009. **106**(40): p. 17217-22.
102. An, S., et al., *Identification and characterization of a melanin-concentrating hormone receptor.* Proc Natl Acad Sci U S A, 2001. **98**(13): p. 7576-81.
103. S Williamson-Hughes, P., K. Grove, and M.S. Smith, *Melanin concentrating hormone (MCH): A novel neural pathway for regulation of GnRH neurons.* 2005. **1041**: p. 117-24.
104. Ward, D.R., et al., *Innervation of gonadotropin-releasing hormone neurons by peptidergic neurons conveying circadian or energy balance information in the mouse.* PLoS One, 2009. **4**(4): p. e5322.
105. Chiocchio, S.R., et al., *Melanin-concentrating hormone stimulates the release of luteinizing hormone-releasing hormone and gonadotropins in the female rat acting at both median eminence and pituitary levels.* Biol Reprod, 2001. **64**(5): p. 1466-72.
106. Murray, J.F., et al., *The influence of gonadal steroids on pre-pro melanin-concentrating hormone mRNA in female rats.* J Neuroendocrinol, 2000. **12**(1): p. 53-9.
107. Gonzalez, M., B. Baker, and C. Wilson, *Stimulatory effect of melanin-concentrating hormone on luteinising hormone release.* Neuroendocrinology, 1997. **66**: p. 254-262.
108. He, H.Y. and H.T. Cline, *What Is Excitation/Inhibition and How Is It Regulated? A Case of the Elephant and the Wisemen.* J Exp Neurosci, 2019. **13**: p. 1179069519859371.
109. Liu, Y., et al., *A Selective Review of the Excitatory-Inhibitory Imbalance in Schizophrenia: Underlying Biology, Genetics, Microcircuits, and Symptoms.* Front Cell Dev Biol, 2021. **9**: p. 664535.
110. Nomura, T., *Interneuron Dysfunction and Inhibitory Deficits in Autism and Fragile X Syndrome.* Cells, 2021. **10**(10).
111. Sakimoto, Y., et al., *Significance of GABA.* Int J Mol Sci, 2021. **22**(22).
112. Li, H.Q. and N.C. Spitzer, *Exercise enhances motor skill learning by neurotransmitter switching in the adult midbrain.* Nat Commun, 2020. **11**(1): p. 2195.
113. Bertels, H., et al., *Neurotransmitter phenotype switching by spinal excitatory interneurons regulates locomotor recovery after spinal cord injury.* Nat Neurosci, 2022. **25**(5): p. 617-629.

114. Meng, D., et al., *Neuronal activity regulates neurotransmitter switching in the adult brain following light-induced stress.* Proc Natl Acad Sci U S A, 2018. **115**(20): p. 5064-5071.
115. Higuchi, H., A. Hasegawa, and T. Yamaguchi, *Transcriptional regulation of neuronal genes and its effect on neural functions: transcriptional regulation of neuropeptide Y gene by leptin and its effect on feeding.* J Pharmacol Sci, 2005. **98**(3): p. 225-31.
116. Quinn, J.P., et al., *Transcriptional control of neuropeptide gene expression in sensory neurons, using the preprotachykinin-A gene as a model.* Can J Physiol Pharmacol, 1995. **73**(7): p. 957-62.
117. Cifani, C., et al., *Regulation of hypothalamic neuropeptides gene expression in diet induced obesity resistant rats: possible targets for obesity prediction?* Front Neurosci, 2015. **9**: p. 187.
118. Lindsay, R.M. and A.J. Harmar, *Nerve growth factor regulates expression of neuropeptide genes in adult sensory neurons.* Nature, 1989. **337**(6205): p. 362-4.

Chapter V. Deletion of VGLUT2 from MCH Neurons Elicits Sex-Specific Effects on Reproductive Development, Energy Balance, and Glucose Handling

Abstract

Hypothalamic melanin-concentrating hormone (MCH) neurons contribute to many fundamental physiological functions including the regulation of energy balance. MCH neurons express numerous genes involved in the synthesis, packaging, and release of the classical neurotransmitters GABA and glutamate, which are the central nervous system's predominant inhibitory and excitatory neurotransmitters, respectively. Both GABA and glutamate are found extensively throughout the hypothalamus and co-released with other hypothalamic neuropeptides. Functional studies in which VGLUT2 was deleted from MCH neurons in adult male mice resulted in altered metabolism, notably increased activity, reduced body weight, and improved glucose tolerance. However, the effect of VGLUT2 deletion in MCH neurons has not been investigated in females. Furthermore, whether loss of glutamatergic signaling from MCH neurons affects other related phenomena such as fertility, which is tightly linked to energy status, has not been addressed. In this study, we use transgenic mouse models to delete VGLUT2 from MCH neurons and investigate the effects on metabolism, reproductive development, and fertility across the lifespan in both male and female mice. We found that loss of VGLUT2 from MCH neurons resulted in sexually dimorphic metabolic and reproductive phenotypes, with females exhibiting delayed reproductive maturation, reduced body weight, and increased energy expenditure while males show some indications of low-grade insulin resistance.

Background

Hypothalamic melanin-concentrating hormone (MCH) neurons, which contribute to many fundamental physiological functions including the regulation of energy balance, express numerous genes involved in the synthesis, packaging, and release of the classical neurotransmitters GABA and glutamate [1-6]. However, the functional relevance of their

capacity for GABAergic and/or glutamatergic neurotransmission remains incompletely understood. Some of the most compelling evidence in support of physiologically relevant glutamate co-release comes from longitudinal metabolism studies utilizing transgenic mouse models to delete VGLUT2 from MCH neurons.

MCH-knockout ("MCH-KO") mice are hyperactive, hypophagic, and lean, and also protected from high fat diet-induced obesity and development of insulin resistance, while MCH overexpression can *cause* obesity and insulin resistance [7-11]. Chemogenetic activation of MCH neurons increases food intake in male rats in an MCHR1 dependent manner [12].

However, when the metabolic phenotypes of male MCH neuron-ablated, MCH-KO, and transgenic *Pmch*-Cre;*Slc17a6*$^{fl/fl}$ mice (which lack VGLUT2 in MCH neurons) are compared, it becomes apparent that there is some functional redundancy between MCH- and glutamatergic neurotransmission in these neurons: all three experimental groups exhibit decreased body weight and adiposity, increased locomotor activity, late-onset hypophagia, attenuated weight gain on high-fat diet, and reductions in circulating leptin [13, 14]. Furthermore, specific indicators of glucose sensing and handling differed between groups, revealing a unique role for glutamate co-release from MCH neurons: MCH neuron ablation and deletion of VGLUT2 from MCH neurons, but not MCH-KO, reduce sucrose preference and improve glucose tolerance [13]. These data suggest that both MCH and glutamate release from MCH neurons are necessary for normal regulation of energy balance and glucose handling.

Importantly, to date, all research on the effect of conditional VGLUT2 deletion from MCH neurons has been carried out exclusively in male mice. This constitutes a significant gap in the field, as biological sex and gonadal hormones are closely linked with metabolism. Of note, glucose handling and type II diabetes risk are particularly different between men and women. For instance, women exhibit higher rates of isolated-impaired glucose tolerance than men [15]. (For review, see [16-18]; additionally, this topic is given extensive coverage in Chapter 1.) It is also unknown how early in development the differences in body weight arise, as only adult mice have been used in published studies.

Relatedly, the reproductive development and function of mice with conditional VGLUT2 deletion from MCH neurons has not been studied despite the close relationship between the neuroendocrine reproductive axis and energy balance. Pubertal timing is intrinsically linked to

nutritional status. Low body weight is associated with delayed puberty, but so is obesity and insulin resistance [19-21]. Adult fertility is also impaired by both under- and overnutrition and by insulin resistance [22, 23]. Furthermore, VGLUT2 deletion in MCH neurons has also been shown to alter sleep and circadian rhythms, which also can impact reproductive development and function [24-30].

To address these gaps, we generated *Pmch*$^{\Delta VGLUT2}$ mice, which lack functional VGLUT2 in MCH neurons. The mice were monitored for numerous measures of metabolic and reproductive function from weaning until 20 weeks of age. We were able to recapitulate some, but not all, of the published findings in males, a fact which may in large part be due to strain differences in metabolism and glucose handling (see *Discussion*). However, most notably, several sexually dimorphic phenotypes were observed, reaffirming the importance of incorporating biological sex variables into all neuroscience research, including the neuroendocrine control of metabolism.

Methods

Mice

Animal Care

Mice were housed in a vivarium at the University of Michigan with a 12/12 light/dark cycle and ad libitum access to food and water. The mice received phytoestrogen-reduced Envigo diet 2016 (16% protein/4% fat), except during breeding when mice were fed phytoestrogen-reduced Envigo diet 2019 (19% protein/8% fat) to accommodate additional nutritional needs of pregnant and nursing dams. Phytoestrogen-reduced diet is routinely used in our laboratory to avoid the effects of exogenous estrogens on mouse physiology. All procedures and experiments were carried out in accordance with the guidelines established by the National Institutes of Health Guide for the Care and Use of Laboratory Animals and approved by the University of Michigan Committee on Use and Care of Animals (Animal Protocol #PRO00010420).

Generation of Pmch$^{\Delta VGLUT2}$ *mice*

Pmch-iCre mice were generated as described in Section II. *Pmch*-iCre$^{+/+}$ mice were crossed with *Slc17a6*^{tm1Lowl}/J ("VGLUT2^{flox}) mice (JAX Stock # 012898) to generate *Pmch*-iCre$^{+/-}$;VGLUT2$^{fl/+}$ mice. *Pmch*-iCre$^{+/-}$;VGLUT2$^{fl/+}$ mice were crossed again to VGLUT2^{flox} mice to generate *Pmch*-iCre$^{+/-}$;VGLUT2$^{fl/fl}$ mice (*Pmch*$^{\Delta VGLUT2}$). Finally, these mice were bred together to generate litters which were all homozygous for VGLUT2^{flox} and either homozygous,

heterozygous, or null for Cre. Mice heterozygous for the *Pmch*-iCre allele were used as "Experimental" animals and mice null for the *Pmch*-iCre allele were used as "Control" animals (*Pmch*$^{\Delta VGLUT2}$ and VGLUT2^{flox}, respectively).

Validation of Pmch$^{\Delta VGLUT2}$ *mouse model*

Deletion of VGLUT2 in *Pmch*$^{\Delta VGLUT2}$ mice was verified using dual-label fluorescent *in situ* hybridization (BaseScope, ACD Bio) as previously described [31]. Briefly, adult male and female mice *Pmch*$^{\Delta VGLUT2}$ and VGLUT2^{flox} mice were deeply anesthetized with isoflurane and euthanized by decapitation. Brains were dissected, embedded in O.C.T. Compound (Tissue-Tek, prod. code 4583), and immediately frozen on dry ice and kept at -80 °C until sectioning. Brains were sectioned using a cryostat at approximately -18 °C onto RNAse-free Superfrost Plus microscope slides (Fisher Scientific, cat. no. 22-037-246) at 16 μm in the coronal plane.

Prior to hybridization, slides were fixed in prechilled 10% NBF for 45 minutes at 4 °C and subsequently dehydrated using a standard ethanol series. The slides were allowed to dry and then borders were drawn around the sections using a hydrophobic barrier pen. Slides were pretreated with hydrogen peroxide for 10 minutes followed by RNAscope Protease IV for 10 minutes before hybridization and signal detection steps. To hybridize, about 150 uL of BaseScope probe mixture was applied to each slide and the slides were incubated at 40°C for 2 hours in a HybEZ oven, then washed with RNAscope Wash Buffer and stored overnight in 5x SSC. On the second day, slides were incubated with reagents AMP1 (30 min at 40 °C) and AMP2 (15 min at 40 °C), rinsing with RNAscope Wash Buffer between each AMP incubation. Slides were then counterstained with hematoxylin and coverslipped with DPX.

Reproductive Phenotyping

Starting at weaning (postnatal day 21 [PD21]), males and females were monitored for external indices of pubertal onset. Males were monitored for balanopreputial separation (BPS), defined as the day the prepuce separates fully from the glans and can be manually retracted [32]. Females were monitored for vaginal opening (VO), determined by a simple visual examination of the vulva [33]. Additionally, once females exhibited VO, vaginal gavage was performed daily. Vaginal smear cytology was assessed to determine the day of first estrus and, subsequently, estrus cyclicity [34]. Because body weight can cause indirect effects on pubertal timing and

estrus cyclicity, mice were weighed daily up to postnatal day 60 and weekly from postnatal day 60 until the end of experiments.

Comprehensive metabolic analysis

Comprehensive metabolic analysis including glucose tolerance testing (GTT) were carried out by the University of Michigan Mouse Metabolic Phenotyping Core.

Animal preparation

Male and female mice were single housed on a 12-12 light/dark cycle (6:00AM-6:00PM) and transferred to the University of Michigan Mouse Metabolic Phenotyping Core one week before analysis. Mice were then transferred to the core's indirect calorimetry system (Promethion System, Sable) for measurement of energy expenditure for three consecutive days. The environment was kept at room temperature (20-23 °C). All animals were given Teklad 2196 reduced phytoestrogen chow throughout the experiment.

Energy expenditure and respiratory quotient

Oxygen consumption (VO_2), carbon dioxide production (VCO_2), and spontaneous motor activity were measured continuously for 120 hours using the Promethion (Comprehensive, High-Resolution Behavioral Analysis Systems, Sable Systems International), an integrated open-circuit calorimeter equipped with an optical beam activity monitoring device. Mice were weighed before the measurements began and then individually placed into the Mouse Cage (Model 3721; 8.1 × 14.4 × 5.5 in) with free access to food and water via equipped feeding and drinking devices located inside the cage. The Promethion food intake, water intake, and body weight monitoring system features high precision sensors capable of measuring in real time for mice [35, 36]. The system was routinely calibrated before the experiment using a standard gas (20.5% O_2 and 0.5% CO_2 in N_2). VO_2 and VCO_2 in each cage were sampled sequentially for 30 seconds in 5 minute intervals and motor activity was recorded every second in X, Y, and Z planes. The air flow rate through the chambers was adjusted at a level that maintained the oxygen differential around 0.3% at resting conditions. Respiratory quotient (RQ), also known as respiratory exchange ratio (RER), was calculated as VCO_2/VO_2. Total energy expenditure, carbohydrate oxidation, and fatty acid oxidation were calculated based on the values of VO_2, VCO_2, and the protein breakdown, estimated from urinary nitrogen excretion. [35-42]

Body composition scan

Body fat, lean mass, free water, and total water were measured using an NMR-based analysis (EchoMRI, 4in1-500). The measurements took less than 2 minutes while conscious mice were placed individually in the measuring tube. The machine is checked daily using a reference sample (canola oil) as recommended by the manufacturer.

Glucose Tolerance Test (GTT)

Mice were fasted for 16 hours starting at 5:00PM the day before the test was to take place. Glucose (25%) was given around 9:00 PM via oral gavage at 2.0 g/kg. Blood samples were collected prior to and after administration at 0, 15, 30, 60, and 120 minutes via tail vein bleeding. Blood levels of glucose were measured using a glucometer (Acucheck, Roche) and plasma levels of insulin were determined using a rat/mouse insulin ELISA kit (Millipore). Animals were restrained for less than 1 minute each time a blood sample was collected.

The total area under the curve (AUC) for glucose and insulin were calculated using the trapezoidal rule [43]. Glucose-Insulin Index, an indicator of insulin resistance, is calculated as the product of the AUC for glucose and insulin [44]. HOMA-IR index was calculated as a homeostatic model assessment of β-cell function and insulin resistance as the product of the fasting glucose and insulin [45].

Fertility assay

Female *Pmch*$^{\Delta VGLUT2}$ and VGLUT2^{flox} littermates were housed two to a cage such that each cage contained a "control" and an "experimental" mouse. A sexually experienced wild-type male mouse was assigned to each cage. Twenty days after the introduction of the male, the three mice were separated into individual cages so that females could be monitored accurately for births. The date of birth was noted, and 21 days before the date of birth was taken to be the date of copulation. In rare instances where pups were born less than 21 days after the introduction of the male, the date of copulation was assumed to be the same as the day the male was introduced. Pups were counted at birth and again at time of weaning (21 days). Body weight for each pup was recorded at the time of weaning.

Analysis methods and generation of photomicrographs

Brain sections were imaged using an Axio Imager M2 microscope (Zeiss) with the Allen brain atlas as a reference (mouse.brain-map.org). Digital images of fluorescent ISH were acquired at

10× and 40× magnification. Illumination and exposure time were kept consistent for each channel at a given magnification. Double-labeled cells were counted at three different levels of the LHA along the rostro-caudal axis.

Data are expressed as mean ± SEM. The unpaired two-tailed Student parametric *t* test with Welch's correction was used for between-comparisons of body weight; spontaneous motor activity; plasma glucose and plasma insulin; age and weight at time of BPS, VO, and first estrus; estrous cyclicity; and female fertility. ANCOVA was used for between-group comparisons of oxygen consumption, carbon dioxide production, respiratory exchange rate, energy expenditure, fat oxidation, and glucose oxidation, where it was necessary to consider body weight as a covariate. T tests were performed using GraphPad Prism software, version 9.4. The ANCOVA analyses done for this work were provided by the NIDDK Mouse Metabolic Phenotyping Centers (MMPC, www.mmpc.org) using their Energy Expenditure Analysis page (http://www.mmpc.org/shared/regression.aspx) and supported by grants DK076169 and DK115255.

A p value of < 0.05 was considered significant in all analyses.

Results

Validation of *Pmch*$^{\Delta VGLUT2}$ mice

Dual-label fluorescent *in situ* hybridization (BaseScope) was performed on one series of brain sections from males and females in each experimental group (2 groups, n=3 per group, 12 brains total) to verify deletion of VGLUT2 from MCH neurons as previously described [48, 49]. However, *Pmch* expression levels are so high that *Slc17a6* signal cannot be seen through the *Pmch* signal, making the images challenging to interpret (Figure 5-1). This protocol will be further optimized prior to submission of this data for publication so that deletion of VGLUT2 from *Pmch*+ neurons can be unambiguously demonstrated.

Male and female *Pmch*$^{\Delta VGLUT2}$ mice exhibit no differences in body weight compared to controls when group housed

The metabolic effects of conditional VGLUT2 deletion in MCH neurons have been documented in male mice, but whether females are differentially affected is unknown. Furthermore, these

metabolic effects have been studied in adult animals but have not, to our knowledge, been monitored across the lifespan. To determine whether conditional VGLUT2 deletion from MCH neurons induces any sexually dimorphic effects on metabolism, we monitored the body weight of *Pmch*$^{\Delta VGLUT2}$ and VGLUT2^{flox} mice from weaning at 21 days of age ("PD21") to about 16 weeks of age (males: n=19 control/34 experimental; females: n=23 control/23 experimental, distributed across three cohorts). Data from all three cohorts was pooled as significant differences were not observed between cohorts. No metabolic differences have been observed as a result of the presence of iCre alone, though this will be documented more systematically and comprehensively prior to publication of the animal model.

Male and female mice were weaned into mixed-genotype cages of 3-5 animals each in their home vivarium. An investigator blinded to their genotypes measured the body weight of each animal daily from PD21-PD60 and, subsequently, once per week up to PD116 (approximately 16 weeks of age). Neither male nor female mice exhibited a difference in body weight between experimental groups at any time point (Figure 5-2A, B).

Female *Pmch*$^{\Delta VGLUT2}$ mice have lower lean mass than controls when single-housed

Although no differences in body weight were observed between experimental groups in either sex, we performed body composition analysis on a subset of mice from each group to determine whether there were any more subtle differences between control and experimental groups. Mice were singly housed leading up to the analysis, and so were separated out of their home cages into individual cages 3 days before experiments were to commence and transferred to the testing room in the University of Michigan Mouse Metabolic Phenotyping Core.

One cohort of mice was sent for comprehensive metabolic testing at 16 weeks of age (males: experimental n=10, experimental n=6; females: control n=7 experimental n=5). When body composition analysis was performed, no changes were observed in males, but single-housed *Pmch*-iCre$^{\Delta VGLUT2}$ females were found to weigh less on average (unpaired t-test with Welch's correction; 19.09 ± 0.52g and 20.82 ± 0.38g, p = 0.033). Interestingly, this result was driven by a significant lean mass (unpaired t-test with Welch's correction; 16.28 ± 0.54g and 17.94 ± 0.37g, p = 0.043); no significant differences were observed in fat mass or either free or total H_2O between groups. (Figure 5-2C, D). No differences were observed between groups when body composition was expressed as a percentage (Figure 5-2E, F). All other metabolic parameters

measured—VCO_2, VO_2, respiratory exchange rate (RER), fat and glucose oxidation, and energy expenditure—were not different between groups (Figure 5-3 and Figure 5-4).

Female *Pmch*$^{\Delta VGLUT2}$ mice exhibit increased locomotor activity when single housed

Because a significant difference in body weight was observed in single-housed, but not group-housed, female *Pmch*$^{\Delta VGLUT2}$ mice, we wondered whether any behavioral differences existed between groups to explain this effect. To that end, food intake, water intake, and spontaneous motor activity were measured continuously for 3 days. Spontaneous activity was measured by quantifying beam breaks in the X, Y, and Z planes. No differences were observed in either sex in the Z plane, comprising jumping and rearing up onto the hind legs. The activity in the X and Y planes, comprising normal ambulatory activity around the cage, were similar to each other in both sexes; the X plane was arbitrarily chosen to represent locomotor activity.

Neither male nor female mice exhibited any significant difference in food or water intake during the testing period, though experimental mice of both sexes appear to trend towards slight suppression of both food and water intake during the light phase (Figure 5-5A-D).

No difference in locomotor activity was observed in either sex when the data was averaged over the three days of testing (Figure 5-5E, F). However, a trend towards increased spontaneous activity was observed in the females during the light phase and over 24 h (unpaired t-tests with Welch's correction*; light phase:* experimental 1416.9 ± 235.6 counts/hr; control 1098.5 ± 329.8 counts/hr; p = 0.09; *24 h:* experimental 1087 ± 140.09 counts/hr; control 821.3 ± 264.6 counts/hr; p = 0.08). Thus, we also analyzed the data by day. Female, but not male, *Pmch*-iCre$^{+/-}$;VGLUT2$^{fl/fl}$ mice were found to be significantly more active than controls on the second and third of the three consecutive days of testing (Figure 5-5G, H). Interestingly, the significant difference over 24 h on the second and third days was driven by differences in the light phase rather than the dark phase, as might have been predicted by the three-day average.

The difference between groups arises after the first day of testing due to a reduction in the control group's spontaneous light phase motor activity, while the spontaneous light phase motor activity in the experimental group remains consistent across the three days of testing. On both the second and third days, the difference between female experimental groups was significant over 24 hours of testing (unpaired t-tests with Welch's correction*; day 2:* experimental 1136.2 ± 61.0 counts/hr; control 726.4 ± 126.2 counts/hr; p = 0.030; *day 3:* experimental 1049.7 ± 78.7

counts/hr; control 726.4 ± 129.0 counts/hr; p = 0.047). No difference was observed during the dark phase; the result is driven by a significant difference during the light phase, when mice are typically less active (unpaired t-tests with Welch's correction*; day 2:* experimental 791.1 ± 49.3 counts/hr; control 492.7 ± 125.7 counts/hr; p = 0.032 *day 3:* experimental 692.0 ± 33.7 counts/hr; control 432.3 ± 100.7 counts/hr; p = 0.019).

Male *Pmch*$^{\Delta VGLUT2}$ mice have elevated insulin compared to controls following a glucose challenge

Published studies have shown that MCH neuronal ablation as well as conditional VGLUT2 deletion from MCH neurons can alter glucose homeostasis, including improving glucose tolerance [13, 50, 51]. However, none of these studies have included female animals, despite extensive documentation of sex differences in glucose handling [15, 52-57]. To determine whether sex differences exist in VGLUT2-mediated MCH neuronal regulation of glucose handling, single housed male and female *Pmch*$^{\Delta VGLUT2}$ and VGLUT2^{flox} mice were subjected to oral glucose tolerance testing. Surprisingly, male *Pmch*$^{\Delta VGLUT2}$ mice showed slight *impairment* to glucose tolerance following delivery of a 2 g/kg bolus of glucose following a 16 hour fast. No significant differences in plasma glucose or insulin were observed at any one time point (15, 30, 60, and 90 minutes following oral gavage) or in the glucose area under the curve (AUC) for either sex (Figure 5-6A, B). However, male *Pmch*$^{\Delta VGLUT2}$ mice had a 15.61% greater insulin AUC on average compared to controls (unpaired t-test with Welch's correction*;* 116.02 ± 5.65 and 134.13 ± 4.28, p = 0.032) (Figure 5-6C). No difference was observed between groups in plasma insulin at any time point or in the AUC in females (Figure 5-6D).

The presence of an increased insulin response without a corresponding difference in plasma glucose is suggestive of low-grade insulin resistance, but no differences were observed between experimental and control males in either of two indirect measures of insulin resistance: the HOMA-IR index, which is calculated as a homeostatic model assessment of β-cell function, and glucose-insulin (G-I) index, calculated as the product of glucose and insulin AUCs (Figure 5-6E). Females also exhibited no significant difference between experimental groups in HOMA-IR index or G-I index (Figure 5-6F).

Female *Pmch*$^{\Delta VGLUT2}$ mice exhibit delayed puberty

To our knowledge, it has not previously been investigated whether conditional VGLUT2 deletion from MCH neurons impacts the reproductive system, despite the fact that metabolic and reproductive control are closely linked. Thus, we monitored external indices of pubertal development to determine whether conditionally deleting VGLUT2 from MCH neurons would impact the timing of pubertal milestones.

Starting at the day of weaning (PD21), the same mice used for longitudinal body weight measurement were also monitored for balanopreputial separation (BPS) and vaginal opening (VO). Once VO was observed, vaginal gavage was also performed daily in females and vaginal epithelium cytology observed to ascertain the date of first estrus.

No differences were observed in day of or weight at time of BPS between experimental and control males (Figure 5-9A). However, female experimental mice exhibited a significant delay in timing of VO (unpaired t-test with Welch's correction, 38.7 ± 2.8 days of age and 36.2 ± 3.7 days of age, $p = 0.014$) (Figure 5-9B). No difference was observed in weight at time of VO (Figure 5-9B).

Day of first estrus was also delayed in experimental mice as compared to controls (unpaired t-test with Welch's correction, 50.3 ± 4.7 days of age and 46.9 ± 5.3 days of age, $p = 0.029$) (Figure 5-10A). One control mouse which never exhibited first estrus or began cycling regularly was omitted from analysis.

Female *Pmch*$^{\Delta VGLUT2}$ mice exhibit normal estrus cyclicity

Since pubertal milestones were found to be delayed in female *Pmch*$^{\Delta VGLUT2}$ mice, we wondered whether these mice would also exhibit impairments in adult reproductive function such as disrupted estrous cyclicity. To that end, vaginal gavage was performed, and vaginal epithelium cytology observed each day for 6 weeks to assess estrous cycle stage.

No differences in estrus cyclicity were observed between experimental groups. Total time spent in each cycle stage (proestrus, estrus, and metestrus/diestrus) as well as average cycle length were found to be consistent between control and experimental females (Figure 5-9D, E).

Female *Pmch*$^{\Delta VGLUT2}$ mice are sub-fertile.

After metabolic assessment was finalized, one control and one experimental female from the same litter (around 20 weeks of age) were placed in cages with one wild-type proven male breeder for a total of 16 females spread across 8 breeding cages. Once pregnancy was noted in at least one female of a cage, the animals were separated into different cages to accurately determine the birth date for each mouse. Birth dates and the number of pups per litter were recorded. Birth date was used to estimate the date of conception. Data was collected for 3 pregnancies per mouse. One pregnancy from a VGLUT2^{flox} mouse was omitted following outlier analysis (ROUT, Q=0.1). No difference in average litter size was observed, but female *Pmch*$^{\Delta VGLUT2}$ mice were found to have increased latency to pregnancy (unpaired t-test with Welch's correction, 6 ± 6.3 days and 1 ± 1.4 days, p = 0.02) (Figure 5-7F).

Discussion

In these experiments, we used *Pmch*$^{\Delta VGLUT2}$ mice, which lack VGLUT2 in MCH neurons, to fill in gaps in the existing literature on the effects of conditional loss of glutamatergic signaling in MCH neurons. Specifically, we incorporated females into our experiments to determine whether biological sex is a modulator of the effects of loss of glutamatergic signaling from MCH neurons. We also measured body weight starting at the time of weaning because *Pmch* expression during early postnatal development, i.e., approximately the first two months of life in the mouse, has been shown to be important for normal energy homeostasis, yet the contributions of co-expressed neurotransmitters in MCH neurons to energy homeostasis during this time period has not been investigated [58]. Our data indicate that during the first two months of life, energy balance is not affected by conditional deletion of VGLUT2 from MCH neurons. Thus, we conclude that the role of MCH neurons in establishing normal energy homeostasis mechanisms does not rely on glutamatergic co-transmission from MCH neurons.

We also expanded beyond the metabolic effects of conditional VGLUT2 deletion in MCH neurons to include indicators of reproductive development and function and found that there is a sex-dependent role for glutamate release from MCH neurons in the timing of pubertal development. In males, no delay to BPS is observed in *Pmch*$^{\Delta VGLUT2}$ mice as compared to controls, but *Pmch*$^{\Delta VGLUT2}$ females exhibit delays to both VO and first estrus. These delays,

which are approximately 2-3 days, are not only statistically but biologically significant: if the lifespan of a mouse vs a human female is taken into account, this can be considered equivalent to nearly a year's delay in puberty in humans.

There are some additional considerations to the interpretation of this data regarding the specific variables measured. VO is an external index of female sexual development and is an apoptosis-mediated event that occurs as a result of rising estradiol [59]. While it coincides with the first estrus in some organisms, such as rats, it typically precedes the first estrus by up to 10 days in the mouse, hence we noted the date of first estrus as a separate variable that is perhaps more directly correlated to reproductive maturity. Similarly, BPS, defined as the day when the prepuce separates fully from the glans of the penis and can be manually retracted, is an androgen mediated event [60, 61].

Once puberty is reached, mice show no difference in estrus cyclicity or the number of pups per litter, but they do have a significant increase in latency to pregnancy. Notably, the delays to both VO and first estrous and the increased latency to pregnancy are not accompanied by significant differences in weight, indicating that these effects are likely a direct effect of VGLUT2 deletion in MCH neurons on HPG axis maturation rather than an indirect effect resulting from altered metabolism. Our results reveal a sex difference which seems to result from interactions between MCH neurons and circulating gonadal hormones.

Alternately, the effects on pubertal timing and fertility could be secondary to sleep disruption, which is known to delay pubertal milestones [29, 30]. Male *Pmch*$^{\Delta VGLUT2}$ mice have been shown to have abnormal diurnal variation in REM sleep. It is therefore likely that our experimental animals could potentially have alterations to sleep [83, 84]. Perhaps a sexual dimorphism in the sleep phenotype of *Pmch*$^{\Delta VGLUT2}$ mice is behind the delayed puberty and subfertility phenotypes in females. These possibilities should be explored more thoroughly in future work.

Contrary to previously published data in male mice, in adult male and female *Pmch*$^{\Delta VGLUT2}$ mice, we observed no alterations to body weight or adiposity between experimental groups except in females that had been single housed for at least 24 hours [13, 14]. We also saw no changes to food intake, which have been documented in mice with VGLUT2 conditionally deleted in MCH neurons, though inconsistently [13]. We did observe an increase in locomotor activity in females, but not in males, whereas previous studies which used only male mice did observe an increase in

locomotor activity [13, 14]. Furthermore, our data shows this increase to be driven by spontaneous light-phase locomotor activity, while previously the increase has been shown to occur during the dark phase [13, 14]. Since mice are usually less active during the light phase, this increase in activity could be secondary to a disruption in circadian rhythm which may be amplified in the female. EEG experiments should be performed to determine whether *Pmch*$^{\Delta VGLUT2}$ mice are sleeping less during the light phase and, if so, whether this effect is sexually dimorphic. Indeed, as aforementioned, an effect on normal diurnal rhythms of REM sleep has been previously observed in male *Pmch*$^{\Delta VGLUT2}$ mice, though females have not been characterized [24].

Recently, it has been shown that VGLUT2 deletion from MCH neurons in male mice reduces anxiety-like behavior in novel environments. Anxious mice are less exploratory in a novel environment [62]. The effects observed to spontaneous activity could thus be a suppression of anxiety associated with the new testing cages. It may not be observed in males because mice are given three days to acclimate to the new test cages before measurements begin, which may be optimized for male mice but inadequate for female mice. Anxiety phenotypes should be systematically characterized in both males and females to evaluate this possibility.

Finally, in male mice we observe an increase in the insulin AUC of experimental mice, but not the glucose AUC or to either the HOMA-IR or G-I indices. The presence of increased plasma insulin without a corresponding difference in plasma glucose suggests low-grade insulin resistance, with a greater insulin response required to handle the same glucose load. This was surprising, as published data has shown that VGLUT2 deletion from MCH neurons *improved* glucose tolerance [13]. Furthermore, the lack of effect on the HOMA-IR and G-I indices, both of which are indirect measures of insulin resistance, contradict that conclusion. GTT will need to be repeated in additional cohorts of mice to determine whether this is a genuine effect and, if so, further studies will be required to understand the mechanism underlying this sex-specific impairment to glucose handling. These studies should include molecular and histological inquiry into whether gene expression in the pancreas is altered in our experimental mice, as there is some evidence for *Pmch* expression in the pancreas and thus Cre-mediated deletion of VGLUT2 could be impacting β-cell function [63].

While unexpected, our results are plausible in the context of documented background strain effects on the effect of MCH neurons on various aspects of metabolic function. These differences are likely due to baseline differences in metabolism that may or may not relate directly to MCH neurons themselves; background strain variations have been reported in many phenotypes, including susceptibility to energy balance and type II diabetes [64-69]. For instance, overexpression of MCH has been shown to cause increased body weight on a C57BL/6 background, but it does not do so on an FVB background [8].

MCH knockout (MCHKO) mice have substantial phenotypic differences based on background strain; the comparison between C57BL/6 and 129 mice has been extensively characterized in male mice, but not females [9]. At baseline, male C57BL/6 mice are susceptible to diet induced obesity and glucose intolerance, while 129 mice are comparatively resistant to such phenotypes [66, 67]. Male C57BL/6 mice exhibit higher spontaneous locomotor activity than their 129 counterparts [66, 67]. MCHKO results in proportionally greater heat production and body weight reduction on a C57BL/6 compared to a 129 background despite inducing a proportionally greater increase in spontaneous motor activity on a 129 background [9]. Because C57BL/6 mice are both heavier and more active at baseline than 129 mice, this may simply be a result of floor/ceiling effects [66, 67]. The fact that we observe lower body weight and elevated locomotor activity specifically in single-housed females could be a result of sex variables interacting with the MCH system, and/or be explained by some interaction of strain- and sex-specific effects.

On a C57BL/6 background, male MCHKO and WT mice consume the same number of calories per day on both chow and HFD, while on 129 background, male MCHKO mice consume more chow than WT mice, though when maintained on HFD they consume the same number of calories per day [9]. This has led to the conclusion that any changes in weight gain observed as a result of MCHKO are due to energy expenditure rather than reduced caloric intake in each strain; indeed, the 129 MCHKO mice might be expected to gain weight relative to WTs on chow if caloric intake alone were considered [9]. However, these values have not been normalized to the body weights of the mice, which presents a challenge to the interpretation of the data given that in this study, the experimental groups had significantly different body weights. We analyzed our food intake data using body weight as a covariate and did not observe any differences in food intake between *Pmch*$^{\Delta VGLUT2}$ and control mice in either males or females. Future work will

include an additional group of experimental and control male and female mice that are maintained on HFD instead of chow so that these results may be analyzed in conjunction with published data more directly.

In male 129 and C57BL/6 mice, glucose tolerance worsens when animals are maintained on a HFD in both WT and MCHKO animals. On a BL/6 background, there is no significant difference in glucose tolerance between MCHKO and WT mice on HFD, whereas on a 129 background, though both WTs and MCHKOs have impairments to glucose tolerance, the MCHKO mice have a significant attenuation of the glucose tolerance impairment compared to WTs when maintained on HFD [9]. High-fat diet also elevates insulin in male C57BL/6 background mice, but no significant effect of high-fat diet on insulin is observed on males of a 129 background [9]. Where background strain has been noted, published studies of conditional VGLUT2 deletion in MCH neurons have used mice on a C57BL/6 background [14]. Conditional deletion of VGLUT2 in male mice on a C57BL/6 background also improves glucose tolerance, suggesting that there may be some functional redundancy between MCH and glutamatergic transmission in MCH neurons, although other studies have failed to replicate alterations to glucose tolerance in MCHKO mice maintained on regular chow diet, so the role for MCH in glucose tolerance may be linked to energy status and more pronounced in the context of positive energy balance [9, 13, 14].

The availability of commercial strains necessitated that we generate our experimental animals by breeding *Pmch*-iCre mice, generated and maintained on a C57BL/6 background, to mixed-background VGLUT2^{flox} mice. These VGLUT2^{flox} mice are on a C57BL/6;FVB;129S6 background. The background strain of our experimental animals therefore includes all three strains for which manipulation of MCH expression has been compared, and all have been found to be different, so it stands to reason that manipulating glutamatergic signaling in these cells could exhibit similar phenotypic variation to the manipulation of MCH itself. These inconsistencies of background strain likely explain why our experiments fails to fully recapitulate the results of any published study over conditional VGLUT2 deletion in MCH neurons. For this reason, it also should not be assumed that there are absolutely no effects of conditional VGLUT2 deletion in MCH neurons during the first two months of postnatal development; this, too, may merely be strain-dependent.

The difference in Cre driver line used must also be considered. Previous studies of VGLUT2 deletion from MCH neurons used the commercially available Tg(*Pmch*-cre)1Lowl/J transgenic mouse line to express Cre recombinase in MCH-expressing neurons and subsequently delete functional VGLUT2 from those cells. This *Pmch*-Cre mouse was developed using a bacterial artificial chromosome (BAC) containing the coding region for Cre recombinase flanked by upstream and downstream regulatory elements of the *Pmch* gene [50]. This technique is reasonably efficient and a very common method of introducing DNA sequences into the genome of a model organism. However, the loci of insertion for the BAC are random: it is incorporated into a genomic site with a unique set of regulatory elements, potentially imposing additional layers of regulation on Cre expression unrelated to the regulation of the target gene.

A BAC may also fail to recapitulate epigenetic regulation that occurs at the native gene locus and relies on enhancers that can be located hundreds of thousands of bases up- or downstream. For instance, it has been hypothesized that MCH is induced in the preoptic area during lactation by prolactin, which upregulates the transcription factor STAT5 [70]. STAT5 in turn targets the sequence TTCN_3GAA [71]. In the 1000 kb upstream of the *Pmch* gene, which represents the upper limit of where one might expect to find regulatory elements for a gene, there are approximately 500 such sites, most of which are, of course, not included in the 80 kb BAC transgene. In spite of this, the existing Tg(Pmch-cre)1Lowl/J transgenic mouse line has proven adequate for a majority of applications; Cre-induced reporter expression is observed in virtually 100% of MCH-immunoreactive cells. However, as discussed in Chapter 2, Cre expression is not observed in the preoptic area of these mice during lactation, despite the fact that the presence of *Pmch* mRNA in the preoptic area during late lactation is well-documented in both mice and rats.

Given our interest in reproductive neuroendocrinology and the role of MCH neurons therein, for our purposes, we required a transgenic mouse that would fully capture the regulatory landscape of the gene and ensure Cre and *Pmch* expression align in **all** physiological states. To that end, as described in Chapter 2, we generated a new *Pmch*-Cre knock-in line. We also used the "codon improved Cre" or "iCre" sequence, which applies mammalian codon usage to the prokaryotic Cre sequence, introducing base substitutions that don't alter the peptide sequence but improve Cre expression and reduce the chances of epigenetic silencing when the Cre sequence is used in transgenic mammals. The combination of these two differences between our new *Pmch*-iCre line

and the preexisting BAC transgenic *Pmch*-Cre line resulted in a new line with Cre-driven reporter gene expression in several areas previously unreported in mice. These novel sites of MCH expression are of putative developmental significance. Because Cre recombinase continues to be expressed in such cells even after developmental expression of the *Pmch* gene has been silenced and the normal adult pattern of peptide expression has been achieved, we must also consider the effect of VGLUT2 deletion from these Cre+ cells which are not MCH+ neurons in adulthood.

We observed Cre-induced GFP expression in two regions where *Pmch* mRNA, but not MCH peptide, has been previously described in the rat brain [72]. Both are affiliated with sensory systems but seem to be specifically important for linking sensory percept with emotional valence. These are the pontine reticular nucleus, especially the caudal part (PRN/PRNc) and the olfactory tubercle (OT), where Cre-induced GFP expression is concentrated primarily in the islands of Calleja. The PRNc is connected with the auditory system via projections to the cochlear nuclei, where we also observe sparse GFP (specifically in the dorsal cochlear nucleus) and contributes to the acoustic startle response [73, 74]. The OT is a site of olfactory processing which seems to link olfactory percept with the reward system and thus, more broadly, to olfaction-related motivated behaviors; indeed, the islands of Calleja are associated with the ventral striatum and substantia nigra compacta [75-77]. It is plausible that an impairment in olfactory integration is affecting sexual receptivity and mating behavior in these mice, as these are largely pheromone-dependent processes in rodents, and thus might contribute to the increased latency to pregnancy observed in $Pmch^{\Delta VGLUT2}$ females. In the future, to accurately interpret the results of our studies, it will be important to ascertain whether any populations of cells that are GFP+/MCH- in adulthood could be responsible for any of the effects observed. Whether the GFP+/MCH- cells observed in our new mouse line are also VGLUT2+ will be carefully evaluated before the publication of this chapter.

Overall, we conclude that, on mixed background mice, conditional deletion of functional VGLUT2 from MCH neurons has sex-specific effects on motor activity, particularly on circadian alignment therein; glucose handling; and the timing of pubertal development. These results are novel as the effect of VGLUT2 deletion in MCH neurons has never before been reported in females. Future work should seek to identify the mechanisms by which MCH neurons interact

with gonadal hormones and other sex variables in order to better understand the sex differences observed in this study. Further, our findings raise additional questions regarding the organizational vs. activational roles of glutamatergic signaling on reproductive physiology and energy balance that necessitate the systematic exploration of *Pmch* in prenatal development as well as its colocalization with VGLUT2.

Acknowledgements

Thank you to Susan Allen, MS and Emily Henson, MS for their help in genotyping and assigning experimental groups for this experiment, and to the University of Michigan Animal Phenotyping Core for conducting the comprehensive metabolic analysis including glucose tolerance testing. The University of Michigan Animal Phenotyping Core is supported by NIH grants DK020572, DK089503, and 1U2CDK110768.

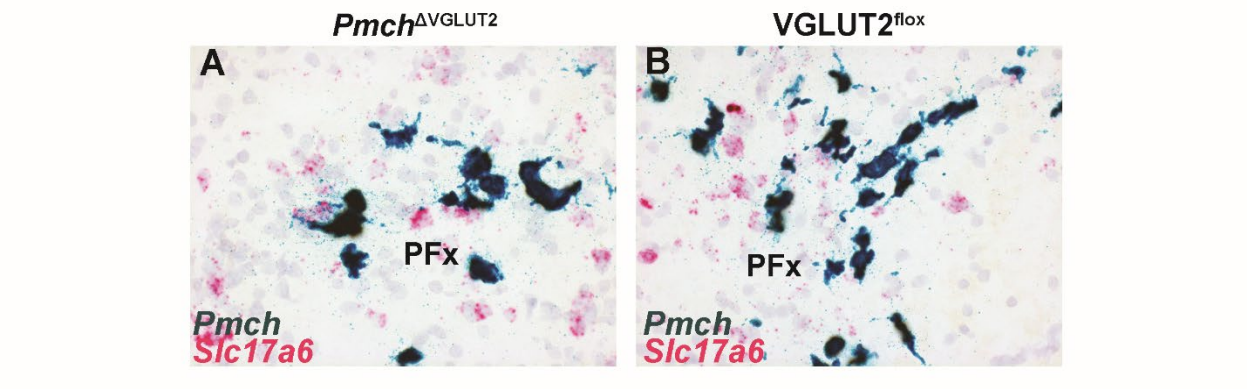

Figure 5-1. *In situ* hybridization for *Pmch* and *Slc17a6* in *Pmch*$^{\Delta VGLUT2}$ and VGLUT2^{flox} mice. *(A) Pmch* and *Slc17a6* mRNA expression in a female *Pmch*$^{\Delta VGLUT2}$ mouse. *(B) Pmch* and *Slc17a6* mRNA expression in a female VGLUT2^{flox} mouse.

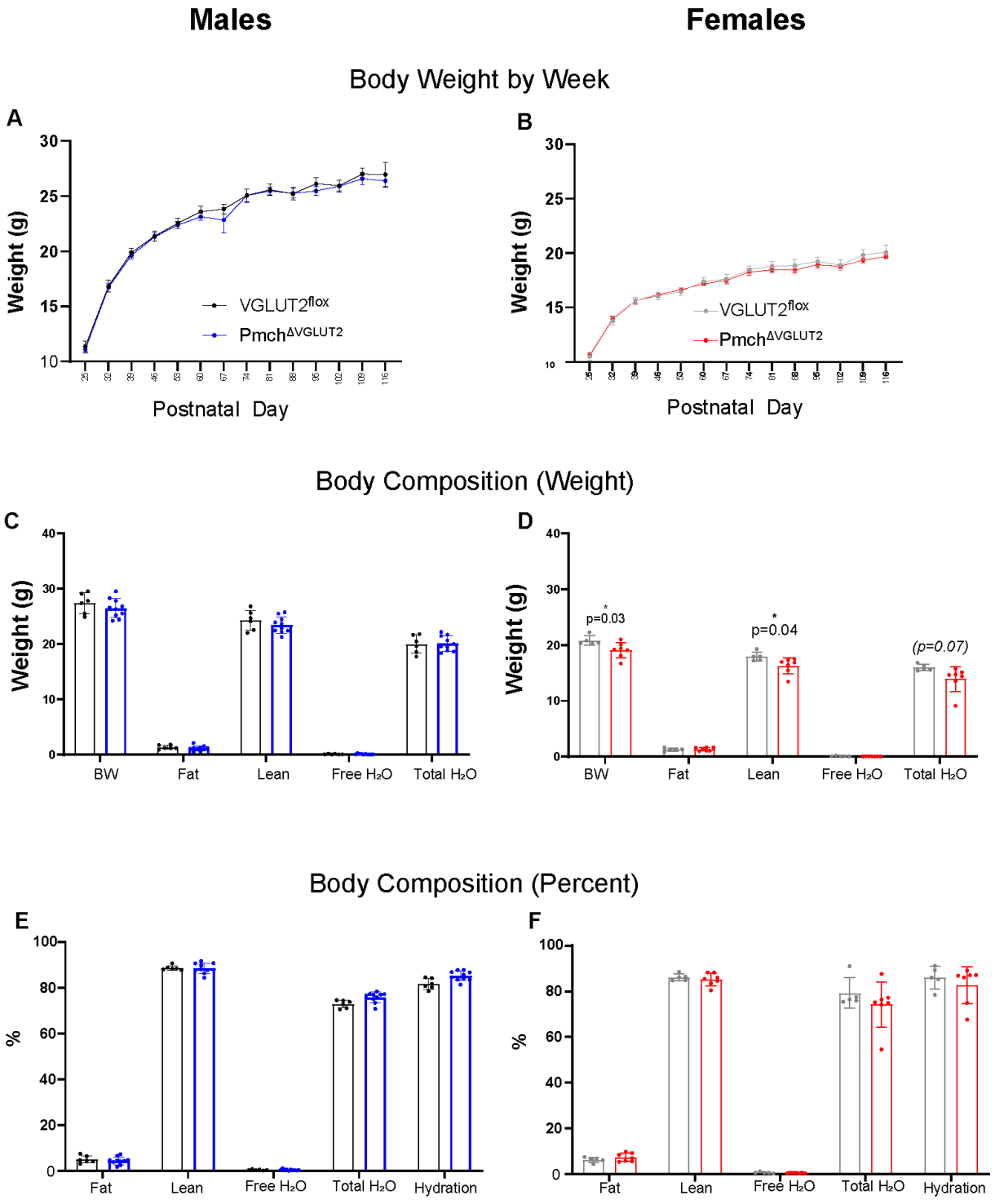

Figure 5-2. Female, but not male, *Pmch*$^{\Delta VGLUT2}$ mice weigh less than VGLUT2^{flox} mice when single housed. *(A, B)* Weekly body weight from PD25 to PD116 in males *(A)* and females *(B)* (Males: n=19 control/34 experimental; females: n=23 control/23 experimental). *(C, D)* Body composition by weight at age ~18 weeks in males *(C)* and females *(D)* (Males: experimental n=10, experimental n=6; females: control n=7 experimental n=5). Note that there is a difference in total body mass driven by a significant reduction in lean mass in *Pmch*-iCre$^{\Delta VGLUT2}$ mice. *(E,F)* Body composition by percentage at age ~18 weeks in males *(E)* and females *(F)* (Males: experimental n=10, experimental n=6; females: control n=7 experimental n=5). There are no significant differences between groups.

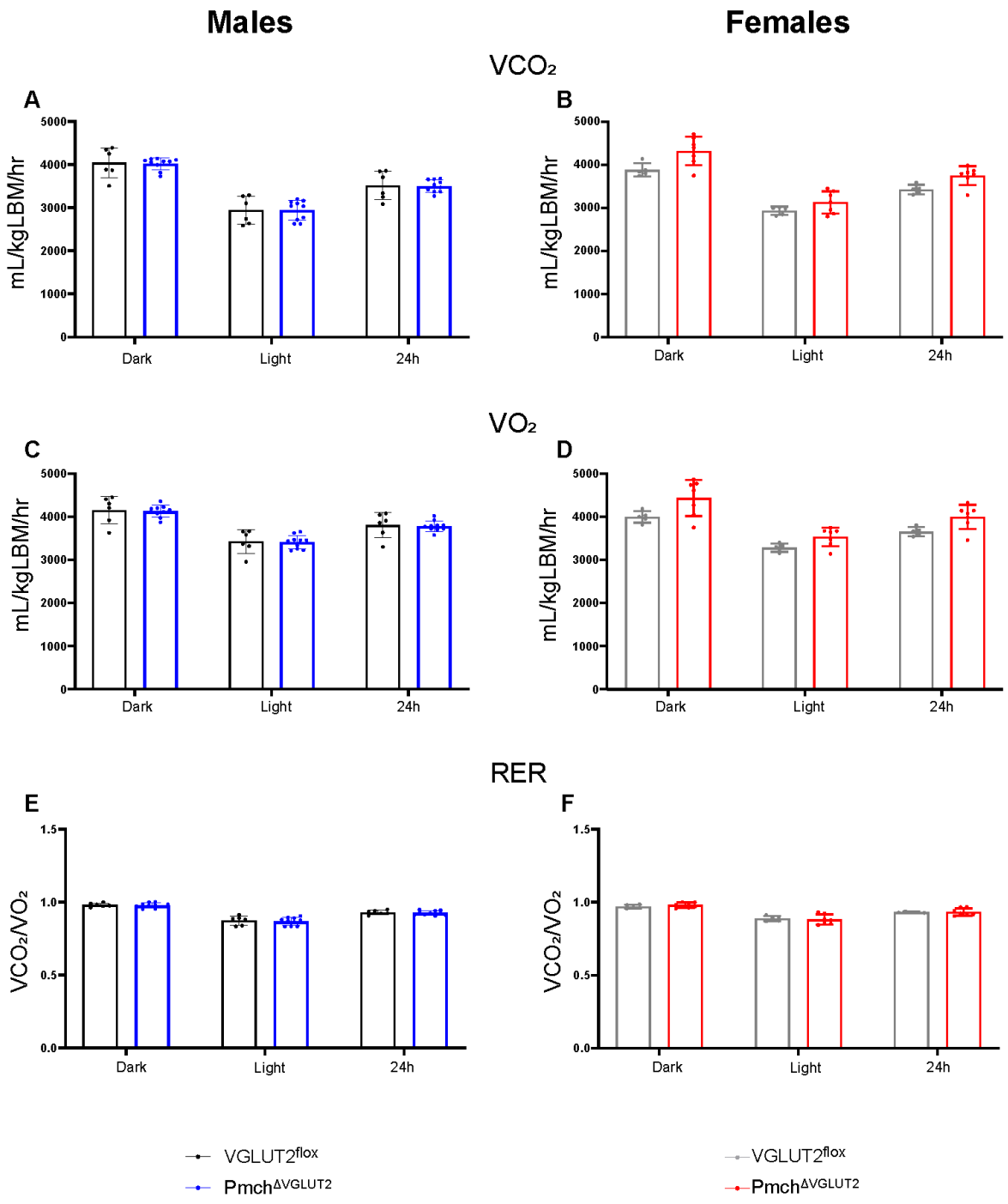

Figure 5-3. Neither male nor female *Pmch*$^{\Delta VGLUT2}$ mice exhibits alterations in respiratory exchange rate. Mice were individually housed with free access to food and water, and VO_2 and VCO_2 in each cage were sampled sequentially for 30s 3×/h for 3 days. (Males: experimental n=10, experimental n=6; females: control n=7 experimental n=5) *(A, B)* Carbon dioxide production (VCO_2) does not differ significantly between male *(A)* or female *(B) Pmch*$^{\Delta VGLUT2}$ and VGLUT2^{flox} mice in the light phase, in the dark phase, or over a 24h period. *(C, D)* Oxygen consumption (VO_2) does not differ significantly between male *(C)* or female *(D) Pmch*$^{\Delta VGLUT2}$ and VGLUT2^{flox} mice in the light phase, in the dark phase, or over a 24h period. *(E, F)* Respiratory exchange ratio (RER), the ratio between VCO_2 and VO_2, does not differ between male *(A)* or female *(B) Pmch*$^{\Delta VGLUT2}$ and VGLUT2^{flox} mice in the light phase, in the dark phase, or over a 24h period.

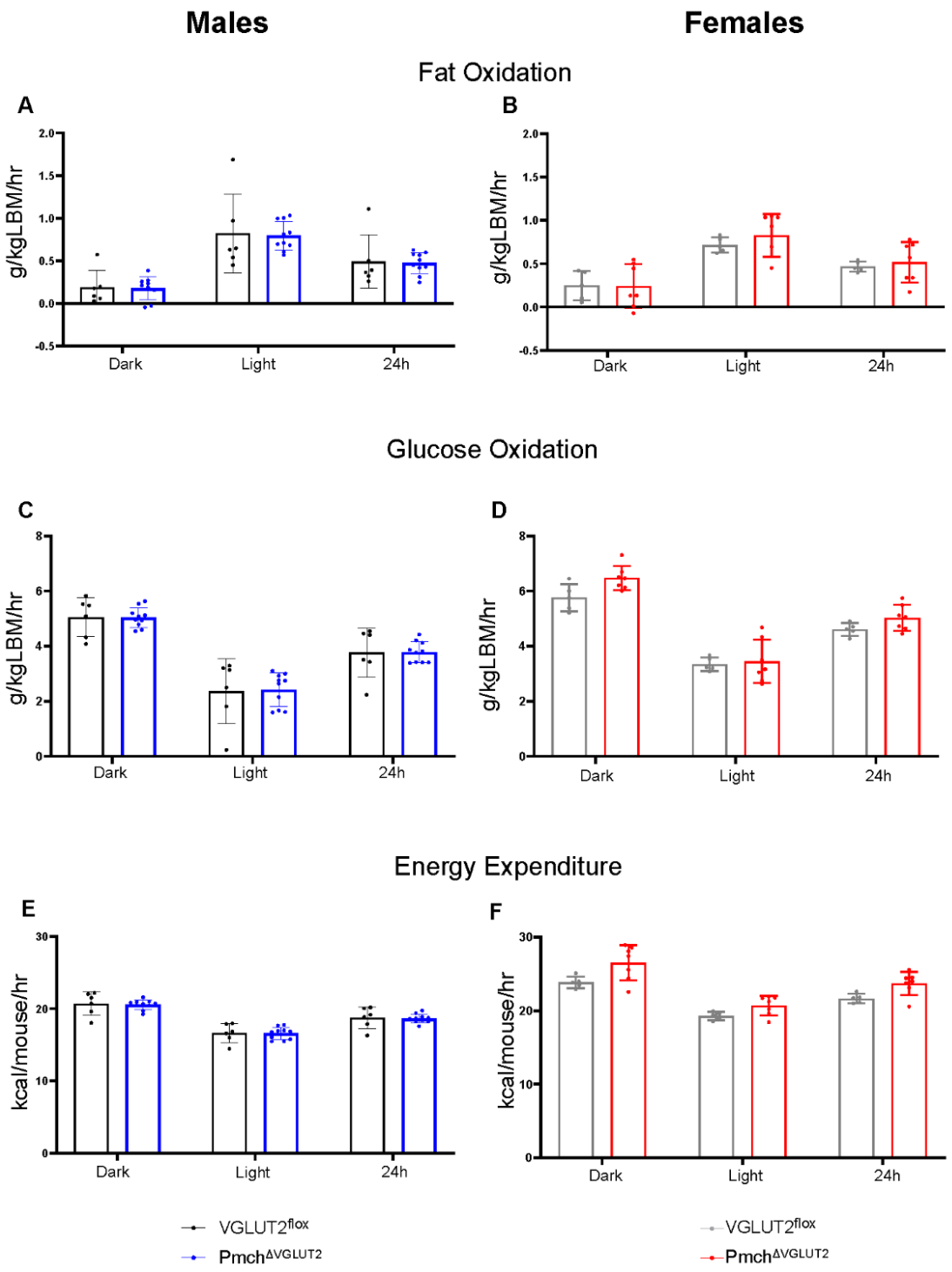

Figure 5-4. Neither male nor female *Pmch*$^{\Delta VGLUT2}$ mice exhibits alterations in rate of energy expenditure. Mice were individually housed with free access to food and water, and VO_2 and VCO_2 in each cage were sampled sequentially for 30s 3×/h for 3 days (Figure 5-3). Total energy expenditure, carbohydrate oxidation, and fatty acid oxidation were calculated respectively based on VO_2, VCO_2, and protein breakdown (estimated from urinary nitrogen excretion). (Males: experimental n=10, experimental n=6; females: control n=7 experimental n=5) *(A, B)* Fat oxidation rate does not differ significantly between male *(A)* or female *(B) Pmch*$^{\Delta VGLUT2}$ and VGLUT2^{flox} mice in the light phase, in the dark phase, or over a 24h period. *(C, D)* Glucose oxidation rate does not differ significantly between male *(C)* or female *(D) Pmch*$^{\Delta VGLUT2}$ and VGLUT2^{flox} mice in the light phase, in the dark phase, or over a 24h period. *(E, F)* Rate of energy expenditure does not differ between male *(E)* or female *(F) Pmch*$^{\Delta VGLUT2}$ and VGLUT2^{flox} mice in the light phase, in the dark phase, or over a 24h period.

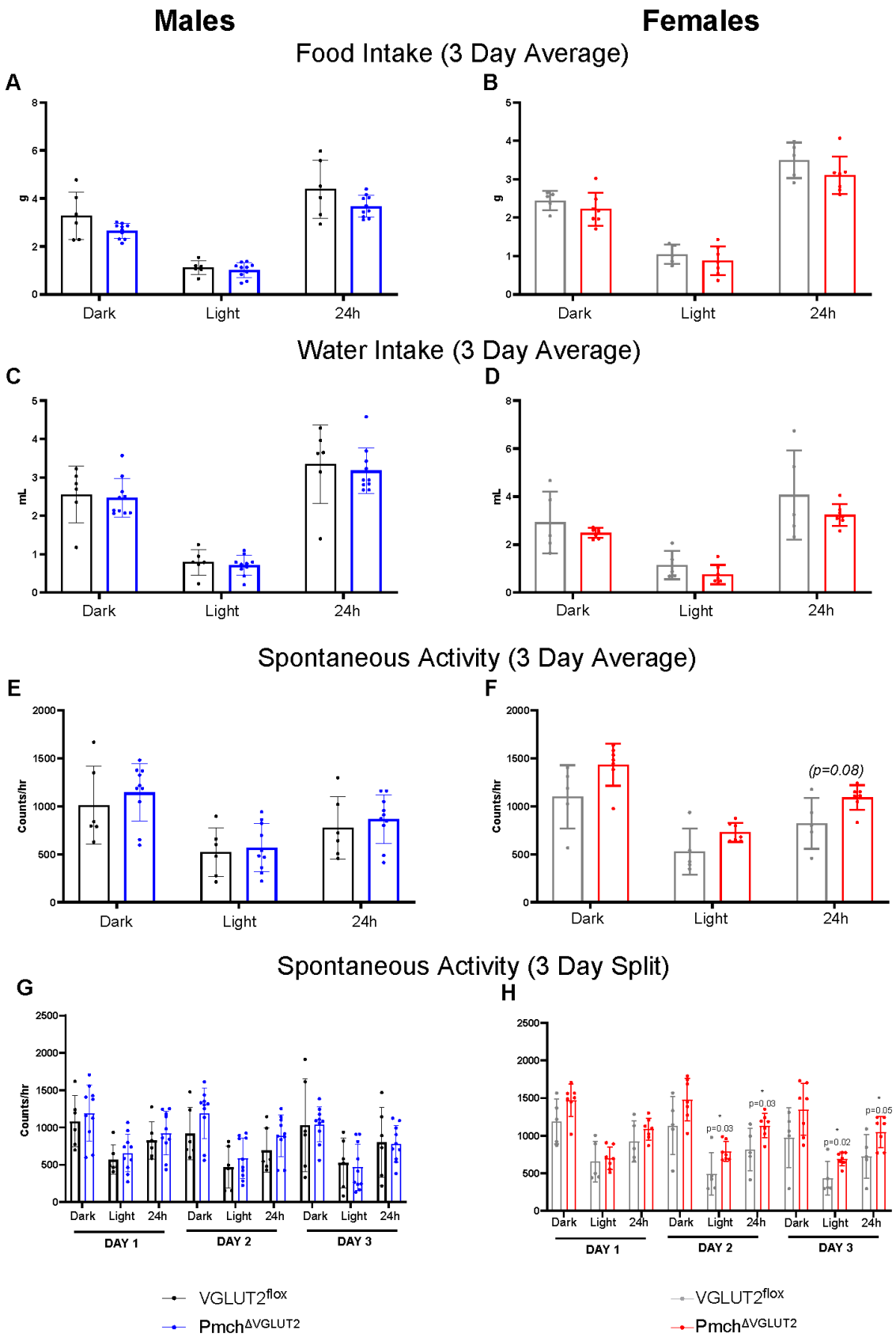
Males
Females
Food Intake (3 Day Average)
A
B
g
Dark
Light
24h
Water Intake (3 Day Average)
C
D
mL
Spontaneous Activity (3 Day Average)
E
F
Counts/hr
(p=0.08)
Spontaneous Activity (3 Day Split)
G
H
DAY 1
DAY 2
DAY 3
p=0.03
p=0.02
p=0.05
VGLUT2flox
PmchΔVGLUT2

Figure 5-5. Female *Pmch*$^{\Delta VGLUT2}$ mice exhibit increased spontaneous activity but no change to food intake. Mice were individually housed with free access to food and water and food intake, water intake, and spontaneous activity were measured using feeding and drinking devices located inside the experimental cages and by optical beam breaks. (Males: experimental n=10, experimental n=6; females: control n=7 experimental n=5) *(A, B)* Food intake in *Pmch*$^{\Delta VGLUT2}$ and VGLUT2^{flox} mice averaged across three experimental days in males *(A)* and females *(B)*. There are no significant differences between groups in the light phase, in the dark phase, or over a 24h period. *(C, D)* Water intake in *Pmch*$^{\Delta VGLUT2}$ and VGLUT2^{flox} mice averaged across three experimental days in males *(C)* and females *(D)*. There are no significant differences between groups in the light phase, in the dark phase, or over a 24h period. *(E,F)* Spontaneous locomotor activity in the X plane in *Pmch*$^{\Delta VGLUT2}$ and VGLUT2^{flox} mice averaged across three experimental days in males *(E)* and females *(F)*. There are no significant differences between groups in the light phase, in the dark phase, or over a 24h period. However, there is a trend towards increased activity in female *Pmch*$^{\Delta VGLUT2}$ mice over 24h. *(G, H)* Spontaneous motor activity compared between groups showing data from the three individual days. On the second and third days of testing, female *Pmch*$^{\Delta VGLUT2}$ mice exhibit increased spontaneous activity over 24h driven by an increase during the light phase. Note that the difference arises not from an increase in activity in experimental mice over the course of testing, but high baseline activity in VGLUT2^{flox} females on the first day compared to the second and third days.

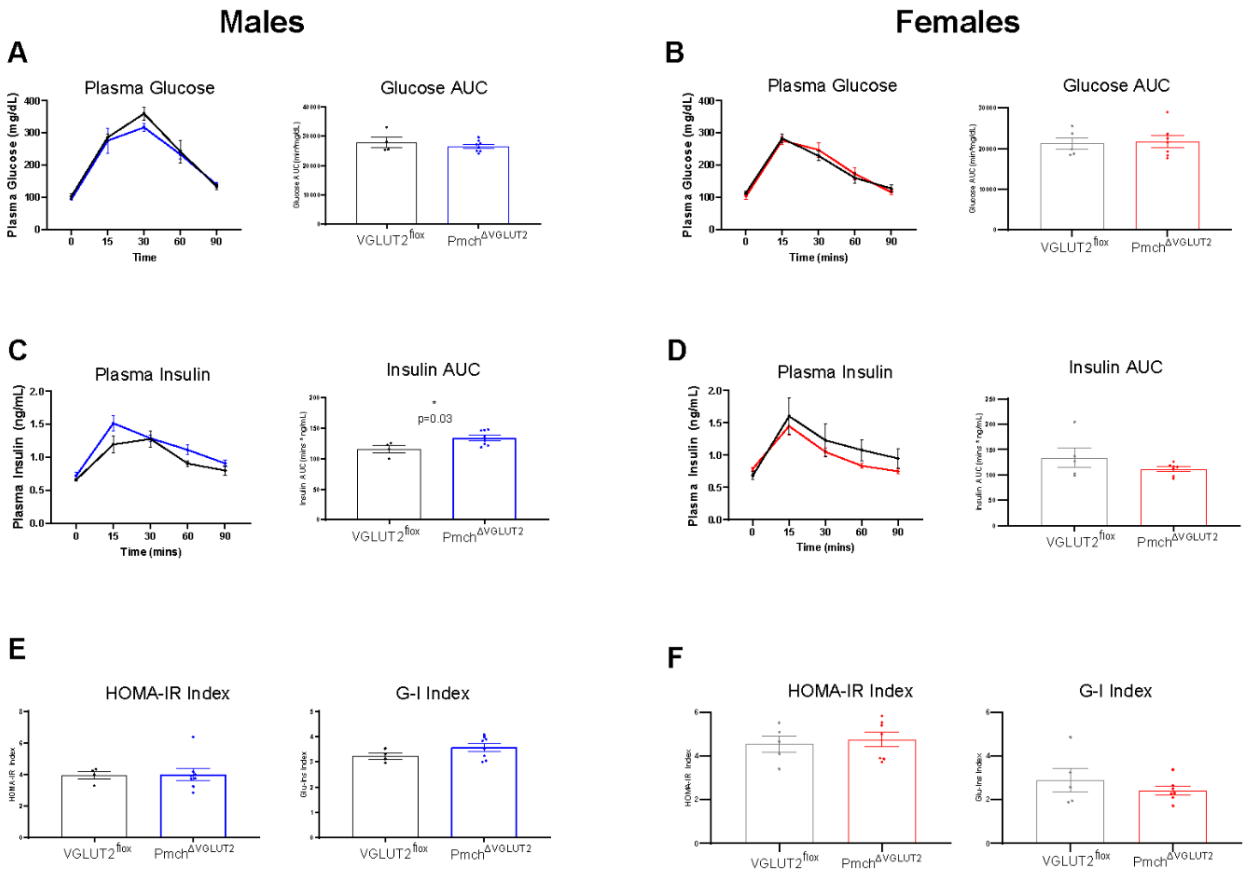

Figure 5-6. Male *Pmch*$^{\Delta VGLUT2}$ mice exhibit elevated insulin AUC following a glucose challenge. Mice were fasted for 16h the day before the test. Glucose (25%) was administered via oral gavage and blood samples were collected from the tail vein immediately prior to and every 15 minutes after glucose administration for 2 hours. Blood glucose and insulin were measured by ELISA. (Males: experimental n=10, experimental n=6; females: control n=7 experimental n=5) *(A, B)* Plasma glucose levels immediately before and 15, 30, 60, and 90 minutes following administration of 2 g/kg bolus of glucose via oral gavage *(left)* and area under the glucose curve (*right*) in male (*A*) and female (*B*) *Pmch*$^{\Delta VGLUT2}$ and VGLUT2^{flox} mice. The glucose AUC is not different between *Pmch*$^{\Delta VGLUT2}$ and VGLUT2^{flox} mice in either sex. *(C, D)* Plasma insulin levels immediately before and 15, 30, 60, and 90 minutes following administration of 2 g/kg bolus of glucose via oral gavage *(left)* and area under the insulin curve (*right*) in male (*C*) and female (*D*) *Pmch*$^{\Delta VGLUT2}$ and VGLUT2^{flox} mice. Note that the insulin AUC is higher in *Pmch*$^{\Delta VGLUT2}$ male mice, but no differences are observed between experimental groups in females. *(E, F)* Two indices of insulin resistance, the Homeostatic Model Assessment of Insulin Resistance (HOMA-IR) test, which indirectly assesses β-cell function and insulin resistance, and the Glucose-insulin (G-I) index, which is the product of the glucose and insulin AUCs and is another indicator of insulin resistance, were calculated for male *(E)* and female *(F)* *Pmch*$^{\Delta VGLUT2}$ and VGLUT2^{flox} mice. No differences were observed between experimental groups for either model in either sex.

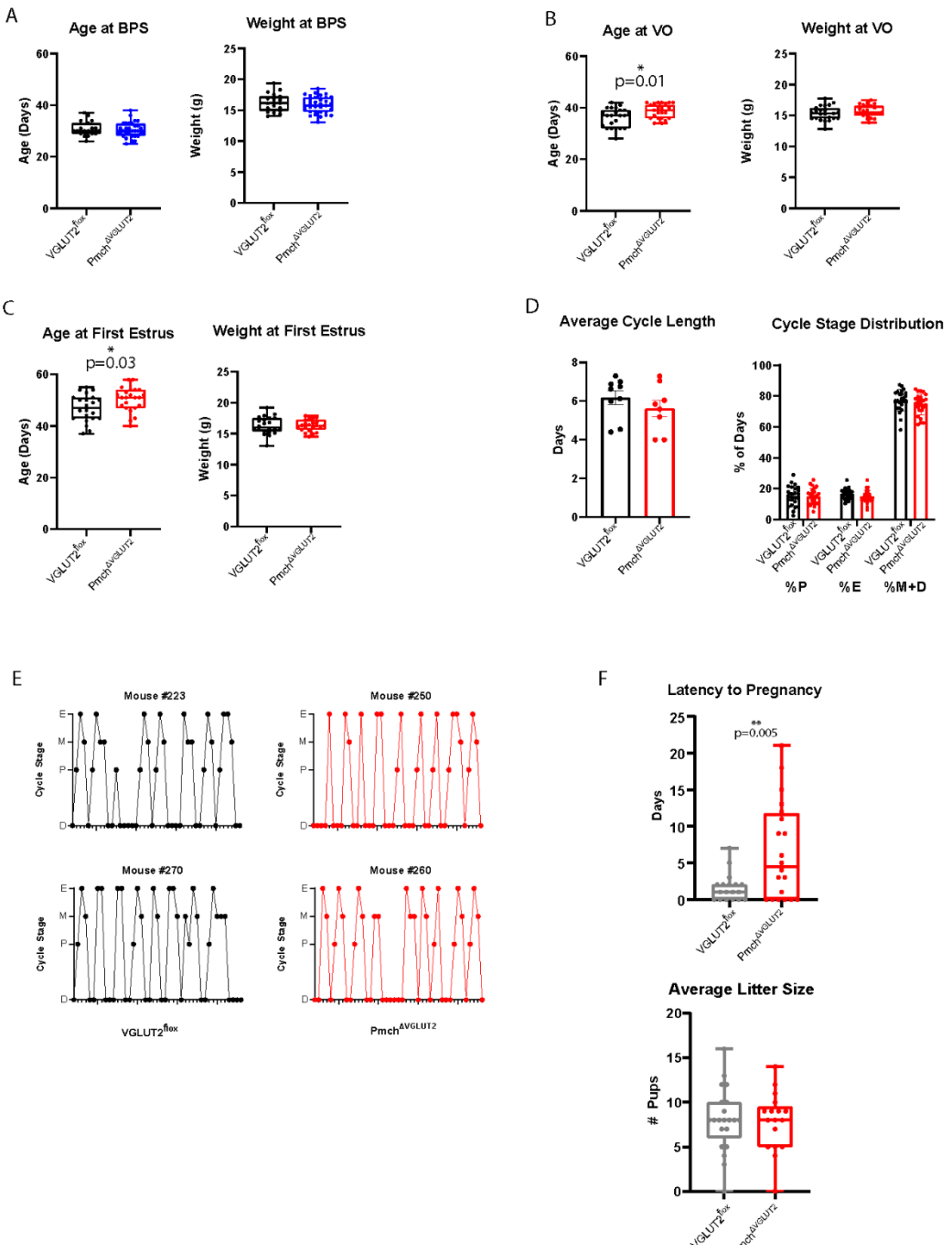

Figure 5-7. Female *Pmch*$^{\Delta VGLUT2}$ mice exhibit delayed pubertal milestones and increased latency to pregnancy. Mice were monitored daily for BPS/VO and, once VO was observed, females were monitored daily for first estrus. Starting at 6 weeks of age, females were subjected to vaginal lavage daily to monitor estrus cyclicity via vaginal epithelial cell morphology. (Males: n=19 control/34 experimental; females: n=23 control/23 experimental). Latency to copulation and average litter size was also compared between *Pmch*$^{\Delta VGLUT2}$ and VGLUT2^{flox} females (experimental n=8, control n=8). *(A)* Age (*left*) and weight (*right*) at time of complete BPS (*A*) or VO (*B*). No differences are observed in males, but female *Pmch*$^{\Delta VGLUT2}$ mice have delayed VO. *(C)* Age (*left*) and weight (*right*) at time of first estrus in females. *Pmch*$^{\Delta VGLUT2}$ mice have delayed first estrus. (*D, E*) Estrus cyclicity in female *Pmch*$^{\Delta VGLUT2}$ and VGLUT2^{flox} mice. No differences are observed in average cycle length (*D, left*) or average time spent in each cycle stage (*D, right*). Representative diagrams showing estrus cyclicity in *Pmch*$^{\Delta VGLUT2}$ and VGLUT2^{flox} (red and black, respectively) are shown in (*E*). (*F*) Fertility compared between *Pmch*$^{\Delta VGLUT2}$ and VGLUT2^{flox} females. Latency to copulation

(*top*) and average litter size (*bottom*) were both highly variable in both groups. No significant differences were observed between groups.

References

1. Mickelsen, L.E., et al., *Neurochemical Heterogeneity Among Lateral Hypothalamic Hypocretin/Orexin and Melanin-Concentrating Hormone Neurons Identified Through Single-Cell Gene Expression Analysis.* eNeuro, 2017. **4**(5).
2. Mickelsen, L.E., et al., *Single-cell transcriptomic analysis of the lateral hypothalamic area reveals molecularly distinct populations of inhibitory and excitatory neurons.* Nat Neurosci, 2019. **22**(4): p. 642-656.
3. Nectow, A.R., et al., *Rapid Molecular Profiling of Defined Cell Types Using Viral TRAP.* Cell Rep, 2017. **19**(3): p. 655-667.
4. Rose, C.R., et al., *Molecular and cellular physiology of sodium-dependent glutamate transporters.* Brain Res Bull, 2018. **136**: p. 3-16.
5. Blanco-Centurion, C., et al., *VGAT and VGLUT2 expression in MCH and orexin neurons in double transgenic reporter mice.* IBRO Rep, 2018. **4**: p. 44-49.
6. Prida, E., et al., *Crosstalk between Melanin Concentrating Hormone and Endocrine Factors: Implications for Obesity.* Int J Mol Sci, 2022. **23**(5).
7. Shimada, M., et al., *Mice lacking melanin-concentrating hormone are hypophagic and lean.* Nature, 1998. **396**(6712): p. 670-4.
8. Ludwig, D.S., et al., *Melanin-concentrating hormone overexpression in transgenic mice leads to obesity and insulin resistance.* J Clin Invest, 2001. **107**(3): p. 379-86.
9. Kokkotou, E., et al., *Mice with MCH ablation resist diet-induced obesity through strain-specific mechanisms.* Am J Physiol Regul Integr Comp Physiol, 2005. **289**(1): p. R117-24.
10. Jeon, J.Y., et al., *MCH-/- mice are resistant to aging-associated increases in body weight and insulin resistance.* Diabetes, 2006. **55**(2): p. 428-34.
11. Tadayyon, M., et al., *Expression of melanin-concentrating hormone receptors in insulin-producing cells: MCH stimulates insulin release in RINm5F and CRI-G1 cell-lines.* Biochem Biophys Res Commun, 2000. **275**(2): p. 709-12.
12. Noble, E.E., et al., *Control of Feeding Behavior by Cerebral Ventricular Volume Transmission of Melanin-Concentrating Hormone.* Cell Metab, 2018. **28**(1): p. 55-68.e7.
13. Schneeberger, M., et al., *Functional analysis reveals differential effects of glutamate and MCH neuropeptide in MCH neurons.* Mol Metab, 2018. **13**: p. 83-89.
14. Whiddon, B.B. and R.D. Palmiter, *Ablation of neurons expressing melanin-concentrating hormone (MCH) in adult mice improves glucose tolerance independent of MCH signaling.* J Neurosci, 2013. **33**(5): p. 2009-16.
15. Zhang, X., et al., *Sex Differences in the Prevalence of and Risk Factors for Abnormal Glucose Regulation in Adults Aged 50 Years or Older With Normal Fasting Plasma Glucose Levels.* Front Endocrinol (Lausanne), 2020. **11**: p. 531796.
16. Tramunt, B., et al., *Sex differences in metabolic regulation and diabetes susceptibility.* Diabetologia, 2020. **63**(3): p. 453-461.
17. Varlamov, O., C.L. Bethea, and C.T. Roberts, *Sex-specific differences in lipid and glucose metabolism.* Front Endocrinol (Lausanne), 2014. **5**: p. 241.
18. Louet, J.F., C. LeMay, and F. Mauvais-Jarvis, *Antidiabetic actions of estrogen: insight from human and genetic mouse models.* Curr Atheroscler Rep, 2004. **6**(3): p. 180-5.

19. Dunger, D.B., M.L. Ahmed, and K.K. Ong, *Early and late weight gain and the timing of puberty.* Mol Cell Endocrinol, 2006. **254-255**: p. 140-5.
20. Frisch, R.E. and R. Revelle, *Height and weight at menarche and a hypothesis of menarche.* Arch Dis Child, 1971. **46**(249): p. 695-701.
21. Ibáñez, L., et al., *Metformin therapy during puberty delays menarche, prolongs pubertal growth, and augments adult height: a randomized study in low-birth-weight girls with early-normal onset of puberty.* J Clin Endocrinol Metab, 2006. **91**(6): p. 2068-73.
22. Kahn, B.E. and R.E. Brannigan, *Obesity and male infertility.* Curr Opin Urol, 2017. **27**(5): p. 441-445.
23. Broughton, D.E. and K.H. Moley, *Obesity and female infertility: potential mediators of obesity's impact.* Fertil Steril, 2017. **107**(4): p. 840-847.
24. Naganuma, F., et al., *Melanin-concentrating hormone neurons promote rapid eye movement sleep independent of glutamate release.* Brain Struct Funct, 2019. **224**(1): p. 99-110.
25. Mahoney, M.M., *Shift work, jet lag, and female reproduction.* Int J Endocrinol, 2010. **2010**: p. 813764.
26. Stocker, L.J., et al., *Influence of shift work on early reproductive outcomes: a systematic review and meta-analysis.* Obstet Gynecol, 2014. **124**(1): p. 99-110.
27. Mosko, S.S., E. Lewis, and J.F. Sassin, *Impaired sexual maturation associated with sleep apnea syndrome during puberty: a case study.* Sleep, 1980. **3**(1): p. 13-22.
28. Chen, Y.H., et al., *Obstructive sleep apnea and the risk of adverse pregnancy outcomes.* Am J Obstet Gynecol, 2012. **206**(2): p. 136.e1-5.
29. Poli, F., et al., *High prevalence of precocious puberty and obesity in childhood narcolepsy with cataplexy.* Sleep, 2013. **36**(2): p. 175-81.
30. Shaw, N.D., et al., *Obstructive sleep apnea (OSA) in preadolescent girls is associated with delayed breast development compared to girls without OSA.* J Clin Sleep Med, 2013. **9**(8): p. 813-8.
31. Baker, A.M., et al., *Robust RNA-based in situ mutation detection delineates colorectal cancer subclonal evolution.* Nat Commun, 2017. **8**(1): p. 1998.
32. Prevot, V., *Puberty in Mice and Rats*, in *Knobil and Neill's Physiology of Reproduction*. 2015, Academic Press: San Diego. p. 13959-1439.
33. S Caligioni, C., *Assessing Reproductive Status/Stages in Mice.* 2009. **Appendix 4**: p. Appendix 4I.
34. Nelson, J.F., et al., *A longitudinal study of estrous cyclicity in aging C57BL/6J mice: I. Cycle frequency, length and vaginal cytology.* Biol Reprod, 1982. **27**(2): p. 327-39.
35. Riachi, M., J. Himms-Hagen, and M.E. Harper, *Percent relative cumulative frequency analysis in indirect calorimetry: application to studies of transgenic mice.* Can J Physiol Pharmacol, 2004. **82**(12): p. 1075-83.
36. Tschöp, M.H., et al., *A guide to analysis of mouse energy metabolism.* Nat Methods, 2011. **9**(1): p. 57-63.
37. Simonson, D.C. and R.A. DeFronzo, *Indirect calorimetry: methodological and interpretative problems.* Am J Physiol, 1990. **258**(3 Pt 1): p. E399-412.
38. Frayn, K.N., *Calculation of substrate oxidation rates in vivo from gaseous exchange.* J Appl Physiol Respir Environ Exerc Physiol, 1983. **55**(2): p. 628-34.

39. Lusk, G., *ANIMAL CALORIMETRY Twenty-Fourth Paper. ANALYSIS OF THE OXIDATION OF MIXTURES OF CARBOHYDRATE AND FAT.* Journal of Biological Chemistry, 1924. **59**: p. 41-42.
40. Ferrannini, E., *The theoretical bases of indirect calorimetry: a review.* Metabolism, 1988. **37**(3): p. 287-301.
41. Kaiyala, K.J., *Mathematical model for the contribution of individual organs to non-zero y-intercepts in single and multi-compartment linear models of whole-body energy expenditure.* PLoS One, 2014. **9**(7): p. e103301.
42. Kaiyala, K.J. and M.W. Schwartz, *Toward a more complete (and less controversial) understanding of energy expenditure and its role in obesity pathogenesis.* Diabetes, 2011. **60**(1): p. 17-23.
43. Allison, D.B., et al., *The use of areas under curves in diabetes research.* Diabetes Care, 1995. **18**(2): p. 245-50.
44. Henriksen, E.J., et al., *Effect of chronic bradykinin administration on insulin action in an animal model of insulin resistance.* Am J Physiol, 1998. **275**(1): p. R40-5.
45. Matthews, D.R., et al., *Homeostasis model assessment: insulin resistance and beta-cell function from fasting plasma glucose and insulin concentrations in man.* Diabetologia, 1985. **28**(7): p. 412-9.
46. Idris, A.I., *Ovariectomy/Orchidectomy in Rodents*, in *Bone Research Protocols*, M.H. Helfrich and S.H. Ralston, Editors. 2012, Humana Press: Totowa, NJ. p. 545-551.
47. Silveira, M.A., et al., *GnRH Neuron Activity and Pituitary Response in Estradiol-Induced vs Proestrous Luteinizing Hormone Surges in Female Mice.* Endocrinology, 2017. **158**(2): p. 356-366.
48. Frazão, R., et al., *Shift in Kiss1 cell activity requires estrogen receptor α.* J Neurosci, 2013. **33**(7): p. 2807-20.
49. Garcia-Galiano, D., et al., *PI3Kα inactivation in leptin receptor cells increases leptin sensitivity but disrupts growth and reproduction.* JCI Insight, 2017. **2**(23).
50. Kong, D., et al., *Glucose stimulation of hypothalamic MCH neurons involves K(ATP) channels, is modulated by UCP2, and regulates peripheral glucose homeostasis.* Cell Metab, 2010. **12**(5): p. 545-52.
51. Burdakov, D., O. Gerasimenko, and A. Verkhratsky, *Physiological changes in glucose differentially modulate the excitability of hypothalamic melanin-concentrating hormone and orexin neurons in situ.* J Neurosci, 2005. **25**(9): p. 2429-33.
52. Veiras, L.C., et al., *Sexual Dimorphic Pattern of Renal Transporters and Electrolyte Homeostasis.* J Am Soc Nephrol, 2017. **28**(12): p. 3504-3517.
53. Rotondo, F., et al., *Effect of sex on glucose handling by adipocytes isolated from rat subcutaneous, mesenteric and perigonadal adipose tissue.* PeerJ, 2018. **6**: p. e5440.
54. Balen, D., et al., *Revised immunolocalization of the Na+-D-glucose cotransporter SGLT1 in rat organs with an improved antibody.* Am J Physiol Cell Physiol, 2008. **295**(2): p. C475-89.
55. Sabolic, I., et al., *Expression of Na+-D-glucose cotransporter SGLT2 in rodents is kidney-specific and exhibits sex and species differences.* Am J Physiol Cell Physiol, 2012. **302**(8): p. C1174-88.
56. Ostenson, C.G., V. Grill, and M. Roos, *Studies on sex dependency of B-cell susceptibility to streptozotocin in a rat model of type II diabetes mellitus.* Exp Clin Endocrinol, 1989. **93**(2-3): p. 241-7.

57. Rossini, A.A., et al., *Sex differences in the multiple-dose streptozotocin model of diabetes.* Endocrinology, 1978. **103**(4): p. 1518-20.
58. Mul, J.D., et al., *Pmch expression during early development is critical for normal energy homeostasis.* Am J Physiol Endocrinol Metab, 2010. **298**(3): p. E477-88.
59. Rodriguez, I., et al., *Mouse vaginal opening is an apoptosis-dependent process which can be prevented by the overexpression of Bcl2.* Dev Biol, 1997. **184**(1): p. 115-21.
60. Korenbrot, C.C., I.T. Huhtaniemi, and R.I. Weiner, *Preputial separation as an external sign of pubertal development in the male rat.* Biol Reprod, 1977. **17**(2): p. 298-303.
61. LYONS, W.R., I. BERLIN, and S. FRIEDLANDER, *CORNIFICATION OF BALANO-PREPUTIAL EPITHELIUM IN NORMAL RATS AND IN CASTRATED RATS TREATED WITH TESTOSTERONE PROPIONATE1.* Endocrinology, 1942. **31**(6): p. 659-663.
62. Sankhe, A.S., et al., *Loss of glutamatergic signalling from MCH neurons reduced anxiety-like behaviours in novel environments.* J Neuroendocrinol, 2023. **35**(1): p. e13222.
63. Pissios, P., et al., *Melanin concentrating hormone is a novel regulator of islet function and growth.* Diabetes, 2007. **56**(2): p. 311-9.
64. Rossmeisl, M., et al., *Variation in type 2 diabetes-related traits in mouse strains susceptible to diet-induced obesity.* Diabetes, 2003. **52**(8): p. 1958-1966.
65. Hofmann, W.E., et al., *Effects of genetic background on thermoregulation and fatty acid-induced uncoupling of mitochondria in UCP1-deficient mice.* Journal of Biological Chemistry, 2001. **276**(15): p. 12460-12465.
66. Surwit, R.S., et al., *Diet-induced changes in uncoupling proteins in obesity-prone and obesity-resistant strains of mice.* Proceedings of the national academy of sciences, 1998. **95**(7): p. 4061-4065.
67. Black, B.L., et al., *Differential effects of fat and sucrose on body composition in AJ and C57BL/6 mice.* Metabolism, 1998. **47**(11): p. 1354-1359.
68. Montagutelli, X., *Effect of the genetic background on the phenotype of mouse mutations.* Journal of the American Society of Nephrology, 2000. **11**(suppl 2): p. S101-S105.
69. Silva, A.J., et al., *Mutant mice and neuroscience: recommendations concerning genetic background.* Neuron, 1997. **19**(4): p. 755-759.
70. Teixeira, P.D.S., et al., *Regulation and neurochemical identity of melanin-concentrating hormone neurons in the preoptic area of lactating mice.* J Neuroendocrinol, 2019: p. e12818.
71. Ehret, G.B., et al., *DNA binding specificity of different STAT proteins. Comparison of in vitro specificity with natural target sites.* J Biol Chem, 2001. **276**(9): p. 6675-88.
72. Bittencourt, J., et al., *The melanin-concentrating hormone system of the rat brain: an immuno-and hybridization histochemical characterization.* Journal of Comparative Neurology, 1992. **319**(2): p. 218-245.
73. Kandler, K. and H. Herbert, *Auditory projections from the cochlear nucleus to pontine and mesencephalic reticular nuclei in the rat.* Brain Res, 1991. **562**(2): p. 230-42.
74. Fendt, M., M. Koch, and H.U. Schnitzler, *Corticotropin-releasing factor in the caudal pontine reticular nucleus mediates the expression of fear-potentiated startle in the rat.* Eur J Neurosci, 1997. **9**(2): p. 299-305.
75. Wesson, D.W. and D.A. Wilson, *Sniffing out the contributions of the olfactory tubercle to the sense of smell: hedonics, sensory integration, and more?* Neurosci Biobehav Rev, 2011. **35**(3): p. 655-68.

76. Talbot, K., N.J. Woolf, and L.L. Butcher, *Feline islands of Calleja complex: I. Cytoarchitectural organization and comparative anatomy.* J Comp Neurol, 1988. **275**(4): p. 553-79.
77. Fallon, J.H., et al., *The islands of Calleja: organization and connections.* J Comp Neurol, 1978. **181**(2): p. 375-95.
78. Poo, C., et al., *Spatial maps in piriform cortex during olfactory navigation.* Nature, 2022. **601**(7894): p. 595-599.
79. Stettler, D.D. and R. Axel, *Representations of odor in the piriform cortex.* Neuron, 2009. **63**(6): p. 854-864.
80. Shiotani, K., et al., *Tuning of olfactory cortex ventral tenia tecta neurons to distinct task elements of goal-directed behavior.* Elife, 2020. **9**.
81. Adams, A.C., et al., *Ablation of the hypothalamic neuropeptide melanin concentrating hormone is associated with behavioral abnormalities that reflect impaired olfactory integration.* Behav Brain Res, 2011. **224**(1): p. 195-200.
82. Beekly, B.G., et al., *Dissociated Pmch and Cre Expression in Lactating Pmch-Cre BAC Transgenic Mice.* Frontiers in Neuroanatomy, 2020. **14**(60).
83. Mondino, A., et al., *Glutamatergic Neurons in the Preoptic Hypothalamus Promote Wakefulness, Destabilize NREM Sleep, Suppress REM Sleep, and Regulate Cortical Dynamics.* J Neurosci, 2021. **41**(15): p. 3462-3478.
84. Vanini, G., et al., *Activation of Preoptic GABAergic or Glutamatergic Neurons Modulates Sleep-Wake Architecture, but Not Anesthetic State Transitions.* Curr Biol, 2020. **30**(5): p. 779-787.e4.
85. Blasco, T.A., et al., *The role of the nucleus raphe pontis and the caudate nucleus in alfentanil rigidity in the rat.* Brain Res, 1986. **386**(1-2): p. 280-6.
86. Buzsáki, G., *Theta oscillations in the hippocampus.* Neuron, 2002. **33**(3): p. 325-340.
87. Zheng, L.M., D.W. Pfaff, and M. Schwanzel-Fukuda, *Electron microscopic identification of luteinizing hormone-releasing hormone-immunoreactive neurons in the medial olfactory placode and basal forebrain of embryonic mice.* Neuroscience, 1992. **46**(2): p. 407-18.
88. Schwanzel-Fukuda, M. and D.W. Pfaff, *The migration of luteinizing hormone-releasing hormone (LHRH) neurons from the medial olfactory placode into the medial basal forebrain.* Experientia, 1990. **46**(9): p. 956-62.
89. Wu, M., et al., *Melanin-concentrating hormone directly inhibits GnRH neurons and blocks kisspeptin activation, linking energy balance to reproduction.* Proc Natl Acad Sci U S A, 2009. **106**(40): p. 17217-22.
90. Wu, M., et al., *Gonadotropin inhibitory hormone inhibits basal forebrain vGluT2-gonadotropin-releasing hormone neurons via a direct postsynaptic mechanism.* J Physiol, 2009. **587**(Pt 7): p. 1401-11.
91. Brock, O., et al., *A Role for Thalamic Projection GABAergic Neurons in Circadian Responses to Light.* J Neurosci, 2022. **42**(49): p. 9158-9179.
92. Hanna, L., et al., *Geniculohypothalamic GABAergic projections gate suprachiasmatic nucleus responses to retinal input.* J Physiol, 2017. **595**(11): p. 3621-3649.
93. BIZZI, E. and D.C. BROOKS, *Pontine reticular formation: relation to lateral geniculate nucleus during deep sleep.* Science, 1963. **141**(3577): p. 270-2.

94. Cohen, B. and M. Feldman, *Relationship of electrical activity in pontine reticular formation and lateral geniculate body to rapid eye movements.* J Neurophysiol, 1968. **31**(6): p. 806-17.
95. Lima, D. and A. Almeida, *The medullary dorsal reticular nucleus as a pronociceptive centre of the pain control system.* Prog Neurobiol, 2002. **66**(2): p. 81-108.
96. Parenti, R., et al., *The projections of the lateral reticular nucleus to the deep cerebellar nuclei. An experimental analysis in the rat.* Eur J Neurosci, 1996. **8**(10): p. 2157-67.
97. Zhan, X. and D.K. Ryugo, *Projections of the lateral reticular nucleus to the cochlear nucleus in rats.* J Comp Neurol, 2007. **504**(5): p. 583-98.

Chapter VI. Indirect Effects of Steroid Hormones on MCH Neuron Modulation of Sleep

Abstract

Sleep disruptions and disorders are associated with alterations in the timing of pubertal development as well as poor fertility outcomes. Despite this, there remains a great paucity of research at the basic and early translational level on the relationship between sleep and reproductive physiology, particularly in female animals. Given the relevance of sleep for women's reproductive health, a deeper understanding of the role of sleep in the maturation and function of the reproductive system that encompasses biological sex differences is imperative for the development of effective interventions and treatments across the life span.

Neuropeptidergic control of vigilance states is complex, but melanin-concentrating hormone (MCH) neurons are key players that have demonstrated effects on pituitary gonadotropin release which vary with the estradiol milieu. We hypothesized that MCH neurons contribute to the temporal integration of sleep and reproductive physiology in a manner dependent on gonadal hormones. We performed antero- and retrograde tracing and immunohistochemistry to characterize a population of MCH neurons that projects to both sleep and reproductive control sites, finding that MCH neurons do not respond directly to gonadal hormones but receive inputs from a population of estrogen-sensing neurons in the arcuate nucleus (ARH). Furthermore, we used optogenetics to activate neuron terminals originating in the ARH in the lateral hypothalamus and perifornical area, where MCH perikarya are found, and observed the effects of so doing on both sleep in males and females in varying estradiol milieu. While male mice and female mice under low estradiol conditions were largely unresponsive, females supplemented with exogenous estradiol exhibited reduced time in both REM and NREM sleep and increased time spent awake during the dark phase. Our findings reveal a previously unrecognized and estradiol-dependent role for the ARH KNDy-PFx MCH neuron circuit in the integration of gonadal steroids and sleep in female mice.

Background

Reduced and fragmented sleep is associated with infertility in humans. Nearly one-fifth of American couples struggle with infertility and, with increasing environmental exposure to sleep and circadian disruptors, deficiencies in pubertal development and fertility will likely continue to increase. Disorders of the reproductive system also have high rates of comorbidity with metabolic dysfunction, certain cancers, and psychiatric illness. Thus, there is an urgent need to better understand the neuroendocrine reproductive axis and how it interacts with sleep.

Sleep is a fundamental neurological function which is conserved across the animal kingdom, though the primary role(s) of sleep and the details of its regulation remain incompletely understood [1-5]. In mammals, sleep can be divided into three basic states using electroencephalography (EEG): (1) wakefulness, for which the EEG is characterized by low amplitude, high frequency waveforms; (2) non-rapid eye movement (NREM) sleep, also known as slow-wave sleep (SWS), for which the EEG is characterized by higher amplitude, slower waveforms, with especially high power in the delta frequency; and (3) rapid eye movement (REM) sleep, also known as paradoxical sleep (PS) for its resemblance to waking EEG signatures [6]. REM sleep, however, may be distinguished from wake by the more organized, "sawtooth"-like theta-frequency waveforms [6].

In spite of its stereotyped and highly conserved nature, variations are observed in sleep between the sexes. Clinical studies suggest that women have lower latency to sleep and increased total sleep time, particularly SWS, as compared to men [7]. Paradoxically, women and girls are twice as likely to report indications of disordered sleep like insomnia, difficulty staying asleep, and daytime tiredness [8].

Variation in sleep quality is also observed across the menstrual cycle. Self-reported sleep disturbances increase during the late luteal phase, particularly in women with dysmenorrhea [9]. Light therapy may improve mood-related premenstrual symptoms, suggesting that circadian disruptions could be related to transient deterioration of sleep quality and constitute a cause of premenstrual negative affect [10, 11]. In some clinical studies, polysomnography and actigraphy recordings confirm that women experience poorer quality sleep during the luteal phase as compared with the follicular and menstrual phases. In Long-Evans rats, cortical EEG, cortical local field potential (CA1 LFP), and electromyography (EMG) recordings revealed that the

proestrus phase of the estrous cycle is characterized by reduced total REM and non-REM sleep during both the dark and light phases as compared to both male rats and female rats in other stages of the estrous cycle [12]. This suppression of sleep was followed by increased total REM and NREM sleep during the estrus phase.

Sleep architecture also varied across the estrous cycle, with females showing alterations to the number and length of bouts of REM and NREM sleep across different phases of the estrous cycle [13]. Finally, more sleep spindles—unique EEG phasic features of NREM sleep observed in the sigma frequency which are involved in learning and memory—are observed during the luteal phase [7-9, 14-16]. Sleep spindles may be related to membrane potential variation in thalamocortical networks; this would suggest a potential broader effect of steroid hormones on neural network dynamics. Taken together, these data indicate that many features of sleep may be modulated by the sex steroid milieu.

Neuropeptidergic control of sleep and wakefulness is complex, but melanin-concentrating hormone (MCH) is well-established as a significant contributor to the process. As detailed in the Introduction, most brain MCH expression is in neurons of the incertohypothalamic area (IHy, alternatively medial zona incerta, ZIm), the perifornical area (PFx), and the lateral hypothalamic area (LHA), all of which have multiple functions that include sleep/wake regulation [17-19]. Notably, MCH neurons are active during sleep, and optogenetic activation of MCH neurons significantly increases sleep duration [20-25]. MCH neurons also project to areas implicated in reproductive control such as the medial preoptic nucleus (MPO) and the median eminence (ME), which harbor gonadotropin-releasing hormone (GnRH) neuron cell bodies and terminals, respectively [26, 27].

At the apex of the neuroendocrine reproductive axis are GnRH neurons. Episodic release of GnRH drives pulsatile secretion of the gonadotropins, luteinizing hormone (LH) and follicle-stimulating hormone (FSH), from the pituitary gland. These in turn act on the gonads to promote gametogenesis and steroidogenesis. A bout of high-frequency LH pulses is required for both pubertal onset and ovulation. Notably, the rise in LH pulse frequency that precipitates puberty occurs during sleep, while in adults, LH pulse frequency is reduced during sleep. The mechanisms governing the temporal relationship between sleep and pituitary gonadotropin

secretion represent a significant gap in the field's understanding of reproductive development and function.

In humans and rodents, MCH terminals are observed in close apposition with GnRH cells, which express MCH receptor 1 (MCHR1) [26-31]. MCH neurons are thus anatomically poised to dually regulate sleep and the reproductive axis. The functional role of MCH neurons in reproductive physiology is less clear, however, with mixed conclusions about the ability of MCH to stimulate LH secretion.

Early studies showed that lesioning the ZIm, where many MCH neurons are found, reduces circulating LH [32]. *In vitro,* hypothalamic explants from adult ovariectomized (OVX) rats can release GnRH following MCH application, but only if the rats are primed with estradiol-2-benzoate (E2) prior to euthanasia and brain dissection [28]. Conversely, when hypothalamic explants from intact male and female prepubertal mice are treated with MCH, a subpopulation of GnRH neurons that is $VGLUT2^{+}$ and kisspeptin-sensitive (which represents 61% of total GnRH neurons) has been reported to be hyperpolarized, ultimately suppressing the ability of kisspeptin to induce GnRH release from these cells [31, 33]. The authors propose that MCH is involved in the relay of metabolic state to the neuroendocrine reproductive axis, suppressing reproductive function in states of negative energy balance. Thus, metabolic state may be another contextual factor which must be considered in the interpretation of data on this topic.

In vivo, MCH injection into the ME and POA increases circulating LH in OVX+E2 rats but not OVX rats treated with vehicle; furthermore, this effect seems to be specific to application of MCH to regions where GnRH neuron perikarya are located, as injection into the ZIm or VMN has no effect in either group [28, 34]. However, intracerebroventricular injection of MCH has also been shown to *attenuate* the anticipated increase in circulating LH in surge-model rats—animals treated with a carefully curated schedule and dosage of both E2 and progesterone (PG) to reliably induce an LH surge [35].

The inconsistency of experimental design renders these data challenging to evaluate concurrently. The valence and magnitude of MCH effects on LH may depend on the site of MCH administration, developmental stage and/or sex steroid milieu at the time of the experiment, and possibly even the species and/or strain of the model organism. As such, none of the data discussed necessarily contradict each other, but rather likely represent different

manifestations of the ability of MCH neurons to integrate numerous peripheral cues and modulate reproduction accordingly.

Another explanation for the discrepancies could be the existence of subpopulations of MCH neurons. MCH neurons migrate from the neural crest in two groups, with an early-arising group that settles in the lateral hypothalamus and projects caudally to the brainstem and a late-arising group settling mainly in the medial hypothalamus which targets hypothalamic and cortical neurons [36, 37]. Thus, it stands to reason that MCH neurons would not all act on the HPG axis in the same way. Sleep architecture also varies with hormonal milieu, suggesting that MCH could coordinate LH secretion with sleep/wake state in a sex-steroid dependent manner [38]. Further support for this notion lies in the fact that this later-arising, more medial population of MCH neurons is known to express the neurokinin-B (NKB) receptor NK3R [39-41]. NKB is a member of the tachykinin family of peptides which participates in the regulation of GnRH neuron firing in conjunction with kisspeptin, potentially by stimulating kisspeptin secretion [42]. NK3R is the preferred receptor for NKB, and loss of NK3R results in severe hypogonadotropic hypogonadism, with or without anosmia [43-48].

We hypothesized that medial MCH neurons, with their expression of NK3R and their projections within the hypothalamus, are involved in the temporal integration of sleep patterns and LH secretion. Furthermore, we predicted that this action could be modulated by gonadal hormones. We performed antero- and retrograde tracing and immunohistochemistry to determine whether a specific population of MCH neurons projects to both sleep and reproductive control sites and whether such a population might be defined by specific projection targets and/or colocalized transcripts. Finally, we used optogenetics to activate a putative NKB-to-MCH neuron circuit and assessed the effects of so doing on both sleep and circulating LH in both sexes and in varying estradiol milieu.

Methods

Mice

Animal Care

Mice were housed in a vivarium at the University of Michigan with a 12/12 light/dark cycle and ad libitum access to food and water. The mice received phytoestrogen-reduced Envigo diet 2016 (16% protein/4% fat), except during breeding when mice were fed phytoestrogen-reduced

Envigo diet 2019 (19% protein/8% fat) to accommodate additional nutritional needs of pregnant and nursing dams and during optogenetic stimulation, when mice received BioServ F0071 Precision pellets (18% protein/5.6% fat). Phytoestrogen-reduced diet is routinely used in our laboratory to avoid the effects of exogenous estrogens on mouse physiology. All procedures and experiments were carried out in accordance with the guidelines established by the National Institutes of Health Guide for the Care and Use of Laboratory Animals and approved by the University of Michigan Committee on Use and Care of Animals (Animal Protocol #PRO00010420).

Pmch-iCre;L10-eGFP Mice

Pmch-iCre;L10-eGFP mice ("MCH-L10") reporter mice were generated by crossing *Pmch*-iCre mice generated in our lab in conjunction with the UM Transgenic Animal Core (see Chapter 2) with B6;129S4-*Gt(ROSA)26Sor*$^{tm9(EGFP/Rpl10a)Amc}$/J line (JAX®; stock #024750, "eGFP-L10a") mice.

Kiss1-Cre;L10-eGFP and Kiss1-Cre;ChR2-eYFP Mice

Kiss1-Cre;L10-eGFP were generated by crossing Tg(*Kiss1*-cre)J2-4Cfe/J (JAX®; stock 023426, "*Kiss1*-Cre") mice with B6;129S4-*Gt(ROSA)26Sor*$^{tm9(EGFP/Rpl10a)Amc}$/J line (JAX®; stock #024750, "eGFP-L10a") mice. *Kiss1*-Cre;ChR2-eYFP mice were generated by crossing *Kiss1*-Cre mice with B6.Cg-*Gt(ROSA)26Sor*$^{tm32(CAG-COP4*H134R/EYFP)Hze}$/J (JAX®; stock # 024109, "ChR2-eYFP") mice.

Surgery

Craniotomy

For injection of anterograde tracers into MCH neurons, adult male and female *Pmch*-Cre;L10-eGFP mice were anaesthetized with isoflurane (2-4%, Fluriso; Vet One) and 50 nL AAV-ChR2-mCherry (Addgene plasmid #18916) was stereotaxically delivered unilaterally into the hypothalamus with a pneumatic picopump (World Precision Instruments) as routinely done in our laboratory and others [49, 50]. This virus has been successfully used previously to label anterograde projections [51]. The coordinates used were AP -4.5 mm from the rostral rhinal vein, ML -0.6 mm from the midline, and DV -4.8 mm from the surface of the dura mater.

After 10 days' recovery from surgery, mice were deeply anesthetized with isoflurane and perfused with 10% formalin and brains were dissected, postfixed for 8 hours in 10% formalin, and cryoprotected overnight using a solution of 20% sucrose in phosphate buffered saline. Coronal sections (30 μm thickness, 4 series) were collected with a freezing microtome and stored in a cryoprotectant solution (20% glycerol/30% ethylene glycol in DEPC-treated PBS) at −20°C. The distribution of mCherry-labeled fibers was mapped following immunohistochemistry.

For injection of anterograde tracers into ARH KNDy neurons, the same basic procedures were followed. Adult male and female *Kiss1*-Cre;eGFP-L10a mice were used (JAX Stock #023426) and the coordinates used were AP -4.6 mm from the rostral rhinal vein, ML -0.2 mm from the midline, and DV -5.6 mm from the surface of the dura mater.

For injection of retrograde tracers into the VLPO and MS/NDB of MCH-Cre;eGFP-L10a mice, the same basic procedures were followed except for the stereotaxic coordinates. For the MS/NDB, the coordinates used were AP -3.0 mm from the rostral rhinal vein, ML on the midline, and DV -4.8 mm from the surface of the dura mater and the tracer injected was Fluoro-Gold ("FG," 1% solution, Fluorochrome). For the VLPO, the coordinates used were AP -2.7 mm from the rostral rhinal vein, ML -1.0 mm from the midline, and DV -4.8 mm from the surface of the dura mater and the tracer injected was cholera toxin, β subunit (Ctb) (1%; List Biological Laboratories, Campbell, CA, USA).

Optical fiber implantation

Adult male and female *Kiss1*-Cre;ChR2-eYFP mice were anaesthetized with isoflurane (2-4%, Fluriso; Vet One) and a metal ferrule optic fiber (400-μm diameter core; BFH37-400 Multimode; NA 0.37; ThorLabs) was implanted unilaterally over the PFx (AP -4.5 mm from the rostral rhinal vein, ML -0.3 mm from the midline, DV -4.8 mm from the surface of the dura mater). Fibers were fixed to the skull using dental acrylic; after the completion of the experiments, mice were euthanized and the locations of optic fiber tips were identified based on the coordinates of Paxinos and Franklin's Mouse Brain in Stereotaxic Coordinates.

EEG/EMG placement

EEG/EMG placement was performed during the same surgery as the optical fiber implantation (above). Mice were implanted with two stainless-steel screws (Frontal: AP: 1.5 mm from Bregma, ML: −1.5 mm; Temporal: AP: −3.5 mm from Bregma, ML: −2.8 mm; Ground: AP:

−3.3 mm from Bregma, ML: −.4 mm) and a pair of multi-strand stainless steel wires inserted into the neck extensor muscles. The EEG and EMG leads were wired to a small electrical connector that is attached to the skull with dental cement. Mice were then kept on a warming pad until awake. All mice were given analgesics (5 mg/kg Meloxicam) preemptively and 24 hours after surgery. Mice were given a minimum of 2 weeks for recovery and 1 week for acclimation before experiments began.

Ovariectomy and estradiol implants

Standard ovariectomy and estrogen replacement procedures were performed as previously described [52]. Briefly, under isoflurane anesthesia, ovaries were externalized through two small incisions on either side of midline just below the rib cage and removed by cauterizing the oviduct. For "OVX+E2" conditions, immediately before experiments, mice were briefly anesthetized again and received a Silastic (Dow Corning) implant containing 0.625 μg 17β-estradiol-3-benzoate (Sigma) dissolved in sesame oil in the scapular region [53].

Optogenetic stimulation and behavioral experiments

Optogenetic stimulation paradigm

Mice received optogenetic stimulation at 20Hz, estimated 10mW at the fiber tip, for four hours on a one second on/four seconds off schedule. Recordings began 30 min into stimulation and data was collected for a total of 3 h per day at a time when the mice will not be disturbed by researchers or care staff entering the room. The study was conducted in a randomized crossover design; each mouse was recorded in both the light and the dark phase with and without optogenetic stimulation such that each animal experienced all four conditions and served as its own control.

Polysomnographic recording and analysis

Polysomnographic signals were digitized at 1000 Hz, with a 0.3-100 Hz bandpass filter applied to the EEG and a 30-100 Hz bandpass filter applied to the EMG, with a National Instruments data acquisition card and collected using a custom MATLAB script. EEG/EMG signals were notch filtered at 60 Hz to account for electrical interference from the recording tether. Mice were recorded for a minimum of 4 sessions: a 12 h dark cycle recording with no optogenetic stimulation, a 12 h light cycle recording with no optogenetic stimulation, a 12 h dark cycle recording with optogenetic stimulation, and a 12 h light cycle recording with optogenetic

stimulation. Polysomnographic signals were analyzed using AccuSleep, an open-source sleep scoring algorithm in MATLAB, and verified by an experienced sleep-scorer [54]. Behavioral states were scored in 5 s epochs as either wake, NREM, or REM sleep.

Histology

Fluorescent in situ hybridization

Neuronal activation induced by optogenetic stimulation was assessed using triple-label fluorescent *in situ* hybridization (RNAscope, ACD Bio). Briefly, adult male and female mice *Pmch*-iCre$^{+/-}$;VGLUT2$^{fl/fl}$ and *Pmch*-iCre$^{-/-}$;VGLUT2$^{fl/fl}$ mice were deeply anesthetized with isoflurane and euthanized by decapitation. Brains were dissected, embedded in O.C.T. Compound (Tissue-Tek, prod. code 4583), and immediately frozen on dry ice and kept at -80 °C until sectioning. Brains were sectioned using a cryostat at approximately -18 °C onto RNAse-free Superfrost Plus microscope slides (Fisher Scientific, cat. no. 22-037-246) at 16 μm in the coronal plane.

Prior to hybridization, slides were fixed in prechilled 10% NBF for 45 minutes at 4 °C and subsequently dehydrated using a standard ethanol series. The slides were allowed to dry and then borders were drawn around the sections using a hydrophobic barrier pen. Slides were pretreated with hydrogen peroxide for 10 minutes followed by RNAscope Protease IV for 15 minutes before hybridization and signal detection steps.

To hybridize, about 150 uL of RNAscope probe mixture was applied to each slide and the slides were incubated at 40°C for 2 hours in a HybEZ oven, then washed with RNAscope wash buffer and stored overnight in 5× SSC. On the second day, amplification of each probe (AMP 1-2) was performed sequentially, incubating for 30 min at 40°C then rinsing in wash buffer after each Multiplex FL v2 Amp solution. Subsequently, the slides were developed using by incubating in RNAscope Multiplex FL v2 HRP-Cn for 15 min at 40°C, rinsing with wash buffer, incubating for 30 min at 40°C with TSA + Fluorescein (Akoya Biosciences, cat. no. SKU NEL741001KT), incubating in RNAscope Multiplex FL v2 HRP blocker for 15 min at 40°C, then rinsing once more with wash buffer. Finally, slides were counterstained with DAPI and coverslipped with ProLong Gold antifade mounting medium (ThermoFisher Scientific).

Single- and dual-label immunohistochemistry

Adult sexually naïve male and female *Pmch*-Cre;eGFP-L10a mice were deeply anesthetized with isoflurane and perfused with 10% formalin. Brains were dissected, postfixed for 2 hours in 10% formalin, and cryoprotected overnight using a solution of 20% sucrose in PBS. Coronal sections (30 μm thickness, 4 series) were collected with a freezing microtome and stored in a cryoprotectant solution (20% glycerol/30% ethylene glycol in DEPC-treated PBS) at −20°C.

Anti-NK3R and anti-AR with TSA Amplification

Brain sections were rinsed 3× in 0.1 M PBS to remove cryoprotectant solution, and in between each step.

Sections were blocked for 10 minutes in 0.3% H_2O_2 in ddH_2O, rinsed 3× in 0.1 M PBS, and subsequently blocked for 30 min in 0.1 M PBS + 0.25% TritonX-100 ("PBST") with 3% normal donkey serum (NDS). Next, sections were incubated overnight in PBST + 3% NDS with chicken anti-GFP (1:10,000, Aves Labs, AB_2307317) and either rabbit-anti NK3R (1:30,000, Novus Biologicals, NB300-102) or rabbit-anti AR (1:200; AbCam, ab133273).

Following primary antibody incubation, sections were incubated in anti-rabbit biotin in 0.1 M PBS for 1 h (1:500; Jackson ImmunoResearch Laboratories, 711-065-152), avidin-biotin complex (ABC) solution in 0.1 M PBS for 1 h (1:1000, Vector Laboratories), and biotinylated tyramide in 0.003% H_2O_2 in ddH_2O for 10 mins (1:250; Perkin Elmer). Finally, sections were incubated in 0.1 M PBS with secondary antisera (1:1000 goat anti-chicken conjugated to Alexa FluorTM 488, AB_2534096, and 1:1000 streptavidin-conjugated AlexaFluor 594, Thermo Fisher Scientific).

Sections were mounted onto gelatin-coated slides, air-dried, and coverslipped with Fluoromount G mounting medium (Electron Microscopy Sciences).

Analysis methods and generation of photomicrographs

Brain sections were imaged in an Axio Imager M2 microscope (Zeiss) except for 3D reconstructions of putative NKB-MCH synapses.

Anatomical tracing data was assembled according to the injection sites using the Allen brain atlas (mouse.brain-map.org) as a reference. Patterns of innervation were assessed in a comparative manner among (i) between male and female mice, and (ii) according to the number

of cells in each subpopulation of MCH neurons that took up the virus, with particular attention to areas related to sleep regulation and reproductive control. Morphology of projecting fibers was analyzed, and terminals defined at 40× or 63× magnification by the presence of varicosities and apparent synaptic bulbs.

Dual-labeled MCH neurons (e.g., NK3R) were quantified in 20× magnification using ImageJ with the Cell Counter plugin. Sexual dimorphisms in colocalization were defined using the student's *t* test (Welch's correction).

Results

MCH neurons of adult male and female mice do not express gonadal steroid receptors

Since numerous features of sleep are affected by biological sex and estrous cycle stage, it is plausible that MCH neurons could be directly regulated by gonadal hormones. Data in rats has found MCH to be coextensive, though not coexpressed, with ERα [55]. However, this has not been verified in mice. Additionally, *Pmch* expression was shown in rats to be increased by DHEA and DHT, though there is no documentation of whether MCH neurons themselves coexpress androgen receptor (AR) [2]. Finally, there is no literature on the expression of progesterone receptor (PGR) in MCH neurons or the ability of progesterone to act directly on MCH neurons. To determine whether this is the case, brain sections from adult male and female *Pmch*-iCre;eGFP-L10a mice were stained with antibodies against GFP and either ERα, AR, or PGR (Figure 6-1). No colocalization of Pmch-Cre;eGFP-L10a was observed with ERα, AR, or PGR in either sex, suggesting that if MCH neuron activity is modulated by sex steroids, this must occur indirectly.

Perifornical MCH neurons of male and female mouse coexpress NK3R

It has been previously shown in male rats and mice that a subpopulation of MCH neurons, mainly in the PFx, express NK3R [40, 41]. To determine whether this was also true in the female mouse brain, we stained sections from male and female *Pmch*-Cre;eGFP-L10a mice with antibodies against GFP and NK3R. We observed that, consistent with previous studies, approximately 50% of GFP+ neurons in the PFx and medial IHy express NK3R while only sparse NK3R is observed in LHA MCH neurons (Figure 6-2). No difference was observed between sexes.

KNDy fibers are in close apposition to PFx MCH neurons

NK3R is the primary receptor of NKB [56, 57]. Most neurons in the arcuate nucleus of the hypothalamus (ARH) express NKB as well as kisspeptin and dynorphin ("KNDy neurons") [58]. These neurons are potently regulated by estradiol via ERα [59, 60]. We sought to determine whether MCH+/NK3R+ neurons are innervated by KNDy neurons. Using antibodies against kisspeptin and silver nitrate/gold chloride amplification, we observed dense labeling of neuronal projections in male and female PFx where MCH/NK3R neurons are found (Figure 6-3A).

We next sought to determine whether NKB+ fibers form synaptic connections with MCH neurons. Using dual-label immunohistochemistry and confocal microscopy, we generated 3D reconstruction images which illustrate that NKB-ir fibers are in close proximity to MCH cells, appearing to synapse onto MCH perikarya and projections (Figure 6-3B).

MCH neurons of the PFx innervate sleep and reproductive control sites

We wondered whether distinct subpopulations of MCH neurons differentially innervate brain sites associated with the regulation of sleep and wakefulness. Specifically, we sought to determine whether PFx MCH neurons possess distinct and/or sexually dimorphic projection targets considering their distinct chemical identity. The Cre-dependent anterograde viral tracer AAV-ChR2-mCherry was used to map the anterograde projections of subpopulations of MCH neurons. Male and female *Pmch*-Cre mice were stereotaxically injected with ~50 nL of virus unilaterally into the hypothalamus. This virus has been successfully used previously to label anterograde projections [51]. The small injection volumes enabled the targeting of small subpopulations of MCH neurons.

Upon examination of the brains of these mice, we identified three regions of interest where MCH neuron fibers were abundant: the medial septum (MS) and adjacent diagonal band (NDB), and the lateral preoptic area (LPO), especially the ventrolateral LPO (VLPO). The MS, NDB, and VLPO are notable because all three of them have an established association with sleep. Lesion studies revealed that the loss of MS neurons reduces NREM sleep and increases REM sleep, and a similar effect is achieved by microinjection of endocannabinoid receptor agonists into the MS [61, 62]. On the other hand, microinjection of glutamate and endocannabinoid receptor antagonists into the MS reduces REM sleep [62, 63]. Granger causality analysis has since been used to demonstrate bidirectional interactions between the hippocampus and MS in the

generation of theta rhythms [64, 65]. Cholinergic neurons of the NDB are also associated with theta rhythm generation; many studies have demonstrated that the NDB and MS work together to this end and thus jointly have an important role in REM sleep [66, 67] (For additional review, see [68] and [69].) Finally, most neurons of the VLPO express the inhibitory neurotransmitters galanin and GABA; they are active during both NREM sleep and REM sleep, and their stimulation promotes sleep onset [70-73].

Interestingly, the density of projections in these three regions was observed to be highly variable by injection site, with the number of infected neurons in the PFx being the best predictor of projection density therein. Representative images of silver-labeled terminals in MS, NDB, and VLPO in male and female brains with injections in the PFx *vs* ZIm can be found in Figure 6-4. Analysis of the superior colliculus was used to confirm that the differences observed were not simply an overall increased abundance of labeled fibers in certain brains as compared to others (Figure 6-4). Thus, these brain regions constitute a group of significant sleep and reproductive control sites which are modulated by a very specific subpopulation of MCH neurons in the rostromedial PFx.

Subsets of PFx MCH neurons projects either to the MS/NDB or to VLPO

Having determined that medial MCH neurons, and in particular neurons of the PFx, send dense projections to MS/NDB and VLPO, our next question was whether individual neurons form connections to all of these regions, or whether PFx MCH neurons might be further subdivided into groups projecting preferentially to different regions of sleep/wakefulness regulation. To answer this question, different retrograde tracers were injected into the MS and VLPO of male and female *Pmch*-iCre;eGFP-L10a mice. Immunostaining was performed against MCH and MCH neurons were examined for colocalization of one or both of these tracers. Mice were stereotaxically injected with Fluorogold (FG) in the MS/NDB and cholera toxin, β subunit (Ctb) in the VLPO. Summaries of the injection sites can be found in Figure 6-5.

This experiment revealed virtually no colocalization of FG and Ctb in MCH neurons. In a given hypothalamic section, between 5 and 50% of Pmch-Cre;L10 neurons expressed Ctb depending on the size and precise location of the injection. Most colocalization was seen in the ZIm and PFx, but some was observed in the LHA and the more lateral parts of the ZI (Figure 6-6).

Interestingly, no colocalization was observed between MCH and FG. FG labeling in the hypothalamus was restricted to a dense cluster of small, round neurons in the tuberal hypothalamus located very close to the fornix (Figure 6-6D). Previous work in our lab has indicated that there is a dense population of PFx neurons with this distinctive morphology which express Cre, but not MCH peptide, in the adult *Pmch*-iCre mouse [74]. Based on the small size and round shape of the cells expressing both Pmch-Cre;L10 and FG, we wondered whether these cells belonged to the Cre+/MCH- population. Indeed, when GFP, rather than MCH, was observed, we found that while virtually no colocalization could be found between MCH- and FG-immunoreactivity, nearly all FG+ neurons in the PFx were also GFP+. We also examined the FG cells to quantify colocalization of Ctb. However, virtually no colocalization of the two tracers was observed even outside of MCH cells. Thus, it appears that there may be a population of PFx cells, some of which are MCH+ and some of which are MCH-, that can be further subdivided into subpopulations targeting the MS/NDB and the VLPO individually.

Optogenetic stimulation of *Kiss1*+ terminals in the PFx alters sleep in female mice in an estrogen- and time-of-day-dependent manner

Having determined that rostromedial MCH neurons of the PFx project to sleep and reproductive control sites and are also situated downstream of estrogen-responsive ARH KNDy neurons, we sought to assess the impact of activating this ARH KNDy neuron → MCH+/NK3R+ neuron circuit on sleep in varying sex steroid milieu. To that end, we implanted optical fibers in the PFx of *Kiss1*-Cre;ChR2-eYFP mice in order to optogenetically stimulate ARH KNDy neuron terminals apposing MCH neurons of the PFx. Cortical EEG electrodes were implanted in the skull to monitor sleep-wake state.

Optogenetic stimulation-induced activity was assessed using the immediate-early gene cFos as a proxy for neuronal activation [75, 76]. Triple-label fluorescent *in situ* hybridization was used to examine *Fos* mRNA expression in the PFx following 90 minutes of optogenetic stimulation. Since all NK3R+ neurons in the PFx are MCH neurons, *Tacr3* mRNA was used as a marker for our MCH neuron population of interest. Because not all ARH KNDy neuron terminals observed in the PFx appear to be in contact with MCH neurons, and there are also ORX/HCRT neurons in the PFx which could receive glutamatergic neurotransmission from ARH KNDy neurons to regulate sleep, we also used probes against *Hcrt* to determine whether *Fos* and *Hcrt* mRNA

colocalized following optogenetic stimulation. *Fos* was visible around the optical fiber implantation site, and the identification of the neurons in which *Fos* is expressed is in progress (Figure 6-7).

While these experiments are still in the pilot phase and thus meaningful statistical analysis cannot yet be performed, the data gathered thus far suggests that in OVX+E2 animals, sleep is reduced when ARH KNDy neurons in the PFx are stimulated in the dark phase. In particular, REM sleep time consistently decreases in OVX+E2 females with stimulation (Figure 6-8), though NREM sleep time is also reduced (Figure 6-9). A corresponding increase in total wake time with stimulation is also observed (Figure 6-10). Consistent effects are not observed on other measures such as average bout length and number of bouts, nor in the other experimental groups.

Discussion

In this study, we sought to determine whether (a) subpopulation(s) of MCH neurons facilitate the temporal relationship between sleep and the regulation of pituitary reproductive hormone secretion. No MCH neurons were found to express sex steroid hormone receptors, eliminating the possibility that a subpopulation of MCH neurons which responds directly to gonadal hormones is implicated in this coordination. However, we found that MCH neurons in the PFx are uniquely poised to coordinate this relationship because in both male and female mice, they project to key sleep and reproductive control sites (VLPO and MS/NDB, respectively), express NK3R, and appear to receive inputs from the ARH, which is a critical modulator of the neuroendocrine reproductive axis and provides an indirect means of sex steroid action on MCH neurons, as the ARH is responsive to and potently regulated by gonadal hormones.

We wondered whether a single population of MCH PFx cells projected to both the MS/NDB and the VLPO, or whether MCH neurons targeting these regions comprised distinct subpopulations within the PFx. When two different retrograde tracers, Ctb and FG, were injected into the VLPO and MS/NDB, respectively, we observed no colocalization of the Ctb and FG in MCH neurons, but we observed virtually no colocalization of FG and MCH immunoreactivity. This finding was at odds with the dense projections observed in the MS/NDB when anterograde tracers were injected into the PFx. However, previous work in our lab has shown that there is a population of Cre+ neurons in the PFx that is not MCH^+; these neurons likely express MCH at some point in development, but not in adulthood. For this reason, we performed the retrograde tracing

experiments in *Pmch*-Cre;eGFP-L10a mice and quantified dual- and triple-labeled cells using both Cre-induced GFP expression and MCH immunoreactivity. Indeed, dual-label FG-GFP cells were observed in the cluster of perifornical cells which we have reported to be Cre+/MCH- in the *Pmch*-Cre mouse.

These cells may express orexin/hypocretin (ORX/HCRT) in adulthood, as their location corresponds to the well-described localization of ORX/HCRT in mice and rats [77, 78]. Furthermore, PFx ORX/HCRT cells are known to send dense projections to the locus coeruleus; the suprachiasmatic nucleus; the septal nuclei, especially the medial septum; and the NDB [77]. Notably, long, thick projections from ORX/HCRT with numerous boutons indicating dense synaptic connections have been documented in the ARH, suggesting that perhaps there is bidirectional communication between this population of PFx cells and KNDy neurons of the ARH [77]. Collectively, these data demonstrate a high likelihood that this cluster of PFx cells is of critical importance to the dual regulation of sleep and the neuroendocrine reproductive axis. Whether the key neuropeptide defining this population is ORX/HCRT or MCH requires further evaluation.

The role of MCH-expressing neurons, at least based on our anatomical tracing data, appears to be more relevant to sleep, as many MCH+ neurons were confirmed using Ctb to innervate the LPO/VLPO, which is less densely innervated by ORX/HCRT neurons of the PFx [77]. More direct action on the HPG axis, via connections both to GnRH neurons themselves in the MS/NDB and to KNDy neurons in the ARH, could originate from either MCH or ORX/HCRT neurons as discussed above and requires additional study.

Nonetheless, the apparent potential ARH KNDy neurons to communicate with MCH neurons via NKB signaling at NK3R still seemed to indicate some ability for the HPG axis to modulate MCH neuron activity. This could constitute a mechanism by which biological sex and circulating gonadal hormones might alter various features of sleep quality and sleep architecture. Since NKB expression is suppressed by estradiol and sleep is more fragmented and reduced overall in high-estradiol conditions, we predicted that NKB excites MCH neurons and is sleep promoting, and this action is reduced when estrogens are high [79]. We hypothesized that activation of NKB terminals in apposition to MCH neurons would be sleep-promoting.

Using mice with channelrhodopsin expressed in KNDy neurons, we optogenetically stimulated KNDy terminals and evaluated changes to sleep, spontaneous activity, and food and water intake in both sexes and in females under distinct gonadal steroid milieu. While Fos activation is observed at the optical fiber implantation site in all mice, male mice and female mice under low estradiol conditions were largely unresponsive to stimulation. However, females supplemented with exogenous estradiol exhibited reduced time in both REM and NREM sleep and increased time spent awake during the dark phase.

It is important to note that while in adult male mice, KNDy neurons are the only sites of kisspeptin expression, in the female, there is an additional site of kisspeptin expression: the anteroventral periventricular area (AVPV) [80]. This makes kisspeptin immunoreactivity an incomplete method of evaluating whether ARH KNDy neurons definitively project to MCH neurons in the female mouse brain. While it seems likely that at least some of the NKB+ fibers in the PFx of the female mouse do originate from the ARH, as they do in the male, it is possible that in females there is an additional contribution from the AVPV. These cells may have distinct projection targets and explain some of the difference between male and female responses to our optogenetic manipulation.

Overall, it seems that other contextual factors, perhaps including global gene expression changes induced by estradiol, may play a role in the ability of KNDy neuron activation to affect changes in sleep. Alternately, our experimental paradigm may not have been optimized to reveal a modulatory, rather than a directly stimulatory, role for KNDy neurons in sleep regulation. For instance, clearer effects may be revealed under circumstances of high sleep pressure (i.e., sleep deprived mice). Collectively, our findings suggest an estradiol-dependent role for KNDy neurons in the regulation of sleep in female mice, though the mechanistic underpinnings and relevant neuronal targets therein remain unclear. Further work is necessary to unravel the mechanisms integrating gonadal steroids and sleep.

Acknowledgements

Special thanks to Christian Burgess and Katherine Furman for lending time, expertise, lab space, and equipment/reagents for optogenetics experiments, and to Emily Henson for performing the RNAscope experiments for this study.

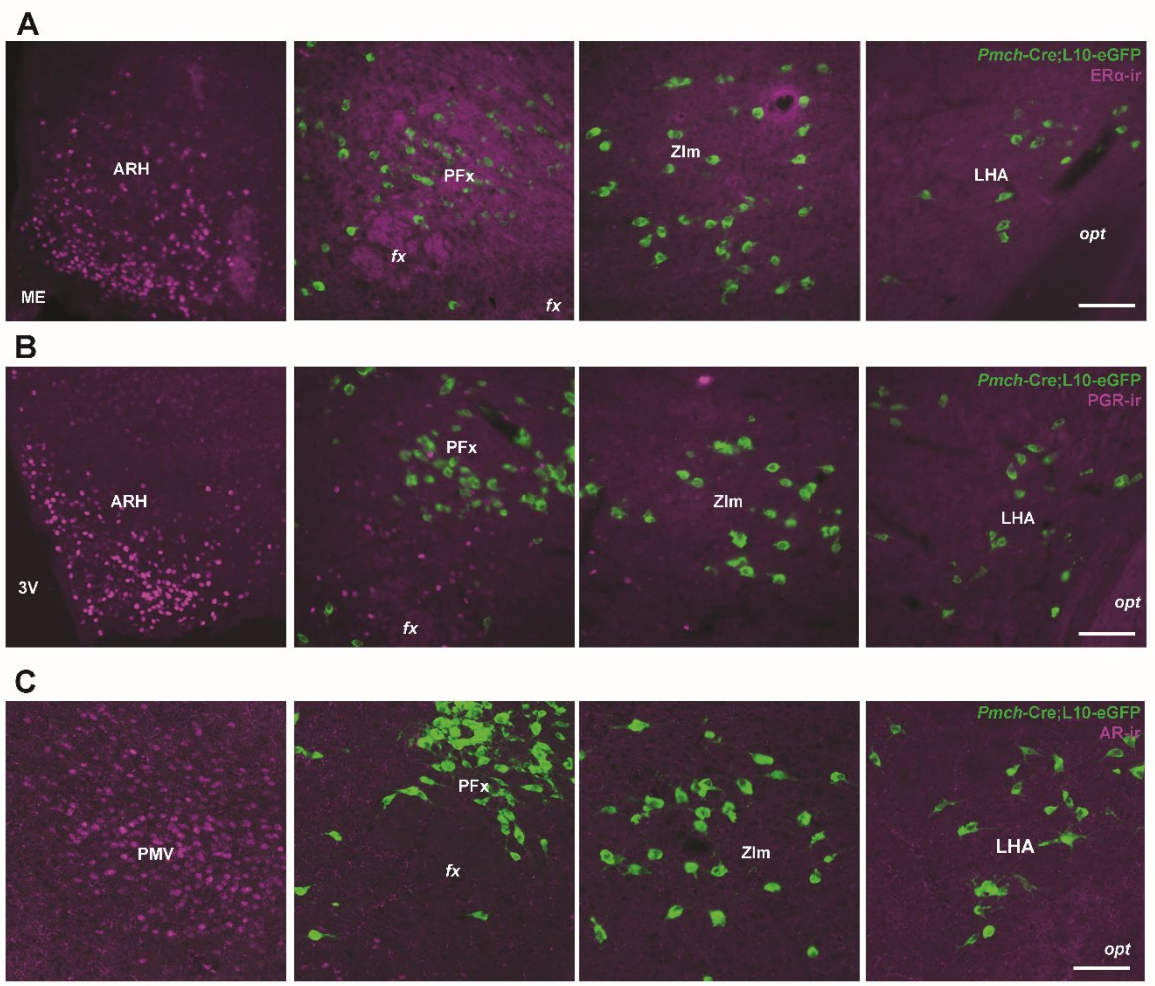

Figure 6-1: MCH neurons do not colocalize gonadal hormone receptors. *(A)* Anti-ERα staining in the brain of adult male and female *Pmch*-iCre;eGFP-L10a mice shows no colocalization of ERα (magenta) with MCH-driven reporter expression (green) in LHA, PFx, or ZIm. Both rostral (top) and caudal (bottom) levels of the PFx are shown. Images shown are from the female brain. *(B)* Anti-PGR staining in the brain of adult male and female *Pmch*-iCre;eGFP-L10a mice shows no colocalization of PGR (magenta) with MCH-driven reporter expression (green) in LHA, PFx, or ZIm. Both rostral (top) and caudal (bottom) levels of the PFx are shown. Images shown are from the female brain. *(C)* Anti-AR staining in the brain of adult male and female *Pmch*-iCre;eGFP-L10a mice shows no colocalization of AR (magenta) with MCH-driven reporter expression (green) in LHA, PFx, or ZIm. Both rostral (top) and caudal (bottom) levels of the PFx are shown. Images shown are from the male brain for AR and the female brain for ERα and PGR. No colocalization is observed in either sex.
Scale bar=100μm. *Abbreviations: ARH=arcuate nucleus of the hypothalamus, fx=fornix, LHA=lateral hypothalamic area, PFx=perifornical area, VMH=ventromedial hypothalamic nucleus, ZIm=zona incerta, medial part.*

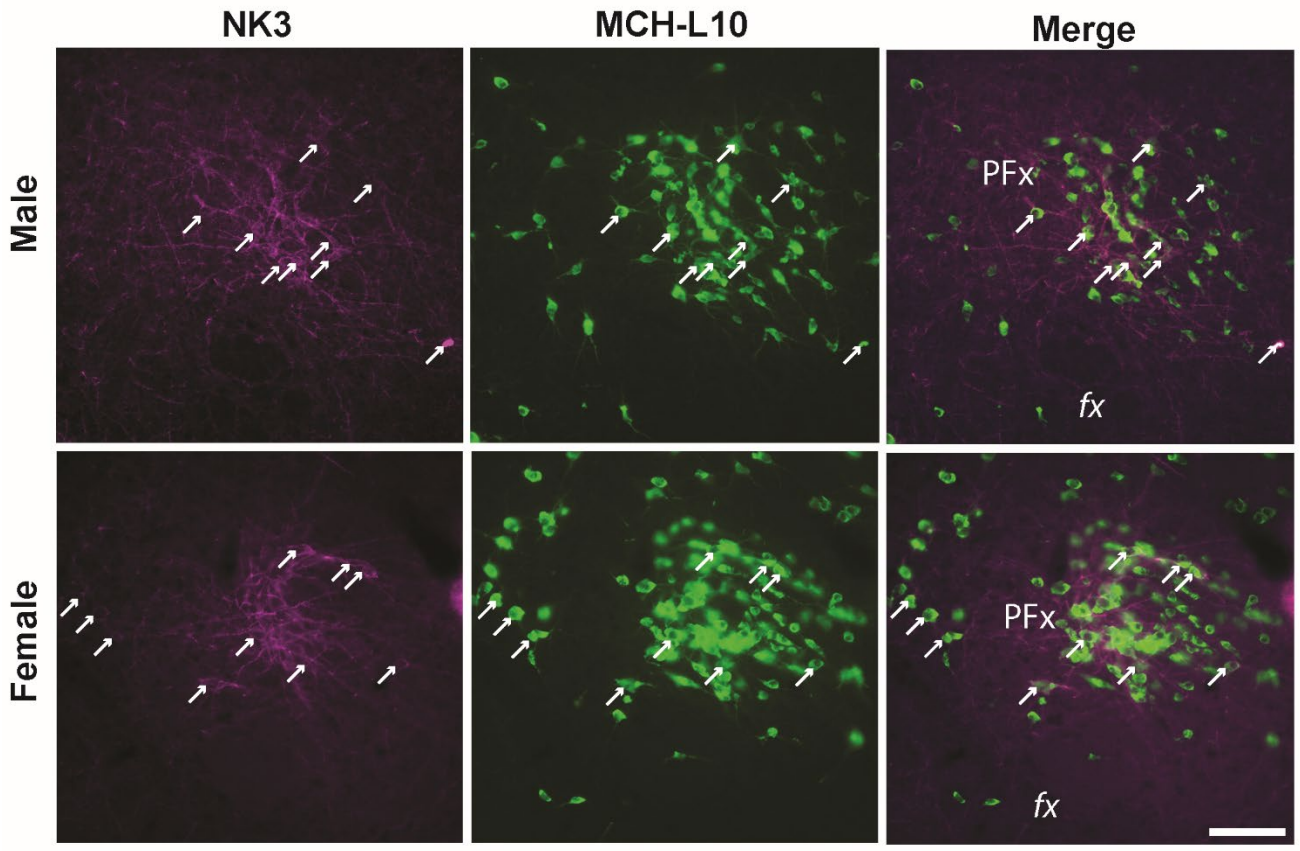

Figure 6-2: A subset of MCH neurons expresses NK3R in both males and females. NK3R (magenta) and Pmch-Cre;L10 in the brains of adult male (top) and female (bottom) *Pmch*-iCre;eGFP-L10a mice. Arrows indicate double-labeled cells. Scale bar=100µm. *Abbreviations: fx=fornix, PFx=perifornical area.*

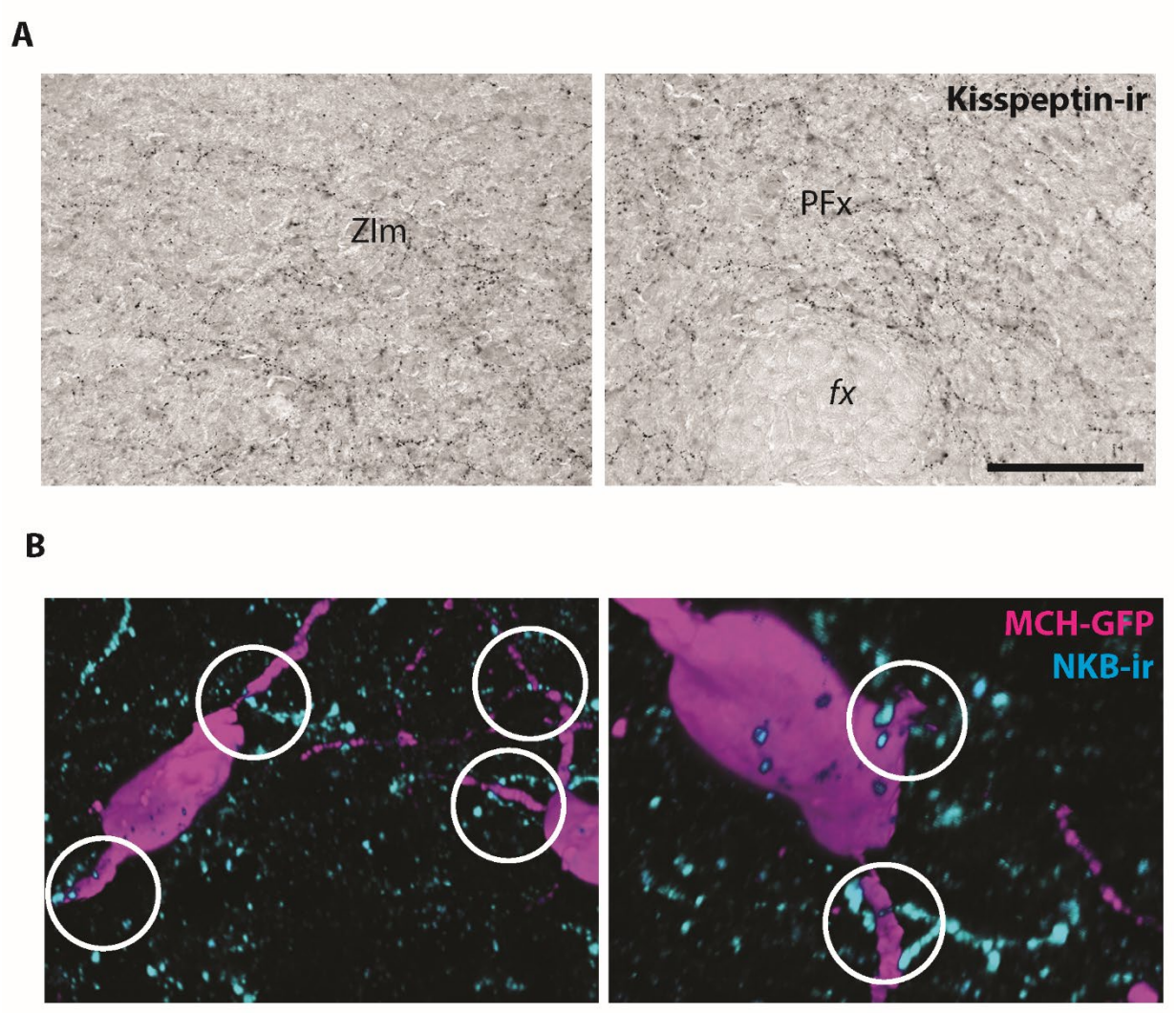

Figure 6-3: MCH neurons are innervated by KNDy neurons. *(A)* Immunostaining for kisspeptin in the male brain reveals projections in the ZIm and PFx, where MCH neuron cell bodies are found. *(B)* 3D reconstruction image of MCH- (magenta) and NKB- (cyan) labeled cells reveals close appositions between NKB+ fibers and MCH axons and perikarya.
Scale bar=100µm. *Abbreviations: fx=fornix, LHA=lateral hypothalamic area, PFx=perifornical area, ZIm=zona incerta, medial part.*

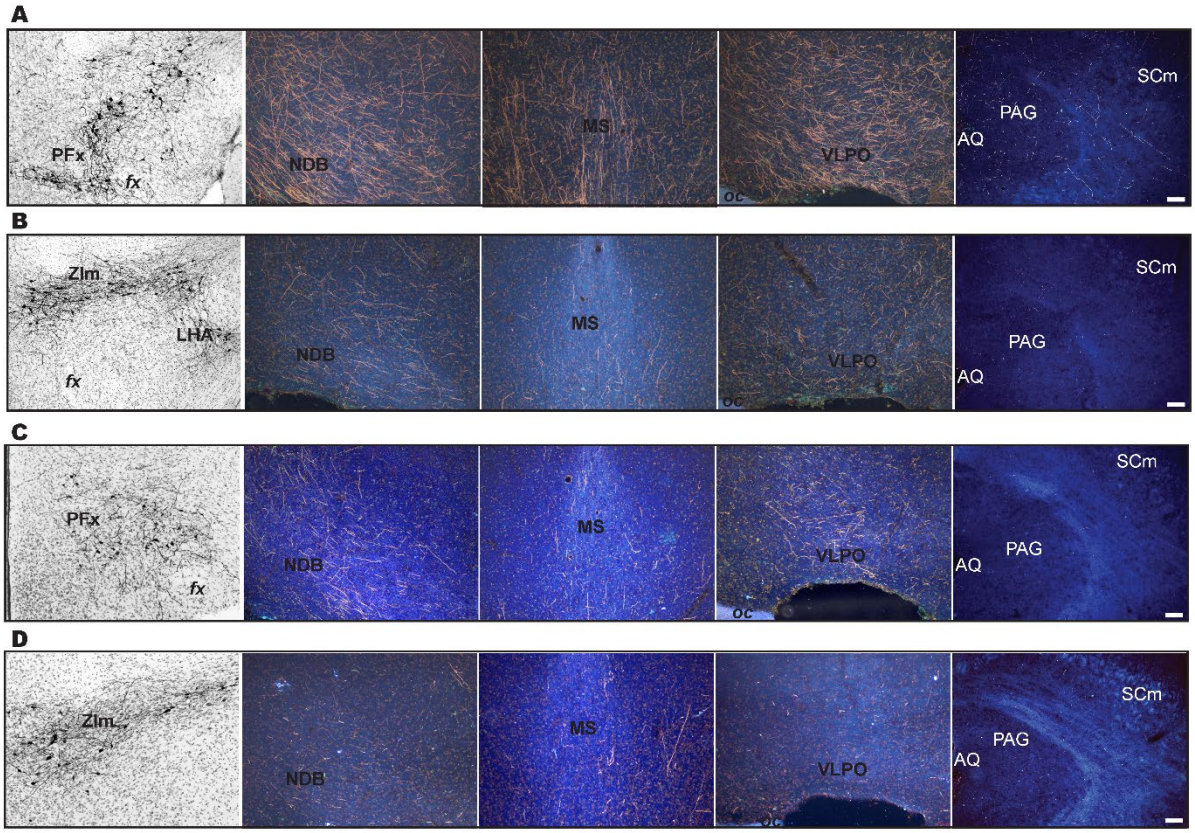

Figure 6-4: MCH neurons in the PFx project to sleep and reproductive control sites. Representative images of AAV-ChR2-mCherry injection sites and resulting visualization of neuron terminals in key brain regions (medial septum, nucleus of the diagonal band, ventrolateral preoptic area) and control regions (periaqueductal gray, superior colliculus [motor related[) of *Pmch*-Cre male (A, B) and female (C, D) mice. (A) Male mouse, PFx injection (170/175 of infected cells in PFx). Note dense projections in MS, NDB, and VLPO. (B) Male mouse, ZIm/LHA injection (20/209 of infected cells in PFx). Note relative lack of labeled terminals in MS, NDB, and VLPO. (C) Female mouse, PFx injection (53/86 of infected cells in PFx). Note terminals in MS, NDB, and VLPO. (D) Female mouse, ZIm injection (5/115 of infected cells in PFx). Note relative lack of labeled terminals in MS, NDB, and VLPO.
Scale bar=100µm. *Abbreviations: AQ=cerebral aqueduct, fx=fornix, LHA=lateral hypothalamic area, MS=medial septum, NDB=diagonal band nucleus, oc=optic chiasm, PAG=periaqueductal gray, PFx=perifornical area, SCm=superior colliculus, motor related, VLPO=ventrolateral preoptic area, ZIm=zona incerta, medial part.*

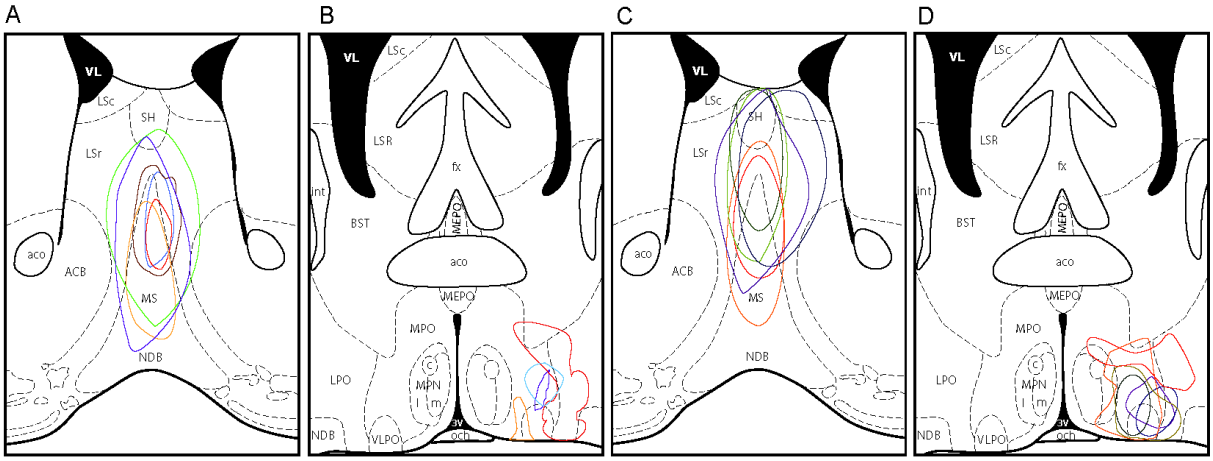

Figure 6-5: Summary of retrograde tracer injection sites in the MS/NDB and VLPO. For the same sex, outlines in the same color represent injections in the same mouse. (A) Sites of fluorogold (FG) injection into the medial septum/diagonal band nucleus (MS/NDB) in the male mouse. (B) Sites of Ctb injection into the VLPO in the male mouse. (C) Sites of FG injection into the MS/NDB in the female mouse. (D) Sites of Ctb injection into the VLPO in the female mouse.
Abbreviations: ACB=nucleus accumbens, aco=anterior commissure, BST=bed nucleus of the stria terminalis, fx=fornix, int=internal capsule, LPO=lateral preoptic area, LSc=lateral septum, caudal part, LSr=lateral septum, rostral part, MEPO=median preoptic nucleus, MPN=medial preoptic nucleus, MPO=medial preoptic area, MS=medial septum, NDB=diagonal band nucleus, och=optic chiasm, SH=septohippocampal nucleus, VL=lateral ventricle, VLPO=ventrolateral preoptic area

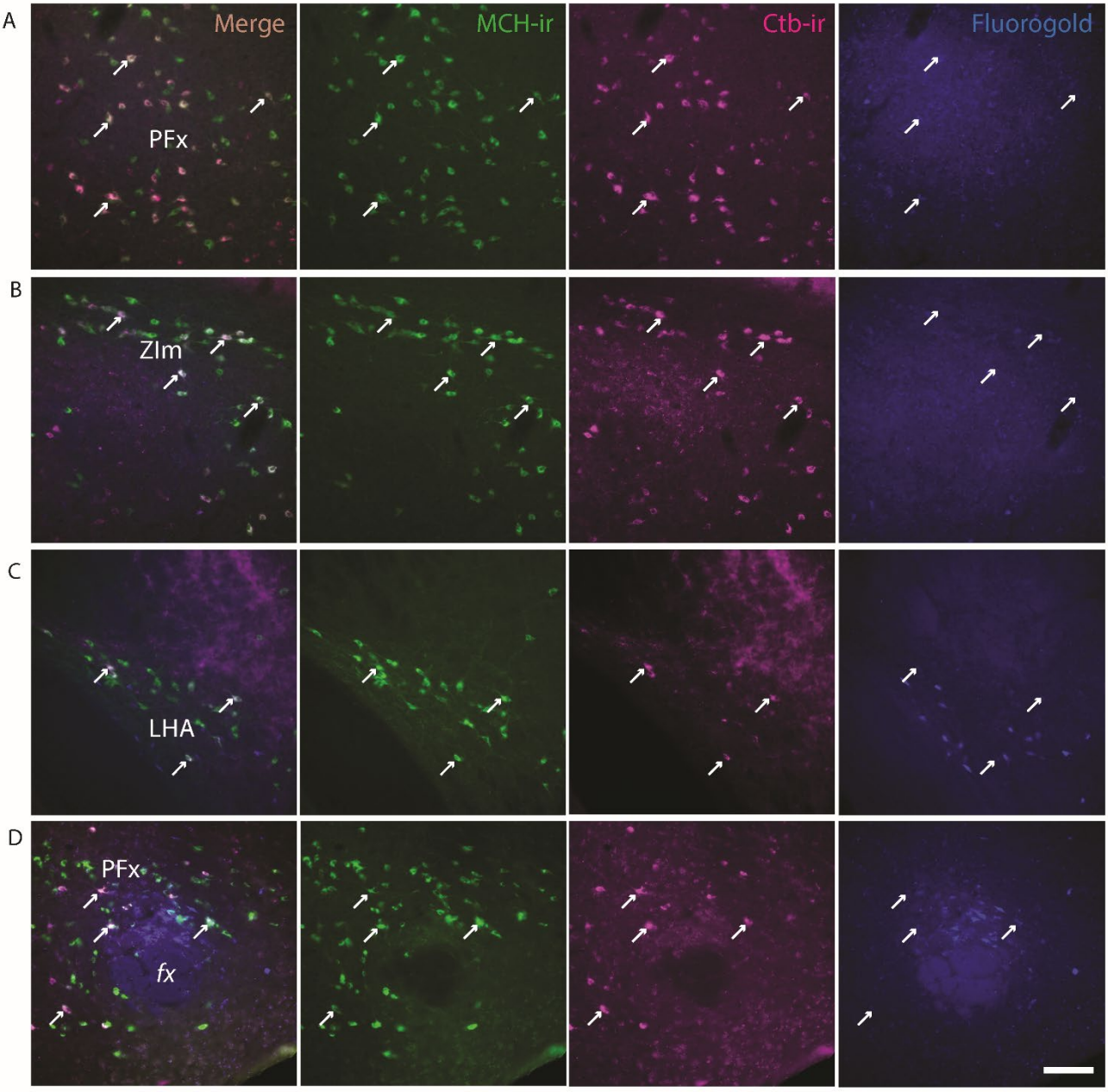

Figure 6-6: Medial septum/diagonal band nucleus- and ventrolateral preoptic area-projecting MCH neurons comprise distinct subpopulations of the PFx. Representative images of anti-MCH, -FG, and -Ctb immunostaining in the adult mouse brain following injection of the retrograde tracers FG into the MS/NDB and Ctb into the VLPO. Images shown are from a female brain; no differences were observed between male and female brains. Note the absence of triple-labeled cells, the presence of Ctb/MCH dual labeled cells, the absence of FG/MCH dual labeled cells, and the localization of FG staining directly anterior to the fornix.
Scale bar=100µm. *Abbreviations: fx=fornix, LHA=lateral hypothalamic area, PFx=perifornical area, ZIm=zona incerta, medial part.*

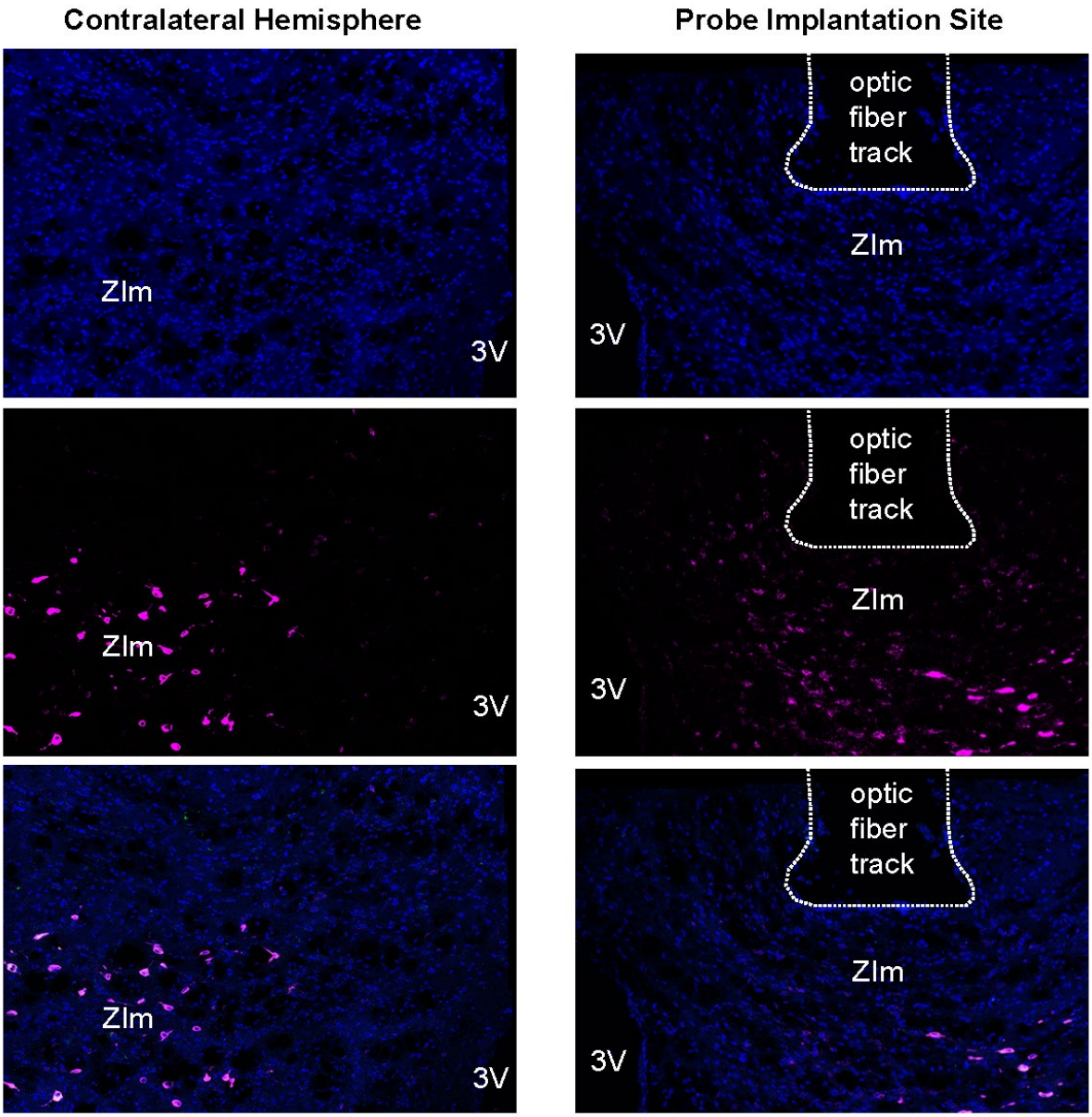

Figure 6-7: Optogenetic stimulation in the PFx of *Kiss1*-Cre;ChR2-eYFP mice induces *Fos* mRNA expression. *(A)* Fluorescent *in situ* hybridization labeling *Fos* (green), *Tacr3* (magenta), and *Hcrt* (white) at the optical fiber implantation site following 2 hours of optogenetic stimulation. *(B)* Fluorescent *in situ* hybridization labeling *Fos* (green), *Tacr3* (magenta), and *Hcrt* (white) at the level of the optical fiber implantation site in the contralateral hemisphere following 2 hours of optogenetic stimulation. Note the elevated *Fos* expression on the side of the optical fiber site and the absence of colocalization with either *Tacr3* or *Hcrt.*
Scale bar=100µm. *Abbreviations: fx=fornix, LHA=lateral hypothalamic area, PFx=perifornical area, ZIm=zona incerta, medial part, 3V=third ventricle.*

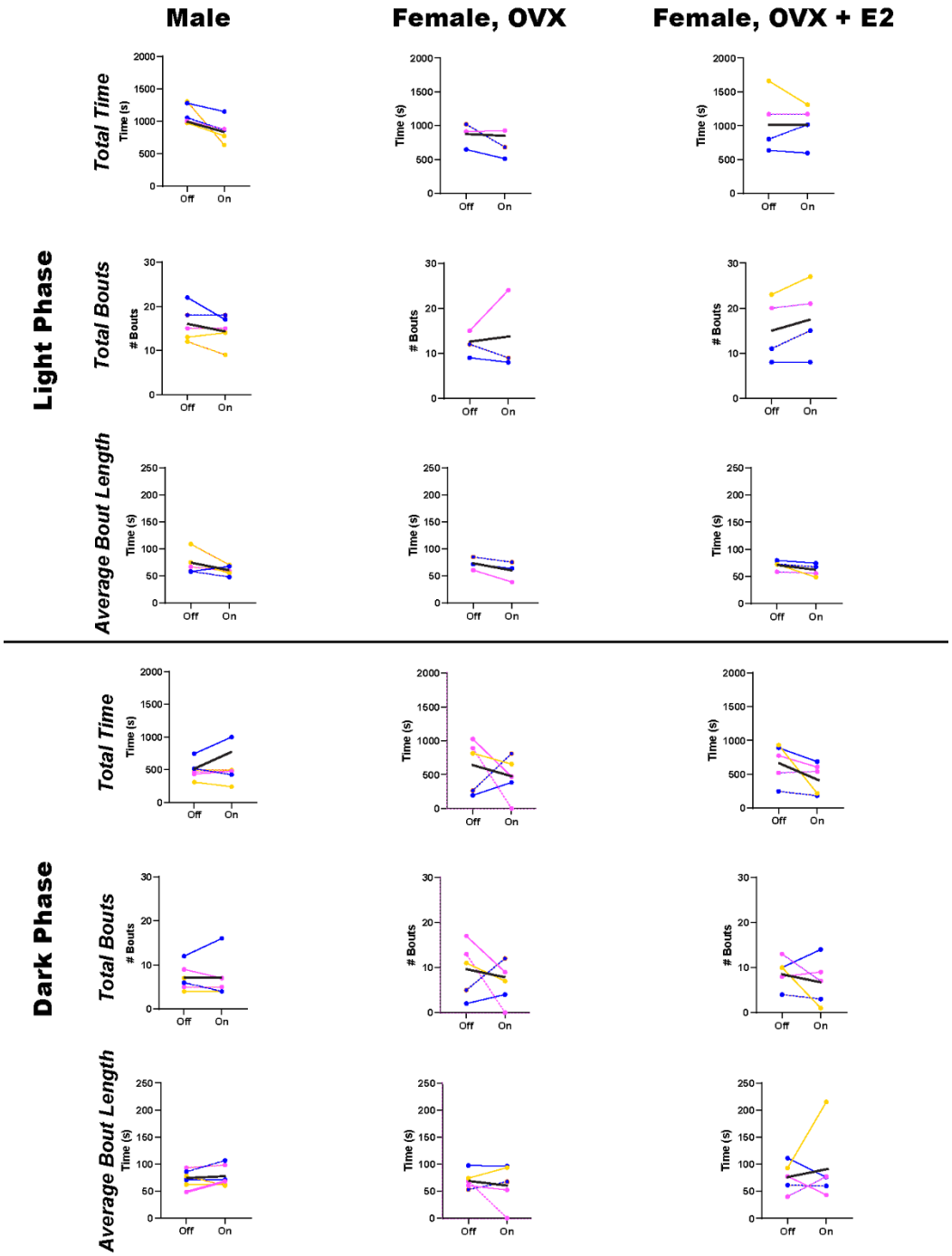

Figure 6-8: Optogenetic stimulation in the PFx of *Kiss1*-Cre;ChR2-eYFP mice decreases time spent in REM sleep in OVX+E2 mice. EEG activity was recorded for 4 hours in both the light and dark phases with and without optogenetic stimulation in a randomized crossover design such that each animal served as its own control. Note that female mice were recorded first following ovariectomy (OVX condition) and subsequently following the implantation of an estradiol implant (OVX+E2 condition) such that individual females may also be compared between estradiol conditions. Yellow lines represent animals in which the center of the optical fiber targeted the tuberal LHA. Pink lines represent animals in which the center of the optical fiber targeted the ZIm. Blue lines represent animals in which the center of the optical fiber targeted the posterior LHA. No clear difference is apparent based on subtle variation in implantation sites. No robust effects of stimulation are observed, but note that OVX+E2 mice largely trend towards reduced total time in REM with stimulation on.

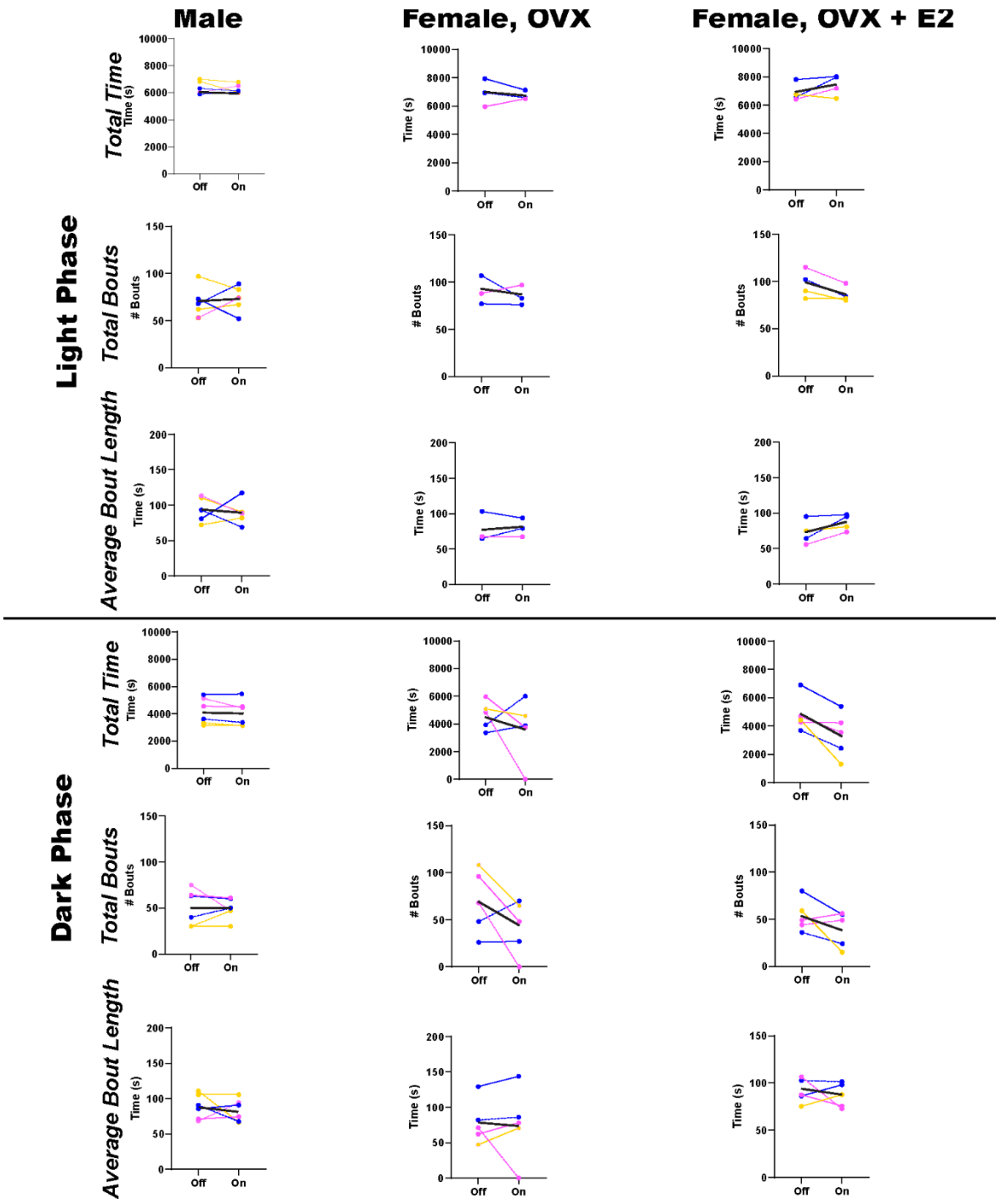

Figure 6-9: Optogenetic stimulation in the PFx of *Kiss1*-Cre;ChR2-eYFP mice decreases time spent in NREM sleep in OVX+E2 mice. EEG activity was recorded for 4 hours in both the light and dark phases with and without optogenetic stimulation in a randomized crossover design such that each animal served as its own control. Note that female mice were recorded first following ovariectomy (OVX condition) and subsequently following the implantation of an estradiol implant (OVX+E2 condition) such that individual females may also be compared between estradiol conditions. Yellow lines represent animals in which the center of the optical fiber targeted the tuberal LHA. Pink lines represent animals in which the center of the optical fiber targeted the ZIm. Blue lines represent animals in which the center of the optical fiber targeted the posterior LHA. No clear difference is apparent based on subtle variation in implantation sites. No robust effects of stimulation are observed, but note that OVX+E2 mice largely trend towards reduced total time in NREM with stimulation on.

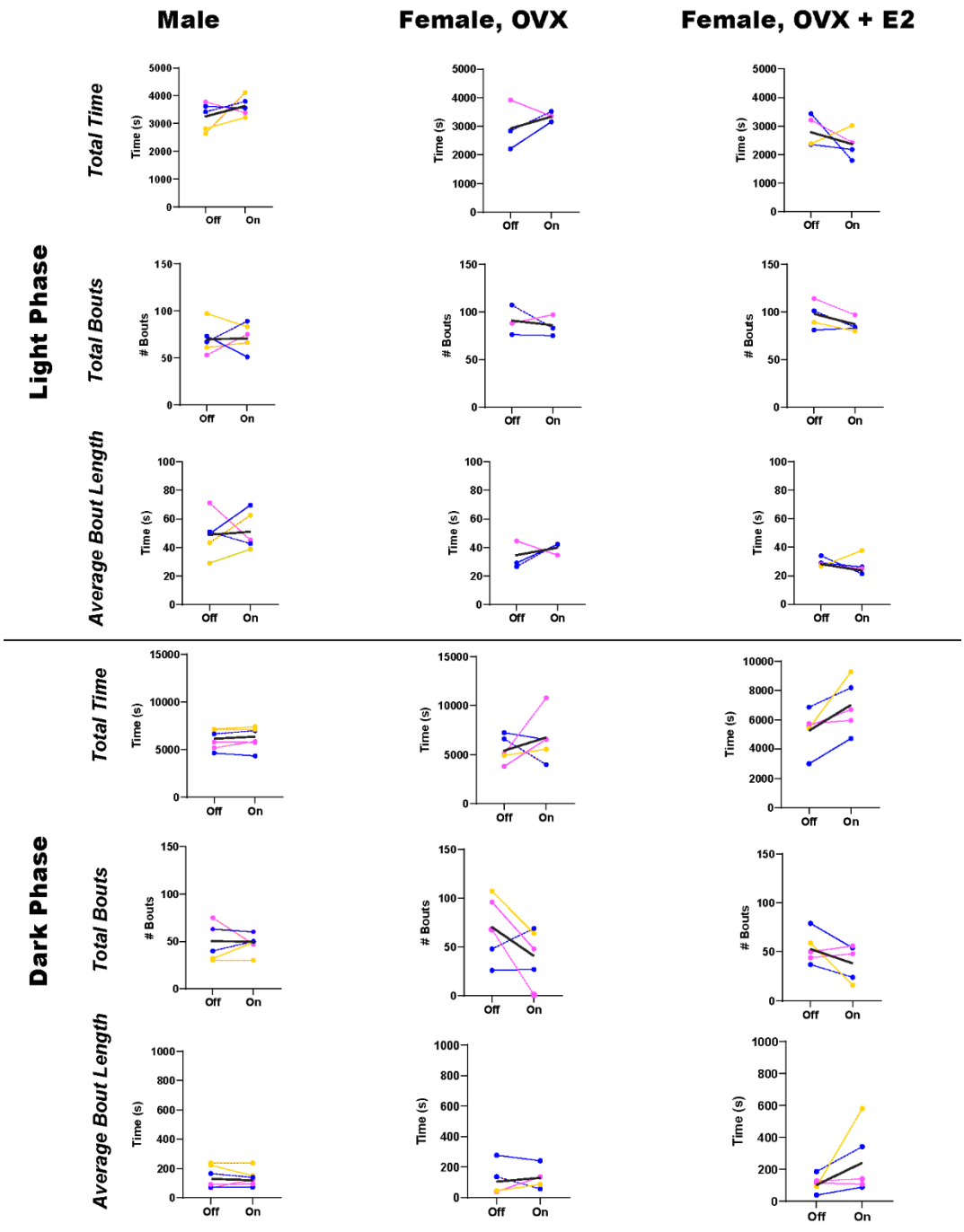

Figure 6-10: Optogenetic stimulation in the PFx of *Kiss1*-Cre;ChR2-eYFP mice increases total wake time in OVX+E2 mice. EEG activity was recorded for 4 hours in both the light and dark phases with and without optogenetic stimulation in a randomized crossover design such that each animal served as its own control. Note that female mice were recorded first following ovariectomy (OVX condition) and subsequently following the implantation of an estradiol implant (OVX+E2 condition) such that individual females may also be compared between estradiol conditions. Yellow lines represent animals in which the center of the optical fiber targeted the tuberal LHA. Pink lines represent animals in which the center of the optical fiber targeted the ZIm. Blue lines represent animals in which the center of the optical fiber targeted the posterior LHA. No clear difference is apparent based on subtle variation in implantation sites. No robust effects of stimulation are observed, but note that OVX+E2 mice largely trend towards increased total time spent awake with stimulation on.

References

1. Maquet, P., *The role of sleep in learning and memory.* Science, 2001. **294**(5544): p. 1048-52.
2. Schmidt, M.H., *The energy allocation function of sleep: a unifying theory of sleep, torpor, and continuous wakefulness.* Neurosci Biobehav Rev, 2014. **47**: p. 122-53.
3. Yamada, R.G. and H.R. Ueda, *Molecular Mechanisms of REM Sleep.* Front Neurosci, 2019. **13**: p. 1402.
4. Malik, D.M., et al., *Circadian and Sleep Metabolomics Across Species.* J Mol Biol, 2020. **432**(12): p. 3578-3610.
5. Siegel, J.M., *Clues to the functions of mammalian sleep.* Nature, 2005. **437**(7063): p. 1264-71.
6. Saper, C.B., et al., *Sleep state switching.* Neuron, 2010. **68**(6): p. 1023-42.
7. Mong, J.A. and D.M. Cusmano, *Sex differences in sleep: impact of biological sex and sex steroids.* Philos Trans R Soc Lond B Biol Sci, 2016. **371**(1688): p. 20150110.
8. Mong, J.A., et al., *Sleep, rhythms, and the endocrine brain: influence of sex and gonadal hormones.* J Neurosci, 2011. **31**(45): p. 16107-16.
9. Baker, F.C. and H.S. Driver, *Self-reported sleep across the menstrual cycle in young, healthy women.* J Psychosom Res, 2004. **56**(2): p. 239-43.
10. Aan Het Rot, M., et al., *Premenstrual mood and empathy after a single light therapy session.* Psychiatry Res, 2017. **256**: p. 212-218.
11. Krasnik, C., et al., *The effect of bright light therapy on depression associated with premenstrual dysphoric disorder.* Am J Obstet Gynecol, 2005. **193**(3 Pt 1): p. 658-61.
12. Colvin, G.B., et al., *Changes in sleep-wakefulness in female rats during circadian and estrous cycles.* Brain Res, 1968. **7**(2): p. 173-81.
13. Swift, K.M., et al., *Sex differences within sleep in gonadally intact rats.* Sleep, 2020. **43**(5).
14. Baker, F.C. and H.S. Driver, *Circadian rhythms, sleep, and the menstrual cycle.* Sleep Med, 2007. **8**(6): p. 613-22.
15. De Gennaro, L. and M. Ferrara, *Sleep spindles: an overview.* Sleep Med Rev, 2003. **7**(5): p. 423-40.
16. Tamminen, J., et al., *Sleep spindle activity is associated with the integration of new memories and existing knowledge.* J Neurosci, 2010. **30**(43): p. 14356-60.
17. Bittencourt, J., et al., *The melanin-concentrating hormone system of the rat brain: an immuno-and hybridization histochemical characterization.* Journal of Comparative Neurology, 1992. **319**(2): p. 218-245.
18. Sita, L., C. Elias, and J. Bittencourt, *Connectivity pattern suggests that incerto-hypothalamic area belongs to the medial hypothalamic system.* 2007. **148**: p. 949-69.
19. Elias, C.F., et al., *Chemically defined projections linking the mediobasal hypothalamus and the lateral hypothalamic area.* J Comp Neurol, 1998. **402**(4): p. 442-59.
20. Hassani, O., M. Gee Lee, and B. Jones, *Melanin-concentrating hormone neurons discharge in a reciprocal manner to orexin neurons across the sleep-wake cycle.* 2009. **106**: p. 2418-2422.
21. Verret, L., et al., *A role of melanin-concentrating hormone producing neurons in the central regulation of paradoxical sleep.* BMC Neurosci, 2003. **4**: p. 19.
22. Jego, S., et al., *Optogenetic identification of a rapid eye movement sleep modulatory circuit in the hypothalamus.* 2013. **16**.

23. Konadhode, R., et al., *Optogenetic Stimulation of MCH Neurons Increases Sleep.* 2013. **33**: p. 10257-63.
24. Tsunematsu, T., et al., *Optogenetic Manipulation of Activity and Temporally Controlled Cell-Specific Ablation Reveal a Role for MCH Neurons in Sleep/Wake Regulation.* 2014. **34**: p. 6896-909.
25. Blanco-Centurion, C., et al., *Dynamic Network Activation of Hypothalamic MCH Neurons in REM Sleep and Exploratory Behavior.* The Journal of Neuroscience, 2019: p. 0305-19.
26. Attademo, A.M., et al., *Neuropeptide Glutamic Acid-Isoleucine May Induce Luteinizing Hormone Secretion via Multiple Pathways.* Neuroendocrinology, 2006. **83**(5-6): p. 313-24.
27. G.P. Gallardo, M., S. R. Chiocchio, and J. H. Tramezzani, *Changes of melanin-concentrating hormone related to LHRH release in the median eminence of rats.* 2005. **1030**: p. 152-8.
28. Murray, J., et al., *Evidence for a Stimulatory Action of Melanin-Concentrating Hormone on Luteinising Hormone Release Involving MCH1 and Melanocortin-5 Receptors.* 2006. **18**: p. 157-67.
29. S Williamson-Hughes, P., K. Grove, and M.S. Smith, *Melanin concentrating hormone (MCH): A novel neural pathway for regulation of GnRH neurons.* 2005. **1041**: p. 117-24.
30. Skrapits, K., et al., *Lateral hypothalamic orexin and melanin-concentrating hormone neurons provide direct input to gonadotropin-releasing hormone neurons in the human.* Front Cell Neurosci, 2015. **9**: p. 348.
31. Wu, M., et al., *Melanin-concentrating hormone directly inhibits GnRH neurons and blocks kisspeptin activation, linking energy balance to reproduction.* Proc Natl Acad Sci U S A, 2009. **106**(40): p. 17217-22.
32. MacKenzie, F., M. James, and C. Wilson, *Changes in dopamine activity in the zona incerta (ZI) over the rat oestrous cycle and the effect of lesions of the ZI on cyclicity: further evidence that the incerto-hypothalamic tract has a stimulatory role in the control of LH release.* Brain Research, 1988. **444**: p. 75-78.
33. Dumalska, I., et al., *Excitatory effects of the puberty-initiating peptide kisspeptin and group I metabotropic glutamate receptor agonists differentiate two distinct subpopulations of gonadotropin-releasing hormone neurons.* J Neurosci, 2008. **28**(32): p. 8003-13.
34. Gonzalez, M., B. Baker, and C. Wilson, *Stimulatory effect of melanin-concentrating hormone on luteinising hormone release.* Neuroendocrinology, 1997. **66**: p. 254-262.
35. Tsukamura, H., et al., *Intracerebroventricular administration of melanin-concentrating hormone suppresses pulsatile luteinizing hormone release in the female rat.* J Neuroendocrinol, 2000. **12**(6): p. 529-34.
36. Croizier, S., et al., *Development of posterior hypothalamic neurons enlightens a switch in the prosencephalic basic plan.* PLoS One, 2011. **6**(12): p. e28574.
37. Cvetkovic, V., et al., *Characterization of subpopulations of neurons producing melanin-concentrating hormone in the rat ventral diencephalon.* J Neurochem, 2004. **91**(4): p. 911-9.
38. Koehl, M., S.E. Battle, and F.W. Turek, *Sleep in female mice: a strain comparison across the estrous cycle.* Sleep, 2003. **26**(3): p. 267-72.

39. Croizier, S., et al., *A comparative analysis shows morphofunctional differences between the rat and mouse melanin-concentrating hormone systems.* PLoS One, 2010. **5**(11): p. e15471.
40. Brischoux, F., et al., *Time of genesis determines projection and neurokinin-3 expression patterns of diencephalic neurons containing melanin-concentrating hormone.* Eur J Neurosci, 2002. **16**(9): p. 1672-80.
41. Fujita, A., et al., *Neurokinin B-Expressing Neurons of the Central Extended Amygdala Mediate Inhibitory Synaptic Input onto Melanin-Concentrating Hormone Neuron Subpopulations.* J Neurosci, 2021. **41**(46): p. 9539-9560.
42. Navarro, V.M., et al., *Regulation of gonadotropin-releasing hormone secretion by kisspeptin/dynorphin/neurokinin B neurons in the arcuate nucleus of the mouse.* J Neurosci, 2009. **29**(38): p. 11859-66.
43. Guran, T., et al., *Hypogonadotropic hypogonadism due to a novel missense mutation in the first extracellular loop of the neurokinin B receptor.* J Clin Endocrinol Metab, 2009. **94**(10): p. 3633-3639.
44. Brioude, F., C.E. Bouvattier, and M. Lombès, *[Hypogonadotropic hypogonadism: new aspects in the regulation of hypothalamic-pituitary-gonadal axis].* Ann Endocrinol (Paris), 2010. **71 Suppl 1**: p. S33-41.
45. Rance, N.E., et al., *Neurokinin B and the hypothalamic regulation of reproduction.* Brain Res, 2010. **1364**: p. 116-28.
46. Semple, R.K. and A.K. Topaloglu, *The recent genetics of hypogonadotrophic hypogonadism - novel insights and new questions.* Clin Endocrinol (Oxf), 2010. **72**(4): p. 427-35.
47. Topaloglu, A.K. and L.D. Kotan, *Molecular causes of hypogonadotropic hypogonadism.* Curr Opin Obstet Gynecol, 2010. **22**(4): p. 264-70.
48. Regoli, D., A. Boudon, and J.L. Fauchére, *Receptors and antagonists for substance P and related peptides.* Pharmacol Rev, 1994. **46**(4): p. 551-99.
49. Donato, J., et al., *Leptin's effect on puberty in mice is relayed by the ventral premammillary nucleus and does not require signaling in Kiss1 neurons.* J Clin Invest, 2011. **121**(1): p. 355-68.
50. Mahany, E.B., et al., *Obesity and High-Fat Diet Induce Distinct Changes in Placental Gene Expression and Pregnancy Outcome.* Endocrinology, 2018. **159**(4): p. 1718-1733.
51. Sarnaik, R. and I.M. Raman, *Control of voluntary and optogenetically perturbed locomotion by spike rate and timing of neurons of the mouse cerebellar nuclei.* Elife, 2018. **7**.
52. Idris, A.I., *Ovariectomy/Orchidectomy in Rodents*, in *Bone Research Protocols*, M.H. Helfrich and S.H. Ralston, Editors. 2012, Humana Press: Totowa, NJ. p. 545-551.
53. Silveira, M.A., et al., *GnRH Neuron Activity and Pituitary Response in Estradiol-Induced vs Proestrous Luteinizing Hormone Surges in Female Mice.* Endocrinology, 2017. **158**(2): p. 356-366.
54. Barger, Z., et al., *Robust, automated sleep scoring by a compact neural network with distributional shift correction.* PLoS One, 2019. **14**(12): p. e0224642.
55. Muschamp, J.W. and E.M. Hull, *Melanin concentrating hormone and estrogen receptor-alpha are coexstensive but not coexpressed in cells of male rat hypothalamus.* Neurosci Lett, 2007. **427**(3): p. 123-6.

56. Hershey, A.D. and J.E. Krause, *Molecular characterization of a functional cDNA encoding the rat substance P receptor.* Science, 1990. **247**(4945): p. 958-62.
57. Nakanishi, S., *Mammalian tachykinin receptors.* Annu Rev Neurosci, 1991. **14**: p. 123-36.
58. Lehman, M.N., L.M. Coolen, and R.L. Goodman, *Minireview: kisspeptin/neurokinin B/dynorphin (KNDy) cells of the arcuate nucleus: a central node in the control of gonadotropin-releasing hormone secretion.* Endocrinology, 2010. **151**(8): p. 3479-89.
59. Clarkson, J., et al., *Kisspeptin-GPR54 signaling is essential for preovulatory gonadotropin-releasing hormone neuron activation and the luteinizing hormone surge.* J Neurosci, 2008. **28**(35): p. 8691-7.
60. Smith, J.T., et al., *Kiss1 neurons in the forebrain as central processors for generating the preovulatory luteinizing hormone surge.* J Neurosci, 2006. **26**(25): p. 6687-94.
61. Srividya, R., H.N. Mallick, and V.M. Kumar, *Sleep changes produced by destruction of medial septal neurons in rats.* Neuroreport, 2004. **15**(11): p. 1831-5.
62. Puskar, P., et al., *Changes in sleep-wake cycle after microinjection of agonist and antagonist of endocannabinoid receptors at the medial septum of rats.* Physiol Behav, 2021. **237**: p. 113448.
63. Mukherjee, D., et al., *Glutamate microinjection in the medial septum of rats decreases paradoxical sleep and increases slow wave sleep.* Neuroreport, 2012. **23**(7): p. 451-6.
64. Kang, D., et al., *Theta-rhythmic drive between medial septum and hippocampus in slow-wave sleep and microarousal: a Granger causality analysis.* J Neurophysiol, 2015. **114**(5): p. 2797-803.
65. Kang, D., et al., *Reciprocal Interactions between Medial Septum and Hippocampus in Theta Generation: Granger Causality Decomposition of Mixed Spike-Field Recordings.* Front Neuroanat, 2017. **11**: p. 120.
66. PETSCHE, H., C. STUMPF, and G. GOGOLAK, *[The significance of the rabbit's septum as a relay station between the midbrain and the hippocampus. I. The control of hippocampus arousal activity by the septum cells].* Electroencephalogr Clin Neurophysiol, 1962. **14**: p. 202-11.
67. Desikan, S., et al., *Target selectivity of septal cholinergic neurons in the medial and lateral entorhinal cortex.* Proc Natl Acad Sci U S A, 2018. **115**(11): p. E2644-E2652.
68. Buzsáki, G., *Theta oscillations in the hippocampus.* Neuron, 2002. **33**(3): p. 325-340.
69. Nuñez, A. and W. Buño, *The Theta Rhythm of the Hippocampus: From Neuronal and Circuit Mechanisms to Behavior.* Front Cell Neurosci, 2021. **15**: p. 649262.
70. Alam, M.N., et al., *Adenosinergic modulation of rat basal forebrain neurons during sleep and waking: neuronal recording with microdialysis.* J Physiol, 1999. **521 Pt 3**: p. 679-90.
71. Sherin, J.E., et al., *Innervation of histaminergic tuberomammillary neurons by GABAergic and galaninergic neurons in the ventrolateral preoptic nucleus of the rat.* J Neurosci, 1998. **18**(12): p. 4705-21.
72. Gong, H., et al., *Activation of c-fos in GABAergic neurones in the preoptic area during sleep and in response to sleep deprivation.* J Physiol, 2004. **556**(Pt 3): p. 935-46.
73. Yang, Q.Z. and G.I. Hatton, *Electrophysiology of excitatory and inhibitory afferents to rat histaminergic tuberomammillary nucleus neurons from hypothalamic and forebrain sites.* Brain Res, 1997. **773**(1-2): p. 162-72.
74. Beekly, B.G., et al., *Dissociated Pmch and Cre Expression in Lactating Pmch-Cre BAC Transgenic Mice.* Frontiers in Neuroanatomy, 2020. **14**(60).

75. Novak, C.M., L. Smale, and A.A. Nunez, *Rhythms in Fos expression in brain areas related to the sleep-wake cycle in the diurnal Arvicanthis niloticus.* Am J Physiol Regul Integr Comp Physiol, 2000. **278**(5): p. R1267-74.
76. Kovács, K.J., *Measurement of immediate-early gene activation- c-fos and beyond.* J Neuroendocrinol, 2008. **20**(6): p. 665-72.
77. Peyron, C., et al., *Neurons containing hypocretin (orexin) project to multiple neuronal systems.* J Neurosci, 1998. **18**(23): p. 9996-10015.
78. Yamanaka, A., et al., *Hypothalamic orexin neurons regulate arousal according to energy balance in mice.* Neuron, 2003. **38**(5): p. 701-13.
79. Yang, J.A., et al., *Regulation of gene expression by 17β-estradiol in the arcuate nucleus of the mouse through ERE-dependent and ERE-independent mechanisms.* Steroids, 2016. **107**: p. 128-138.
80. Smith, J.T., et al., *Regulation of Kiss1 gene expression in the brain of the female mouse.* Endocrinology, 2005. **146**(9): p. 3686-92.

Chapter VI. Indirect effects of steroid hormones on MCH neuron modulation of sleep

Abstract

Sleep disruptions and disorders are associated with alterations in the timing of pubertal development as well as poor fertility outcomes. Despite this, there remains a great paucity of research at the basic and early translational level on the relationship between sleep and reproductive physiology, particularly in female animals. Given the relevance of sleep for women's reproductive health, a deeper understanding of the role of sleep in the maturation and function of the reproductive system that encompasses biological sex differences is imperative for the development of effective interventions and treatments across the life span.

Neuropeptidergic control of vigilance states is complex, but melanin-concentrating hormone (MCH) neurons are key players that have demonstrated effects on pituitary gonadotropin release which vary with the estradiol milieu. We hypothesized that MCH neurons contribute to the temporal integration of sleep and reproductive physiology in a manner dependent on gonadal hormones. We performed antero- and retrograde tracing and immunohistochemistry to characterize a population of MCH neurons that projects to both sleep and reproductive control sites, finding that MCH neurons do not respond directly to gonadal hormones but receive inputs from a population of estrogen-sensing neurons in the arcuate nucleus (ARH). Furthermore, we used optogenetics to activate neuron terminals originating in the ARH in the lateral hypothalamus and perifornical area, where MCH perikarya are found, and observed the effects of so doing on both sleep in males and females in varying estradiol milieu. While male mice and female mice under low estradiol conditions were largely unresponsive, females supplemented with exogenous estradiol exhibited reduced time in both REM and NREM sleep and increased time spent awake during the dark phase. Our findings reveal a previously unrecognized and estradiol-dependent role for the ARH KNDy-PFx MCH neuron circuit in the integration of gonadal steroids and sleep in female mice.

Background

Reduced and fragmented sleep is associated with infertility in humans. Nearly one-fifth of American couples struggle with infertility and, with increasing environmental exposure to sleep and circadian disruptors, deficiencies in pubertal development and fertility will likely continue to increase. Disorders of the reproductive system also have high rates of comorbidity with metabolic dysfunction, certain cancers, and psychiatric illness. Thus, there is an urgent need to better understand the neuroendocrine reproductive axis and how it interacts with sleep.

Sleep is a fundamental neurological function which is conserved across the animal kingdom, though the primary role(s) of sleep and the details of its regulation remain incompletely understood [1-5]. In mammals, sleep can be divided into three basic states using electroencephalography (EEG): (1) wakefulness, for which the EEG is characterized by low amplitude, high frequency waveforms; (2) non-rapid eye movement (NREM) sleep, also known as slow-wave sleep (SWS), for which the EEG is characterized by higher amplitude, slower waveforms, with especially high power in the delta frequency; and (3) rapid eye movement (REM) sleep, also known as paradoxical sleep (PS) for its resemblance to waking EEG signatures [6]. REM sleep, however, may be distinguished from wake by the more organized, "sawtooth"-like theta-frequency waveforms [6].

In spite of its stereotyped and highly conserved nature, variations are observed in sleep between the sexes. Clinical studies suggest that women have lower latency to sleep and increased total sleep time, particularly SWS, as compared to men [7]. Paradoxically, women and girls are twice as likely to report indications of disordered sleep like insomnia, difficulty staying asleep, and daytime tiredness [8].

Variation in sleep quality is also observed across the menstrual cycle. Self-reported sleep disturbances increase during the late luteal phase, particularly in women with dysmenorrhea [9]. Light therapy may improve mood-related premenstrual symptoms, suggesting that circadian disruptions could be related to transient deterioration of sleep quality and constitute a cause of premenstrual negative affect [10, 11]. In some clinical studies, polysomnography and actigraphy recordings confirm that women experience poorer quality sleep during the luteal phase as compared with the follicular and menstrual phases. In Long-Evans rats, cortical EEG, cortical local field potential (CA1 LFP), and electromyography (EMG) recordings revealed that the

proestrus phase of the estrous cycle is characterized by reduced total REM and non-REM sleep during both the dark and light phases as compared to both male rats and female rats in other stages of the estrous cycle [12]. This suppression of sleep was followed by increased total REM and NREM sleep during the estrus phase.

Sleep architecture also varied across the estrous cycle, with females showing alterations to the number and length of bouts of REM and NREM sleep across different phases of the estrous cycle [13]. Finally, more sleep spindles—unique EEG phasic features of NREM sleep observed in the sigma frequency which are involved in learning and memory—are observed during the luteal phase [7-9, 14-16]. Sleep spindles may be related to membrane potential variation in thalamocortical networks; this would suggest a potential broader effect of steroid hormones on neural network dynamics. Taken together, these data indicate that many features of sleep may be modulated by the sex steroid milieu.

Neuropeptidergic control of sleep and wakefulness is complex, but melanin-concentrating hormone (MCH) is well-established as a significant contributor to the process. As detailed in the Introduction, most brain MCH expression is in neurons of the incertohypothalamic area (IHy, alternatively medial zona incerta, ZIm), the perifornical area (PFx), and the lateral hypothalamic area (LHA), all of which have multiple functions that include sleep/wake regulation [17-19]. Notably, MCH neurons are active during sleep, and optogenetic activation of MCH neurons significantly increases sleep duration [20-25]. MCH neurons also project to areas implicated in reproductive control such as the medial preoptic nucleus (MPO) and the median eminence (ME), which harbor gonadotropin-releasing hormone (GnRH) neuron cell bodies and terminals, respectively [26, 27].

At the apex of the neuroendocrine reproductive axis are GnRH neurons. Episodic release of GnRH drives pulsatile secretion of the gonadotropins, luteinizing hormone (LH) and follicle-stimulating hormone (FSH), from the pituitary gland. These in turn act on the gonads to promote gametogenesis and steroidogenesis. A bout of high-frequency LH pulses is required for both pubertal onset and ovulation. Notably, the rise in LH pulse frequency that precipitates puberty occurs during sleep, while in adults, LH pulse frequency is reduced during sleep. The mechanisms governing the temporal relationship between sleep and pituitary gonadotropin

secretion represent a significant gap in the field's understanding of reproductive development and function.

In humans and rodents, MCH terminals are observed in close apposition with GnRH cells, which express MCH receptor 1 (MCHR1) [26-31]. MCH neurons are thus anatomically poised to dually regulate sleep and the reproductive axis. The functional role of MCH neurons in reproductive physiology is less clear, however, with mixed conclusions about the ability of MCH to stimulate LH secretion.

Early studies showed that lesioning the ZIm, where many MCH neurons are found, reduces circulating LH [32]. *In vitro,* hypothalamic explants from adult ovariectomized (OVX) rats can release GnRH following MCH application, but only if the rats are primed with estradiol-2-benzoate (E2) prior to euthanasia and brain dissection [28]. Conversely, when hypothalamic explants from intact male and female prepubertal mice are treated with MCH, a subpopulation of GnRH neurons that is $VGLUT2^{+}$ and kisspeptin-sensitive (which represents 61% of total GnRH neurons) has been reported to be hyperpolarized, ultimately suppressing the ability of kisspeptin to induce GnRH release from these cells [31, 33]. The authors propose that MCH is involved in the relay of metabolic state to the neuroendocrine reproductive axis, suppressing reproductive function in states of negative energy balance. Thus, metabolic state may be another contextual factor which must be considered in the interpretation of data on this topic.

In vivo, MCH injection into the ME and POA increases circulating LH in OVX+E2 rats but not OVX rats treated with vehicle; furthermore, this effect seems to be specific to application of MCH to regions where GnRH neuron perikarya are located, as injection into the ZIm or VMN has no effect in either group [28, 34]. However, intracerebroventricular injection of MCH has also been shown to *attenuate* the anticipated increase in circulating LH in surge-model rats—animals treated with a carefully curated schedule and dosage of both E2 and progesterone (PG) to reliably induce an LH surge [35].

The inconsistency of experimental design renders these data challenging to evaluate concurrently. The valence and magnitude of MCH effects on LH may depend on the site of MCH administration, developmental stage and/or sex steroid milieu at the time of the experiment, and possibly even the species and/or strain of the model organism. As such, none of the data discussed necessarily contradict each other, but rather likely represent different

manifestations of the ability of MCH neurons to integrate numerous peripheral cues and modulate reproduction accordingly.

Another explanation for the discrepancies could be the existence of subpopulations of MCH neurons. MCH neurons migrate from the neural crest in two groups, with an early-arising group that settles in the lateral hypothalamus and projects caudally to the brainstem and a late-arising group settling mainly in the medial hypothalamus which targets hypothalamic and cortical neurons [36, 37]. Thus, it stands to reason that MCH neurons would not all act on the HPG axis in the same way. Sleep architecture also varies with hormonal milieu, suggesting that MCH could coordinate LH secretion with sleep/wake state in a sex-steroid dependent manner [38]. Further support for this notion lies in the fact that this later-arising, more medial population of MCH neurons is known to express the neurokinin-B (NKB) receptor NK3R [39-41]. NKB is a member of the tachykinin family of peptides which participates in the regulation of GnRH neuron firing in conjunction with kisspeptin, potentially by stimulating kisspeptin secretion [42]. NK3R is the preferred receptor for NKB, and loss of NK3R results in severe hypogonadotropic hypogonadism, with or without anosmia [43-48].

We hypothesized that medial MCH neurons, with their expression of NK3R and their projections within the hypothalamus, are involved in the temporal integration of sleep patterns and LH secretion. Furthermore, we predicted that this action could be modulated by gonadal hormones. We performed antero- and retrograde tracing and immunohistochemistry to determine whether a specific population of MCH neurons projects to both sleep and reproductive control sites and whether such a population might be defined by specific projection targets and/or colocalized transcripts. Finally, we used optogenetics to activate a putative NKB-to-MCH neuron circuit and assessed the effects of so doing on both sleep and circulating LH in both sexes and in varying estradiol milieu.

Methods

Mice

Animal Care

Mice were housed in a vivarium at the University of Michigan with a 12/12 light/dark cycle and ad libitum access to food and water. The mice received phytoestrogen-reduced Envigo diet 2016 (16% protein/4% fat), except during breeding when mice were fed phytoestrogen-reduced

Envigo diet 2019 (19% protein/8% fat) to accommodate additional nutritional needs of pregnant and nursing dams and during optogenetic stimulation, when mice received BioServ F0071 Precision pellets (18% protein/5.6% fat). Phytoestrogen-reduced diet is routinely used in our laboratory to avoid the effects of exogenous estrogens on mouse physiology. All procedures and experiments were carried out in accordance with the guidelines established by the National Institutes of Health Guide for the Care and Use of Laboratory Animals and approved by the University of Michigan Committee on Use and Care of Animals (Animal Protocol #PRO00010420).

Pmch-iCre;L10-eGFP Mice

Pmch-iCre;L10-eGFP mice ("MCH-L10") reporter mice were generated by crossing *Pmch*-iCre mice generated in our lab in conjunction with the UM Transgenic Animal Core (see Chapter 2) with B6;129S4-*Gt(ROSA)26Sor*$^{tm9(EGFP/Rpl10a)Amc}$/J line (JAX®; stock #024750, "eGFP-L10a") mice.

Kiss1-Cre;L10-eGFP and Kiss1-Cre;ChR2-eYFP Mice

Kiss1-Cre;L10-eGFP were generated by crossing Tg(*Kiss1*-cre)J2-4Cfe/J (JAX®; stock 023426, "*Kiss1*-Cre") mice with B6;129S4-*Gt(ROSA)26Sor*$^{tm9(EGFP/Rpl10a)Amc}$/J line (JAX®; stock #024750, "eGFP-L10a") mice. *Kiss1*-Cre;ChR2-eYFP mice were generated by crossing *Kiss1*-Cre mice with B6.Cg-*Gt(ROSA)26Sor*$^{tm32(CAG-COP4*H134R/EYFP)Hze}$/J (JAX®; stock # 024109, "ChR2-eYFP") mice.

Surgery

Craniotomy

For injection of anterograde tracers into MCH neurons, adult male and female *Pmch*-Cre;L10-eGFP mice were anaesthetized with isoflurane (2-4%, Fluriso; Vet One) and 50 nL AAV-ChR2-mCherry (Addgene plasmid #18916) was stereotaxically delivered unilaterally into the hypothalamus with a pneumatic picopump (World Precision Instruments) as routinely done in our laboratory and others [49, 50]. This virus has been successfully used previously to label anterograde projections [51]. The coordinates used were AP -4.5 mm from the rostral rhinal vein, ML -0.6 mm from the midline, and DV -4.8 mm from the surface of the dura mater.

After 10 days' recovery from surgery, mice were deeply anesthetized with isoflurane and perfused with 10% formalin and brains were dissected, postfixed for 8 hours in 10% formalin, and cryoprotected overnight using a solution of 20% sucrose in phosphate buffered saline. Coronal sections (30 μm thickness, 4 series) were collected with a freezing microtome and stored in a cryoprotectant solution (20% glycerol/30% ethylene glycol in DEPC-treated PBS) at −20°C. The distribution of mCherry-labeled fibers was mapped following immunohistochemistry.

For injection of anterograde tracers into ARH KNDy neurons, the same basic procedures were followed. Adult male and female *Kiss1*-Cre;eGFP-L10a mice were used (JAX Stock #023426) and the coordinates used were AP -4.6 mm from the rostral rhinal vein, ML -0.2 mm from the midline, and DV -5.6 mm from the surface of the dura mater.

For injection of retrograde tracers into the VLPO and MS/NDB of MCH-Cre;eGFP-L10a mice, the same basic procedures were followed except for the stereotaxic coordinates. For the MS/NDB, the coordinates used were AP -3.0 mm from the rostral rhinal vein, ML on the midline, and DV -4.8 mm from the surface of the dura mater and the tracer injected was Fluoro-Gold ("FG," 1% solution, Fluorochrome). For the VLPO, the coordinates used were AP -2.7 mm from the rostral rhinal vein, ML -1.0 mm from the midline, and DV -4.8 mm from the surface of the dura mater and the tracer injected was cholera toxin, β subunit (Ctb) (1%; List Biological Laboratories, Campbell, CA, USA).

Optical fiber implantation

Adult male and female *Kiss1*-Cre;ChR2-eYFP mice were anaesthetized with isoflurane (2-4%, Fluriso; Vet One) and a metal ferrule optic fiber (400-μm diameter core; BFH37-400 Multimode; NA 0.37; ThorLabs) was implanted unilaterally over the PFx (AP -4.5 mm from the rostral rhinal vein, ML -0.3 mm from the midline, DV -4.8 mm from the surface of the dura mater). Fibers were fixed to the skull using dental acrylic; after the completion of the experiments, mice were euthanized and the locations of optic fiber tips were identified based on the coordinates of Paxinos and Franklin's Mouse Brain in Stereotaxic Coordinates.

EEG/EMG placement

EEG/EMG placement was performed during the same surgery as the optical fiber implantation (above). Mice were implanted with two stainless-steel screws (Frontal: AP: 1.5 mm from Bregma, ML: −1.5 mm; Temporal: AP: −3.5 mm from Bregma, ML: −2.8 mm; Ground: AP:

−3.3 mm from Bregma, ML: −.4 mm) and a pair of multi-strand stainless steel wires inserted into the neck extensor muscles. The EEG and EMG leads were wired to a small electrical connector that is attached to the skull with dental cement. Mice were then kept on a warming pad until awake. All mice were given analgesics (5 mg/kg Meloxicam) preemptively and 24 hours after surgery. Mice were given a minimum of 2 weeks for recovery and 1 week for acclimation before experiments began.

Ovariectomy and estradiol implants

Standard ovariectomy and estrogen replacement procedures were performed as previously described [52]. Briefly, under isoflurane anesthesia, ovaries were externalized through two small incisions on either side of midline just below the rib cage and removed by cauterizing the oviduct. For "OVX+E2" conditions, immediately before experiments, mice were briefly anesthetized again and received a Silastic (Dow Corning) implant containing 0.625 μg 17β-estradiol-3-benzoate (Sigma) dissolved in sesame oil in the scapular region [53].

Optogenetic stimulation and behavioral experiments

Optogenetic stimulation paradigm

Mice received optogenetic stimulation at 20Hz, estimated 10mW at the fiber tip, for four hours on a one second on/four seconds off schedule. Recordings began 30 min into stimulation and data was collected for a total of 3 h per day at a time when the mice will not be disturbed by researchers or care staff entering the room. The study was conducted in a randomized crossover design; each mouse was recorded in both the light and the dark phase with and without optogenetic stimulation such that each animal experienced all four conditions and served as its own control.

Polysomnographic recording and analysis

Polysomnographic signals were digitized at 1000 Hz, with a 0.3-100 Hz bandpass filter applied to the EEG and a 30-100 Hz bandpass filter applied to the EMG, with a National Instruments data acquisition card and collected using a custom MATLAB script. EEG/EMG signals were notch filtered at 60 Hz to account for electrical interference from the recording tether. Mice were recorded for a minimum of 4 sessions: a 12 h dark cycle recording with no optogenetic stimulation, a 12 h light cycle recording with no optogenetic stimulation, a 12 h dark cycle recording with optogenetic stimulation, and a 12 h light cycle recording with optogenetic

stimulation. Polysomnographic signals were analyzed using AccuSleep, an open-source sleep scoring algorithm in MATLAB, and verified by an experienced sleep-scorer [54]. Behavioral states were scored in 5 s epochs as either wake, NREM, or REM sleep.

Histology

Fluorescent in situ hybridization

Neuronal activation induced by optogenetic stimulation was assessed using triple-label fluorescent *in situ* hybridization (RNAscope, ACD Bio). Briefly, adult male and female mice *Pmch*-iCre$^{+/-}$;VGLUT2$^{fl/fl}$ and *Pmch*-iCre$^{-/-}$;VGLUT2$^{fl/fl}$ mice were deeply anesthetized with isoflurane and euthanized by decapitation. Brains were dissected, embedded in O.C.T. Compound (Tissue-Tek, prod. code 4583), and immediately frozen on dry ice and kept at -80 °C until sectioning. Brains were sectioned using a cryostat at approximately -18 °C onto RNAse-free Superfrost Plus microscope slides (Fisher Scientific, cat. no. 22-037-246) at 16 μm in the coronal plane.

Prior to hybridization, slides were fixed in prechilled 10% NBF for 45 minutes at 4 °C and subsequently dehydrated using a standard ethanol series. The slides were allowed to dry and then borders were drawn around the sections using a hydrophobic barrier pen. Slides were pretreated with hydrogen peroxide for 10 minutes followed by RNAscope Protease IV for 15 minutes before hybridization and signal detection steps.

To hybridize, about 150 uL of RNAscope probe mixture was applied to each slide and the slides were incubated at 40°C for 2 hours in a HybEZ oven, then washed with RNAscope wash buffer and stored overnight in 5× SSC. On the second day, amplification of each probe (AMP 1-2) was performed sequentially, incubating for 30 min at 40°C then rinsing in wash buffer after each Multiplex FL v2 Amp solution. Subsequently, the slides were developed using by incubating in RNAscope Multiplex FL v2 HRP-Cn for 15 min at 40°C, rinsing with wash buffer, incubating for 30 min at 40°C with TSA + Fluorescein (Akoya Biosciences, cat. no. SKU NEL741001KT), incubating in RNAscope Multiplex FL v2 HRP blocker for 15 min at 40°C, then rinsing once more with wash buffer. Finally, slides were counterstained with DAPI and coverslipped with ProLong Gold antifade mounting medium (ThermoFisher Scientific).

Single- and dual-label immunohistochemistry

Adult sexually naïve male and female *Pmch*-Cre;eGFP-L10a mice were deeply anesthetized with isoflurane and perfused with 10% formalin. Brains were dissected, postfixed for 2 hours in 10% formalin, and cryoprotected overnight using a solution of 20% sucrose in PBS. Coronal sections (30 μm thickness, 4 series) were collected with a freezing microtome and stored in a cryoprotectant solution (20% glycerol/30% ethylene glycol in DEPC-treated PBS) at −20°C.

Anti-NK3R and anti-AR with TSA Amplification

Brain sections were rinsed 3× in 0.1 M PBS to remove cryoprotectant solution, and in between each step.

Sections were blocked for 10 minutes in 0.3% H_2O_2 in ddH_2O, rinsed 3× in 0.1 M PBS, and subsequently blocked for 30 min in 0.1 M PBS + 0.25% TritonX-100 ("PBST") with 3% normal donkey serum (NDS). Next, sections were incubated overnight in PBST + 3% NDS with chicken anti-GFP (1:10,000, Aves Labs, AB_2307317) and either rabbit-anti NK3R (1:30,000, Novus Biologicals, NB300-102) or rabbit-anti AR (1:200; AbCam, ab133273).

Following primary antibody incubation, sections were incubated in anti-rabbit biotin in 0.1 M PBS for 1 h (1:500; Jackson ImmunoResearch Laboratories, 711-065-152), avidin-biotin complex (ABC) solution in 0.1 M PBS for 1 h (1:1000, Vector Laboratories), and biotinylated tyramide in 0.003% H_2O_2 in ddH_2O for 10 mins (1:250; Perkin Elmer). Finally, sections were incubated in 0.1 M PBS with secondary antisera (1:1000 goat anti-chicken conjugated to Alexa FluorTM 488, AB_2534096, and 1:1000 streptavidin-conjugated AlexaFluor 594, Thermo Fisher Scientific).

Sections were mounted onto gelatin-coated slides, air-dried, and coverslipped with Fluoromount G mounting medium (Electron Microscopy Sciences).

Analysis methods and generation of photomicrographs

Brain sections were imaged in an Axio Imager M2 microscope (Zeiss) except for 3D reconstructions of putative NKB-MCH synapses.

Anatomical tracing data was assembled according to the injection sites using the Allen brain atlas (mouse.brain-map.org) as a reference. Patterns of innervation were assessed in a comparative manner among (i) between male and female mice, and (ii) according to the number

of cells in each subpopulation of MCH neurons that took up the virus, with particular attention to areas related to sleep regulation and reproductive control. Morphology of projecting fibers was analyzed, and terminals defined at 40× or 63× magnification by the presence of varicosities and apparent synaptic bulbs.

Dual-labeled MCH neurons (e.g., NK3R) were quantified in 20× magnification using ImageJ with the Cell Counter plugin. Sexual dimorphisms in colocalization were defined using the student's *t* test (Welch's correction).

Results

MCH neurons of adult male and female mice do not express gonadal steroid receptors

Since numerous features of sleep are affected by biological sex and estrous cycle stage, it is plausible that MCH neurons could be directly regulated by gonadal hormones. Data in rats has found MCH to be coextensive, though not coexpressed, with ERα [55]. However, this has not been verified in mice. Additionally, *Pmch* expression was shown in rats to be increased by DHEA and DHT, though there is no documentation of whether MCH neurons themselves coexpress androgen receptor (AR) [2]. Finally, there is no literature on the expression of progesterone receptor (PGR) in MCH neurons or the ability of progesterone to act directly on MCH neurons. To determine whether this is the case, brain sections from adult male and female *Pmch*-iCre;eGFP-L10a mice were stained with antibodies against GFP and either ERα, AR, or PGR (Figure 6-1). No colocalization of Pmch-Cre;eGFP-L10a was observed with ERα, AR, or PGR in either sex, suggesting that if MCH neuron activity is modulated by sex steroids, this must occur indirectly.

Perifornical MCH neurons of male and female mouse coexpress NK3R

It has been previously shown in male rats and mice that a subpopulation of MCH neurons, mainly in the PFx, express NK3R [40, 41]. To determine whether this was also true in the female mouse brain, we stained sections from male and female *Pmch*-Cre;eGFP-L10a mice with antibodies against GFP and NK3R. We observed that, consistent with previous studies, approximately 50% of GFP+ neurons in the PFx and medial IHy express NK3R while only sparse NK3R is observed in LHA MCH neurons (Figure 6-2). No difference was observed between sexes.

KNDy fibers are in close apposition to PFx MCH neurons

NK3R is the primary receptor of NKB [56, 57]. Most neurons in the arcuate nucleus of the hypothalamus (ARH) express NKB as well as kisspeptin and dynorphin ("KNDy neurons") [58]. These neurons are potently regulated by estradiol via ERα [59, 60]. We sought to determine whether MCH+/NK3R+ neurons are innervated by KNDy neurons. Using antibodies against kisspeptin and silver nitrate/gold chloride amplification, we observed dense labeling of neuronal projections in male and female PFx where MCH/NK3R neurons are found (Figure 6-3A).

We next sought to determine whether NKB+ fibers form synaptic connections with MCH neurons. Using dual-label immunohistochemistry and confocal microscopy, we generated 3D reconstruction images which illustrate that NKB-ir fibers are in close proximity to MCH cells, appearing to synapse onto MCH perikarya and projections (Figure 6-3B).

MCH neurons of the PFx innervate sleep and reproductive control sites

We wondered whether distinct subpopulations of MCH neurons differentially innervate brain sites associated with the regulation of sleep and wakefulness. Specifically, we sought to determine whether PFx MCH neurons possess distinct and/or sexually dimorphic projection targets considering their distinct chemical identity. The Cre-dependent anterograde viral tracer AAV-ChR2-mCherry was used to map the anterograde projections of subpopulations of MCH neurons. Male and female *Pmch*-Cre mice were stereotaxically injected with ~50 nL of virus unilaterally into the hypothalamus. This virus has been successfully used previously to label anterograde projections [51]. The small injection volumes enabled the targeting of small subpopulations of MCH neurons.

Upon examination of the brains of these mice, we identified three regions of interest where MCH neuron fibers were abundant: the medial septum (MS) and adjacent diagonal band (NDB), and the lateral preoptic area (LPO), especially the ventrolateral LPO (VLPO). The MS, NDB, and VLPO are notable because all three of them have an established association with sleep. Lesion studies revealed that the loss of MS neurons reduces NREM sleep and increases REM sleep, and a similar effect is achieved by microinjection of endocannabinoid receptor agonists into the MS [61, 62]. On the other hand, microinjection of glutamate and endocannabinoid receptor antagonists into the MS reduces REM sleep [62, 63]. Granger causality analysis has since been used to demonstrate bidirectional interactions between the hippocampus and MS in the

generation of theta rhythms [64, 65]. Cholinergic neurons of the NDB are also associated with theta rhythm generation; many studies have demonstrated that the NDB and MS work together to this end and thus jointly have an important role in REM sleep [66, 67] (For additional review, see [68] and [69].) Finally, most neurons of the VLPO express the inhibitory neurotransmitters galanin and GABA; they are active during both NREM sleep and REM sleep, and their stimulation promotes sleep onset [70-73].

Interestingly, the density of projections in these three regions was observed to be highly variable by injection site, with the number of infected neurons in the PFx being the best predictor of projection density therein. Representative images of silver-labeled terminals in MS, NDB, and VLPO in male and female brains with injections in the PFx *vs* ZIm can be found in Figure 6-4. Analysis of the superior colliculus was used to confirm that the differences observed were not simply an overall increased abundance of labeled fibers in certain brains as compared to others (Figure 6-4). Thus, these brain regions constitute a group of significant sleep and reproductive control sites which are modulated by a very specific subpopulation of MCH neurons in the rostromedial PFx.

Subsets of PFx MCH neurons projects either to the MS/NDB or to VLPO

Having determined that medial MCH neurons, and in particular neurons of the PFx, send dense projections to MS/NDB and VLPO, our next question was whether individual neurons form connections to all of these regions, or whether PFx MCH neurons might be further subdivided into groups projecting preferentially to different regions of sleep/wakefulness regulation. To answer this question, different retrograde tracers were injected into the MS and VLPO of male and female *Pmch*-iCre;eGFP-L10a mice. Immunostaining was performed against MCH and MCH neurons were examined for colocalization of one or both of these tracers. Mice were stereotaxically injected with Fluorogold (FG) in the MS/NDB and cholera toxin, β subunit (Ctb) in the VLPO. Summaries of the injection sites can be found in Figure 6-5.

This experiment revealed virtually no colocalization of FG and Ctb in MCH neurons. In a given hypothalamic section, between 5 and 50% of Pmch-Cre;L10 neurons expressed Ctb depending on the size and precise location of the injection. Most colocalization was seen in the ZIm and PFx, but some was observed in the LHA and the more lateral parts of the ZI (Figure 6-6).

Interestingly, no colocalization was observed between MCH and FG. FG labeling in the hypothalamus was restricted to a dense cluster of small, round neurons in the tuberal hypothalamus located very close to the fornix (Figure 6-6D). Previous work in our lab has indicated that there is a dense population of PFx neurons with this distinctive morphology which express Cre, but not MCH peptide, in the adult *Pmch*-iCre mouse [74]. Based on the small size and round shape of the cells expressing both Pmch-Cre;L10 and FG, we wondered whether these cells belonged to the Cre+/MCH- population. Indeed, when GFP, rather than MCH, was observed, we found that while virtually no colocalization could be found between MCH- and FG-immunoreactivity, nearly all FG+ neurons in the PFx were also GFP+. We also examined the FG cells to quantify colocalization of Ctb. However, virtually no colocalization of the two tracers was observed even outside of MCH cells. Thus, it appears that there may be a population of PFx cells, some of which are MCH+ and some of which are MCH-, that can be further subdivided into subpopulations targeting the MS/NDB and the VLPO individually.

Optogenetic stimulation of *Kiss1*+ terminals in the PFx alters sleep in female mice in an estrogen- and time-of-day-dependent manner

Having determined that rostromedial MCH neurons of the PFx project to sleep and reproductive control sites and are also situated downstream of estrogen-responsive ARH KNDy neurons, we sought to assess the impact of activating this ARH KNDy neuron → MCH+/NK3R+ neuron circuit on sleep in varying sex steroid milieu. To that end, we implanted optical fibers in the PFx of *Kiss1*-Cre;ChR2-eYFP mice in order to optogenetically stimulate ARH KNDy neuron terminals apposing MCH neurons of the PFx. Cortical EEG electrodes were implanted in the skull to monitor sleep-wake state.

Optogenetic stimulation-induced activity was assessed using the immediate-early gene cFos as a proxy for neuronal activation [75, 76]. Triple-label fluorescent *in situ* hybridization was used to examine *Fos* mRNA expression in the PFx following 90 minutes of optogenetic stimulation. Since all NK3R+ neurons in the PFx are MCH neurons, *Tacr3* mRNA was used as a marker for our MCH neuron population of interest. Because not all ARH KNDy neuron terminals observed in the PFx appear to be in contact with MCH neurons, and there are also ORX/HCRT neurons in the PFx which could receive glutamatergic neurotransmission from ARH KNDy neurons to regulate sleep, we also used probes against *Hcrt* to determine whether *Fos* and *Hcrt* mRNA

colocalized following optogenetic stimulation. *Fos* was visible around the optical fiber implantation site, and the identification of the neurons in which *Fos* is expressed is in progress (Figure 6-7).

While these experiments are still in the pilot phase and thus meaningful statistical analysis cannot yet be performed, the data gathered thus far suggests that in OVX+E2 animals, sleep is reduced when ARH KNDy neurons in the PFx are stimulated in the dark phase. In particular, REM sleep time consistently decreases in OVX+E2 females with stimulation (Figure 6-8), though NREM sleep time is also reduced (Figure 6-9). A corresponding increase in total wake time with stimulation is also observed (Figure 6-10). Consistent effects are not observed on other measures such as average bout length and number of bouts, nor in the other experimental groups.

Discussion

In this study, we sought to determine whether (a) subpopulation(s) of MCH neurons facilitate the temporal relationship between sleep and the regulation of pituitary reproductive hormone secretion. No MCH neurons were found to express sex steroid hormone receptors, eliminating the possibility that a subpopulation of MCH neurons which responds directly to gonadal hormones is implicated in this coordination. However, we found that MCH neurons in the PFx are uniquely poised to coordinate this relationship because in both male and female mice, they project to key sleep and reproductive control sites (VLPO and MS/NDB, respectively), express NK3R, and appear to receive inputs from the ARH, which is a critical modulator of the neuroendocrine reproductive axis and provides an indirect means of sex steroid action on MCH neurons, as the ARH is responsive to and potently regulated by gonadal hormones.

We wondered whether a single population of MCH PFx cells projected to both the MS/NDB and the VLPO, or whether MCH neurons targeting these regions comprised distinct subpopulations within the PFx. When two different retrograde tracers, Ctb and FG, were injected into the VLPO and MS/NDB, respectively, we observed no colocalization of the Ctb and FG in MCH neurons, but we observed virtually no colocalization of FG and MCH immunoreactivity. This finding was at odds with the dense projections observed in the MS/NDB when anterograde tracers were injected into the PFx. However, previous work in our lab has shown that there is a population of Cre+ neurons in the PFx that is not MCH^+; these neurons likely express MCH at some point in development, but not in adulthood. For this reason, we performed the retrograde tracing

experiments in *Pmch*-Cre;eGFP-L10a mice and quantified dual- and triple-labeled cells using both Cre-induced GFP expression and MCH immunoreactivity. Indeed, dual-label FG-GFP cells were observed in the cluster of perifornical cells which we have reported to be Cre+/MCH- in the *Pmch*-Cre mouse.

These cells may express orexin/hypocretin (ORX/HCRT) in adulthood, as their location corresponds to the well-described localization of ORX/HCRT in mice and rats [77, 78]. Furthermore, PFx ORX/HCRT cells are known to send dense projections to the locus coeruleus; the suprachiasmatic nucleus; the septal nuclei, especially the medial septum; and the NDB [77]. Notably, long, thick projections from ORX/HCRT with numerous boutons indicating dense synaptic connections have been documented in the ARH, suggesting that perhaps there is bidirectional communication between this population of PFx cells and KNDy neurons of the ARH [77]. Collectively, these data demonstrate a high likelihood that this cluster of PFx cells is of critical importance to the dual regulation of sleep and the neuroendocrine reproductive axis. Whether the key neuropeptide defining this population is ORX/HCRT or MCH requires further evaluation.

The role of MCH-expressing neurons, at least based on our anatomical tracing data, appears to be more relevant to sleep, as many MCH+ neurons were confirmed using Ctb to innervate the LPO/VLPO, which is less densely innervated by ORX/HCRT neurons of the PFx [77]. More direct action on the HPG axis, via connections both to GnRH neurons themselves in the MS/NDB and to KNDy neurons in the ARH, could originate from either MCH or ORX/HCRT neurons as discussed above and requires additional study.

Nonetheless, the apparent potential ARH KNDy neurons to communicate with MCH neurons via NKB signaling at NK3R still seemed to indicate some ability for the HPG axis to modulate MCH neuron activity. This could constitute a mechanism by which biological sex and circulating gonadal hormones might alter various features of sleep quality and sleep architecture. Since NKB expression is suppressed by estradiol and sleep is more fragmented and reduced overall in high-estradiol conditions, we predicted that NKB excites MCH neurons and is sleep promoting, and this action is reduced when estrogens are high [79]. We hypothesized that activation of NKB terminals in apposition to MCH neurons would be sleep-promoting.

Using mice with channelrhodopsin expressed in KNDy neurons, we optogenetically stimulated KNDy terminals and evaluated changes to sleep, spontaneous activity, and food and water intake in both sexes and in females under distinct gonadal steroid milieu. While Fos activation is observed at the optical fiber implantation site in all mice, male mice and female mice under low estradiol conditions were largely unresponsive to stimulation. However, females supplemented with exogenous estradiol exhibited reduced time in both REM and NREM sleep and increased time spent awake during the dark phase.

It is important to note that while in adult male mice, KNDy neurons are the only sites of kisspeptin expression, in the female, there is an additional site of kisspeptin expression: the anteroventral periventricular area (AVPV) [80]. This makes kisspeptin immunoreactivity an incomplete method of evaluating whether ARH KNDy neurons definitively project to MCH neurons in the female mouse brain. While it seems likely that at least some of the NKB+ fibers in the PFx of the female mouse do originate from the ARH, as they do in the male, it is possible that in females there is an additional contribution from the AVPV. These cells may have distinct projection targets and explain some of the difference between male and female responses to our optogenetic manipulation.

Overall, it seems that other contextual factors, perhaps including global gene expression changes induced by estradiol, may play a role in the ability of KNDy neuron activation to affect changes in sleep. Alternately, our experimental paradigm may not have been optimized to reveal a modulatory, rather than a directly stimulatory, role for KNDy neurons in sleep regulation. For instance, clearer effects may be revealed under circumstances of high sleep pressure (i.e., sleep deprived mice). Collectively, our findings suggest an estradiol-dependent role for KNDy neurons in the regulation of sleep in female mice, though the mechanistic underpinnings and relevant neuronal targets therein remain unclear. Further work is necessary to unravel the mechanisms integrating gonadal steroids and sleep.

Acknowledgements

Special thanks to Christian Burgess and Katherine Furman for lending time, expertise, lab space, and equipment/reagents for optogenetics experiments, and to Emily Henson for performing the RNAscope experiments for this study.

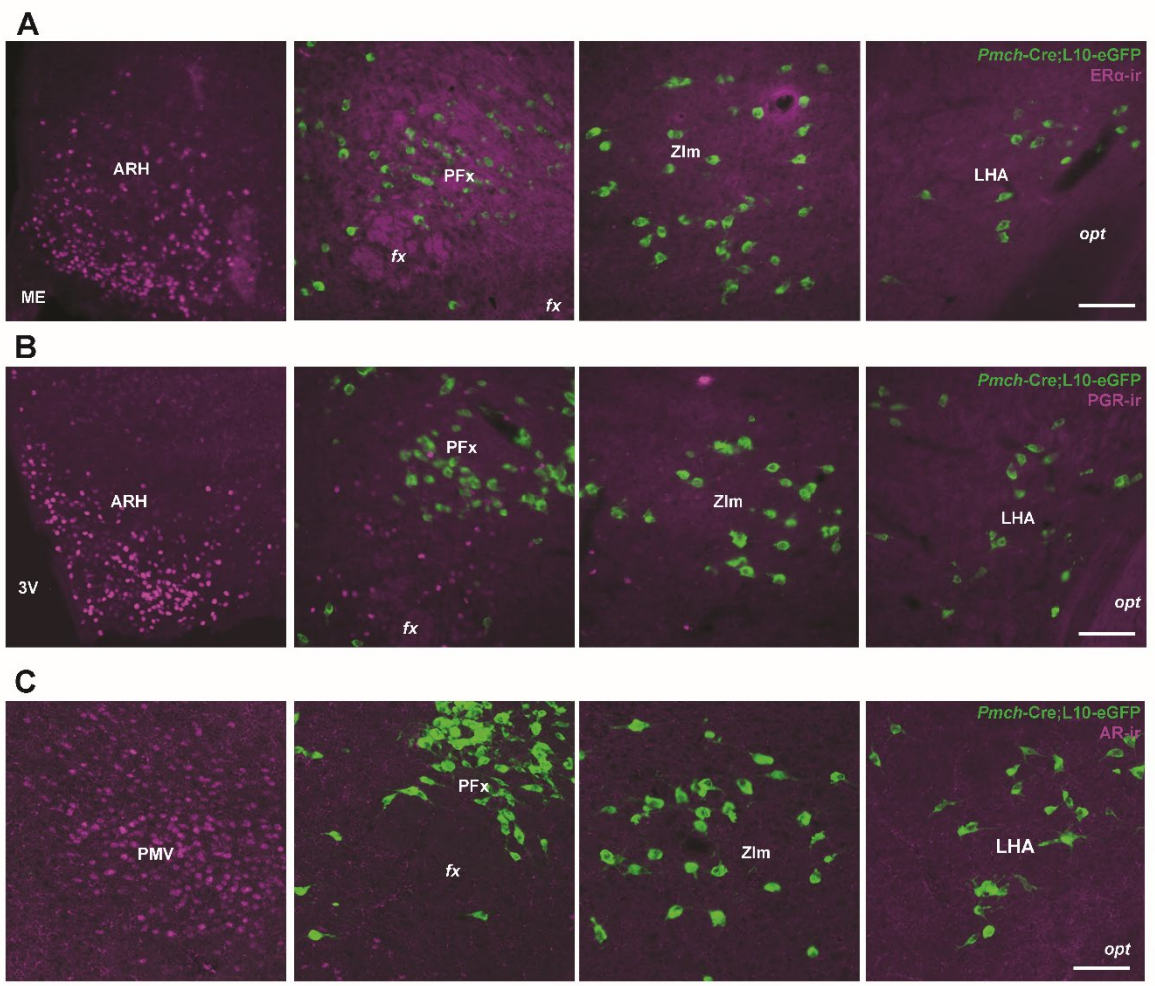

Figure 6-1: MCH neurons do not colocalize gonadal hormone receptors. *(A)* Anti-ERα staining in the brain of adult male and female *Pmch*-iCre;eGFP-L10a mice shows no colocalization of ERα (magenta) with MCH-driven reporter expression (green) in LHA, PFx, or ZIm. Both rostral (top) and caudal (bottom) levels of the PFx are shown. Images shown are from the female brain. *(B)* Anti-PGR staining in the brain of adult male and female *Pmch*-iCre;eGFP-L10a mice shows no colocalization of PGR (magenta) with MCH-driven reporter expression (green) in LHA, PFx, or ZIm. Both rostral (top) and caudal (bottom) levels of the PFx are shown. Images shown are from the female brain. *(C)* Anti-AR staining in the brain of adult male and female *Pmch*-iCre;eGFP-L10a mice shows no colocalization of AR (magenta) with MCH-driven reporter expression (green) in LHA, PFx, or ZIm. Both rostral (top) and caudal (bottom) levels of the PFx are shown. Images shown are from the male brain for AR and the female brain for ERα and PGR. No colocalization is observed in either sex.
Scale bar=100μm. *Abbreviations: ARH=arcuate nucleus of the hypothalamus, fx=fornix, LHA=lateral hypothalamic area, PFx=perifornical area, VMH=ventromedial hypothalamic nucleus, ZIm=zona incerta, medial part.*

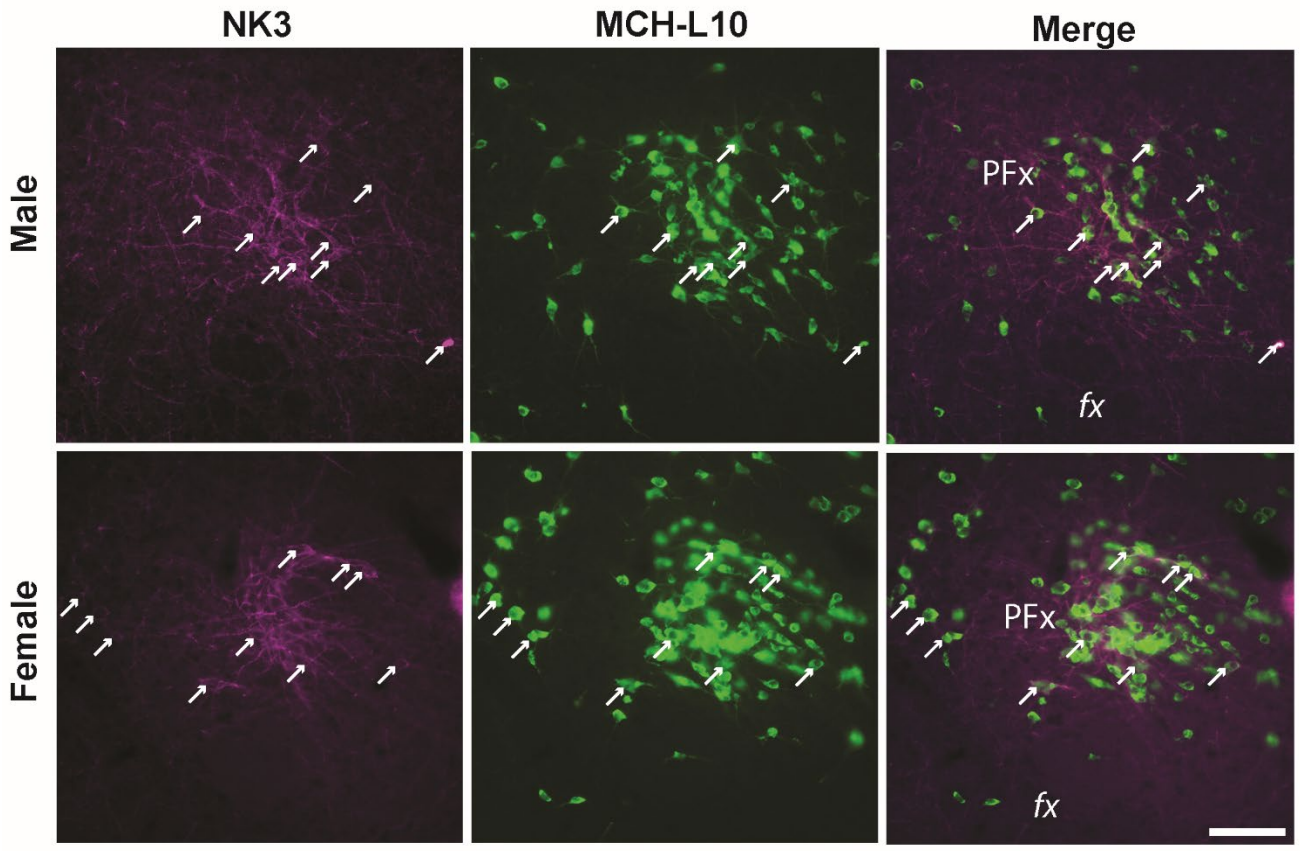

Figure 6-2: A subset of MCH neurons expresses NK3R in both males and females. NK3R (magenta) and Pmch-Cre;L10 in the brains of adult male (top) and female (bottom) *Pmch*-iCre;eGFP-L10a mice. Arrows indicate double-labeled cells. Scale bar=100µm. *Abbreviations: fx=fornix, PFx=perifornical area.*

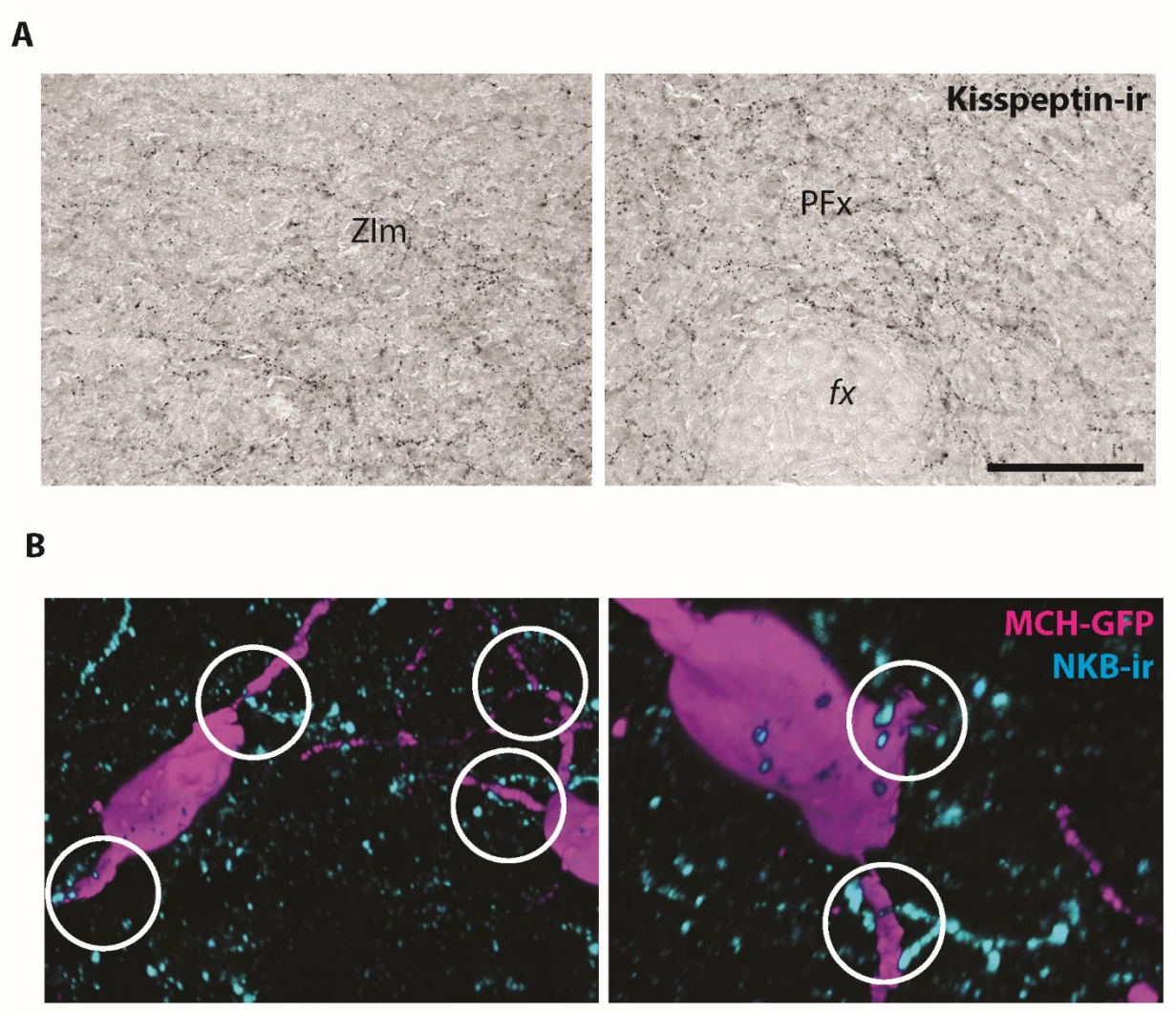

Figure 6-3: MCH neurons are innervated by KNDy neurons. *(A)* Immunostaining for kisspeptin in the male brain reveals projections in the ZIm and PFx, where MCH neuron cell bodies are found. *(B)* 3D reconstruction image of MCH- (magenta) and NKB- (cyan) labeled cells reveals close appositions between NKB+ fibers and MCH axons and perikarya.
Scale bar=100µm. *Abbreviations: fx=fornix, LHA=lateral hypothalamic area, PFx=perifornical area, ZIm=zona incerta, medial part.*

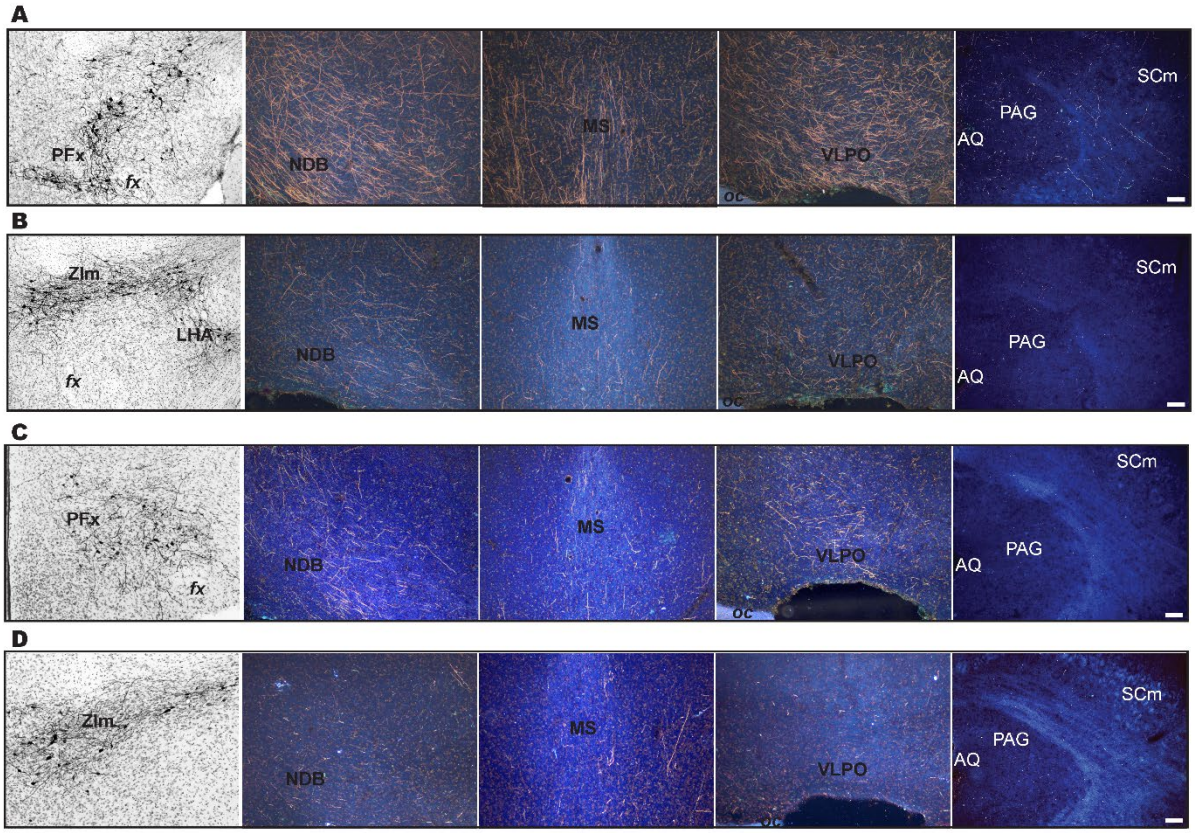

Figure 6-4: MCH neurons in the PFx project to sleep and reproductive control sites. Representative images of AAV-ChR2-mCherry injection sites and resulting visualization of neuron terminals in key brain regions (medial septum, nucleus of the diagonal band, ventrolateral preoptic area) and control regions (periaqueductal gray, superior colliculus [motor related[) of *Pmch*-Cre male (A, B) and female (C, D) mice. (A) Male mouse, PFx injection (170/175 of infected cells in PFx). Note dense projections in MS, NDB, and VLPO. (B) Male mouse, ZIm/LHA injection (20/209 of infected cells in PFx). Note relative lack of labeled terminals in MS, NDB, and VLPO. (C) Female mouse, PFx injection (53/86 of infected cells in PFx). Note terminals in MS, NDB, and VLPO. (D) Female mouse, ZIm injection (5/115 of infected cells in PFx). Note relative lack of labeled terminals in MS, NDB, and VLPO.
Scale bar=100µm. *Abbreviations: AQ=cerebral aqueduct, fx=fornix, LHA=lateral hypothalamic area, MS=medial septum, NDB=diagonal band nucleus, oc=optic chiasm, PAG=periaqueductal gray, PFx=perifornical area, SCm=superior colliculus, motor related, VLPO=ventrolateral preoptic area, ZIm=zona incerta, medial part.*

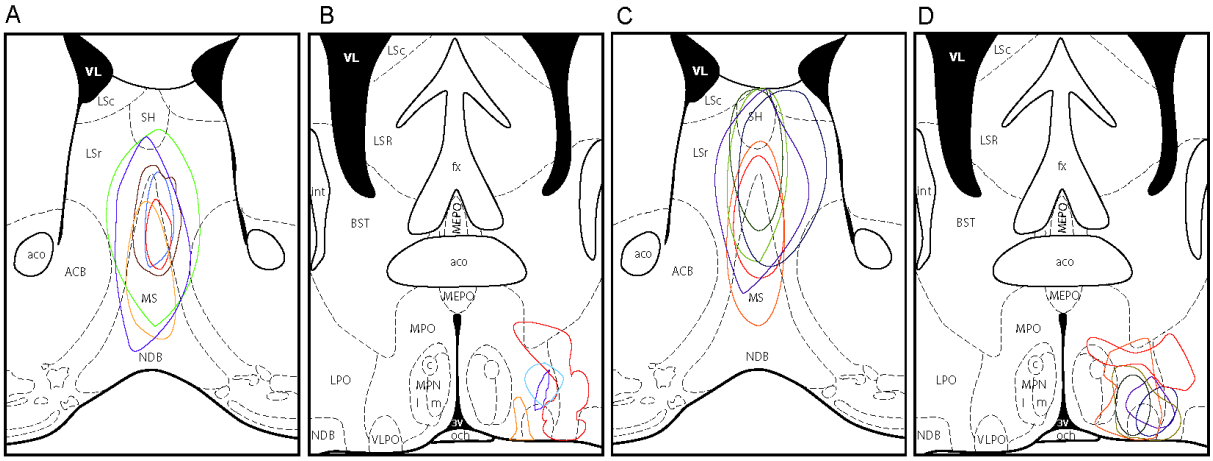

Figure 6-5: Summary of retrograde tracer injection sites in the MS/NDB and VLPO. For the same sex, outlines in the same color represent injections in the same mouse. (A) Sites of fluorogold (FG) injection into the medial septum/diagonal band nucleus (MS/NDB) in the male mouse. (B) Sites of Ctb injection into the VLPO in the male mouse. (C) Sites of FG injection into the MS/NDB in the female mouse. (D) Sites of Ctb injection into the VLPO in the female mouse.
Abbreviations: ACB=nucleus accumbens, aco=anterior commissure, BST=bed nucleus of the stria terminalis, fx=fornix, int=internal capsule, LPO=lateral preoptic area, LSc=lateral septum, caudal part, LSr=lateral septum, rostral part, MEPO=median preoptic nucleus, MPN=medial preoptic nucleus, MPO=medial preoptic area, MS=medial septum, NDB=diagonal band nucleus, och=optic chiasm, SH=septohippocampal nucleus, VL=lateral ventricle, VLPO=ventrolateral preoptic area

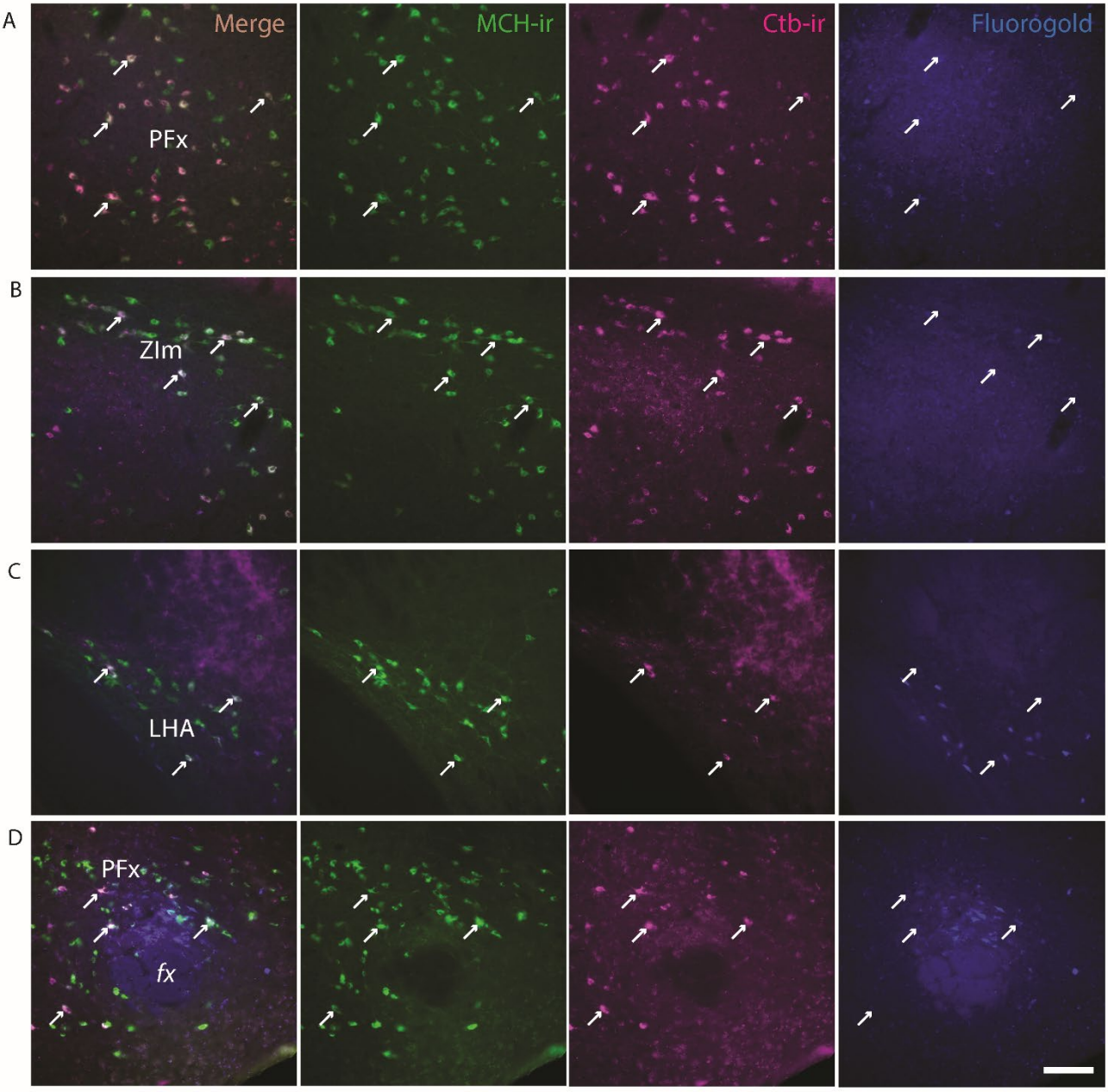

Figure 6-6: Medial septum/diagonal band nucleus- and ventrolateral preoptic area-projecting MCH neurons comprise distinct subpopulations of the PFx. Representative images of anti-MCH, -FG, and -Ctb immunostaining in the adult mouse brain following injection of the retrograde tracers FG into the MS/NDB and Ctb into the VLPO. Images shown are from a female brain; no differences were observed between male and female brains. Note the absence of triple-labeled cells, the presence of Ctb/MCH dual labeled cells, the absence of FG/MCH dual labeled cells, and the localization of FG staining directly anterior to the fornix.
Scale bar=100µm. *Abbreviations: fx=fornix, LHA=lateral hypothalamic area, PFx=perifornical area, ZIm=zona incerta, medial part.*

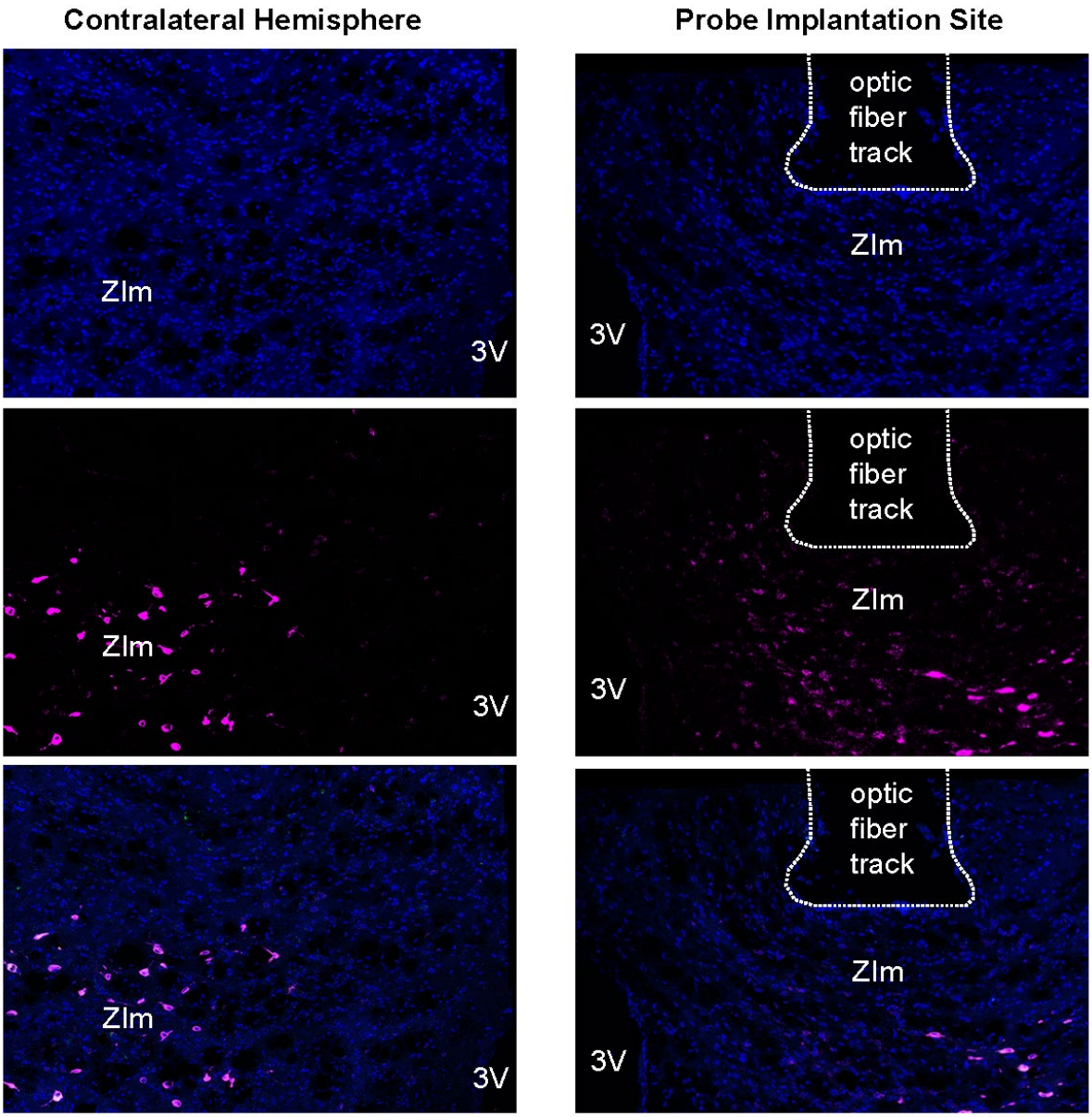

Figure 6-7: Optogenetic stimulation in the PFx of *Kiss1*-Cre;ChR2-eYFP mice induces *Fos* mRNA expression. *(A)* Fluorescent *in situ* hybridization labeling *Fos* (green), *Tacr3* (magenta), and *Hcrt* (white) at the optical fiber implantation site following 2 hours of optogenetic stimulation. *(B)* Fluorescent *in situ* hybridization labeling *Fos* (green), *Tacr3* (magenta), and *Hcrt* (white) at the level of the optical fiber implantation site in the contralateral hemisphere following 2 hours of optogenetic stimulation. Note the elevated *Fos* expression on the side of the optical fiber site and the absence of colocalization with either *Tacr3* or *Hcrt.*
Scale bar=100µm. *Abbreviations: fx=fornix, LHA=lateral hypothalamic area, PFx=perifornical area, ZIm=zona incerta, medial part, 3V=third ventricle.*

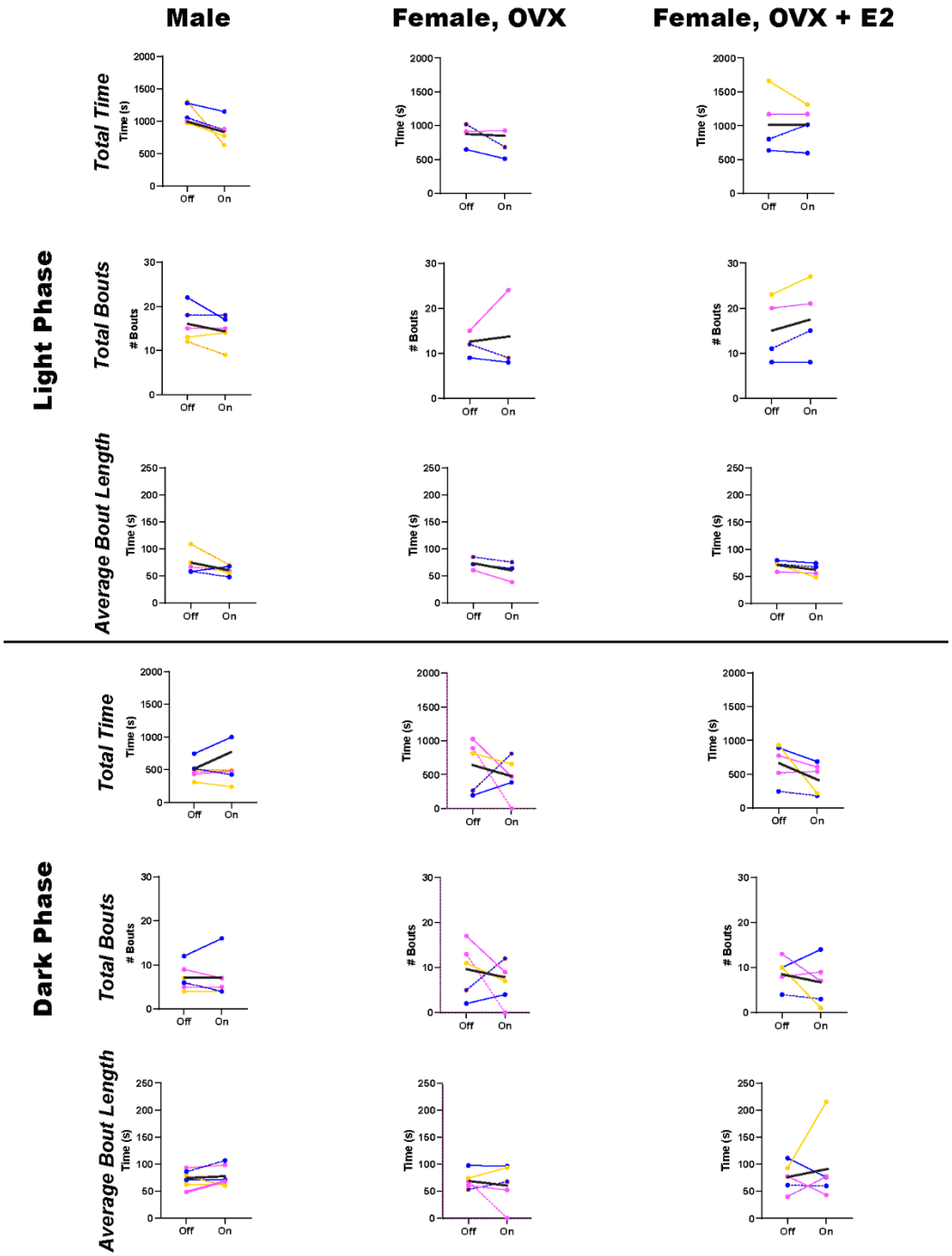

Figure 6-8: Optogenetic stimulation in the PFx of *Kiss1*-Cre;ChR2-eYFP mice decreases time spent in REM sleep in OVX+E2 mice. EEG activity was recorded for 4 hours in both the light and dark phases with and without optogenetic stimulation in a randomized crossover design such that each animal served as its own control. Note that female mice were recorded first following ovariectomy (OVX condition) and subsequently following the implantation of an estradiol implant (OVX+E2 condition) such that individual females may also be compared between estradiol conditions. Yellow lines represent animals in which the center of the optical fiber targeted the tuberal LHA. Pink lines represent animals in which the center of the optical fiber targeted the ZIm. Blue lines represent animals in which the center of the optical fiber targeted the posterior LHA. No clear difference is apparent based on subtle variation in implantation sites. No robust effects of stimulation are observed, but note that OVX+E2 mice largely trend towards reduced total time in REM with stimulation on.

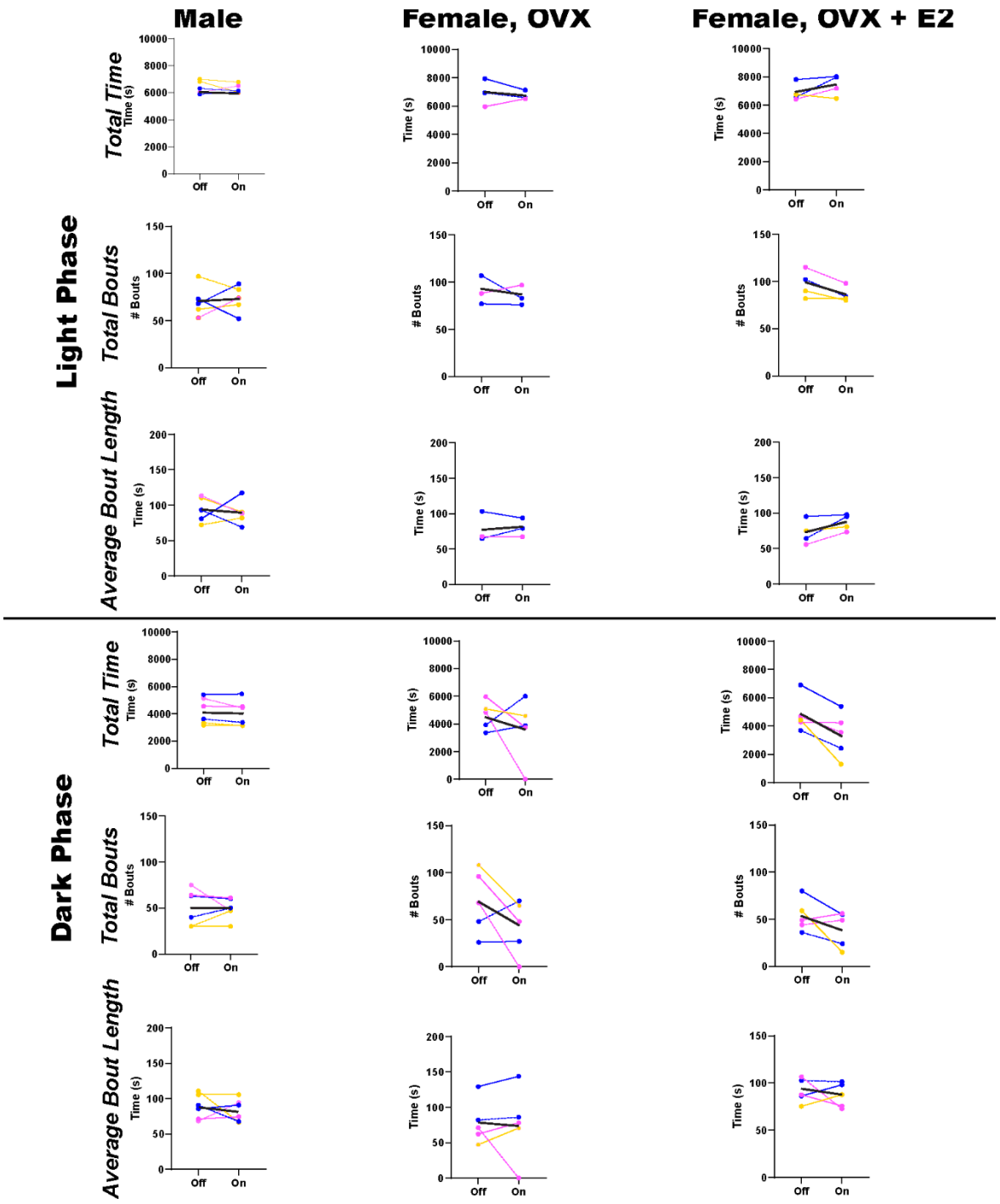

Figure 6-9: Optogenetic stimulation in the PFx of *Kiss1*-Cre;ChR2-eYFP mice decreases time spent in NREM sleep in OVX+E2 mice. EEG activity was recorded for 4 hours in both the light and dark phases with and without optogenetic stimulation in a randomized crossover design such that each animal served as its own control. Note that female mice were recorded first following ovariectomy (OVX condition) and subsequently following the implantation of an estradiol implant (OVX+E2 condition) such that individual females may also be compared between estradiol conditions. Yellow lines represent animals in which the center of the optical fiber targeted the tuberal LHA. Pink lines represent animals in which the center of the optical fiber targeted the ZIm. Blue lines represent animals in which the center of the optical fiber targeted the posterior LHA. No clear difference is apparent based on subtle variation in implantation sites. No robust effects of stimulation are observed, but note that OVX+E2 mice largely trend towards reduced total time in NREM with stimulation on.

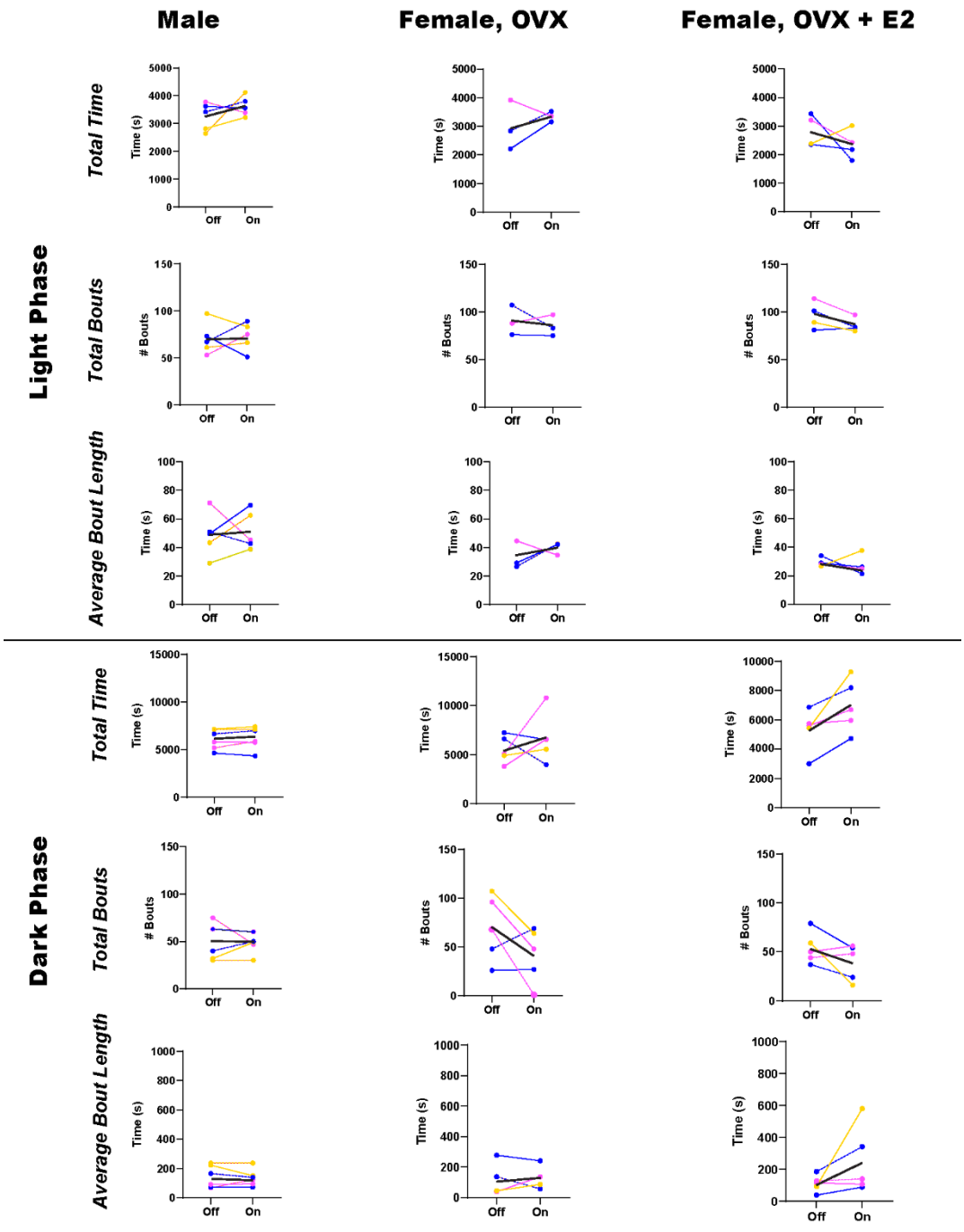

Figure 6-10: Optogenetic stimulation in the PFx of *Kiss1*-Cre;ChR2-eYFP mice increases total wake time in OVX+E2 mice. EEG activity was recorded for 4 hours in both the light and dark phases with and without optogenetic stimulation in a randomized crossover design such that each animal served as its own control. Note that female mice were recorded first following ovariectomy (OVX condition) and subsequently following the implantation of an estradiol implant (OVX+E2 condition) such that individual females may also be compared between estradiol conditions. Yellow lines represent animals in which the center of the optical fiber targeted the tuberal LHA. Pink lines represent animals in which the center of the optical fiber targeted the ZIm. Blue lines represent animals in which the center of the optical fiber targeted the posterior LHA. No clear difference is apparent based on subtle variation in implantation sites. No robust effects of stimulation are observed, but note that OVX+E2 mice largely trend towards increased total time spent awake with stimulation on.

References

1. Maquet, P., *The role of sleep in learning and memory.* Science, 2001. **294**(5544): p. 1048-52.
2. Schmidt, M.H., *The energy allocation function of sleep: a unifying theory of sleep, torpor, and continuous wakefulness.* Neurosci Biobehav Rev, 2014. **47**: p. 122-53.
3. Yamada, R.G. and H.R. Ueda, *Molecular Mechanisms of REM Sleep.* Front Neurosci, 2019. **13**: p. 1402.
4. Malik, D.M., et al., *Circadian and Sleep Metabolomics Across Species.* J Mol Biol, 2020. **432**(12): p. 3578-3610.
5. Siegel, J.M., *Clues to the functions of mammalian sleep.* Nature, 2005. **437**(7063): p. 1264-71.
6. Saper, C.B., et al., *Sleep state switching.* Neuron, 2010. **68**(6): p. 1023-42.
7. Mong, J.A. and D.M. Cusmano, *Sex differences in sleep: impact of biological sex and sex steroids.* Philos Trans R Soc Lond B Biol Sci, 2016. **371**(1688): p. 20150110.
8. Mong, J.A., et al., *Sleep, rhythms, and the endocrine brain: influence of sex and gonadal hormones.* J Neurosci, 2011. **31**(45): p. 16107-16.
9. Baker, F.C. and H.S. Driver, *Self-reported sleep across the menstrual cycle in young, healthy women.* J Psychosom Res, 2004. **56**(2): p. 239-43.
10. Aan Het Rot, M., et al., *Premenstrual mood and empathy after a single light therapy session.* Psychiatry Res, 2017. **256**: p. 212-218.
11. Krasnik, C., et al., *The effect of bright light therapy on depression associated with premenstrual dysphoric disorder.* Am J Obstet Gynecol, 2005. **193**(3 Pt 1): p. 658-61.
12. Colvin, G.B., et al., *Changes in sleep-wakefulness in female rats during circadian and estrous cycles.* Brain Res, 1968. **7**(2): p. 173-81.
13. Swift, K.M., et al., *Sex differences within sleep in gonadally intact rats.* Sleep, 2020. **43**(5).
14. Baker, F.C. and H.S. Driver, *Circadian rhythms, sleep, and the menstrual cycle.* Sleep Med, 2007. **8**(6): p. 613-22.
15. De Gennaro, L. and M. Ferrara, *Sleep spindles: an overview.* Sleep Med Rev, 2003. **7**(5): p. 423-40.
16. Tamminen, J., et al., *Sleep spindle activity is associated with the integration of new memories and existing knowledge.* J Neurosci, 2010. **30**(43): p. 14356-60.
17. Bittencourt, J., et al., *The melanin-concentrating hormone system of the rat brain: an immuno-and hybridization histochemical characterization.* Journal of Comparative Neurology, 1992. **319**(2): p. 218-245.
18. Sita, L., C. Elias, and J. Bittencourt, *Connectivity pattern suggests that incerto-hypothalamic area belongs to the medial hypothalamic system.* 2007. **148**: p. 949-69.
19. Elias, C.F., et al., *Chemically defined projections linking the mediobasal hypothalamus and the lateral hypothalamic area.* J Comp Neurol, 1998. **402**(4): p. 442-59.
20. Hassani, O., M. Gee Lee, and B. Jones, *Melanin-concentrating hormone neurons discharge in a reciprocal manner to orexin neurons across the sleep-wake cycle.* 2009. **106**: p. 2418-2422.
21. Verret, L., et al., *A role of melanin-concentrating hormone producing neurons in the central regulation of paradoxical sleep.* BMC Neurosci, 2003. **4**: p. 19.
22. Jego, S., et al., *Optogenetic identification of a rapid eye movement sleep modulatory circuit in the hypothalamus.* 2013. **16**.

23. Konadhode, R., et al., *Optogenetic Stimulation of MCH Neurons Increases Sleep.* 2013. **33**: p. 10257-63.
24. Tsunematsu, T., et al., *Optogenetic Manipulation of Activity and Temporally Controlled Cell-Specific Ablation Reveal a Role for MCH Neurons in Sleep/Wake Regulation.* 2014. **34**: p. 6896-909.
25. Blanco-Centurion, C., et al., *Dynamic Network Activation of Hypothalamic MCH Neurons in REM Sleep and Exploratory Behavior.* The Journal of Neuroscience, 2019: p. 0305-19.
26. Attademo, A.M., et al., *Neuropeptide Glutamic Acid-Isoleucine May Induce Luteinizing Hormone Secretion via Multiple Pathways.* Neuroendocrinology, 2006. **83**(5-6): p. 313-24.
27. G.P. Gallardo, M., S. R. Chiocchio, and J. H. Tramezzani, *Changes of melanin-concentrating hormone related to LHRH release in the median eminence of rats.* 2005. **1030**: p. 152-8.
28. Murray, J., et al., *Evidence for a Stimulatory Action of Melanin-Concentrating Hormone on Luteinising Hormone Release Involving MCH1 and Melanocortin-5 Receptors.* 2006. **18**: p. 157-67.
29. S Williamson-Hughes, P., K. Grove, and M.S. Smith, *Melanin concentrating hormone (MCH): A novel neural pathway for regulation of GnRH neurons.* 2005. **1041**: p. 117-24.
30. Skrapits, K., et al., *Lateral hypothalamic orexin and melanin-concentrating hormone neurons provide direct input to gonadotropin-releasing hormone neurons in the human.* Front Cell Neurosci, 2015. **9**: p. 348.
31. Wu, M., et al., *Melanin-concentrating hormone directly inhibits GnRH neurons and blocks kisspeptin activation, linking energy balance to reproduction.* Proc Natl Acad Sci U S A, 2009. **106**(40): p. 17217-22.
32. MacKenzie, F., M. James, and C. Wilson, *Changes in dopamine activity in the zona incerta (ZI) over the rat oestrous cycle and the effect of lesions of the ZI on cyclicity: further evidence that the incerto-hypothalamic tract has a stimulatory role in the control of LH release.* Brain Research, 1988. **444**: p. 75-78.
33. Dumalska, I., et al., *Excitatory effects of the puberty-initiating peptide kisspeptin and group I metabotropic glutamate receptor agonists differentiate two distinct subpopulations of gonadotropin-releasing hormone neurons.* J Neurosci, 2008. **28**(32): p. 8003-13.
34. Gonzalez, M., B. Baker, and C. Wilson, *Stimulatory effect of melanin-concentrating hormone on luteinising hormone release.* Neuroendocrinology, 1997. **66**: p. 254-262.
35. Tsukamura, H., et al., *Intracerebroventricular administration of melanin-concentrating hormone suppresses pulsatile luteinizing hormone release in the female rat.* J Neuroendocrinol, 2000. **12**(6): p. 529-34.
36. Croizier, S., et al., *Development of posterior hypothalamic neurons enlightens a switch in the prosencephalic basic plan.* PLoS One, 2011. **6**(12): p. e28574.
37. Cvetkovic, V., et al., *Characterization of subpopulations of neurons producing melanin-concentrating hormone in the rat ventral diencephalon.* J Neurochem, 2004. **91**(4): p. 911-9.
38. Koehl, M., S.E. Battle, and F.W. Turek, *Sleep in female mice: a strain comparison across the estrous cycle.* Sleep, 2003. **26**(3): p. 267-72.

39. Croizier, S., et al., *A comparative analysis shows morphofunctional differences between the rat and mouse melanin-concentrating hormone systems.* PLoS One, 2010. **5**(11): p. e15471.
40. Brischoux, F., et al., *Time of genesis determines projection and neurokinin-3 expression patterns of diencephalic neurons containing melanin-concentrating hormone.* Eur J Neurosci, 2002. **16**(9): p. 1672-80.
41. Fujita, A., et al., *Neurokinin B-Expressing Neurons of the Central Extended Amygdala Mediate Inhibitory Synaptic Input onto Melanin-Concentrating Hormone Neuron Subpopulations.* J Neurosci, 2021. **41**(46): p. 9539-9560.
42. Navarro, V.M., et al., *Regulation of gonadotropin-releasing hormone secretion by kisspeptin/dynorphin/neurokinin B neurons in the arcuate nucleus of the mouse.* J Neurosci, 2009. **29**(38): p. 11859-66.
43. Guran, T., et al., *Hypogonadotropic hypogonadism due to a novel missense mutation in the first extracellular loop of the neurokinin B receptor.* J Clin Endocrinol Metab, 2009. **94**(10): p. 3633-3639.
44. Brioude, F., C.E. Bouvattier, and M. Lombès, *[Hypogonadotropic hypogonadism: new aspects in the regulation of hypothalamic-pituitary-gonadal axis].* Ann Endocrinol (Paris), 2010. **71 Suppl 1**: p. S33-41.
45. Rance, N.E., et al., *Neurokinin B and the hypothalamic regulation of reproduction.* Brain Res, 2010. **1364**: p. 116-28.
46. Semple, R.K. and A.K. Topaloglu, *The recent genetics of hypogonadotrophic hypogonadism - novel insights and new questions.* Clin Endocrinol (Oxf), 2010. **72**(4): p. 427-35.
47. Topaloglu, A.K. and L.D. Kotan, *Molecular causes of hypogonadotropic hypogonadism.* Curr Opin Obstet Gynecol, 2010. **22**(4): p. 264-70.
48. Regoli, D., A. Boudon, and J.L. Fauchére, *Receptors and antagonists for substance P and related peptides.* Pharmacol Rev, 1994. **46**(4): p. 551-99.
49. Donato, J., et al., *Leptin's effect on puberty in mice is relayed by the ventral premammillary nucleus and does not require signaling in Kiss1 neurons.* J Clin Invest, 2011. **121**(1): p. 355-68.
50. Mahany, E.B., et al., *Obesity and High-Fat Diet Induce Distinct Changes in Placental Gene Expression and Pregnancy Outcome.* Endocrinology, 2018. **159**(4): p. 1718-1733.
51. Sarnaik, R. and I.M. Raman, *Control of voluntary and optogenetically perturbed locomotion by spike rate and timing of neurons of the mouse cerebellar nuclei.* Elife, 2018. **7**.
52. Idris, A.I., *Ovariectomy/Orchidectomy in Rodents*, in *Bone Research Protocols*, M.H. Helfrich and S.H. Ralston, Editors. 2012, Humana Press: Totowa, NJ. p. 545-551.
53. Silveira, M.A., et al., *GnRH Neuron Activity and Pituitary Response in Estradiol-Induced vs Proestrous Luteinizing Hormone Surges in Female Mice.* Endocrinology, 2017. **158**(2): p. 356-366.
54. Barger, Z., et al., *Robust, automated sleep scoring by a compact neural network with distributional shift correction.* PLoS One, 2019. **14**(12): p. e0224642.
55. Muschamp, J.W. and E.M. Hull, *Melanin concentrating hormone and estrogen receptor-alpha are coexstensive but not coexpressed in cells of male rat hypothalamus.* Neurosci Lett, 2007. **427**(3): p. 123-6.

56. Hershey, A.D. and J.E. Krause, *Molecular characterization of a functional cDNA encoding the rat substance P receptor.* Science, 1990. **247**(4945): p. 958-62.
57. Nakanishi, S., *Mammalian tachykinin receptors.* Annu Rev Neurosci, 1991. **14**: p. 123-36.
58. Lehman, M.N., L.M. Coolen, and R.L. Goodman, *Minireview: kisspeptin/neurokinin B/dynorphin (KNDy) cells of the arcuate nucleus: a central node in the control of gonadotropin-releasing hormone secretion.* Endocrinology, 2010. **151**(8): p. 3479-89.
59. Clarkson, J., et al., *Kisspeptin-GPR54 signaling is essential for preovulatory gonadotropin-releasing hormone neuron activation and the luteinizing hormone surge.* J Neurosci, 2008. **28**(35): p. 8691-7.
60. Smith, J.T., et al., *Kiss1 neurons in the forebrain as central processors for generating the preovulatory luteinizing hormone surge.* J Neurosci, 2006. **26**(25): p. 6687-94.
61. Srividya, R., H.N. Mallick, and V.M. Kumar, *Sleep changes produced by destruction of medial septal neurons in rats.* Neuroreport, 2004. **15**(11): p. 1831-5.
62. Puskar, P., et al., *Changes in sleep-wake cycle after microinjection of agonist and antagonist of endocannabinoid receptors at the medial septum of rats.* Physiol Behav, 2021. **237**: p. 113448.
63. Mukherjee, D., et al., *Glutamate microinjection in the medial septum of rats decreases paradoxical sleep and increases slow wave sleep.* Neuroreport, 2012. **23**(7): p. 451-6.
64. Kang, D., et al., *Theta-rhythmic drive between medial septum and hippocampus in slow-wave sleep and microarousal: a Granger causality analysis.* J Neurophysiol, 2015. **114**(5): p. 2797-803.
65. Kang, D., et al., *Reciprocal Interactions between Medial Septum and Hippocampus in Theta Generation: Granger Causality Decomposition of Mixed Spike-Field Recordings.* Front Neuroanat, 2017. **11**: p. 120.
66. PETSCHE, H., C. STUMPF, and G. GOGOLAK, *[The significance of the rabbit's septum as a relay station between the midbrain and the hippocampus. I. The control of hippocampus arousal activity by the septum cells].* Electroencephalogr Clin Neurophysiol, 1962. **14**: p. 202-11.
67. Desikan, S., et al., *Target selectivity of septal cholinergic neurons in the medial and lateral entorhinal cortex.* Proc Natl Acad Sci U S A, 2018. **115**(11): p. E2644-E2652.
68. Buzsáki, G., *Theta oscillations in the hippocampus.* Neuron, 2002. **33**(3): p. 325-340.
69. Nuñez, A. and W. Buño, *The Theta Rhythm of the Hippocampus: From Neuronal and Circuit Mechanisms to Behavior.* Front Cell Neurosci, 2021. **15**: p. 649262.
70. Alam, M.N., et al., *Adenosinergic modulation of rat basal forebrain neurons during sleep and waking: neuronal recording with microdialysis.* J Physiol, 1999. **521 Pt 3**: p. 679-90.
71. Sherin, J.E., et al., *Innervation of histaminergic tuberomammillary neurons by GABAergic and galaninergic neurons in the ventrolateral preoptic nucleus of the rat.* J Neurosci, 1998. **18**(12): p. 4705-21.
72. Gong, H., et al., *Activation of c-fos in GABAergic neurones in the preoptic area during sleep and in response to sleep deprivation.* J Physiol, 2004. **556**(Pt 3): p. 935-46.
73. Yang, Q.Z. and G.I. Hatton, *Electrophysiology of excitatory and inhibitory afferents to rat histaminergic tuberomammillary nucleus neurons from hypothalamic and forebrain sites.* Brain Res, 1997. **773**(1-2): p. 162-72.
74. Beekly, B.G., et al., *Dissociated Pmch and Cre Expression in Lactating Pmch-Cre BAC Transgenic Mice.* Frontiers in Neuroanatomy, 2020. **14**(60).

75. Novak, C.M., L. Smale, and A.A. Nunez, *Rhythms in Fos expression in brain areas related to the sleep-wake cycle in the diurnal Arvicanthis niloticus.* Am J Physiol Regul Integr Comp Physiol, 2000. **278**(5): p. R1267-74.
76. Kovács, K.J., *Measurement of immediate-early gene activation- c-fos and beyond.* J Neuroendocrinol, 2008. **20**(6): p. 665-72.
77. Peyron, C., et al., *Neurons containing hypocretin (orexin) project to multiple neuronal systems.* J Neurosci, 1998. **18**(23): p. 9996-10015.
78. Yamanaka, A., et al., *Hypothalamic orexin neurons regulate arousal according to energy balance in mice.* Neuron, 2003. **38**(5): p. 701-13.
79. Yang, J.A., et al., *Regulation of gene expression by 17β-estradiol in the arcuate nucleus of the mouse through ERE-dependent and ERE-independent mechanisms.* Steroids, 2016. **107**: p. 128-138.
80. Smith, J.T., et al., *Regulation of Kiss1 gene expression in the brain of the female mouse.* Endocrinology, 2005. **146**(9): p. 3686-92.

Chapter VII. Conclusions

Overview

The MCH system is implicated in a wide range of physiological functions including metabolism, sleep, and reproduction. In addition to the MCH peptide itself, co-release of classical neurotransmitters from MCH neurons is a critical component of their function.

In Chapter 2, we demonstrate that *Pmch* mRNA is transiently expressed in the POA, PVH, and other forebrain nuclei of the lactating female mouse, and that these transient populations are GABAergic while constitutive MCH populations in the IHy/LHA/PFx are glutamatergic. Furthermore, we show that Cre-induced reporter gene expression is dissociated from *Pmch* mRNA expression in the forebrain and rostral hypothalamus of lactating female BAC transgenic *Pmch*-Cre mice. Thus, in Chapter 3, we describe the generation of a new *Pmch*-iCre mouse line using CRISPR/Cas9 technology to fully capture the regulatory landscape of the *Pmch* gene.

In Chapter 4, we review the literature regarding amino acid neurotransmission from MCH neurons and make a case for greater flexibility in our conceptualization of neurochemical identity. We suggest that MCH neurons likely possess the molecular machinery to synthesize both GABA and glutamate but may preferentially release one or the other depending on some combination of factors related to both the internal and external environment.

In Chapter 5, we show that VGLUT2 deletion from MCH cells has sex-specific effects on reproduction and metabolism. Female $Pmch^{\Delta VGLUT2}$ mice exhibit delayed pubertal development and increased latency to pregnancy compared with control littermates. Female $Pmch^{\Delta VGLUT2}$ mice also have higher locomotor activity than controls, while male $Pmch^{\Delta VGLUT2}$ mice show indications of slightly impaired glucose tolerance.

Due to the sex differences observed in Chapter 5, in Chapter 6 we investigated the potential role of gonadal steroids on the regulation of sleep in male and female mice. We describe the projection patterns and transcriptional profiles of MCH neurons and use this information to define subsets of the MCH neuron populations, most notably, a subpopulation of MCH neurons in the PFx that targets both sleep and reproductive control sites and expresses the neurokinin-B (NKB) receptor, NK3R. We proposed a mechanism by which estrogen-sensing kisspeptin-neurokinin B-dynorphin (KNDy neurons) modulate activity of this subpopulation of MCH neurons via NKB signaling and tested this hypothesis by optogenetically stimulating NK3R terminals in the PFx of male and female mice. While male mice and female mice under low estradiol conditions were largely unresponsive, females supplemented with exogenous estradiol exhibited reduced time in both REM and NREM sleep and increased time spent awake during the dark phase. Our findings reveal a previously unrecognized and estradiol-dependent role for the KNDy-MCH neuron circuit in the integration of gonadal steroids and sleep in female mice.

Limitations of the Work and Proposed Solutions

Animals

The *Pmch*-iCre mouse model we generated (Chapter 3) and used for many of the experiments described in Chapters 5 and 6 effectively exhibited Cre-inducible reporter gene expression in MCH+ cells in the LHA, IHy, and PFx. However, reporter gene expression is also observed in a number of MCH- cells in the PFx, the dorsal aspect of the ZIm, several pontine nuclei including the pontine reticular nucleus, caudal part (PRNc) and other sites in the forebrain and rostral hypothalamus including the olfactory tubercle (OT). *Pmch* mRNA has been reported in the PRNc and OT of the rat brain, but never mouse, and the Cre+/MCH- cells of the PFx have been previously described by our lab. However, the majority of the sites in which we observe Cre-induced reporter gene expression in the absence of MCH-immunoreactive cells are not documented sites of MCH expression.

These populations are likely sites of developmental *Pmch* expression, and several of them are VGLUT2+ in adulthood. *Pmch* expression is observed as early as embryonic day 11 in mice [1]. Thus, Cre-mediated deletion of VGLUT2 (Chapter 5) began during important periods of neurogenesis and central nervous system organization, and it is possible that it also affected

additional neuronal populations beyond the MCH+ neurons of the LHA, IHy, and PFx. This has the potential to confound the interpretation of our data, as there could be both organizational and activational effects of VGLUT2 deletion from MCH neurons, and conversely, compensatory mechanisms resulting from disruption of the MCH system in early development could mask an effect of disrupting VGLUT2 signaling in adult MCH neurons.

In future work, it will be important to verify using ISH and/or IHC in developing brains that sites of Cre-induced reporter gene expression contain *Pmch* mRNA at some point in development and are not off-target effects. Furthermore, dual-label ISH/IHC should be performed to determine the neurochemical identity of *Pmch*-expressing populations in order to parse the potential effects of VGLUT2 deletion in developmental *Pmch*-expressing cells from the effects in LHA/IHy/PFx MCH cells in adulthood. Finally, it would be constructive to devise a means of inducing Cre-mediated deletion of VGLUT2 in adulthood in order to determine the effect of loss of glutamatergic signaling from MCH neurons in adult animals in which this system developed normally.

The *Kiss1*-Cre;ChR2-eYFP mice used for optogenetics experiments in Chapter 6 showed robust YFP labeling in the arcuate nucleus and YFP-labeled terminals in the PFx in apposition to MCH neurons. Additionally, cFos induction is clear at the optical fiber implantation site in *Kiss1*-Cre;ChR2-eYFP mice. Thus, we can assume that optogenetic stimulation is affecting neuronal activation, and the fact that males and OVX females are largely unresponsive is not simply a matter of lack of activation. However, it is important to consider that while all kisspeptin-expressing neurons in the male brain are located in the ARH, and thus we can assume that all *Kiss1*-Cre;ChR2-eYFP terminals being stimulated in the PFx of male mice are coming from ARH KNDy neurons, females have an additional kisspeptin-expressing population in the AVPV. Thus, in future experiments, the relative contributions of inputs from the AVPV and the ARH must be assessed, particularly as a sex- and estradiol-specific trend has been observed in the effect of our paradigm on sleep. One answer to this would be the use of retrograde tracers to evaluate the relative numbers of Fos-activated cells which receive inputs from the ARH vs the AVPV, or the use of AAV-ChR2 anterograde tracer injections in commercially available *Tac2*-Cre mice in the manner used to label MCH neuron projections in Chapter 6.

Technical Limitations Around LH Measurement

Some insight into the ways in which LH pulsatility fluctuates with vigilance state across the lifespan has been gained from studies in humans [2-11]. However, the study of the precise mechanisms behind the integration of vigilance state and LH release have proven challenging to approach from an experimental design perspective. The insights that might be gained by aligning continuous measurements of circulating LH levels with EEG, particularly in combination with the ability to use chemo- or optogenetic manipulation to target various components of sleep circuitry and/or the neuroendocrine reproductive axis, are sizeable. However, the continuous sampling of blood from rodents on the time scale that would be necessary to gain such insights is not feasible given the small volume of blood that can be removed without causing harm to the animal. It is also impractical, as blood cannot be collected from the tail vein in sleeping mice because this is an invasive and stressful procedure, and automated blood collection methodologies such as the Culex system are not compatible with the specialized cages required for optogenetic stimulation, sleep recordings, etc. Thus, we have sought to better understand how MCH neurons might integrate sleep and various aspects of reproductive physiology from a largely anatomical perspective, but our ability to actually observe real-time effects of manipulations to the circuit we have identified on sleep and circulating LH simultaneously is limited.

To combat this, we designed a second new transgenic mouse model which has a fluorescent tag fused to the beta subunit of LH. Our hope is that we will be able to use this animal to estimate circulating LH levels in real time using fluorescence as a proxy for LH concentration in the blood. We are currently working with collaborators to optimize a system for detecting this fluorescence in blood reliably and reproducibly. The low levels of circulating LH and the high autofluorescence of the blood make this a challenging technical conundrum in its own right, but based on our calculations the endeavor is feasible in principle. If we can optimize the detection of the fluorescent protein, the ability to gather continuous, real-time data about circulating LH levels has the potential to transform how we study LH release and serve as proof of concept for assaying other circulating hormones in a similar manner.

Effects of VGLUT2 Deletion in MCH Neurons using the *Pmch*-iCre mouse model

There are numerous documented effects of VGLUT2 deletion from MCH neurons on metabolism, sleep, and anxiety. Male *Pmch*-Cre$^{\Delta VGLUT2}$ mice exhibit decreased body weight and adiposity, increased locomotor activity, late-onset hypophagia, attenuated weight gain on high-fat diet, reductions in circulating leptin, reduced sucrose preference, and altered glucose tolerance [12, 13]. VGLUT2 deletion from MCH neurons also reduces REM sleep during the dark phase and increases the diurnal variability of REM sleep in male mice [14]. Finally, VGLUT2 deletion from MCH neurons has been associated with reduced anxiety-like behavior [15].

In our experiments, we did not observe most of these reported metabolic effects of VGLUT2 deletion from MCH neurons, which is likely an effect of background strain differences. However, we do observe a trend towards an increase in VCO_2, VO_2, glucose and fatty oxidation, and rate of energy expenditure. In the future, we will increase the size of our experimental groups sent for comprehensive metabolic testing to determine whether a more statistically powered study reveals differences in basal metabolic rate in *Pmch*$^{\Delta VGLUT2}$ male and/or female mice. We do see a slight but significant reduction in body weight in females when they are single housed, and the effect is driven by lean mass. The legitimacy of this effect and, if it is replicable and not an artefact of the specific subset of females used for comprehensive metabolic testing, its etiology will be important to explore in future studies.

We report that male mice have increased area under the curve for plasma insulin following an oral glucose challenge, suggesting mild insulin resistance. While no significant effect was observed in females, they trend towards reduced AUC for insulin which would imply slightly enhanced insulin tolerance. Future studies will expand the sample size for both males and females. Furthermore, as there are some reports of *Pmch* expression in the pancreas, we will use both histology and qPCR to assess whether VGLUT2 deletion in MCH cells could be affecting the pancreas and whether this might explain alterations in glucose handling.

We also did not explore the effects of high-fat diet on *Pmch*-Cre$^{\Delta VGLUT2}$ mice. This has not previously been investigated in females, so it will be important both to determine whether we replicate existing findings in our mice as well as whether females exhibit a unique phenotype. We will also investigate hormone feedback effects on metabolism by performing longitudinal

body weight monitoring, comprehensive metabolic analysis, and glucose tolerance testing in ovariectomized females with and without estradiol replacement on both chow and high fat diet.

In addition to these metabolic effects, we report several novel sex-specific findings on reproductive physiology in *Pmch*-Cre$^{\Delta VGLUT2}$ mice. Female *Pmch*-Cre$^{\Delta VGLUT2}$ mice exhibit delayed VO and first estrus, and while they appear to cycle normally, they have an increased latency to pregnancy as compared to control littermates. Future work should endeavor to further understand the mechanisms behind these effects.

Potential Mechanisms of MCH Neuron Integration of Sleep and LH Release Timing

We report that MCH neurons do not express sex steroid receptors, but that a subpopulation therein, located in the PFx, does express the neurokinin B receptor (NKB; NK3R) and receives inputs from estradiol-responsive KNDy neurons in the ARH. Furthermore, we observed that, when Cre-dependent anterograde tracers are injected into MCH neurons, the specific targeting of the injection is a clear predictor of the location of target cells, with injections situated primarily in the PFx innervating regions associated with reproductive control much more densely than injections targeting more lateral MCH neurons. This led us to believe that medial MCH neurons located primarily in the PFx are the most likely candidates for MCH-mediated integration of sleep and reproductive physiology.

Pilot studies using optogenetics to activate a putative ARH KNDy → PFx MCH circuit elicit only modest effects, and minimal *Fos* mRNA expression in MCH neurons themselves. Ovariectomized females with estradiol replacement do largely trend towards reduced total time spent in both REM and NREM sleep during the dark phase and increased time spent awake in the dark phase. A consistent response to stimulation is not apparent in males or in ovariectomized females without estradiol replacement. This may reinforce the idea that some aspect of KNDy neuron modulation of sleep is gated by estradiol, a theory which is supported both by studies of LH secretion and sleep: MCH administration differentially alters LH secretion under different estradiol milieu, and sleep is more fragmented when estradiol is high. However, these studies are still in the pilot stage, and it will be important to increase our sample sizes until we have a statistically powered study before the finalization of conclusions and the publication of this work.

It is also important to consider the KNDy neurons express additional neuropeptides and neurotransmitters. Of course, they express kisspeptin and dynorphin; while the kisspeptin receptor *Kiss1r* is not located in the same region as MCH neurons, MCH cells are known to colocalize the kappa opioid receptor (KOR) for which the dynorphins comprise endogenous ligands [16, 17]. Thus, action at KORs by dynorphin could also be affecting MCH neuron activity, which could also explain the absence of *Fos* labeling in MCH neurons. Activation of KORs would result in neuronal inhibition, and thus would not induce *Fos.* Additionally, KNDy neurons express VGLUT2 and thus the neuronal activation we observe could be the result of glutamatergic excitation of another population of neurons in the PFx. Different and even contrasting effects could be resulting from our optogenetic manipulations as a result of the different neuropeptides and neurotransmitters that are synthesized in KNDy neurons, which may muddy the interpretation of our behavioral data. The use of selective antagonists for glutamate receptors, KOR, and NK3R could be employed in the future to parse the unique effects of the different neurotransmitters that may be released when KNDy terminals are stimulated.

Finally, we should revisit our experimental design and assess whether our parameters are optimal for detecting a modulatory, rather than a directly excitatory or inhibitory, role for this ARH KNDy → PFx circuit. It may be beneficial, for instance, to sleep deprive mice beforehand to observe a sleep-suppressing effect of this circuit, or to provide some wake-promoting stimulus in order to be able to observe a sleep-promoting effect. Alternately, recording neuronal activity, either *in vitro* or *in vivo*, could offer some insights into precisely what is happening downstream of ARH KNDy neurons in the PFx and give some insight into the likely behavioral effects that may result.

Final Conclusions

My dissertation work has shown that *Pmch* may have previously unknown developmental roles; that the MCH system is an important player in the integration of sleep and the neuroendocrine reproductive axis; that glutamatergic neurotransmission in MCH neurons has sex-specific effects on metabolism and reproductive development and efficiency; and finally, that ARH KNDy neuron action at several potential targets in the PFx, including but not limited to MCH neurons, is a potential mediator of gonadal steroid effects on sleep architecture. Future studies should

characterize the developmental expression of *Pmch*; elucidate the mechanisms by which glutamatergic neurotransmission from MCH neurons affects the neuroendocrine reproductive axis and neuroendocrine control of metabolism; and define the specific neuronal targets of KNDy neurons in the PFx with the potential to modify sleep. A more complete understanding of the role of MCH neurons in both male and female animals across the lifespan, including during embryonic development, is important for conceptualization of how the neural circuits governing sleep, metabolism, and reproduction work synergistically as well as how dysfunction in one of these areas may impact health in the others. Additionally, a greater mechanistic understanding of the neuronal populations integrating gonadal steroids and sleep is critical to developing understanding and therapeutic interventions for sex-mediated sleep pathologies, which are both a major quality of life burden and associated with many other comorbid disorders. Finally, our data revealed sex-dependent effects that may not have been predicted based on MCH neurons' absence of gonadal steroid receptors; these findings underscore the vital importance of using male and female animals in all basic science research.

References

1. Croizier, S., et al., *Development of posterior hypothalamic neurons enlightens a switch in the prosencephalic basic plan.* PLoS One, 2011. **6**(12): p. e28574.
2. Kapen, S., et al., *Effect of Sleep-Wake Cycle Reversal on Luteinizing Hormone Secretory Pattern in Puberty.* 1974. **39**: p. 293-9.
3. Apter, D., et al., *Gonadotropin-releasing hormone pulse generator activity during pubertal transition in girls : pulsatile and diurnal patterns of circulating gonadotropins.* Journal of Clinical Endocrinology and Metabolism, 1993 **76**(4): p. 940-949.
4. Dunkel, L., et al., *Developmental changes in 24-hour profiles of luteinizing hormone and follicle-stimulating hormone from prepuberty to midstages of puberty in boys.* 1992. **74**: p. 890-7.
5. Landy, H., et al., *Sleep Modulation of Neuroendocrine Function: Developmental Changes in Gonadotropin-Releasing Hormone Secretion during Sexual Maturation.* 1990. **28**: p. 213-7.
6. Mitamura, R., et al., *Diurnal Rhythms of Luteinizing Hormone, Follicle-Stimulating Hormone, and Testosterone Secretion before the Onset of Male Puberty 1.* 1999. **84**: p. 29-37.
7. E. Oerter, et al., *Gonadotropin Secretory Dynamics During Puberty in Normal Girls and Boys.* 1990. **71**: p. 1251-8.
8. Penny, R., N. O. Olambiwonnu, and S. D. Frasier, *Episodic fluctuations of serum gonadotropins in pre and post-pubertal girls and boys.* 1977. **45**: p. 307-11.

9. Boyar, R., et al., *Synchronization of Augmented Luteinizing Hormone Secretion with Sleep during Puberty.* 1972. **287**: p. 582-6.
10. R. McCartney, C., *Maturation of Sleep–Wake Gonadotrophin-Releasing Hormone Secretion Across Puberty in Girls: Potential Mechanisms and Relevance to the Pathogenesis of Polycystic Ovary Syndrome.* 2010. **22**: p. 701-9.
11. Shaw, N., et al., *Insights into Puberty: The Relationship between Sleep Stages and Pulsatile LH Secretion.* 2012. **97**.
12. Schneeberger, M., et al., *Functional analysis reveals differential effects of glutamate and MCH neuropeptide in MCH neurons.* Mol Metab, 2018. **13**: p. 83-89.
13. Whiddon, B.B. and R.D. Palmiter, *Ablation of neurons expressing melanin-concentrating hormone (MCH) in adult mice improves glucose tolerance independent of MCH signaling.* J Neurosci, 2013. **33**(5): p. 2009-16.
14. Naganuma, F., et al., *Melanin-concentrating hormone neurons promote rapid eye movement sleep independent of glutamate release.* Brain Struct Funct, 2019. **224**(1): p. 99-110.
15. Sankhe, A.S., et al., *Loss of glutamatergic signalling from MCH neurons reduced anxiety-like behaviours in novel environments.* J Neuroendocrinol, 2023. **35**(1): p. e13222.
16. Ozaki, S., et al., *Region-specific changes in brain kisspeptin receptor expression during estrogen depletion and the estrous cycle.* Histochem Cell Biol, 2019. **152**(1): p. 25-34.
17. Parks, G.S., et al., *Identification of neuropeptide receptors expressed by melanin-concentrating hormone neurons.* J Comp Neurol, 2014. **522**(17): p. 3817-33.